10. WATANA DEVELOPMENT DESCRIPTION

This section provides a description of the main project works and the factors that were considered in selecting the preliminary designs for the major features. The site access and transmission facilities are described in other sections – Site Access Facilities are described in Section 8 and Transmission and Interconnection Facilities are described in Section 11.

10.1. Introduction

10.1.1. Site Survey and Mapping

The site survey and base mapping was created during 2012. After initial layouts were crafted using topography obtained by digitizing the 1980s topographical maps, the first new topographic data became available for the current feasibility studies using the Interferometric Synthetic Aperture Radar elevation data and the MatSu-North Susitna Bare Earth Data (both datasets are using Horizontal North American Datum of 1983 [NAD83] and North American Vertical Datum of 1988 [NAVD88]).

On the drawings prepared in the 1980s, the vertical datum has been described as "USC & GS MSL" or "Mean Sea Level". In APA document No. 14, "Horizontal and Vertical Control Surveys", dated March 1981, by R&M Consultants, it is stated that "Elevations are based on a local NGS mean sea-level datum which approximates the U.S. sea-level datum of 1929".

Although no single document serves as the official defining document for NAVD 88 (www.ngs.noaa.gov/datums/vertical), detailed information is available in an NGS-NOAA Special Report, "Results of the General Adjustment of the North American Vertical Datum of 1988". This document indicates that for the 48 adjacent states, the vertical difference in datums between NAVD 88 and NGVD 29 ranges from -40 cm (-1.31 ft.) to +150 cm (4.92 ft.), and that in Alaska, the differences range from +94 cm (3.08 ft.) to +240 cm (7.87 ft.). The NGS-NOAA Special Report also indicates that the NGVD 29 to NAVD 88 datum conversion in Fairbanks is +160 cm (5.25 ft.), and in Anchorage it is +190 cm (6.23 ft.).

Given that no official datum conversion is available in the vicinity of Watana Dam, a reasonable approximation could potentially be determined from a current resurvey of benchmarks (brass cap monuments) near Watana Dam. Among the monuments in the project area, difference varies between a maximum value of 5.950 ft. and a minimum value of 5.821 ft., for a range of 0.129 ft. (1.5 inches) among the 10 benchmarks. The average difference is 5.901 ft. and the benchmark closest to Watana Dam (22-C) has a difference between datums of 5.899 ft. The vertical datum differences at the benchmarks also fall between the given values for Fairbanks (5.25 ft.) and

Anchorage (6.23 ft.). From this, it appears that the vertical datum differential at Watana Dam between NAVD 88 and NGVD 29 can be given as about 5.9 ft.

10.1.2. Project General Arrangement

The proposed Watana Dam will create a reservoir approximately 42 miles long, with a surface area of about 23,500 acres, and a gross storage capacity of 5,170,000 acre-feet (ac-ft.) at the normal maximum operating level (NMOL) of El. 2050 ft. as shown in Figure 1.6-2.

The maximum water surface elevation of the project shown in the accompanying figures during probable maximum flood (PMF) conditions will be El. 2064.5 ft. The minimum operating level of the reservoir will be El. 1850 ft., providing 3,380,000 acre-ft. of active storage during normal operation.

The dam will be a concrete gravity structure constructed using roller compacted concrete (RCC) methodology. The dam will have a central section with a curved axis radius equal to 2,600 ft. at the upstream edge of the crest. At each abutment there will be straight gravity sections (with downstream slopes of 0.85H to 1.0V) acting as "thrust blocks" and intersecting the curved section at tangent points. The downstream face of the dam will be curved (vertically) at a radius of 1,650 ft. from the crest which will be 45-ft.-wide. The upstream face will be vertical except for a batter with a slope of 0.1H to 1.0V below El. 1770 ft. The nominal crest elevation of the dam will be El. 2065 ft., with a maximum dam height of approximately 705 ft. above the foundation. The crest length will be approximately 2,810 ft. The total volume of the RCC concrete structure will be approximately 5,215,000 cubic yards, with an additional 456,000 cubic yards of conventional concrete placed in the dam crest, spillway and outlet works. During construction, the Susitna River will be diverted through a concrete-lined diversion tunnel on the north side of the river, 36 ft. in diameter and approximately 2,060 ft. long. A 44 ft. by 44 ft. square sluice will be constructed through the dam to provide supplemental river diversion capacity.

Each installed generating unit will be served by a single power intake located on the upstream face of the dam. Each power intake will be a concrete structure with multi-level gates capable of operating over the full reservoir operating range. From each intake structure, a steel penstock with an internal diameter of 19 ft. will penetrate the concrete dam and will be anchored to the downstream face of the dam leading to the powerhouse complex. The steel penstock will be surrounded in a concrete encasement where it is positioned on the downstream face of the dam.

The powerhouse will house three generating units with vertical shaft Francis-type hydraulic turbines driving direct connected synchronous generators. A fourth penstock will pass through

the concrete dam, and the downstream end will be semi permanently capped—to be removed if and when an additional generating unit is eventually installed in the future.

Access to the powerhouse floor level will be by means of a shotcrete-lined access tunnel from the north (right) side of the valley, necessary because of the steep valley sides, and a road from the north bank of the downstream river valley. Turbine discharge will flow through three draft tubes (one per unit) and into the common tailrace.

One three-phase generator step up transformer for each unit will be mounted on the powerhouse deck, downstream of the powerhouse building, together with a spare transformer. From the transformer bushings there will be 230 kilovolt (kV) high voltage lines that will connect to a switchyard on the left downstream abutment. The switchyard will provide switching to three transmission lines.

The intakes for the low-level outlet facilities will be located on the upstream face of the dam to the north side of the spillway, with a total combined capacity of approximately 32,000 cubic feet per second (cfs) at a surcharge of 7.5 ft. In combination with the average powerhouse flow of 7,830 cfs, the arrangement provides for the storing and releasing of the 50-year flood without raising the pool level above El. 2057.5 ft. and without spillway operation.

The spillway located on the north side of the powerhouse will consist of an upstream ogee control structure with four radial gates and an inclined concrete chute and flip bucket designed to pass a maximum discharge of 250,000 cfs. This spillway, together with the outlet facilities, will be capable of discharging 282,000 cfs – the routed peak discharge from the estimated PMF inflow of 310,000 cfs, while maintaining a maximum water level of El. 2064.5 ft. Additionally, emergency release facilities will be located in the diversion tunnel after closure to allow controlled filling and for lowering of the reservoir – after the low level outlets have drawn the water down to El. 1850 ft. – over a period of time for emergency inspection or repair of impoundment structures.

The general arrangement of the dam and powerhouse facilities is shown in Figure 1.6-2 and on Drawing 04-01C002.

10.2. Site Facilities

The site facilities covered by this section include the construction facilities, temporary construction camp, permanent village, water supply, wastewater treatment, and solid waste disposal, shown in Figure 1.1-3. Refer to Drawing 01-00G001 for details.

The siting of these facilities was originally examined during the 1980s feasibility studies and documented in the Watana Support Facilities–Master Plan, dated July 1985. The methodology used in, and the results of, that report have been used in preparing the project arrangement shown on the drawings.

The proposed facilities assume that workers performing summer (seasonal) tasks such as RCC placement, would remain at the project site throughout the whole construction season, while those performing year-round tasks (such as tunneling or conventional concrete placement) would be subject to a rotational method of working (such as two weeks on, one week off) similar to other major infrastructure developments in Alaska.

Key infrastructure includes:

- temporary construction camp;
- contractor facilities;
- permanent village for operators (used during construction for supervising staff);
- temporary housing at the permanent village (removed at the end of construction);
- water treatment facilities;
- wastewater treatment facilities; and,
- solid waste facilities.

Other temporary facilities, such as the quarry development, construction roads, concrete batching facilities, etc., are described in construction planning in Section 13. The airstrip, the camp at the railroad offloading area, and the permanent site access roads, all of which are important to construction, are described in Section 8.

10.2.1. Location of Facilities

The site facilities will be located to the north of the Project as shown on Drawing 01-00G001. The permanent village will be located around the panhandle lake as shown, although the exact position will be defined after wetland and other environmental surveys have been completed. The temporary construction camp will be located alongside the adjacent long lake, which (with the addition of a small dock) is long enough to be used for float plane access. In a similar manner to the permanent village, the exact position of the construction camp will be defined after wetland and environmental surveys. It is expected that the detailed layout of the accommodation facilities will be adjusted to minimize wetlands impacts.

The water treatment facilities and waste water facilities will be located between the construction camp and the permanent village so that they can be left in place to conveniently service the permanent village.

An area available for a temporary camp for site investigations is also shown – although to date alternative arrangements have been made.

10.2.2. Temporary Construction Camp

The temporary construction camp and contractors' facilities will provide housing for the contractors' workforce, and buildings and facilities for the management of the workforce and the maintenance of contractors' equipment. With the exception of particular buildings/workshops, it is proposed that all buildings are removed at the end of construction, and the area landscaped and revegetated.

Manpower planning has been carried out concurrently with construction schedule preparation, and the cost estimation, and recognizes the difference between seasonal workers and those performing tasks year-round. Those working during the summer season are assumed to remain on the site all season, while those with year-round work will rotate. Accommodation planning assumes that every worker will need a single room to themselves, and those that are working on a rotational basis will not "vacate" their rooms. Therefore, more rooms will be needed than there are workers on site.

The construction camp will provide temporary housing for up to 1,200 contractors' personnel, including laborers, foremen, section managers, etc. although normally there will be a lower number in residence. The senior management staff are assumed to be accommodated in the (enlarged) permanent village described in Section 10.2.4. Support facilities for the temporary accommodation will include:

- kitchen
- dining hall
- administration offices
- store
- laundry facilities
- recreational facilities, such as a movie theatre, gym, and recreation hall
- playing fields

- medical facility sized for the project site (located near the airstrip to facilitate evacuation in case of a serious medical condition)

Fire fighting vehicles/pumps will be located at the airstrip, but will service the whole project site during construction and permanent operation.

The construction camp will be fenced to minimize human/bear interactions.

It is expected that the construction camp will be primarily single status.

Based on the proposed schedule and the balance of all season and rotational workers, the residential accommodation will be sufficient for 1,200 individuals, and at any one time 800 are expected to be in residence and using the common facilities.

To mobilize workers to commence construction, including the construction of a temporary construction camp at the site, the initial work will be performed based on a temporary camp at the railhead. It is estimated that this would need to accommodate between 60 and 300 persons. During the construction of the access road and the mobilization stage, this will be used as a base of operation, but production will suffer because of the long daily "commute" to the site. However, as soon as a temporary camp at the dam site is partially complete and available for occupancy, the base of operations will shift from the railhead to the site, leaving the facilities at the railhead for their ongoing intended use.

The temporary facilities at the railhead will include:

- kitchen
- dining hall
- administration offices
- laundry facilities
- recreational facilities, such as a gym, and recreation hall

Power and fiber optic services will be required at the railhead. The power will be drawn from a tapping on the intertie – which will also be used to service the main construction – and a tapping will be made to the fiber optic cables that are within the ARRC right of way. There will be water and wastewater facilities constructed at the location.

The railhead facilities will provide for those supporting the logistics chain there, as well as some "emergency" accommodation for drivers or those prevented from using the road or rail because of inclement weather.

10.2.3. Contractor Facilities

The contractor facilities will include:

- offices
- store
- mechanical workshop
- tire workshop
- electrical shop
- lumber shop
- covered storage
- fenced outdoor storage
- fuel storage
- explosives storage (located remote from other facilities)
- bar bending shop

A transport hub, including waiting room will be located at the airstrip, to facilitate the rotation of a significant proportion of the contractors' workers each Monday and Friday.

10.2.4. Permanent Village

The village will provide housing for management personnel, AEA staff and consultants, and guest accommodation for visitors during the construction of the Project. A portion of the village around the lake shore will be constructed as permanent housing suitable for long-term use by families after completion of the Project. The permanent housing in the village is expected to comprise two-bedroom homes, and one-bedroom apartments. In addition, extra two-bedroom housing units will be temporarily located in the village, and will be removed at the end of construction to leave the appropriate number of houses for permanent operators, as further described in Section 10.2.6.

Included in the village will be a block with small units (one bedroom) for single staff – which at the end of construction will be removed – and a block of studio apartments for construction site visitors that will be refurbished and retained for large maintenance groups who might relocate to the site, during operation, for major maintenance. After construction this block will be maintained, and heated, but will only be opened for use during major maintenance.

In addition to the accommodation, the village will include:

- dining facilities
- gymnasium
- recreation hall/club
- sports fields

The permanent village will be robustly fenced to minimize human/bear interactions.

The temporary housing will be removed at the completion of construction, and the appropriate areas landscaped, and the medical facilities and fire station constructed for the construction phase will be refurbished for long term use.

10.2.5. Owner Offices

Construction supervision offices will be constructed at the site for AEA staff, construction management staff retained by AEA and the design consultants. They will comprise offices, conference rooms, document storage, a drafting group office, and a small kitchen. There will also be a laboratory for ongoing testing of construction materials and concrete.

At the present time, it is assumed that these offices will be removed at the end of construction, and the requisite offices for ongoing operation will be in the powerhouse. However, if preferred by AEA, a permanent owner/operator office building could be constructed on the right (north) abutment.

10.2.6. Operators Accommodation

During the operation of the project, it is assumed that AEA or its contracted operator will require the staff listed in Table 10.2-1, who will reside at the project:

Table 10.2-1. Typical Operations Staffing

Staff	Number
Plant Manager (non-shift work)	1
Operators (shift work)	3
Electric lead technician (shift work)	3
Electric labor (non-shift work)	2
Mechanical lead technician (shift work)	3
Mechanical labor (non-shift work)	2
Civil lead technician (non-shift work)	1

Staff	Number
Civil labor (non-shift work)	3
Administrative manager	1
Security	5-10
Total FTEs	24-29

Note: FTE – full time equivalents

As noted, it is expected that a security staff of between 5–10 persons will be required.

At this time it is assumed that all these staff members would be full time at the site, and would not work on a rotating basis, so 29 family houses will be necessary. For occasional guests it is suggested that other houses also be left in place (and kept heated). As mentioned above, these houses will be built as part of the temporary facilities and will be used by management personnel, AEA staff, consultants, and guests during the construction of the project, but will be built more robust to later serve as permanent housing.

In addition, the apartment building to be included in the permanent village which will house single management personnel and guests during construction will be remodeled after construction of the Project is complete. That building will be reconfigured as approximately 50 studio apartments for the use of larger maintenance crews when they are sent to the project for extended periods for rebuilds, additions or expansions. The building will include a kitchen/dining facility and recreation rooms, but will not normally be open, and will be maintained with nominal heating until needed.

10.2.7. Water Supply

10.2.7.1. General

A water supply system will be provided for the construction camp and will be left in place for the permanent village, powerhouse and any permanent office building. This water system will include adequate supply for drinking (potable) water, fire protection, laboratory operations and miscellaneous uses for the construction of the Project and on-going operations after completion.

The following Table 10.2-2 presents the preliminary water system design criteria which were used to generally size the water and wastewater supply and treatment facilities for both the construction camp and permanent village. Water supply for construction activities including the concrete batch plant will be sized separately and will be the responsibility of the selected main contractor.

Table 10.2-2. Preliminary Water System Design Criteria

Parameter	Construction	Permanent
Population Served	1,200	80
Average Daily Per Capita Usage, gpcd	100	100
Daily Average Water Usage, mgd	0.12	0.03
Maximum Day Water Usage, mgd	0.22	0.05
Maximum Hour Water Usage, mgd	0.32	0.08
Fire Flow, gpm	1,060	560
Fire Demand, gallons	318,000	134,400

Note: gpcd: gallons per capita per day
mgd: million gallons per day
gpm: gallons per minute

The water supply system will include the following key components:

- Raw water intake, and pump station in a prefabricated building;
- Raw water pipeline and raw water storage tank;
- Water treatment system including low-pressure microfiltration membrane treatment with primary disinfection by ultraviolet light irradiation;
- Treated water storage tank;
- Treated water pumping and distribution system; and,
- Fire protection pumping and piping system (assuming that untreated water is used for fire protection supply).

A process diagram for these facilities is shown on Drawing 03-13-C001. Each of the systems is described in greater detail in the subsections below.

10.2.7.2. Raw Water Intake and Pump Station

The water supply system will include a raw water intake utilizing a sub-surface intake gallery. Preliminary assessment of the site indicates year round water will be available from Deadman Creek, northeast of the proposed construction camp site, making this a favored location for the intake. This type of intake has been demonstrated to be successful at providing year-round water supplies in cold, arctic regions. During the winter months, the intake gallery will be heated using conventional electric heat tracing to prevent freezing. A pump station located in a well-insulated prefabricated building above the intake will have a firm pumping capacity (i.e., assuming one pump out of service) of approximately 200,000 gallons per day (gpd) to meet maximum day usage requirements.

It is proposed that the pump station be designed for continuous operation, with continuous water recirculation (even when the treatment systems are offline) to avoid the plugging and freezing issues that are prevalent with start/stop operations in cold weather. Continuous operation, along with the raw water storage described below, will also reduce the need for operational changes during peak flows. The intake and pump station will be designed such that the installation can be easily "down-sized" after the construction camp is decommissioned to a lower pumping rate of approximately 50,000 gpd for the permanent facility needs. The pump station will convey water through the raw water pipeline to the raw water storage tank located in a building between the construction camp and the permanent village.

Additional fire protection supply may also be available on a seasonal basis from the lakes adjacent to the construction camp and permanent village sites (designated, respectively, Lake A and Lake B). During detailed design, the feasibility of using the lakes as a supply for fire suppression should be investigated and if acceptable, raw water intakes and pump stations will be designed and constructed at one or both lakes to supply untreated water directly to the fire protection system. As noted elsewhere, the fire protection system for the power facilities will be based on extraction from the tailrace. Further discussion on the fire protection system is presented below.

The power for the raw water pump station will come from the main construction camp power supply, with backup power provided by an additional 100-kW diesel generator located at the water/wastewater treatment building. At the end of construction, the normal power supply will be provided from the power facilities. Electrical conduits buried along the raw water pipeline alignment will supply power to the raw water pump station.

Instrumentation and controls will be installed at the raw water pump station to allow for remote monitoring of pump status and provide alarms in the event of equipment failures. These signals will be relayed to a control panel in the water/wastewater treatment building for easy control and operation by the operator(s) during the construction phase with further relaying to the main power facilities control room after construction is complete.

Deadman Creek is located a significant distance from both the construction camp and permanent village, which adds cost and operational difficulties. Further investigation with regard to the soils and groundwater levels surrounding the permanent village would be beneficial to determine if wells or galleries in locations closer to the point of use could be a reliable, cost-effective alternative. Another possible alternative raw water supply is the Susitna River, although this alternative would require the creation of settling basins. These options will be more thoroughly investigated during detailed design.

There will be significant use of raw water during construction including the following activities:

- Aggregate production
- RCC and CVC production
- Aggregate heating
- Abutment warming
- Abutment cleaning
- Drilling and Grouting
- RCC and CVC curing
- Dust suppression

The majority of the use is on the left (south) abutment, so the contractor can be expected to pump water out of the main river on the left bank, or possibly Fog Lake, creating a distribution system for raw water from the river around the site.

10.2.7.3. Raw Water Pipeline and Raw Water Storage Tank

The raw water pipeline will convey water approximately 3.6 miles to an approximate 0.3 million gallons (MG) raw water storage tank located inside a building and adjacent to the water treatment plant also inside the same treatment building. The tank has been shown in the drawings at grade, but during detailed design it may be relocated lower for enhanced insulation.

The raw water pipeline will comprise two separate three-inch diameter pipes. Using this configuration, adequate scouring velocities will be maintained for both the construction phase (using both pipelines simultaneously) and the permanent village (using a single pipeline) flow regimes, without having to install new piping in the future. To the extent possible continuous circulation through the two pipes will be practiced. The raw water pipelines will need to either be buried sufficiently deep, or be insulated, for its entire length to prevent freezing of the water in the pipes. A decision will be made after site investigations have been carried out, but (apart from insulation considerations) burying is preferable to prevent damage by wildlife. Given the proximity of bedrock in this area, buried raw water pipelines may not be feasible making insulated, heat-traced pipe the sole option. In either case, continuously delivering or recirculating the raw water through these pipelines, as discussed above, will help prevent freezing.

To minimize disturbance to the land during construction and thereafter, the pipeline route will be selected to collocate with other facilities as far as possible. Therefore, as far as possible the pipeline will be located alongside permanent roads and the airstrip.

The raw water storage tank will be located inside a climate-controlled water/wastewater treatment building to avoid freezing and to maintain a higher water temperature to improve treatability, as discussed below.

The proposed raw water storage tank provides several functions including:

- Serves as a buffer/feed tank for the water treatment plant (WTP) to improve system reliability due to the long distance between the intake and the WTP;
- Serves as a feed tank for the fire protection supply with a full tank meeting the estimated fire flow volume as discussed below; and,
- Can provide supply for some construction water uses, if demands are relatively low.

It is proposed that the raw water tank be co-located with the WTP and treated water storage tank and appurtenant systems which will be located inside a common building adjacent to the camp and village areas.

If further investigation finds that raw water is not available during the winter months, additional raw water storage in a lined reservoir could be required. Such a lined raw water reservoirs, will – typical of cold region water systems – be designed with adequate depth to allow for freezing of the surface while maintaining a sufficient useable volume below the ice layer. If such winter storage was required, an estimated usable volume of up to 18 MG of storage might be required to serve the construction camp during the projected five-month freezing period – depending on the occupancy. This requirement will be further investigated during detailed design, when water source investigations have been performed in greater detail.

Given the distance between the raw water intake and the treatment plant there may be difficulty maintaining the raw water pipeline during the winter. An alternative system of wells in closer proximity to the treatment plant building will be installed to provide nominal water supply to avoid complete breakdown during inclement weather. Availability of groundwater in this area will be examined in detail during detailed design.

10.2.7.4. Water Treatment System

A pre-engineered package-type water treatment system is appropriate for the location. Determination of the specific characteristics of a water treatment system for the proposed source will depend on the raw water quality, treatment goals, regulatory requirements when commissioned, and operation and maintenance (O&M) requirements. Potable water will be required to meet all Federal Maximum Contaminant Levels as well as any state-specific regulations adopted prior to construction. Two types of pre-engineered (package-type) treatment systems can be considered including:

- Conventional flocculation/sedimentation/granular media filtration; and
- Low-pressure membrane filtration.

Both systems can be pressurized without a free water surface inside the tankage, or have a free water surface within the tankage. Further analysis of the options will be considered after more extensive analysis of raw water quality data from Deadman Creek or an alternate raw water source. Key water quality parameters which can affect treatment process selection include temperature, turbidity, color, pH, alkalinity, total organic carbon, and iron/manganese. However, a low pressure membrane filtration system is included in this conceptual design for cost estimating purposes. A membrane water treatment system has many advantages, including providing robust treatment in a compact footprint.

Ultraviolet disinfection downstream of filtration is included for enhanced disinfection. Following ultra violet (UV) disinfection, chlorine will be added to maintain a free-chlorine residual in the distribution system. A process flow diagram for the water treatment system is shown on Drawing 03-13C002.

An on-site hypochlorite generation system which uses salt as the primary delivered chemical is proposed for chlorine supply. Other chemicals will also be required to support operations of the WTP, such as coagulant and clean-in-place chemicals for membrane units (including caustic soda, acid, and sodium bisulfite). Some of these chemicals can be shared with the wastewater treatment system.

Other features of the treated water supply will include:

- 0.3 MG treated water storage tank;
- Treated water pumps with a hydropneumatic (pressure) tank to deliver water to the distribution system; and,
- Backup power generator to provide basic water supply needs during periods of prolonged outages of the primary camp power supply.

During detailed design of the facilities, to the extent that State regulations allow it, consideration should be given to the supply of interior fire protection water, toilets and outside water for automobile washing etc. direct from the raw water tank through a separate distribution system. Such a dual system should reduce demand for treatment chemicals etc.

10.2.7.5. Water / Wastewater Treatment Building

It is proposed that the raw water tank, water treatment plant, and treated water storage tank and appurtenant water supply systems be co-located inside a common building adjacent to the camp

and village areas (alternatively, a location suitable for the construction camp could be chosen and the equipment and tankage could be relocated near the permanent village after construction). This building will be climate-controlled to reduce the effects of freezing temperatures on the treatment processes and equipment. A conceptual layout for the building is shown on Drawing 03-13C002. For speed of construction a pre-engineered metal building is suggested to allow for ease of material delivery and construction in the remote construction camp location, however careful design and construction of the building foundation will be required to prevent failure from permafrost or to protect against frost jacking. The building will be heavily insulated and contain areas for electrical/HVAC equipment, chemical storage, and operations/office space.

It is also proposed that the wastewater treatment system be co-located in the treatment building. Precautions will need to be taken to segregate the wastewater system from any drinking water system components including segregation of O&M tasks. At this level of feasibility, the building plan has been defined with no direct connection (doors) between the wastewater treatment and raw water treatment sections of the building.

10.2.8. Wastewater Collection and Treatment

10.2.8.1. General

A wastewater collection, treatment, and disposal system will be provided for the construction camp, permanent village, airport facilities and construction yard area.

Table 10.2-3 presents the preliminary wastewater system design criteria used to size the wastewater treatment and discharge facilities.

Table 10.2-3. Preliminary Wastewater System Design Criteria

	Construction Camp	Permanent Facilities
Population Served	1,200	80
Avg. Daily Per Capita Flow, gpcd	100	100
Avg. Daily Wastewater Flow, mgd	0.12	0.03
Max. Daily Wastewater Flow, mgd	0.19	0.05

Note: gpcd: gallons per capita per day
mgd: million gallons per day

The average daily flows will be affected by the typical daily diurnal flow variations common to most municipal wastewater treatment systems. This will be mitigated, to some degree, by the 24-hour operation schedule that will be employed during the summer months. Reduction of operations – and thus camp staff – in the winter will help reduce the overall load on the wastewater treatment plant when cold water will make treatment less efficient. A batching

system, or equalization tank, at the head of the wastewater treatment plant will help to balance daily fluctuations in wastewater flow and will improve overall system capacity and performance.

Wastewater will require secondary treatment to meet state and federal standards. This includes compliance with the "30/30 rule," limiting the 30-day average wastewater discharge to no more than 30 mg/L of BOD_5 (five day biochemical oxygen demand) and 30 mg/L of Total Suspended Solids. Additional treatment requirements for nutrients and/or toxics (regulated constituents with a reasonable potential for toxicity to human or aquatic life) such as metals may also be applicable depending on a biological opinion on the receiving waters. Careful analysis of the chosen raw water source will also be beneficial to the wastewater system planning, to determine if any constituents of concern are prevalent.

The wastewater system, as provided in the current concept, consists of the following key components:

- Wastewater collection system and raw wastewater pump stations located in a subsurface collection tanks;
- Influent equalization tank;
- Influent screens;
- Packaged submerged membrane wastewater treatment plant;
- Inline UV disinfection;
- Treated wastewater discharge pipeline and outfall (gravity flow); and,
- Sludge handling system including mechanical dewatering and dewatered sludge storage.

Other alternative treatment methods, such as the use of Sequencing Batch Reactor technology might also be an appropriate fit, depending ultimately on the long-term treatment goals of the facility. For space allocation and costing purposes at this planning level phase, submerged membrane technology as the primary treatment system adequately serves as a placeholder until further investigation during detailed design determines that other treatment methods are more beneficial.

Special "fogs" treatment (fats, oils, and grease) would be applied at the source – the largest of which will be the contractor's yard.

10.2.8.2. Collection System and Influent Pump Station

The wastewater collection system will consist of both gravity and pumped connections. Ideally, the construction camp wastewater will flow by gravity to a centrally-located collection tank and

then will be pumped into the wastewater treatment facility. For the permanent village, a similar but separate gravity collection system to a central storage/transfer tank is recommended. The collection system piping will consist mostly of high-density polyethylene pipe, which has a key advantage over other types of pipe as it can be frozen full of water with reduced probability of damage.

From the collection tank, wastewater will be pumped to the wastewater treatment system. Similar to the raw water pipeline, as discussed above, buried depth, heat tracing and insulation considerations will require careful evaluation for freeze protection of the collection system piping during detailed design.

10.2.8.3. Wastewater Treatment System

Wastewater treatment will be accomplished in a packaged, pre-manufactured treatment plant. The most common types of package wastewater treatment plants are extended aeration plants, sequencing batch reactors, oxidation ditches, contact stabilization plants, rotating biological contactors, and membrane biological reactors. Of these, the most applicable systems for this site are extended aeration plants, sequencing batch reactors, and membrane biological reactors. The current conceptual design utilizes membrane biological reactors, with the membranes being located submerged within stainless steel extended aeration tanks. This system is advantageous as it provides:

- A compact footprint, advantageous for indoor installation;
- Modular systems that can support the construction camp, but also be easily pared down for the permanent village;
- Ease of construction with factory assembled treatment modules delivered to the site with minimal field construction required;
- Excellent effluent water quality, capable of meeting more stringent requirements for nutrients and metals if required as discussed above; and,
- Low maintenance.

The packaged treatment plant will feature aerobic wastewater treatment to remove biochemical oxygen demand (BOD) as well as membrane filtration to remove solids, bacteria, and viruses. To facilitate a compact design, while maintaining systematic redundancy, it is recommended that the membranes be submerged within each of two tanks, which will operate as batch systems cycling through aeration and decant (membrane filtration) modes. A process flow diagram for the wastewater treatment system is shown on Drawing 03-13C001.

Treated wastewater will be discharged to the Susitna River upstream of the dam. Careful planning of the outfall will be required to make sure this remains free flowing throughout the year. This includes consideration of ice depth and water movement as needed to produce an adequate mixing zone, if allowed by the discharge permit, even during the cold winter months. An effluent storage tank may be necessary to store treated wastewater and discharge it in batches to prevent freezing in the pipeline and outfall.

10.2.8.4. Sludge Handling

Both the water treatment and wastewater treatment plants will generate a significant amount of residual waste streams including sludge. These treatment by-products will need to be dewatered and disposed of appropriately. The most typical method of treatment sludge disposal in cold regions is the use of a sludge pit, but these are often messy and difficult to operate in the winter. Sludge thickening and/or dewatering is recommended to reduce the volume of sludge needed to be disposed. A belt press thickener is recommended for sludge dewatering for its simple mechanics and ease of operation. The dewatered sludge can then be trucked to the dewatered sludge disposal site. The disposal site should be a solid waste landfill or separate sludge drying basins, depending on the level of dewatering achieved. Co-processing of the water treatment plant sludge may be possible with careful isolation (air gaps) of the water treatment sludges from the wastewater treatment systems.

10.2.9. Solid Waste Disposal

The temporary construction camp as well as the permanent operations village will require a solid waste collection system and disposal site. Steel dumpsters are often best suited for refuse collection as they are typically easily available, large enough to hold several days of accumulation, can be locked for prevention of bear ingress, and can easily be prevented from blowing over in strong winds.

The solid waste landfill will also require careful siting and sizing to protect public and environmental health especially with relation to the water source. The location relative to the airstrip is also a consideration to avoid bird hazards. Acceptable land area and adequate soil cover material is likely available adjacent to both temporary and permanent communities. Fencing will be necessary to prevent animal use (such as bears).

It is recommended that both the solid waste and the sludge (solid waste) generated by the water/wastewater treatment processes be combined into a single disposal site. A single, lined sanitary landfill will reduce the disposal site footprint, streamline the collection process, and minimize waste-wildlife interactions. The proposed disposal site is located to the North of the

airstrip at a distance of 10,000 ft., or, another area could be chosen that maximizes the distance from the airstrip and is not within the aircraft approach/departure path to minimize bird hazards.

Preliminary design calculations were completed assuming occupants in the construction camp for an eight year construction period and a permanent village design life (before major refurbishment) of 50 years following construction (total design life of 58 years). Analogous to similarly-sized cold weather, remote, communities, the solid waste landfill can be expected to contain approximately 290,000 cubic yards of material at the completion of its design life. A lined disposal site footprint of 600 ft. by 450 ft. (approximately six acres) and a nominal solid waste depth of 30 ft. will provide necessary volume. Additional capacity could be achieved by introducing an effort to compact the refuse. At the end of construction, that part of the landfill site used for the construction period could be permanently sealed and landscaped, because annual demands on the site will dramatically reduce after the construction is completed.

To reduce conflicts with wildlife, specifically bears, approximately 2,500 linear ft. of bear-proof fencing will be installed around the perimeter of the landfill facility. Typically, electrified fencing is the most effective in deterring bears. This would result in an approximate area of seven acres within the fence line – but when the sealing and landscaping is performed at the end of construction the fencing could be reduced to that needed for permanent occupation of the housing.

The total combined solid waste volume of the construction camp with an eight year construction time and the permanent village with a 50 year design life is shown in Table 10.2-4.

Table 10.2-4. Total Combined Solid Waste Volume

	Municipal Solid Waste (CY)	Sludge Solid Waste (CY)
Construction Camp	64,500	11,500
Permanent Village	191,000	21,500
Type Total	255,500	33,000
Total Volume:	288,500	

The volume of watered sludge cake (using belt presses) from the water and wastewater treatment systems is based on the assumption of 15 percent solids production. This equates to approximately three wet tons/day and 0.8 wet tons/day for the camp and village, respectively, with a bulk density of approximately 50 pounds per cubic foot.

10.2.10. Fire Protection System

The construction camp facilities and permanent village will be equipped with a reliable method for fire protection, and alarm. Any occupied buildings will be equipped with interior fire sprinklers which will be connected to the water distribution system. The State of Alaska has adopted the International Fire Code as its standard on fire protection systems. The systems will comply with the applicable requirements of the International Fire Code and the National Fire Protection Association codes and standards.

In addition to the interior system, a large capacity fire protection system, serving hydrants around the construction camp and permanent infrastructure facilities, will also be installed to provide greater flows during severe events. A raw water storage and piping system separate from the treated water distribution system will be required. The large diameter fire protection pipeline serving the various hydrants would remain dry under normal conditions (to prevent freezing) and would be pressurized when needed.

As described above, it is proposed to provide fire protection water supply by using the raw water storage tank which serves as the feed tank for the water treatment plant. A fire booster pump station located adjacent to the tank will be required to deliver adequate flow/pressure from the tank into the large capacity fire pipeline system.

Ideally, fire protection supply would be available "by gravity" and not require use of electro-mechanical systems (pumps and generator) during an emergency. However, use of an elevated tank to store untreated and/or treated water at the camp location is not feasible due to winter temperatures. As mentioned above, an additional fire protection supply may be available on a seasonal basis from the lakes (denoted A and B) adjacent to the construction camp and permanent village site.

At the end of construction, the large capacity facilities for the construction camp will be removed, leaving the system serving the permanent housing and facilities, and the airport. A fire pump truck will be garaged at the airport available for use around the site during operation. Firefighting at the power facilities will be accomplished using water pumped from the tailrace.

10.3. Geotechnical Design Considerations

The foundation characterization necessary for engineering analyses and feasibility design decisions is usually performed with the benefit of a focused site investigation. In this case, until the full site investigation and laboratory testing has been completed, including completion of drilling in the river channel, geophysical surveys, exploratory adits and in situ testing, it has been necessary to characterize the foundation based on the geotechnical information available from studies performed in the 1970s and 80s and those performed through the 2014 investigation program. An exploration and testing work plan has been developed of which a portion of the recommended investigations for feasibility has been completed (MWH, 2013). The site investigation and testing program are a "work in progress".

10.3.1. Engineering Geology

The general geological setting and site conditions are described in Section 6.3. The engineering geology characterization, design parameters and considerations related to the overburden; bedrock units; discontinuities (e.g., joints; shears, and fracture zones), weathering and alteration; geological features and the relict channel are described below.

10.3.1.1. Overburden

Overburden in the dam site area consists of till, colluvium, and talus the limits of which are shown on Drawing 01-01GT003. The overburden thickness in the dam abutments is typically less than 20 ft. thick but in areas may reach a thickness of 50 ft. or more (e.g., left abutment upstream of the dam axis. Subsurface investigations indicate that the contact between the overburden and bedrock is relatively unweathered and distinct. For additional information refer to the top of bedrock contour map (Drawing 01-01GT004).

In the river channel, alluvium beneath the proposed dam site area is typically between 70 to 80 ft. thick, but it is up to 140 ft. thick (Drawing 01-01GT007) within the two bedrock depressions located upstream of the dam. Within the dam footprint, alluvium ranges from about 60 to 105 ft. thick. The alluvium is comprised primarily of well-graded coarse-grained gravels, sandy gravels, and gravelly sands with cobbles and boulders (Harza-Ebasco 1983). The boulders are visible on the gravel bars and banks of the river and generally range from 1 to 3 ft. in diameter but some are as large as 5 ft. in diameter. Near the south abutment the alluvium transitions to a thick talus deposit of diorite boulders.

10.3.1.2. Bedrock Units

The dam site is primarily underlain by Tertiary volcanic intrusions that range in composition from diorite to quartz diorite to granodiorite (Drawing 01-01GT006). Therefore, the foundation for the dam, spillway, powerhouse and all other principal structures will involve diorite lithology. The bedrock is medium to dark green gray, fine to medium grained, generally hard to very hard, strong to very strong, competent, and generally fresh. However, bedrock is typically slightly to moderately weathered at the top of rock and along discontinuities to depths of 50 to 80 ft. Below the surficial zone of weathering, the rock mass is typically closely to moderately closely fractured. In outcrop, joints are typically tight to open, although they are mostly tight at greater depths, rough to smooth in profile, planar, and some contain iron stains, carbonate deposits or are slickensided. At depth, weathering locally can occur in areas of highly fractured rock, and the fractured rock may also contain shear zones with clay and breccia and/or be hydrothermally altered.

Bedrock directly downstream of and at higher elevations above the left abutment of the dam site consists of extrusive volcanics, mostly andesite porphyry which varies locally to dacite or latite. Andesite is not known to occur in the foundation of the dam or appurtenant structures. The andesite is similar in chemical composition to the diorite and is generally dark gray to black, slightly weathered, strong to very strong, competent and in places contains diorite xenoliths.

The diorite pluton has been intruded by mafic and felsic dikes that are generally a few feet wide, and exhibit contacts that are tight and competent. Felsic dikes are observed in outcrop as well as boreholes. The dikes are light gray, aphanitic to medium grained, fresh, hard, and strong to very strong. Mafic dikes are less common than felsic dikes but were observed in outcrop and in several boreholes. The mafic dikes typically consist of andesite and are less than 5 ft. wide. They are dark gray to green-gray, fine-grained, fresh, hard, and strong.

In a number of boreholes, hydrothermally altered diorite was encountered. The degree of alteration encountered is highly variable, but in the areas of severe alteration, the rock can be weak to extremely weak and contain zones of rock completely altered to clay minerals over several inches. These altered zones are rarely seen in outcrop because the bedrock has been eroded into gullies where alteration is moderate to severe. Where encountered in rock cores, the (apparent) width of the altered zones in boreholes range up to 20 ft. but are typically less than 5 ft., and altered rock is often associated with close fracturing, fracture zones, or shear zones. The transition between fresh and altered rock is gradational over a few inches to few feet.

Representative NQ and HQ rock core samples were tested to determine the engineering properties of the diorite, andesite, and altered diorite. Since the properties of diorite, quartz diorite, and granodiorite were found to be similar, they were all recorded under the heading for

diorite. It should be noted that in general samples from the upper 250 to 300 ft. were selected as these are considered more representative of conditions affecting foundation design. However, where the number of samples was limited (e.g. sonic velocity), results from all depths were considered.

Due to the quality and extent of moderately to highly altered rock, which occurs in some locations over intervals of a few feet of core, high quality samples could not be collected or tested reliably and are therefore not well represented in the testing and results below. Such samples are expected to be of lower density, strength, and deformability.

The rock test results reported in the following sections include data from studies performed in the 1980s and the current studies, 2011 to 2014 and the level of investigations and testing is considered adequate for feasibility level design purposes. Additional geotechnical work including drilling, down-hole testing, geophysics, exploratory adits, laboratory and in situ testing, will be required as part of the detailed design.

10.3.1.3. Engineering Properties of Rock Material

10.3.1.3.1. Unit Weight

Tests for unit weights were performed in conjunction with unconfined compression and tensile strength tests. The results from testing are summarized in Table 10.3-1:

Table 10.3-1. Summary of Unit Weight Tests

Rock Type	Number of Tests	Minimum (pcf)	Maximum (pcf)	Mean ± Standard Deviation (pcf)
Diorite	22	164.8	172.0	168.0 ± 1.6
Andesite	10	162.6	166.9	164.8 ± 1.7
Altered Diorite	1	165.6	165.6	165.6

The results are consistent for these rock types, and the unit weight of altered diorite is slightly less than that of fresh diorite, which is expected since some of the minerals have been altered to clay.

10.3.1.3.2. Unconfined Compressive Strength

The results from unconfined compressive strength (UCS) tests are summarized in Table 10.3-2.

Table 10.3-2. Summary of Unconfined Compression Strength Tests

Rock Type	Number of Tests	Minimum (psi)	Maximum (psi)	Mean ± Standard Deviation (psi)
Diorite	33	7,610	31,130	21,590 ± 6,200
Andesite	10	6,100	26,210	17,000 ± 6,100
Altered Diorite	9	1,580	15,500	7,600 ± 4,100

The diorite and andesite are both classified as strong to very strong. Excluding the altered diorite, more than 90 percent of andesite and diorite samples have UCS greater than 12,000 psi.

Although not represented, zones where the rock is highly weathered and altered may be classified as very weak to weak over short (few feet) intervals.

10.3.1.3.3. Point Load Index Testing

Point load index testing was performed at regular intervals on core from two boreholes drilled in 1984 and at select locations during other campaigns. The ease of this test enables a large number of samples to be tested covering a wider range of sample quality than UCS testing. The point load index (PLI) strength tests were used to estimate the compressive strength of the rock by applying a UCS:PLI ratio equal to 24.9 (HQ-size core) and 21.9 (NQ-size core) for samples from 1984. A ratio of 19 was used for samples tested in 2012 (HQ – size core) based on an evaluation of the testing data. The results from point load index tests are summarized in Table 10.3-3.

Table 10.3-3. Summary of Point Load Index Strengths

Rock Type	Number of Tests	Minimum (psi)	Maximum (psi)	Mean ± Standard Deviation (psi)
Diorite	77	4,760	31,330	18,460 ± 5,830
Andesite	6	--	--	19,620 ± 3,150
Altered Diorite	13	3,710	26,620	11,590 ± 6,600

In addition to the results presented above, more than 300 point load tests were performed during the 1980-1981 study, but detailed test data are not available for analysis. In general, the 1980-1981 tests had correlated compressive strengths ranging from less than 10,000 psi to more than 40,000 psi. Although the strengths from testing in 1980-1981 are higher than those from 1984 and 2011 to 2012, both data sets indicate the rock is strong to very strong, but less so in areas of localized alteration.

In general, the compressive strengths estimated from point load index testing are in the same range as unconfined compressive strength tests and indicate that fresh, sound andesite and diorite bedrock is strong to very strong, and zones of slightly altered rock can be moderately strong to strong.

10.3.1.3.4. Tensile Strength

Brazilian tensile strength (T_{BR}) results summarized in Table 10.3-4 indicate a high tensile strength. The ratio of the mean tensile strength to the UCS (T_{BR} / UCS) ranges from about 8 percent and 10 percent for the three rock types. In general, the tensile strength is between 5 and 10 percent of the UCS; thus, the test results are consistent with expectations.

Table 10.3-4. Summary of Brazilian Tensile Strength Tests

Rock Type	Number of Tests	Minimum (psi)	Maximum (psi)	Mean ± Standard Deviation (psi)	T_{BR} / UCS (%)
Diorite	9	1,820	2,360	2,160 ± 170	10%
Andesite	3	1,620	1,720	1,680 ± 60	9.9%
Altered Diorite	2	470	810	640 ± 240	8.4%

10.3.1.3.5. Intact Rock Deformation Properties

Elastic properties were measured on intact samples under unconfined compression using electronic strain gages bonded to the sample in the horizontal and vertical directions. Stress, axial, diametric, and volumetric strain were measured and plotted against axial stress from which the intact modulus and Poisson's ratio were calculated at 50 percent failure load. The tangent modulus was calculated for the tests performed in the 1980s, and the secant modulus was calculated for the 2012 and 2014 tests. The results from all testing are combined in Table 10.3-5.

Table 10.3-5. Summary of Intact Rock Modulus Parameters

Rock Type	Number of Tests	Minimum (x 10^6 psi)	Maximum (x 10^6 psi)	Mean ± Standard Deviation (x 10^6 psi)	Poisson's Ratio
Diorite	21	6.7	12.8	10.0 ± 1.4	0.23 + 0.04
Andesite	4	5.6	10.5	8.6 ± 2.2	0.25 + 0.01
Altered Diorite	7	2.0	10.9	6.7 ± 3.3	0.21 + 0.06

10.3.1.3.6. Dynamic Elastic Properties

Compressional (V_p) and shear (V_s) wave velocities were measured on five samples of intact diorite. The results of the tests are summarized in Table 10.3-6.

Table 10.3-6. Summary of Compressional and Shear Wave Velocities and Dynamic Properties

Rock Type	Number of Tests	V_p (ft./s)	V_s (m/s)	Dynamic Modulus (x10^6 psi)	Dynamic Poisson's Ratio
Diorite	5	17,050 ± 820	9,670 ± 320	9.0 ± 1.0	0.28 ± 0.03
Andesite	0	--	--	--	--
Altered Diorite	0	--	--	--	--

Note: Mean values and standard deviations are reported.

The sonic velocity testing of intact samples indicates that the static and dynamic deformation properties for intact diorite are similar.

10.3.1.4. Rock Mass Characterization and Properties

The rock mass characterization and material properties used in the analyses of the proposed design configuration draws heavily on the studies performed in the 1980s but is supplemented by information collected in 2012 and 2014.

10.3.1.4.1. Rock Quality Designation

Rock Quality Designation (RQD) was determined for all rock cores extracted during the 1980s and the current investigations (2011 to 2014). Some of the boreholes implemented during the USACE studies were rotary drilled without core recovery so RQDs values are not available from them and the data from the 2014 investigations has not yet been verified, but available results since 2011 are consistent with results from previous investigations.

Rock quality encountered in the drilling was generally good to excellent with RQD values averaging between 75 and 90 percent. In general, rock quality improves with depth, with the upper 50 to 80 ft. of rock being weathered and more fractured and RQD averaging between 40 and 70 percent. Below this weathered zone, rock quality is good to excellent (85 percent to 100 percent) with localized zones of fractured, sheared, or altered rock, which are generally one to five feet thick, but can occasionally be up to 30 ft. thick. RQD correlates well with the hydraulic conductivity (sometimes referred to as "rock mass permeability") testing data (see Section 0), which is normally a function of rock quality.

In general, weathering appears to be primarily physical in nature, with weathered rock being restricted to the upper 40 ft. at the dam site. The weathering is light to moderate in joints, with penetration generally less than an inch from the joint wall. Rock within shear and fracture zones is more weathered, and many of these zones exhibit chemical weathering and hydrothermal alteration.

10.3.1.4.2. Rock Mass Characterization

Geological field data and empirical methods were used to assess rock mass properties for the feasibility design. This consisted of the following:

- Evaluate foundation geologic conditions by performing geologic mapping, core drilling, and in situ testing.
- Identify different engineering geologic units having generally uniform properties with respect to rock strength, degree of fracturing, and weathering.
- Characterize and develop rock mass classification for each engineering geologic unit and assign material properties.

Using data from the studies through 2012 and 2014 geologic mapping in and adjacent to the dam site footprint area, rock mass classifications were carried out in order to identify and differentiate distinct engineering units using the 1989 Bieniawski rock mechanics rating system (RMR_{89}). RMR_{89} is computed using the following six parameters:

- Uniaxial compressive strength;
- RQD;
- Spacing of discontinuities;
- Condition of discontinuities;
- Groundwater conditions; and
- Adjustment for orientation of discontinuities.

The borehole log for each hole was reviewed, and the character of the rock in each core run was evaluated to estimate the RMR_{89} for each run. The Geological Strength Index (GSI; Hoek and Marinos 2000) was then estimated using Bieniawski's (1989) joint condition (Jcond) and an evaluation of the Rock Quality Designation (RQD) using the relationship proposed by Hoek et al. (2013) as described below:

$$GSI = 1.5Jcond_{89}+RQD/2$$

In addition to empirical relationship between GSI and RMR from the drilling investigation, GSI is typically assessed during mapping. At the dam site, the outcrops generally have a blocky to massive appearance with two or three prominent joints sets plus minor sets. Typically JS1 and JS2 were encountered and one of the minor sets or random sets formed the other prominent set. Block sizes ranged from small (2.5 inches to 8 inches per side) to large (2 ft. to 6 ft. per side), but were typically medium sized (8 inches to 2 ft. per side). Medium-sized blocks typically form the boulder talus observed on steep slopes, below rock outcrops, and in gullies throughout the dam site.

The jointing creates a blocky to very blocky rock mass structure with good to fair quality joint surfaces when evaluated with respect to GSI. The tight to open joints give the rock mass a tight to slightly loosened structure with a moderate to high degree of block interlocking. Based on these characterizations, the GSI for all measured outcrops ranged between 40 and 75. However, the GSI was typically between 55 and 65, and overall averaged about 60 in outcrop.

Overall, the dam site is underlain by relatively lightly to moderately fractured diorite intersected by discrete geologic features and linear zones of moderately to highly fractured rock, narrow shear zones and zones of hydrothermal alteration. Considering the type of rock, distribution, and quality that has been encountered, the bedrock is divided into three engineering units, which are expected to have distinctly different engineering properties. It is important to distinguish between different materials because heterogeneous foundation materials can introduce stress concentrations into the foundation and structure, which need to be accounted during design. The following describes each of the units and Table 10.3-7 summarizes the GSI for each of the units.

1. **Engineering Unit 1** – Sound Bedrock – Fresh, hard, strong to very strong, and lightly to moderately fractured and jointed diorite. The rock mass is characterized as blocky to very blocky. Joints are typically rough to smooth, slightly weathered to fresh, and tight. In the upper 20 ft. of the foundation, where the bedrock may be slightly more weathered, the GSI generally ranges from about 40 to 70, and averages about 55. Below 20 ft. depth, the GSI for Engineering Unit 1 generally ranges from about 50 to 80 and averages about 65.

2. **Engineering Unit 2** – Moderately to Highly Fractured Bedrock – Fresh to slightly weathered, hard, strong, and moderately to highly fractured diorite (refer to Section 10.3.1.5.3). The rock mass is characterized as very block to sheared/disturbed/seamy with joints that are rough to smooth, slightly to moderately weathered to fresh, and tight. The character of the rock within the upper 20 ft. of the foundation is similar to that at depth. The GSI for Engineering Unit 2 generally ranges from about 30 to 50, and averages about 40.

3. **Engineering Unit 3** – Sheared and Altered Bedrock – Bedrock within discrete 5 to 30 ft. wide zones (apparent width) consisting of highly fractured rock with shear zones up to 2 ft. wide and zones of alteration (see Section 10.3.1.5.4 and Section 10.3.1.5.5). The rock mass is moderately to highly weathered/altered, weak to strong, and characterized as sheared/disturbed/seamy. Joints are smooth to slickensided, slightly to moderately weathered and altered, tight to partly open. The GSI for this engineering unit generally ranges from about 15 to 40, and averages about 25.

Table 10.3-7. Ranges and Average GSI for Engineering Units

Material	Depth Below Ground Surface (feet)	GSI		
		Min	Maximum	Recommended
Engineering Unit 1	0 to 20 [1]	40	70	55
	Greater than 20	60	80	65
Engineering Unit 2 [2]	All	30	50	40
Engineering Unit 3 [2]	All	15	30	25

Note:
1. Recommended value based on geologic mapping of outcrops in 2014 and degree of weathering observed in rock cores in the upper 20 ft.
2. The minimum, maximum, and recommended GSI values for Engineering Unit 2 and Unit 3 are slightly higher at depths greater than 20 ft., but the difference is considered minor (less than five); thus, these units are described as having a single set of values.

10.3.1.4.3. Rock Mass Strength and Deformability

Rock mass strength and deformation properties are developed using empirical relationships that combined rock mass characterization with the results from laboratory testing.

Strength and deformation parameters for each of the engineering units are computed using RocLab software (RocScience, Inc.) and empirically based formulations and the anticipated foundation loading conditions. The rock mass strength is based on the generalized non-linear Hoek-Brown criterion (Hoek et al. 2002), from which equivalent Mohr-Coulomb strength parameters for the rock mass in terms of cohesion and friction angle are calculated. The rock mass deformation modulus is calculated using the formulation by Hoek and Diederichs (2006).

For each of the three engineering units at the dam site foundation the parameters listed in Table 10.3-8 are recommended to be used to estimate the rock mass strength and deformation parameters – based on sample characteristics from all the site investigations to date. Recommended rock mass strength and deformation parameters are listed in Table 10.3-9.

Table 10.3-8. Recommended Intact Rock Properties

Material	Depth Interval (feet)	Unit Weight (pcf)	UCS (psi)	Hoek-Brown constant (m_i)	Intact Rock Modulus (1×10^6 psi)	Poisson's Ratio
Engineering Unit 1	0 to 20	168	21,590	25	10	0.23
	Greater than 20	168	21,590	25	10	0.23
Engineering Unit 2	All	168	15,300	20	8.6	0.23
Engineering Unit 3	All	165	7,600	20	2.0	0.21

Table 10.3-9. Recommended Rock Mass Strength and Deformation Parameters

Material	Depth Interval (feet)	GSI	Cohesion (psi)	Friction Angle	Rock Mass Deformation Modulus ($\times 10^6$ psi)
Engineering Unit 1	0 to 20	55	340	53°	4.1
	Greater than 20	65	500	57°	6.3
Engineering Unit 2	All	40	240	48°	1.4
Engineering Unit 3	All	25	130	38°	0.12

Note:
1. Based on confining pressure of about 720 psi based on unit weight of rock and assuming a dam height of about 700 feet.
2. The Disturbance Factor, D varies from 0 to 1. The effects of the disturbance due to blasting are expected to be shallow with some minor stress relief occurring within 10 feet of the ground surface. This depth is relatively minor compared to the depth influence of the dam on the foundation or high slopes. Therefore, a D = 0 is recommended for calculating the rock mass strength and deformation modulus.

10.3.1.4.4. Rock Mass Permeability

Water pressure tests were performed in exploratory boreholes during all investigations phases. Rock mass permeability is controlled by the jointing, fracturing, weathering, and if present, ice within joints.

The rock mass permeability is based on the secondary permeability formed by joints since the intact rock is considered impermeable. The rock mass permeability of the bedrock generally ranges between 1×10^{-6} cm/sec to 2×10^{-4} cm/sec. As would be expected in fractured rock near the surface or in localized areas of fracture zones, rock mass permeability can be as much as 4×10^{-4} cm/sec to 7×10^{-4} cm/sec. In a few instances, water takes exceeded the pump capacity and the desired injection pressures could not be achieved. In such cases the rock mass permeability may be on the order of 1×10^{-3} cm/s or greater. Overall, the rock mass permeability tends to decrease with depth as joint frequency is reduced and joints have narrower aperture.

Artesian conditions were encountered in borehole BH-12 along the upper left abutment at a depth of about 325 ft., which corresponded with the altered and sheared contact between diorite

and andesite. Because of the structural relationship of these two rock units, greater hydraulic conductivity is likely to be expected at the contact.

Frozen ground conditions are believed to be present locally within the rock mass and likely has an effect on rock mass permeability. Ice-filled joints restrict flow through the rock mass, thereby giving misleading values of low rock mass permeability values. Therefore, thawing of localized areas of the foundation and/or post-construction foundation treatment will be required to obtain more reliable estimates and for foundation treatments, such as grouting. Refer to Section 0 for additional discussion of approaches to grouting of frozen ground.

10.3.1.5. Rock Mass Structure

From geologic mapping and core drilling at the dam site, three major classes of discontinuities have been identified in the rock mass. As described in Section 6.3, the most common and pervasive class through the site are joints. Fracture zones, which are less common than joints, consist primarily of closely spaced or concentrated areas of jointed rock. Least common are shear zones, which exhibit some evidence of relative displacement such as the presence of gouge, breccia, and/or slickensides. The most prominent of the fracture and shear zones have been termed "Geologic Features" beginning with reports by Acres (1982a). Joints, fracture, shear, and alteration zones exhibit a wide range of characteristics. More detailed characteristics of each type of discontinuity are described in the following subsections.

10.3.1.5.1. Joints

Mapping performed during the 1980s and site investigations performed between 2012 and 2014 have identified four joint sets at the site. The orientations of these four sets, which includes two primary and two secondary sets are summarized in Table 10.3-10. Some minor subsets and other random joints are also encountered in outcrop and boreholes. The joint sets are common to all rock types at the dam site. For detailed discussion of joints refer to Section 6.3 of this report.

Table 10.3-10. Summary of Joint Set Orientations

Joint Set	Strike (Azimuth)	Strike Average (Azimuth)	Dip
JS1	270° to 330°	300°	80° SW to 70° NE
JS2	025° to 060°	040°	80° SE to 70° NW
JS3	340° to 020°	350°	70° E to 80° W
JS4	Variable	Variable	Less than 35°

Note: Strikes are reported in the upper hemisphere regardless of the dip direction.

Orientations were also evaluated with respect to four quadrants (e.g., NE, SE) around the dam axis and for the north and south banks to evaluate potential spatial variations. Figure 10.3-1 shows stereonets with contoured poles representing the orientation of discontinuities from 2014 surface geologic mapping, in which northwest-southeast trending set, northeast-southwest set, and shallow dipping sets were identified. Minor variations were observed when evaluating the data for the north and south banks. However, the northwest quadrant exhibited a greater abundance of north-south trending discontinuities (JS3) than in other quadrants, which was similarly reported by Acres (1982b). These joints sets and some minor subsets were used to evaluate three dimensional wedges in each abutment which were subjected to limit equilibrium sliding stability analyses described in Section 10.3.3.2.

The discontinuity data from downhole logging performed in 2012 and 2014 are shown in Figure 10.3-2. The downhole survey encountered discontinuities that are mostly shallow dipping; the northwest-southeast trending set is less prominent; and the northeast-southwest trending joint set is nearly absent. This inconsistency, when compared to the surface mapping data set, is attributable to the bias introduced by the orientation of the boreholes drilled and the linear nature of downhole logging, as well as the selected borehole orientation with respect to JS1 and JS2.

The 2012 and 2014 boreholes in the dam site footprint area are steeply inclined and trend to the northeast-southwest or north-south directions. Holes of this orientation and inclination will encounter shallow dipping features with greater frequency than steeply inclined joints or those that tend to parallel the borehole. Bias correction was applied during the stereographic analysis, but the bias cannot be eliminated. Furthermore, the data sets cannot be combined due to number of discontinuities within each data set. It is easy for the analyst to identify discontinuities on the borehole image such that a large number of discontinuities can be selected – in this case 3312 discontinuities – including many closely spaced joints of the same set. During geologic mapping of rock outcrops, the focus was on identifying the major and minor sets (plus prominent random joints) within each outcrop but limiting the number of measurements to only those sets present, and this approach yielded about 558 measurements. Therefore, the data sets from surface mapping and the downhole logging were evaluated separately and then compared to verify that the relevant joint sets have been identified.

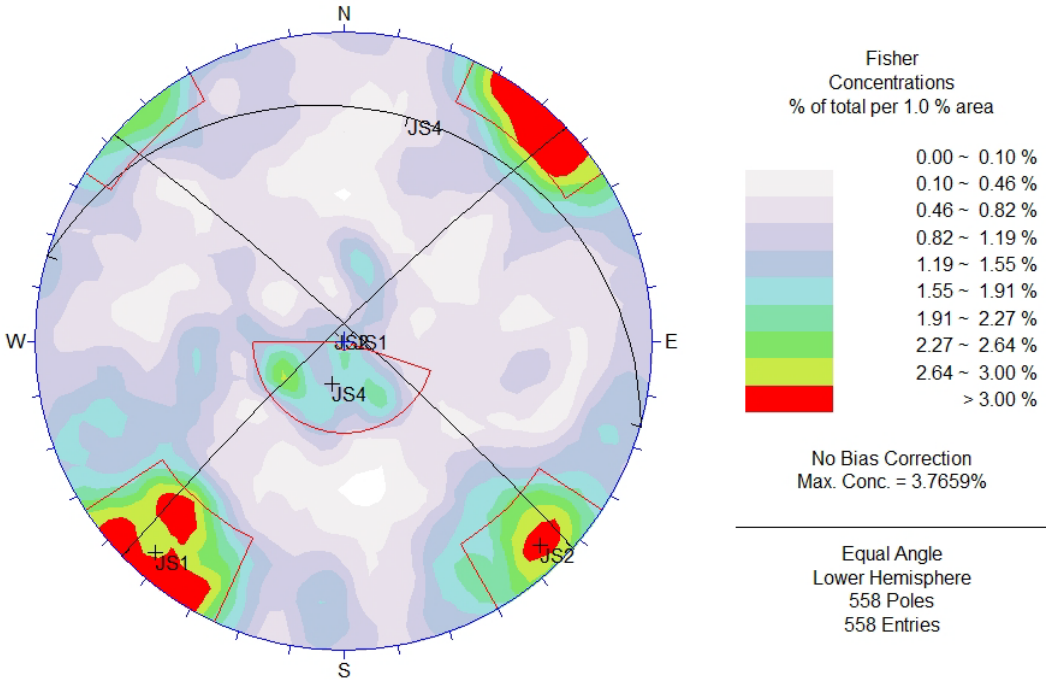

Figure 10.3-1. Lower Hemisphere, Equal Angle Stereograph Plots of Principal Joint Sets from Surface Mapping

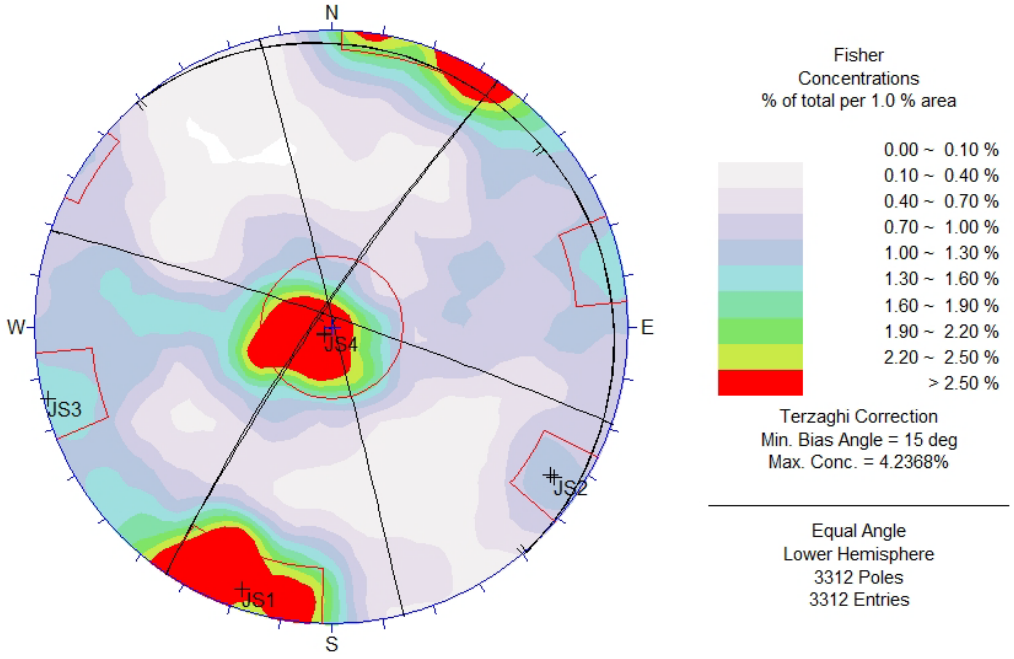

Figure 10.3-2. Lower Hemisphere, Equal Angle Stereograph Plots of Principal Joint Sets from Downhole Logging

After the joint sets were identified, the individual discontinuities recorded during mapping were assigned to respective joint sets and grouped so that the characteristics of each joint set could be evaluated. Joints were described in accordance with International Society for Rock Mechanics (ISRM) guidelines (1978) such that joint engineering properties could be developed. In addition, the joint spacing was evaluated to estimate the approximate block size formed by the intersecting joints. The characteristics of the joint sets are summarized in Table 10.3-11 and are described below.

Table 10.3-11. Summary of Joint Set Characteristics from Geologic Mapping

Joint Set	Joint Spacing	Typical Persistence (ft.)	Shape and Surface Roughness	Aperture and Filling	Amplitude Roughness (JRC)
JS1	16" (4" to 4')	10 to 60	Planar, rough to locally smooth	Tight to open, clean with local iron staining and carbonate infill	9 (4 to 16)
JS2	15" (2" to 3')	3 to 30	Planar, rough to locally smooth	Very tight to open, clean with local iron staining	9 (2 to 16)
JS3	10" (4" to 12")	Less than 3 to 30	Planar to locally irregular, rough to smooth	Tight to open, iron staining or carbonate infill	9 (6 to 14)
JS4	16" (1" to 5')	3 to 30	Planar, rough to locally smooth	Tight to very wide, clean with local iron staining and carbonate infill	8 (2 to 16)

Note: Parenthetic value is the range.

Joint Set 1 (JS1) and JS2 are major sets that occur throughout the site area, although the orientation of JS2 varies slightly around the site. JS3 is generally more prominent downstream of the dam site, particularly in the northwest quadrant. JS4 is also widely distributed throughout the site but has shallow dips in all directions. Other minor subsets and random joints are also present, but the focus is on the four principal joint sets.

Joint surfaces for JS1 are typically planar, smooth to rough, and exhibit minor iron staining and carbonate deposits. The joint spacing typically ranges from 4 inches and 4 ft. and average about 16 inches. The joints typically have medium to high persistence, 10 to 60 ft., but is often dependent on the height of the outcrop, which can be more than 60 ft. in some places. These joints are generally tight, but open joints of this set are found in outcrop. The larger amplitude roughness (JRC) ranges from 4 to 16 and averages about 9. Fracture zones, shear zones, and alteration zones are most frequently oriented parallel to JS1.

Downstream of the dam JS2 joints typically dip to the northwest. The joints are generally planar, rough to smooth, and are clean or can have iron staining and carbonate deposits. Joint spacing typically ranges from 2 inches to 3 ft. and averages approximately 15 inches. JS2 joints have moderate persistence, typically between 10 and 30 ft. Joints are very tight to open, and in outcrop were generally open. The larger amplitude roughness (JRC) ranged from 2 to 16 and

averages about 9. No fracture, shear, or alteration zones that have been identified are associated with JS2.

JS3 is considered a minor set, although it is locally prominent downstream of the dam, particularly in the northern bank. The joint spacing typically ranges from 4 inches to 12 inches, and averages about 10 inches. Joints are generally planar to irregular, and rough to smooth. Joints are tight to open with minor carbonate and iron staining. The larger amplitude roughness (JRC) ranged from 6 to 14 and averages about 9. Fracture and shear zones parallel to JS3 were mapped at a number of locations, but these tend to be less critical features with respect to the dam footprint than structures of JS1.

Shallow dipping joints comprise JS4 and are found throughout the dam site and dip less than 30 in nearly all directions, although there is slightly greater percentage dipping to the northeast. Joints in this set are planar, smooth to rough, tight to very wide open and in some locations show carbonate deposits and iron staining. The joint spacing ranges from about 1 inch to 5 ft. and averages about 16 inches. Joints from this set typically have low to moderate persistence, 3 to 30 ft. The larger amplitude roughness (JRC) ranged from 2 to 16 and averages about 8. No significant mineralization, shearing, fracture, or alteration zones appear to be associated with this joint set.

It has been postulated that gently inclined and flat lying joints (less than 30° dip) may be the result of stress relief after glacial unloading and/or erosion of the river valley. The data from the 2012 and 2014 downhole televiewer logs were evaluated to assess the ratio of shallow joints per linear foot of vertical depth below ground surface to total joints per linear foot of survey for depth in increments of 50 ft. (i.e. depth below ground surface 0 to 50 ft., 50 to 100 ft., etc.). If related to stress relief, one would expect the ratio of shallow dipping joints to decrease with depth below ground surface (adjustments were made to account for hole inclination and depth of discontinuity).

The analysis indicates that joints dipping less than 30° account for about 40 percent of joints down to depths of 600 ft. below ground surface (see Figure 10.3-3). The percentages of joints dipping less than 15° were also plotted against depth, and again the percentage of shallow dipping joints remains fairly uniform with depth, generally ranging from 12 to 20 percent. The relatively consistent percentage of shallow dipping joints to depths as much as 600 ft. below ground surface suggests the effect of stress relief extends to depths below 600 ft. or that shallow dipping joints are not related to stress relief or rebound but are instead formed by other geologic processes.

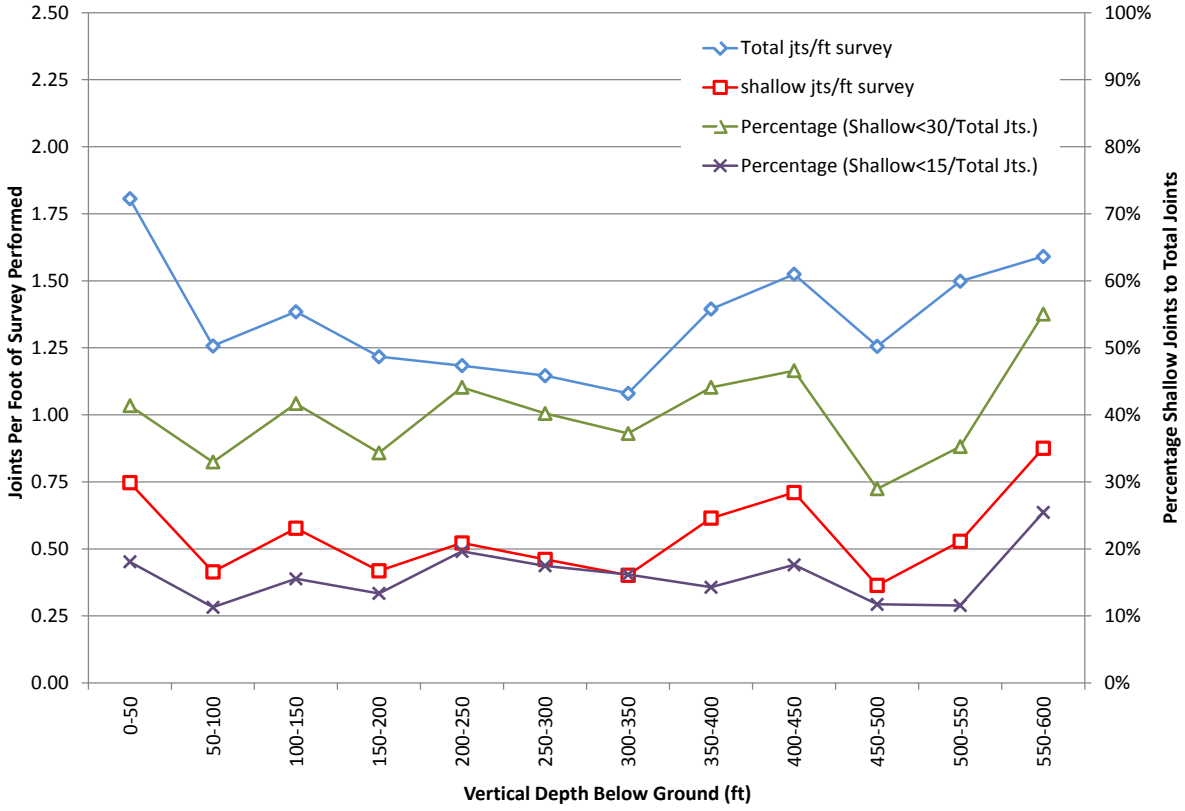

Figure 10.3-3. Evaluation of Shallow Joints from Downhole Logs

10.3.1.5.2. Fracture, Shear, and Alteration Zones

As described in Section 6.3 fracture, shear, and alteration zones and combinations thereof have been mapped at the site, although the majority of mapped features are less than 10 ft. wide and discontinuous. Where zones more than 10 ft. wide were identified, both boundaries have been delineated on the geologic maps and sections. In general, these features are aligned with JS1 and some with JS3. The characteristics of fracture, shear, and alteration zones are detailed in Section 6.3 and summarized below. The primary focus here is on those geologic features that are expected to be evident in the footprint of the dam foundation.

10.3.1.5.3. Fracture Zones

Fracture zones consist of very closely to closely spaced (less than 1 inch to 8 inches) typically over widths less than 10 ft. of jointed rock where no apparent relative movement has occurred. Fracture zones are common to all rock types and are generally encountered in boreholes and less frequently observed in outcrop. In general, fracture zones consist of rock that is more fractured,

very close to closely fractured zones comprised of poorer quality rock mass. In addition, the RQD and GSI within fracture zones may be quite low and such zones are generally associated with increased hydraulic conductivity.

10.3.1.5.4. Shear Zones

A shear zone is defined as a zone of rock along which there has been measurable or discernable displacement characterized by breccia, gouge, and/or slickensides indicating relative movement and cataclasis. Such shear zones are common to all rock types at the site and are most frequently associated with fracture zones and moderately to severely altered rock. These shear zones typically trend northwest-southeast (paralleling JS1), and particularly trend this direction within the dam footprint. Infilling within shear zones typically consists of coarse to fine sand-size rock fragments weathered to tan-yellow, orange, brown and sometimes includes a narrow zone (few inches) of silt or clay gouge within the central portion. Both the breccia and gouge are soft to medium stiff, friable, and erodible. Thicknesses of these shear zones in the dam footprint based on the current geologic mapping are generally less than 1 to 2 ft. wide. In the broader dam site area, Acres (1982b) had reported that shear zones vary from less than 0.1 inch up to 10 ft. (apparent thickness). The reason for this discrepancy is unclear but it may be due to how a shear zone is defined.

10.3.1.5.5. Alteration Zones

Alteration zones are areas where hydrothermal solutions have caused the chemical breakdown of the feldspars and mafic minerals. The products of alteration are kaolinitic clay from feldspar and chlorite from mafic minerals. These zones are found in both the diorite and in the andesite porphyry but appear to be less common in the andesite porphyry.

Most of the information regarding alteration zones is from the boreholes since alteration zones are rarely seen in outcrop because they are relatively easily eroded. They are exposed on the surface on the north bank in one outcrop at river level near the dam axis. The degree of alteration is highly variable ranging from slight, where the feldspars show discoloration, to complete where the feldspars and mafics are completely altered to clay and chlorite. Widths of these zones most often range up to 20 ft. but are generally less than 5 ft. An exception is in the inclined borehole BH-12, on the south bank and downstream of the dam, which encountered very thick zones of alternation (slight or moderate) over a length of approximately 260 ft. with discrete shears and zones of shearing The orientation of the zones of alteration with respect to the borehole are not known, however if it assumed that each zone has a similar orientation and is near vertical the maximum apparent width may be on the order of 215 ft.

No increase in joint frequency is evident in association with these alteration zones. Thin (less than 2 inches wide) shear zones are associated with a number of the alteration zones. RQDs are generally low; however, core recovery is generally more than 90 percent within the alteration zones. The transition from fresh to altered rock is gradational, generally occurring over less than one foot.

Given the character of the altered zones with respect to the dimensions of the dam foundation, these features are not anticipated to be sources of major structural weaknesses in the otherwise sound bedrock foundation. However, foundation preparation will require local dental treatment to remove soft materials at the foundation level and replacement with dental concrete. If associated with fracture zones and shear zones, localized grouting may also be necessary to control seepage, prevent piping, and to improve strength and deformability of the foundation.

10.3.1.5.6. Geologic Feature GF4B

In general, fracture, shear and alteration zones will be encountered through the project area in all types of excavations. Analysis and review of the existing data on the dam site geology was made and site investigations were performed that included lineament analysis of the dam site using the newly acquired digital elevation data and abutment geologic mapping of and drilling across the largely northwest-trending structural features. The goal was to identify and characterize the geologic features that will intersect the dam foundation. Refer to Section 6.3 and Drawing 01-01GT006 for additional detailed descriptions of the geologic features.

GF4B consists of multiple discrete fracture zones, splays or branches, oriented in the northwest-southeast direction, that intersect a north-south trending fracture zone. The fracture zones, which may contain narrow shear zones typically less than 8 inches wide consisting of breccia and clay gouge, are correlated to several prominent gullies immediately upstream of the dam right abutment between the shoreline to about El. 1850 ft. that are as much as 40 to 50 ft. wide. Although the gullies appear wide at the surface, information from mapping and drilling suggest that the fracture zones are much narrower and the geomorphic expressions are a manifestation of erosion processes.

Based on a review of rock core from DH12-3, bedrock in this area of the foundation alternates between zones of very closely to closely fractured rock in the upper 300 ft. It is postulated that the more highly fractured zones correlate with gullies manifested at the ground surface and less fractured core correlates with more competent outcrops. Some of the fracture zones contain some minor shear zones (i.e. less than 1-ft. wide). Below 300 ft., fracture zones in this borehole are generally less than about 5 to 7 ft. wide and occur less frequently in what is generally moderately close fractured rock. Discontinuities within fracture zones are typically tight, surfaces are rough to smooth with iron oxide staining, white carbonate deposits, or chlorite, and

some surfaces contain clay infilling with slickensides. The fracture zones appear to contain some minor shear zones, which are typically less than a few feet wide.

Although considered relatively minor features with respect to the dimensions of the dam, due to the location and trend of these fracture zones and similar fracture zones and minor shear zones, the project structures were moved slightly downstream, to reduce the potential impacts these or similar structural features could have on the dam foundation. However, where encountered in the foundation, highly fractured rock and shear zones might need to require mitigation by means of dental excavation and backfilling, consolidation grouting to improve strength and deformability, and stitch grouting to reduce seepage.

Projecting GF4B to the north and northwest would intersect the alignments of the diversion tunnel and access tunnel excavations. Localized sections of highly fractured rock are anticipated to be encountered in the tunnels which may require increased rock support to achieve suitably stable openings. In addition, the more highly fractured rock may be a source of groundwater infiltration and may require water control grouting to reduce groundwater inflow and to facilitate placement of concrete and shotcrete linings.

10.3.1.5.7. Geologic Feature GF5

GF5 consists of multiple fracture zones with some minor shear zones that cross the dam footprint on the lower right abutment. The geologic structures comprising GF5 are similar to those of GF4B and trend northwest-southeast (310° to 320°). The structures are steeply dipping, and are anticipated to be encountered in the dam and spillway foundations and diversion tunnel excavations.

Although there is no topographic expression of this fracture and shear zones at the surface on the north abutment above about El. 1700 ft., GF5 was correlated with several shear and fracture zones intersected in borehole DH-9 (Acres 1982b). However, the orientation of the fracture zone is not known and therefore cannot be positively correlated with GF5. Regardless, the joints and fractures in DH-9 are generally iron stained and carbonate-coated, and faint slickensides occur on some surfaces. The RQDs in DH-9 are low, with an average of 57 percent. Hydraulic conductivities are generally between 10^{-1} cm/sec and 10^{-3} cm/sec, and decrease with depth.

In 2012 and 2014, inclined boreholes DH12-4 and DH14-11 were drilled across this gully on the right abutment approximately normal to GF5. Based on the site investigations and a review of the previous studies, it appears that GF5 consists of several fracture zones typically ranging from about 5 to 10 ft. in width and some contain shear zones up 20 inches wide. While data relative to GF5 lacks compelling demonstration for the presence of a significant, through-going fault or shear zone, it is depicted as the widest and most continuous feature in the dam foundation.

It is expected that GF5 may require special treatment in the dam foundation, including measures such as over-excavation or dental excavation and replacement with concrete. In addition, consolidation and stitch grouting area may be required to improve foundation characteristics.

GF5 is also expected to intersect the proposed diversion tunnel and access tunnel and may require additional rock support to achieve suitable stable openings. In addition, it could be a source of groundwater infiltration, which may necessitate grouting and drainage to control seepage during construction and installation of tunnel linings.

10.3.1.5.8. Strength of Discontinuities

Direct shear tests have been performed on natural, saw-cut, and polished surfaces to estimate the peak and residual (or basic) shear strength. Direct shear tests were conducted on saw-cut surfaces; natural calcite coated surface inferred to be an in situ healed joint; a natural, iron oxide-stained joint surface; polished rock surfaces; polished rock surface against mortar; and some joints from altered rock and some with calcite or other fillings. The results of the direct shear tests are provided in the Geotechnical Data Report, included in Appendix B1.

The natural joints show relatively high peak and residual friction angles. The peak friction angles of natural joints ranged from about 36° to 48°, neglecting cohesion. Analyses of vertical and horizontal displacements in samples from BH-8 indicate an approximately 10° incline, which appears to reflect the asperity angle of the natural joint.

Polished rock, as expected, resulted in the lowest basic friction angle of 18°. This angle is not considered representative of joints since it does not include effects of asperities as found in situ. Typically the basic friction angle of the rock is estimated for saw cut joints, which for these tests ranged from 21° to 35° degrees. Literature indicates the basic friction angle for medium grained granitic-type rocks are typically in the range of 29° to 35°. This suggests that the tests that have lower strengths (DH12-8, DS1) may be anomalous or may be at least partly due to sample alteration (DH12-8, DS6) or the infillings.

The bedrock is intersected by several types of discontinuities such as joints, formation contacts, and shear zones or alteration zones. The shear strength parameters of discontinuities are based on the Barton-Bandis non-linear strength criterion. The friction angle and apparent cohesion used in stability analyses are the “instantaneous” values taken as the tangent to the Barton-Bandis strength envelope for the applicable normal load associated with the particular loading condition being analyzed. The Barton-Bandis equation is given below:

$$\tau = \sigma_n \tan\left(\phi_r + JRC \log_{10}\left(\frac{JCS}{\sigma_n}\right)\right)$$

where:

τ: shear strength along the joint
φ_r: residual friction angle
JRC: joint roughness coefficient
JCS: joint wall compressive strength

For fresh, clean discontinuities (tight, no infilling material) in diorite, based on experience, the following values are recommended for use in feasibility level analysis:

Residual Friction Angle, φ_r ..... 30°
Joint Roughness Coefficient, JRC 8–10
Joint Wall Compressive Strength, JCS ..... 21,590 psi

For joints and shear zones or alteration zones with clay infilling and no rock-wall contact, the strength of the discontinuity will be governed by the infilling material and will be lower.

10.3.1.6. In Situ Stresses

No direct measurements of in situ rock stresses have been undertaken as part of the previous or present feasibility-level site investigation and testing programs. Although the magnitudes of in situ stresses are not known, the approximate orientations of the principal in situ stresses can be assessed based on observations and evaluation of the contemporary stress regime, as defined by current plate tectonic models, GPS observations, earthquake focal mechanisms and Quaternary faulting. A qualitative evaluation indicates that the project area is subject to northwest-southeast oriented sub-horizontal compressive stress associated with the subduction of the Pacific Plate in south-central Alaska. This is the maximum in situ principal stress direction, which is sub horizontal.

It is common practice to assume that the three in situ principal stresses are orthogonal to each other. Because the project area has been undergoing uplift due to glacial rebound, it can be surmised that the vertical in situ principal stress is the minimum in situ principal stress, leaving the intermediate in situ principal stress oriented in the horizontal direction and oriented in the northeast-southwest direction.

Due to the present tectonic stress regime, it is worth noting that ratio of vertical to horizontal could be much less than 1.0. This could present some conditions that need to be evaluated further in next phase of study – including evaluation of the potential for heave and excessive

loosening in foundation excavations, potential for grout-jacking in the vertical direction and other stress related effects.

10.3.2. Construction Materials Sources

For the RCC dam, the bulk construction materials required for the project will largely be aggregate obtained from quarry sources. Additionally, some impervious and rip rap materials will be needed for cofferdam construction.

The 1980s investigations and license application contemplated sequential development of Watana and Devils Canyon dam, which would have formed a reservoir extending to the tailrace of the Watana Dam. Under these conditions, it would have been feasible to contemplate the use of construction materials from gravel borrow areas downstream of the Susitna-Watana Project, as they would be inundated by the Devils Canyon reservoir.

In contemplating sources of construction materials for the proposed project, site investigations and laboratory testing focused on evaluation of previously defined rock aggregate material source, Quarry A, and identification and delineation of new aggregate material sources adjacent to the proposed dam. The change in the dam type from the rockfill embankment of the 1980s to a RCC dam dictated a change in the construction material requirements for the project. Field investigations were conducted in 2011 and 2012 of potential quarry sites that could produce suitable aggregate for the project. These were Quarry A, identified in the 1970s and immediately south of the dam site, and a new quarry, designated Quarry M, just upstream of the dam site on the left abutment. Bedrock at these two proposed sites differs; andesite to dacite porphyry is found at Quarry A and diorite is found at Quarry M. Rock core and bulk samples have been tested for alkali reactivity, freeze thaw, soundness and abrasion, to determine the suitability of the material as an aggregate in the production of both RCC and conventional concrete. Any altered seams of diorite materials found in the quarry will be selectively wasted within quarry management protocols. A spoil area has been designated upstream of the Quarry M site.

Based on preliminary testing, the results indicate these rock types are of overall good physical-mechanical quality. This was reflected by their generally low sulfate soundness losses (less than one percent), low LA abrasion losses (dacite around 14 percent, diorite about 20 percent), absorption of less than 1.2 percent, and reasonable density values. Alkali-Aggregate Reactivity (AAR) characteristics were evaluated on a very limited basis and indicate that these rock types are considered as “inconclusive” to “potentially reactive”, depending upon the criteria being used. With the use of an appropriate supplementary cementitious material (e.g., fly ash) in the concrete and RCC mixes (which is planned to limit the heat of hydration anyway) potential expansion would be mitigated.

At the feasibility stage, it was decided that some simple tests should be performed to verify that the aggregate available could have AAR potential mitigated with the mixes being considered.

Petrographic examinations – in accordance with ASTM C 295 and CSA A 23.2-15A – were performed on the samples. As recorded in the laboratory results from samples in DH 12-2 the extent to which the quartz diorite could be alkali reactive depends on the nature of the quartz. Although examination of thin sections indicated that the samples lacked undulatory extinction (an indicator of strained quartz), it is universally acknowledged that some strained quartz may cause a deleterious alkali-silica reaction if present as a constituent of concrete aggregate in sufficient amounts. Some papers have suggested that the criterion for reactive strained quartz is to be more than 20 percent strained quartz with an average undulatory extinction angle greater than 15 degrees. Length changes of mortar bars containing such strained quartz will be 0.025 and 0.040 percent (or more) at 6 and 12 months.

Crushed samples from "quarry" drill holes were used in accelerated mortar bar testing, based on ASTM C 1260 and C 1567. Because the testing was only performed to verify that the sorts of mixes considered were appropriate to mitigate reaction, they deviated from these standards in two respects: cementitious proportion and length of test.

The tests were performed using two types of fly ash – Class C and Class F – both provided from the Centralia thermal plant in Washington State, which would be the probable source if the project is constructed before 2028 when the plant is due to close.

The tests were performed on two mixes:

- A "mass concrete" mix using a fly ash replacement of 35 percent and a total cementitious content of 71.2 percent of the mass specified in ASTM C 1260 and C 1567.
- A RCC mix using a fly ash replacement of 45 percent and a total cementitious content of 17 percent of the mass specified in ASTM C 1260 and C 1567. This mix represents the lower envelope of fly ash content that might be considered for RCC, and it is expected that a greater proportion will in fact be specified.

For each mix, in each case, the length in the mortar bars was measured through 28 days, and then at 60, 90, 120 days.

For the "RCC" mix, the expansion in the mortar bar ranged from 0.026 percent to 0.034 percent at 28 days, and from 0.062 percent to 0.088 percent at 120 days. Although not performed strictly in accordance with the ASTM requirements, the results indicate that the amount of fly ash being considered for the RCC mix is sufficient to render the mix safe against AAR. For the feasibility

design– and the associated estimation of cost of cement and fly ash - this result is seen as acceptable.

With respect to the conventional concrete mix tested, the expansion in the mortar bar ranged from 0.069 percent to 0.083 percent at 28 days and from 0.24 percent to 0.29 percent at 120 days. This level of expansion is seen to warrant further testing during detailed design in order to determine the required specification for the adopted conventional concrete mix.

Freeze-thaw testing was also conducted and indicates both the dacite and diorite have low losses. Historical data from Acres (1982) reported slightly over two percent loss for 150 cycles on both rock types in Quarry A. A test on split NQ core of dacite from Quarry A in 2011 had a loss of 10 percent after 55 cycles. The later test may be attributable to pre-existing fractures and therefore does not appear to be representative of the loss for unfractured material. In addition, two freeze-thaw tests on rock from Quarry M were conducted on samples of diorite collected in talus below the outcrops. These tests resulted in 0.01 percent and 0.02 percent loss after 55 cycles. These loss percentages are very low. The results from the laboratory testing are summarized in the Geotechnical Data Report in Appendix B1.

Additional field investigation and testing is required to better define the quality of the material, potential wastage, available reserves, etc. This should include a small quarry development to perform test blasts. During final design, the material should be crushed for trial mixes of RCC and conventional concrete and for RCC trial placement. It is not envisaged that the quarry will be sufficiently developed in time to provide material for the cofferdams. Required materials could be obtained from the dam foundation excavations on the abutments.

The impervious core material for the cofferdams may be available from the removal and stripping of overburden (till) from the upper abutment slopes or could be obtained from a nearby borrow area, which consists of compact and dense glacial deposits, primarily consisting of till, outwash and lacustrine materials. Extensive field investigations and testing of the materials in Borrow Area D near Deadman Creek were conducted in the 1980s to characterize this impervious construction material source. The soil type for the till (e.g., Units M, G', and J') and much of the outwash (e.g., Units E/F and I) soils is a silt-sand (SM) which both contain cobbles and boulders (which are not part of the soil classification). Clayey sand (SC) and cohesive clayey and silty (CL, ML) soils are also common to the glacial lacustrine and till deposits.

Acres (1982a, 1982b) reported that the engineering properties of the materials include a moisture content of 11 to 12 percent and Atterberg Limits for the more granular material contains relatively low plasticity (PL 15 percent, PI 5 percent) constituents except for the tills and lacustrine deposits that are cohesive and have a high plasticity. Compaction testing of a composite material using a Standard Proctor Test indicate that the material has a maximum dry

density of about 128 to 134 pcf at an optimum moisture content of 8 percent to 10.4 percent while Modified Proctor Test results (material <¾ inch sieve) indicate a maximum dry density of 135 pcf at 7.5 percent moisture content. Consolidation compressive indices (Cc) of 0.061 and 0.091, respectively at 2 percent above optimum moisture content.

Processing and blending of outwash (Units E/F) with some other soils (Unit M) is required to achieve the proper gradation and moisture content while removing oversized material. Thus, construction material source includes suitable percentage of fine particles, e.g., silty-sands (SM), which can be compacted to achieve relatively low hydraulic conductivity. The underlying lacustrine deposit (Unit G), characterized by high moisture content (23 percent) of the sandy silts (Unit G) material, is considered unsuitable.

10.3.3. Design and Construction Considerations

10.3.3.1. Slope Stability

Cut slopes in soil for foundation excavation are anticipated to vary from 2H:1V to 1.5H:1V for permanent cuts in overburden with temporary cuts at 1H:1V to 1.5H:1V. The steepness of these cuts is necessitated by the topography of the site, and slope stabilization will be required in several areas to prevent sloughing.

Rock discontinuities (e.g., joints) will control the design of rock excavations and rock slopes and are used to evaluate foundation and abutment stability. The design of rock slopes and excavation openings consider the orientation of the joint sets with respect to the orientation of the excavation face, and the joint characteristics. Excavation cuts in rock will vary from 1H:2V to 1H:3V in weathered material but will generally be 1H:4V in fresh rock.

The slopes of rock cuts will be designed as stable excavations without rock reinforcement, but where this is not feasible, slopes will be reinforced with pattern or spot bolts and shotcrete (or concrete) with proper drainage as needed. Flattening of slopes, rock bolting, wire mesh and shotcrete will also be necessary in areas of more fractured rock, and in areas exhibiting unfavorable dip, to stabilize rock blocks and wedges. It is anticipated that rock reinforcement and slope protection of permanent rock slopes will include rock dowels and bolts, wire mesh and possibly reinforced shotcrete, and drainage will be necessary in local areas, such as highly weathered rock.

All rock cuts will have surface drainage ditches established at the top of the cut, on intermediate benches, and at the toe of the slope to collect and channel water away to reduce water infiltration and thereby improve slope stability. Drain holes will be drilled into the face of the rock cuts as necessary to relieve ground water pressure deeper within the rock mass and patterned weep holes

will be drilled to shallow depths to relieve pressure acting against shotcrete or concrete. Rock fencing and rock fall netting could also be provided on benches for protection of roads and other temporary and permanent facilities.

Cut slopes will be reexamined during detailed design considering the orientations and continuity of the local structure, slope orientation, and consider local fracture and shear zones as well.

10.3.3.2. Dam Abutment Stability Analysis

A key factor in the design of any dam is the abutment stability. For a concrete arch dam, in which the abutment is expected to carry thrust loads, abutment stability is of critical importance. Therefore, the stability of major (and minor) rock blocks and wedges subjected to the imposed dam loads, steady-state seepage, and during seismic events is paramount. The stereoplots from the 1980s studies were used in the analysis of rock wedges on the left and right abutments. The results from the 2014 mapping and investigations are generally consistent with the prior studies.

A series of preliminary limit equilibrium analyses have been carried out to evaluate and confirm the stability of the left and right abutments of the dam. These analyses, which used simplified dam geometry, were carried out to determine the overall impact of critical structural geology features on abutment sliding stability, and not to design the project. It was intended to determine: (a) the possible impact of the identified discontinuity sets on abutment stability; and, (b) the influence of varying piezometric loads. These simplistic analyses were intended to explore the potential for any major design issues that would need to be addressed in later design phases. However, the analyses employed are not considered to be precise design tools and therefore the results are not to be used as a basis for detailed design.

The following section summarizes the abutment stability analyses conducted in support of the current feasibility study.

10.3.3.2.1. Abutment and Rock Block Arrangement

A series of preliminary limit equilibrium analyses were carried out to provide a general assessment of the stability of the left and right abutments considering the critical orientations of geologic features and discontinuities. In general, the joint orientations described in Table 10.3-10 were used in the analysis, although different nomenclature was used. In addition, the stability analysis was completed before the 2014 mapping was performed and the joint sets were updated. Thus, the stability analysis needs to be updated to more accurately reflect the orientations within each abutment.

The general layout of the hypothetical abutment rock blocks (wedges) within the abutments of a curved concrete gravity dam is shown schematically on Figure 10.3-4. For the proposed dam, a

total of eight 3-D tetrahedral wedges were analyzed, four in each abutment. Typical plans and sections of the wedges in the left abutment are shown on Figure 10.3-5, Figure 10.3-6 and Figure 10.3-7. The basal planes of all wedges are made up by a series of gently dipping planes at different elevations in the abutments, intended to simulate with the shallow dipping joint set. The side planes are defined by a steeply inclined joint set in the left and right abutments. The grout curtain forms the upstream limit of each wedge. Each wedge daylights in the slope immediately downstream of the dam. Analyses for static loading conditions and normal reservoir levels were carried out for each of the eight wedges. In addition seismic stability analyses were conducted to assess the impact of pseudostatic earthquake loadings on rock stability.

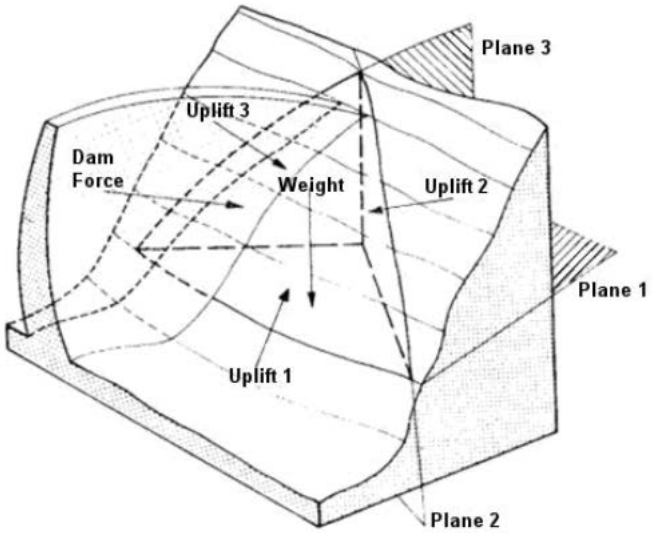

Plane 1, Plane 2, and Plane 3 are Discontinuity Planes; Uplift 1, Uplift 2, and Uplift 3 are Water Forces; W is the Block Weight; and Dam Force is the Thrust from the Dam (From Scott, G.A. 1999, "Guidelines Foundation and Geotechnical Studies for Existing Concrete Dams", USBR, adapted from Londe

Figure 10.3-4. Schematic Rock Block within the Abutment of an Arch Dam

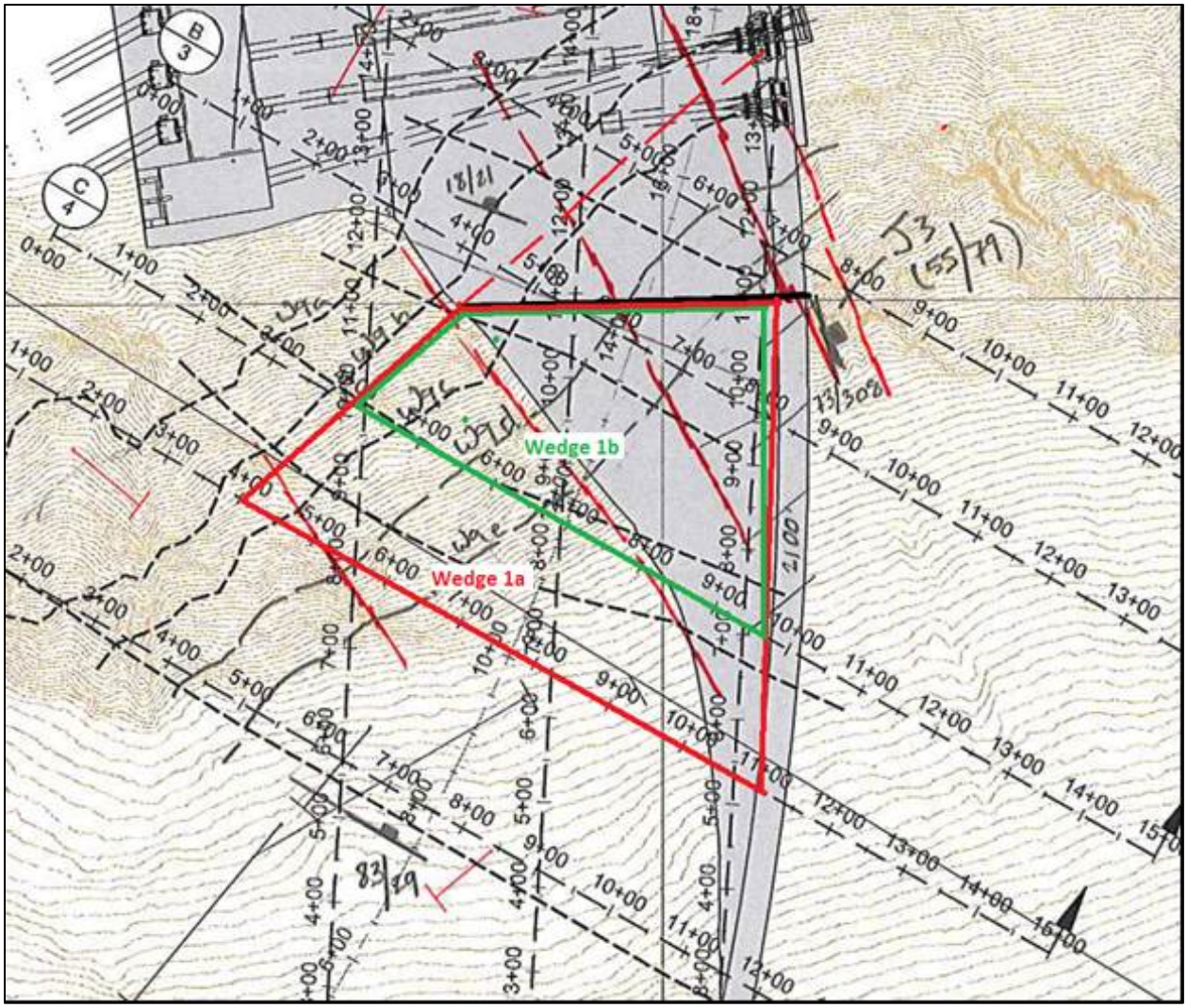

Figure 10.3-5. Plan, Left Abutment Wedges 1a and 1b

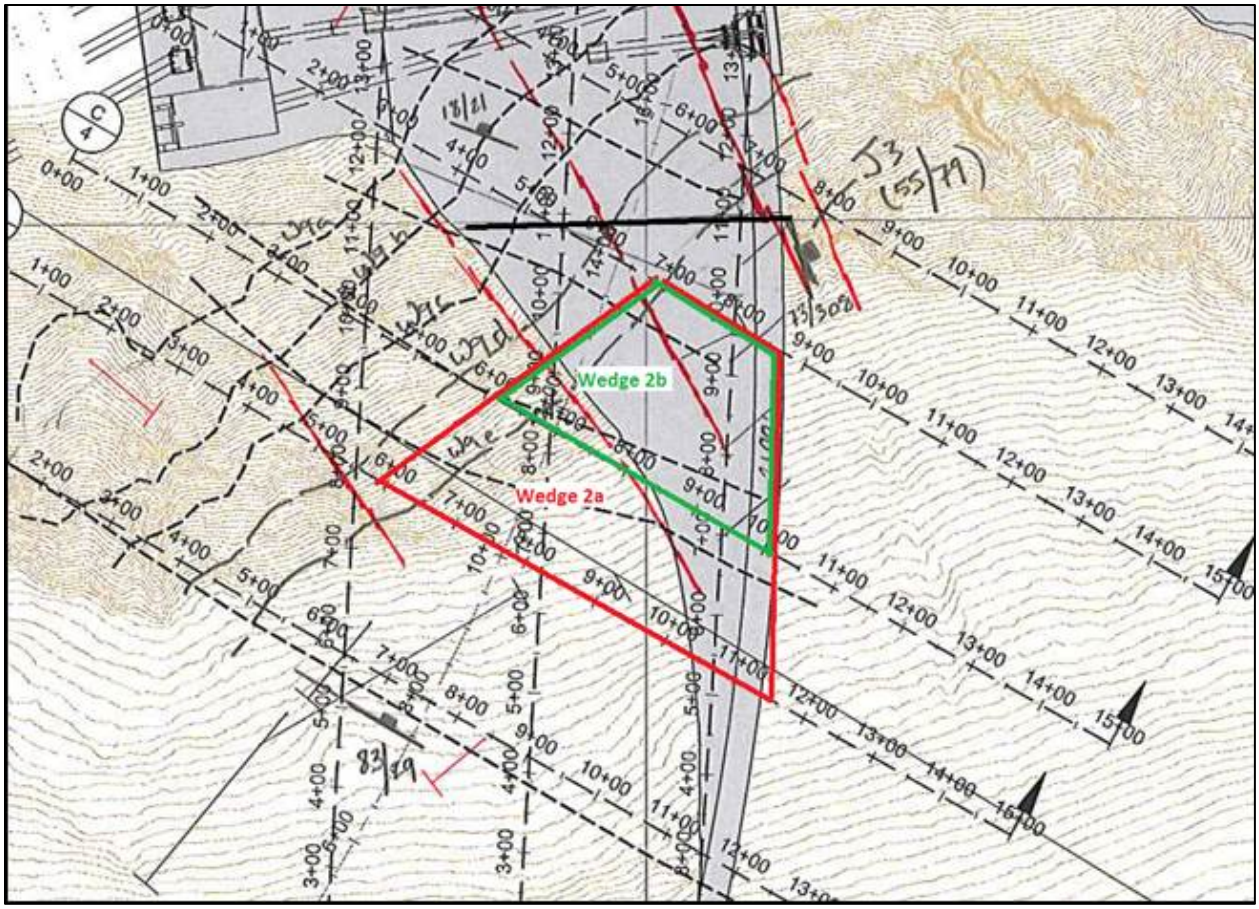

Figure 10.3-6. Plan, Left Abutment Wedges 2a and 2b

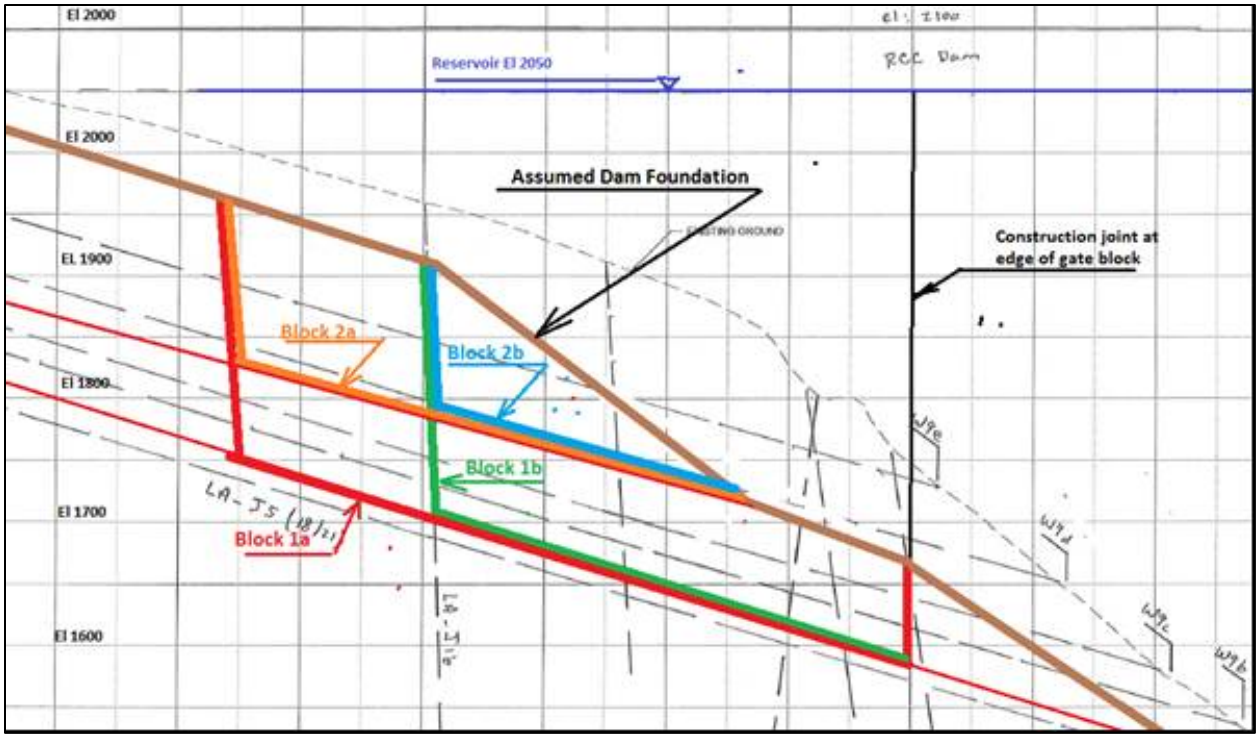

Figure 10.3-7. Schematic Profile along Dam Axis Left Abutment showing Wedges 1a, 1b 2a and 2b; Scale of Wedge Boundaries is Approximate

10.3.3.2.2. Limit Equilibrium Analysis

Static limit equilibrium analyses were carried out on multiple wedges in the left and right abutments for normal to extreme piezometric loading conditions and approximated pseudostatic loads using kinematic analysis and DIPS software. The analyses incorporate the following:

- Wedge weight.
- Dam weight load applied to the top of the wedge. Thrust loads from the dam were not included.
- Water pressure distribution on each block face. Hydrostatic loadings were applied on the J1 side plane and J5 basal plane of the wedge. It was assumed that the water pressure in these planes declines linearly from the grout curtain to the point where the discontinuity daylights in the slope downstream of the dam. Parametric studies were carried out to evaluate the effects of drainage by varying the uplift at the downstream side of the grout curtain from 100 percent (no effective drainage) to zero (100 percent effective drainage). It should be noted that, based on precedent experience in arch dam abutments, a 33 percent uplift case would be considered a reasonable design assumption. The other cases

show the effects of varying uplift pressures from the design ideal. Drilled drain holes – including those drilled from any required extension of the adits that might be needed to address wedge drainage – will extend far enough to intersect the lowest critical plane that daylights.

- Pseudostatic loads (most critical blocks only). Given that the wedge would actually have a complex internal response to seismic shaking, it was considered that the simplistic application of a single horizontal seismic load was sufficient for a preliminary estimate of stability. More rigorous seismic analysis of critical wedges will be carried out during the final design of the project.
- Orientations of the discontinuities and block face.
- Friction cone contours at 5° increments plotted on stereoplot.
- The resultant force vector plotted on the stereoplot.
- Inspect the friction cone contours and resultant plots.
- Establish the friction angles (Φreq) needed for limit equilibrium (FOS = 1.0) and compute the factor of safety (FOS) against sliding as per the procedures described by Londe, Goodman and other authorities assuming the sliding plane has no cohesion and a friction strength (Φ_{disc}) of 45°.

The results of the stability analyses are provided in Appendix B5, but are summarized below. The analyses of the left abutment indicate the following:

- The wedges have acceptable static (FOS > 2.0) and seismic stability (FOS > 1.0) for the 33 percent uplift case. This is a normal design uplift assumption that assumes that foundation drainage is two thirds effective. For this drainage case, the required friction resistance for FOS=1.0 varies from 24° to 27° for the static case and 32° to 43° for the earthquake case. The FOS for assumed Φdisc = 45°, varies from about 2.0 to 2.2 for the static case and from about 1.07 to 1.6 for the earthquake case.
- In all drainage cases, the static FOS is greater than 1.0. The earthquake FOS values are less than 1.0 when the drainage efficiency is 33 percent or less (67 percent uplift) in Wedge 1a.
- Overall stability is very sensitive to the hydraulic uplift forces in the side (J1) and base (J5) planes. As piezometric load increases, the direction of the resultant vector rotates northwards, towards the valley. Thus, the sliding FOS is reduced by almost half when the hydraulic loadings in these planes are increased from 33 to 100 percent. This confirms the requirement for a well-constructed grout curtain and effective drainage of the foundation and abutments.

- The stereoplots show that critical sliding and thrust loads are directed along the basal J5 plane and there are no significant loadings across the J1 plane. The orientations of the resultant vectors show that sliding stability is controlled by the shear strength of the J5 plane and indicate that the strength of the J1 plane has very little influence on stability.

The analyses of the right abutment indicate the following:

- The right abutment wedges have acceptable static (FOS $\geq$ 2.0) and pseudostatic seismic stability (FOS$\geq$1.0) for the 33 percent uplift case. This is a normal design assumption that assumes that foundation drainage is two thirds effective. For this drainage case, the required friction resistance for FOS=1.0 varies from 11° to 25° (Φ_{req}). The FOS for assumed Φ_{disc} = 45°, varies from about 2.1 to 5.1 for the static case and the FOS is greater than 1.0 for all drainage cases.
- Overall stability is very sensitive to the hydraulic uplift forces in the side (J1) and base (J5) planes. As piezometric load increases, the direction of the resultant vector rotates southwards, towards the valley. Thus, the sliding FOS is reduced by almost half when the hydraulic loadings in these planes are increased from 33 to 100 percent. This confirms the requirement for a well-constructed grout curtain and effective drainage of the foundation and abutments.
- The stereonets show that critical sliding and thrust loads are directed along the J4 basal planes on the left bank and there are no significant loadings across the J2 side plane. The orientations of the resultant vectors show that sliding stability is controlled by the shear strength of the J4 plane and indicate that the strength of the J2 plane has very little influence on stability.

The results of this preliminary analysis are considered to be conservative because:

- Dam loading forces were represented by the dead weight of the dam plus the water load on the upstream face of the dam. Thrust loads resulting from the dam curvature, which direct some of the loadings into the abutment (with consequent increase of the sliding FOS) were conservatively excluded from this analysis.
- The theoretical hydraulic loadings used for the three discontinuity planes are usually reduced when flow net values, which consider head losses along the flow paths, are used.
- Cohesion resistance along the sliding planes was not considered. It is assumed that shear strength is controlled by friction resistance. Given that the basal sliding planes are made up of a series of en-echelon, discontinuous joints, it is probable that failure planes would have to shear through a number of intact and competent rock bridges along the failure path imparting a significant cohesion strength component.

10.3.3.2.3. Conclusions

The results from preliminary analyses of theoretical abutment blocks indicate that the left and right abutments have acceptable sliding stability for reservoir loads under static and assumed pseudostatic seismic conditions. The analyses used conservative shear strength parameters and piezometric uplift assumptions in the rock mass. While considered preliminary, the analyses indicate that the abutments have robust stability for the "arch action" expected from the planned curved gravity dam design.

It must be pointed out that the pseudostatic earthquake stability assessment is a rough approximation of earthquake loadings but is sufficient for feasibility level design. The analyses carried out herein demonstrate that the abutments are expected to have a robust resistance to uniform horizontal loadings, but the analyses do not accurately assess the effects of the final chosen design loading cases. More detailed dynamic stability assessments will be required during detailed design. In addition, since this analysis was performed – because of ongoing development of the dam configuration – the dam has been rotated (by less than 5° on the left abutment), and the robust stability should not be impacted greatly by the repositioning.

It should be noted that this assessment is based on incomplete geological information with respect to the geotechnical properties of the critical discontinuity sets. Future foundation and joint characterization from the planned exploratory adit investigations needs to be incorporated into the geologic model to enable more representative analyses of the right and left abutments based on improved information on the subsurface geologic conditions including persistence of sub horizontal discontinuities and the presence and persistence of ice-filled discontinuities, final dam configuration, and completion of a seepage analysis to evaluate the hydraulic forces.

10.3.3.3. Dam Foundation Design

The foundation area for the proposed curved RCC dam has a considerably reduced area compared to the 1980s proposal for an ECRD. However, the integrity of the foundation of an RCC dam is paramount to the stability and safety of the dam, and a more detailed characterization of the foundation will be necessary to perform detailed design of the dam. To that end, before future detailed design, a more extensive site investigation program is recommended to be implemented, which would include excavating adits and the associated drilling, in situ testing, and instrumentation monitoring within the adits in both abutments.

For this report, the existing information derived from the 1980s and site investigations and geologic mapping from the 2012 and 2014 investigations was used to characterize the foundations. Rock elevations and quality were plotted using the new site contours derived from the LiDAR ground surface contours, together with the borehole data from the 1980s studies. The

data were adjusted from the NAD27 datum, Alaska State Planes coordinate system used in the 1980s studies to the NAD83 datum coordinate system currently in use together with NAVD88. Based on the revised bedrock contours and assessment of rock quality at the dam site including rock outcrops, a plot of the rock surface was made to estimate excavations necessary to achieve an acceptable dam foundation (Drawing 01-01GT004). In addition, the following assumptions and design and construction considerations pertinent to project include:

- The bedrock foundation level has been chosen so that the foundation of the dam will be non-erodible under the projected and calculated seepage gradients.
- The foundation level has been chosen so that the contact between the dam and the bedrock surface will be on fresh to slightly weathered or altered, strong and sound rock. Dental excavation will be performed to remove significant bedrock irregularities to provide a smoothly varying foundation surface.
- Dental excavation and treatment will be performed in the bedrock foundation at locations of highly fractured, sheared, and moderately to highly altered zones (e.g., where geologic features GF4B and GF5) are present in the foundation. Conventional concrete infill will be placed in these areas of extra excavation.
- The potential for encountering bedrock on the left abutment and lower right abutments at temperatures slightly below freezing and the variations in the rock surface temperatures over the dam footprint are likely to require special procedures for placement of RCC and conventional concrete against the cold rock. Having a large foundation area against which concrete will be placed, will necessitate development of special procedures during detailed design. Construction methodology will need to be developed to facilitate thawing of the foundation prior to placement of concrete and foundation treatments.

As part of the preliminary design, the dam foundation design includes characterization of the foundation, preliminary finite element analyses, and assessments of dam foundation treatments necessary to provide a foundation suitable for carrying intended loads.

10.3.3.3.1. Finite Element Analysis

A key aspect of evaluating the feasibility of the RCC dam is to understand the behavior of the dam and how it interacts with the foundation. To understand the stresses and deformations that might be experienced by the dam and foundation in response to the anticipated loading, preliminary finite element analyses (FEA) were performed using ANSYS and LS-DYNA.

The 3-D ANSYS foundation model included sensitivity of dam stability and performance of the structure relative to changes in discrete foundation elements with differing deformation parameters. The diagrams shown in Figure 10.3-8 show the basic zoning used for the analyses –

which was compiled before the geological mapping of 2014, and the subsequent reinterpretation of the geological features in the dam foundation. Generally the reinterpretation of the foundation has postulated narrower and less continuous geological features than previous interpretations, so the simplified model used in the analysis is conservative – with regard to size of feature and continuity – compared to that which will be used in the detailed design analysis. The preliminary analyses examined static and dynamic stability of the dam using a relatively coarse mesh for the foundation, which required simplification of the geologic interpretation of the foundation geology presented on Drawing 01-01GT006. In particular, in the Acres interpretation used, the lower right abutment of the dam foundation is shown to be comprised of several fracture zones (Engineering Unit 2) and narrow altered/shear zones (Engineering Unit 3) within the area of geologic features GF4B and GF5 that are separated by more intact rock (Engineering Unit 1). Because the dimensions of the elements forming the FEA mesh are larger than the width of the fracture zones, the lower right abutment was oversimplified as a wider zone having rock mass properties that are a composite of the three engineering units.

While not directly correlated with the Engineering Units defined in Table 10.3-9 since the preliminary modeling was completed before the foundation parameters were finalized, Zone A is approximately equivalent to Engineering Unit 1 below a depth of 20 ft. and the "Weak Layer" approximates the upper 20 ft. of the foundation. Zone B is modeled using a deformation modulus that covers the estimated range for Engineering Unit 1, Unit 2, and Unit 3. The properties incorporated into the finite element analyses are summarized in Table 10.3-12. The model was run using linear elastic materials, thus the rock mass strength parameters are not pertinent.

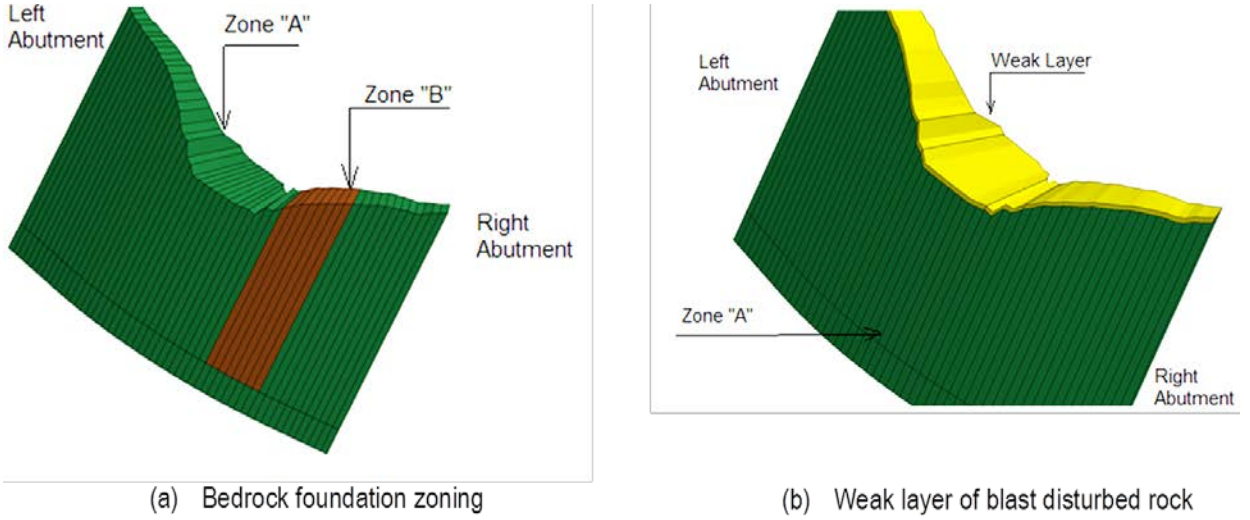

Figure 10.3-8. ANSYS Foundation Models Showing Principal Bedrock Zones

Table 10.3-12. Foundation Parameters for Preliminary 3-D FEA

Analysis Case	Description	Deformation Modulus, E (x 10^6 psi)		
		Weak Layer	Zone A	Zone B
Layout 3 – ANSYS	Homogeneous Foundation	–	3.5	3.5
Layout 4 – ANSYS	Base Case	–	3.5	1.5
	Sensitivity – High	–	7.0	3.0
	Sensitivity – Low	–	1.75	0.75
Layout 4 – (Modified) ANSYS and LS-DYNA	Homogeneous Foundation	2.8	3.5	3.5
	Homogeneous Foundation	2.0	3.5	3.5
	Base Case	–	3.5	1.5

10.3.3.3.2. Consolidation Grouting

Although controlled blasting will be used for the final excavation of the dam foundation (and other structures such as the spillway and powerhouse) it is prudent to assume that rock within about 20 ft. of the excavated surface may have experienced stress release and loosening of joints. Therefore, in accordance with normal practice for large dams, consolidation grouting will be performed to improve the rock quality and modulus under the entire dam contact area and up to 30 ft. upstream and downstream of the footprint. In addition, consolidation grouting is assumed under the spillway structure, powerhouse, and other appurtenant structures.

It has been assumed at this time that consolidation grout holes approximately 25 ft. deep will be drilled into the dam foundation on a 10 ft. by 10 ft. grid, except in the areas where ground temperatures are below freezing, which will require a tighter spacing, 6 ft. by 6 ft. (e.g., left abutment). In addition, localized consolidation grouting may be necessary in localized zones of fracturing associated with fracture, shear, or altered bedrock to improve the strength and deformability of the rock mass. The holes will be oriented such that they intersect as many of the discontinuity sets as is reasonable. Based on the information available at the present time, Joint Set 1 and Joint Set 2 are the dominant joint sets and are near vertical and there is a shallow dipping joint set. Thus, holes will be oriented a maximum of 15° from vertical.

From data available from the existing borehole instrumentation, it is postulated that the bedrock may be at a stable residual temperature of about 30°F within much of the lower left abutment, and potentially in pockets on the right abutment. The low temperature zone appears to extend more than 200 ft. below the ground surface in the left abutment bedrock. A ground temperature of more than 40°F is normally required for grouting. Therefore, for consolidation grouting to

achieve its purpose, it is envisaged that the ambient bedrock temperature must be raised to at least 40°F.

Grouting of bedrock that exhibits a temperature below freezing point of water (and may contain ice filled joints) will require some approaches that differ from conventional grouting. Planning for this aspect of the project is very important, and it is envisaged that, during future site investigations, a test grouting program will be initiated to assess the merits of various alternative methods and procedures for consolidation grouting and curtain grouting particularly with regard to frozen bedrock. In the meantime, the following methodologies for grouting frozen ground are postulated for raising the rock mass temperature some of which are discussed in Section 10.9 with respect to preparation of the foundation for placement of RCC. Allowances have been included in the cost estimates for the following measures, as appropriate:

1. Closer consolidation hole spacing.
2. Early stripping of overburden and rock materials to promote thawing. Insulate and heat the areas over winter.
3. Circulate hot water in consolidation holes.
4. Circulate steam in consolidation holes.
5. Install electric heaters in holes.

Where structural features (sheared and altered zones and poor quality bedrock) pass through the dam foundation, additional stitch grouting will be performed as required if it has been determined that structural features are potential pathways for seepage. In general, where encountered, such zones will be capped with conventional concrete, and then a number of inclined holes will be drilled from each side to intersect with the feature at various depths, and from which grouting can be carried out. Structural features will be carefully mapped, and if considered necessary, extra or lengthened galleries will be introduced into the RCC so that higher pressure grouting of the feature is possible after the RCC has been placed, and to measure and remediate seepage through the feature after impoundment.

10.3.3.3.3. Curtain Grouting

Curtain grouting will be performed to reduce seepage and reduce the potential for piping of weak foundation materials or joint infillings. The challenges relating to curtain grouting at the dam site, as with the consolidation grouting, primarily relate to encountering ice-filled discontinuities. Otherwise, curtain grouting is expected to follow standard industry practice.

The grout curtain will be constructed beneath the dam foundation, along the dam axis extending up both abutments. The maximum depth of the curtain will be approximately 375 ft. below

foundation level (i.e., 50 percent of maximum total head). Foundation grouting will be performed from galleries within the dam that will collect water from foundation drain holes drilled downstream of the grout curtain. In accordance with modern practice, a single row grout curtain is assumed to have holes inclined holes 15° from vertical and oriented in the upstream direction. This arrangement is suitable to intersect the large number of discontinuities dominated by JS1, JS2, and JS3. Standard split-spacing techniques will be used beginning with primary holes drilled at 20-ft. spacing, followed by secondary holes and together with tertiaries and quaternary holes as required to achieve closure. In specific areas, as dictated by the final evaluation of the dam foundation and optimization of treating frozen ground, an additional row (or rows) of grout holes may be used.

In accordance with modern practice for dam construction, grouting will be performed using balanced, stabilized grout mixes consisting of water and Portland cement having a water:cement (W:C) ratio generally between 0.5 and 2.0 (by weight) and super-plasticizer, additives, and admixtures to meet criteria with respect to viscosity, density, stability, set times, and bleed. Grouting pressures will be limited to prevent the possibility of foundation jacking or uplift of the dam. For feasibility level design, it is assumed that the target residual hydraulic conductivity for the grout curtain is about 3 Lugeons. Closure will be based on a preliminary established value of cubic feet of grout per foot injected. This value will be assessed during an initial test grout program prior to production grouting.

The objective of curtain grouting will be to fill discontinuities within the dam foundation down to approximately 50 ft., and for the rest of the curtain to reduce turbulent flow through discontinuities to a manageable level. Although, for the purposes of cost estimating a fixed grout curtain depth has been assumed, the work will take into account the actual rock conditions encountered during the program and will be modified on site.

While multiple holes for consolidation grouting might be required to facilitate thawing in the near surface bedrock, it is less practical to thaw the bedrock at great depths to facilitate curtain grouting, although in areas of ice-filled joints extra rows or holes may be needed locally or over limited depth intervals. It is envisaged that thawing could take longer, if it is not achieved by delivery of appropriately warm grout. However, grouting will be performed from the adits in the abutments and the galleries within the dam and thus it can continue year round, and if required even after the dam is complete. Additional holes in the left abutment have been allowed for in the cost estimate where rock temperatures are known to be below 32°F.

It is prudent to allow for further grouting during the initial years of project operation after foundation thawing has occurred due to the reservoir impoundment. Additional grouting would

also be done from the galleries and adits, and an allowance for this work is included in the O&M costs during the early years of operation.

Where the diversion tunnel plug will be aligned with the grout curtain, extensive contact, consolidation grouting and radial grouting will be performed from the diversion tunnel to tie the tunnel plug grouting to the dam grout curtain and provide a continuous cutoff. Contact grouting will also be performed in the annular space around all other tunnel linings and the concrete plug placed in the sluice through the base of the dam.

10.3.3.3.4. Foundation Drainage

A drainage curtain will be constructed downstream of the grout curtain to intercept seepage, and to relieve hydraulic pressure beneath the dam. Drain holes will be drilled from the drainage galleries and the adits that extend into the abutments.

A single row of drains will be drilled downstream of the grout curtain, 10 ft. apart, to a depth estimated between 60 and 80 percent of the grout curtain depth, although seepage analysis will be performed during detailed design to finalize the required level of the drainage curtain. Seepage will be collected by gutters in the invert of the gallery and directed to the lower points in the dam for measurement and for discharge. It is important that facilities are also included for measuring seepage flows at specific locations or for particular, discrete, areas of the foundation for purposes of monitoring drain performance.

10.3.4. Underground Excavations

10.3.4.1. Diversion Tunnel

The orientation of the diversion tunnel on the right bank has been selected for the best hydraulic performance and to suit the project layout, while accommodating issues that might arise with respect to the stability of the portal. The joint set orientations will control the support requirements for the diversion tunnel together with any geological features encountered such as GF4B and GF5 (see Section 6.3). It appears that an east-west tunnel orientation is favorable as it crosses the two major joint sets at about 45°. Controlled blasting methods will be employed to reduce the potential for damaging the rock during excavation of the 36 ft. diameter horseshoe tunnel (and the enlarged 45 ft. section). The most efficient method of excavating the diversion tunnel will be to use a top heading and bench. Primary support of the excavation will consist of rock bolts (where needed), wire mesh and shotcrete. However, it is anticipated that zones of fracturing, shearing, and alteration will be encountered and will require steel channels or ribs or lattice girders for support. After excavation is complete, the tunnel will be lined with 12 inches of reinforced concrete, and an 18-inch-thick lining will be placed in the emergency release

chamber. Fracture, shear, and alteration zones are anticipated to be sources of groundwater inflow, which will require grouting to reduce inflows, for contractor construction safety, and to facilitate placement of shotcrete and final concrete linings.

The diversion tunnel will be converted to an emergency release tunnel, after the plug has been inserted and will require that the floor of the tunnel be excavated a further 46 ft. deep. This excavation could be performed during the original excavation of the diversion tunnel (and temporarily backfilled and a concrete floor placed). However, in order to facilitate diversion, it is likely that second-stage excavation would be performed after the temporary plug is inserted and while the final diversion plug is being placed. The appropriate method and sequence should be left to the contractor to suite its means and methods.

The approach channels to the portals will be excavated through talus and bedrock. Due to the thickness of the loose talus upslope of these cuts, large excavations and significant rock stabilization methods of the adjacent slopes will be required.

A challenge that has arisen at some projects – where there is limited cover over the diversion tunnel downstream of the closure gate – relates to the rapid external loading (as the reservoir fills) of the diversion tunnel lining during initial reservoir filling and before the completion of the plug. For Watana this difficulty has been mitigated because the sluice through the dam will remain open until the plug has been completed and the diversion tunnel gates have been removed. Thus the diversion tunnel lining upstream of the plug will never be subject to high external loading and there will be greater flexibility in the final on-site choice of the upstream portal of the diversion tunnel.

10.3.4.2. Access Tunnels

The location of the powerhouse at the toe of the dam necessitates the use of a tunnel for access, because the walls of the canyon are too steep for an open cut road to be practical.

Delivery of equipment for the powerhouse will be through the access tunnel. The largest pieces of equipment that will be transported through the tunnel include the generator step up transformers, the turbine runner, the powerhouse crane beam and possibly penstock pipe sections. The tunnel has been dimensioned to accommodate these items.

The tunnel excavation will be reinforced with rock dowels and reinforced shotcrete lining. Careful analysis of support requirements will be necessary for the spur tunnel used to store the standby generator and for the vertical shaft that extends to the low level outlet valve gallery.

The configuration at the crossing of the diversion tunnel and the access tunnel will require careful analysis, design, and construction, as the intersection of the two will alter the effective rock stress. Care will need to be taken in design. The diversion tunnel will never be pressurized, and it is envisaged at this time that the limited vertical separation between the two tunnels can be mitigated by an over excavation of the diversion tunnel and the inclusion of a (reinforced) structural concrete "bridge" forming part of the diversion tunnel lining crown and the floor of the access tunnel. It is assumed that rock tendons will be required in each of the tunnels at that location to stabilize the intersection. During detailed design, the option of reconfiguring the access tunnel to increase the vertical separation of the tunnels will be investigated.

Pattern drain holes will be required in the access tunnels to relieve pressure on the lining, and flows will be directed to a formed drainage channel in the concrete invert.

10.3.5. Cofferdams

Zoned embankments will be constructed upstream and downstream of the proposed dam to close river flow and maintain diversion of the river through the diversion tunnel.

When the powerhouse substructure has reached an elevation of El. 1476 ft. and the upstream section of the RCC has reached an elevation of approximately El. 1530 ft., the cofferdams can be allowed to fall into disrepair. Until that time, they are necessary to divert the river flow through the diversion tunnel, although under certain circumstances the upstream cofferdam can be overtopped so that ice or water flows through the sluice.

There is a considerable thickness of alluvial deposits beneath the river consisting of gravelly sand with cobbles and boulders, and the banks of the river the talus deposits consist of angular cobbles and boulders, all of which are highly pervious. Therefore, a slurry cut-off wall will be necessary, constructed from the cofferdam and extend through the alluvium. The cutoff is not expected to fully cutoff seepage, and continuous dewatering will be required to remove seepage from the excavation until the structures have achieved the elevations noted above.

The cofferdams should be located to avoid deeper alluvium cover (greater than 100 ft. thick) and where possible, avoid significant geologic features (fracture and/or shear zones) beneath the impervious material.

The diversion is described in detail in Section 10.4, but the initial closure will be achieved using rockfill stockpiled on either bank and then dozed into the river from either side. It is most convenient to perform closure at the lowest possible flow, even when the river is frozen, when it may be possible to use the ice as a working surface. After closure has been achieved, and the river has been diverted through the diversion tunnel, the closure cofferdam will be enhanced as

necessary by the placement of a choker course of silt on the upstream side. The next step will be to complete the cutoff wall behind the closure dyke, and then complete the remainder of the upstream cofferdam. The final work on the upstream cofferdam will be the excavation of bypass channels to allow flow and ice to pass the cofferdam without damage and flow through the sluice when flows exceed the capacity of the diversion tunnel, or during ice "breakout" when and if the diversion tunnel became blocked with ice. Because of the speed of placement of RCC, this situation is considered to constitute a risk for only one "breakout" season.

The design and construction of the downstream cofferdam is very similar to that of the upstream cofferdam. At completion, the downstream cofferdam must be removed to form a suitable tailrace. The upstream cofferdam can be left in place and will be inundated by the reservoir.

10.3.6. Watana Relict Channel

Studies performed in the 1980s indicate the existence of a deep buried valley (relict channel) that crosses from the north bank of the Susitna River gorge, upstream from the proposed dam site, and extends to Tsusena Creek, a distance of about 1.5 miles. Along the buried valley thalweg, the highest bedrock surface is estimated to be located at approximate El. 1750 ft., which is about 300 ft. below the NMOL of the proposed reservoir (El. 2050 ft.). The maximum hydraulic gradient along the buried channel (El. 2050 ft. to Tsusena Creek) would be low, approximately 4.3 percent.

Potential challenges posed by the relict channel are:

- Subsurface leakage from the reservoir through potentially permeable material along the buried channel.
- Thawing of permafrost, if present, in the relict channel over time resulting in increased seepage.

The average hydraulic gradient along the channel is considered low, and there may be no need to make any provisions for remedial treatment. However remedial measures currently being considered for the deep buried valley are placement of a downstream toe drain at Tsusena Creek, a filtered exit, to control the potential problem of piping. In addition, long-term monitoring to determine the hydraulic gradient and rate of thaw of permafrost that may be realized following initial reservoir impoundment is also considered.

The final proposal treatment will be determined during detailed design and after the completion of additional investigations (e.g., pumping tests). In the meantime, for the project cost estimate an allowance has been included for remedial measures.

10.4. River Diversion

10.4.1. General

The 1985 Federal Energy Regulatory Commission (FERC) license application adopted a twin 36 ft. circular tunnel configuration for diversion based on a design flow of 77,000 cfs, equivalent to a 50-year return period flood. The criteria used were appropriate for a clay core embankment dam, and an upstream cofferdam elevation of El. 1550 ft. During the comparison of alternative configurations performed for this report, the potential for alternative, more economic diversion arrangements was investigated for the RCC dam and for the CFRD variants.

The available hydrological analysis has been updated for the project site to include about 30 more years of flood data than was available in the 1980s. The updated flood frequency is presented in Table 10.4-1.

Table 10.4-1. Flood Frequency at Watana Dam Site

Return Period (years)	Flow (cfs)
2	38,500
5	50,500
10	59,200
20	68,300
25	71,300
50	80,800
100	91,300
500	116,300
1,000	128,400

As noted previously, the arrangements adopted for the chosen RCC dam project will comprise a single diversion tunnel through the north (right) bank and a sluice incorporated within the dam. The tunnel will be converted to serve as emergency release facilities upon completion of the Project and the sluice will be completely filled with concrete and grouted.

10.4.2. Criteria

The diversion tunnel will be concrete-lined throughout.

Because the annual peak flow frequently occurs in conjunction with the spring river ice cover breakup, the diversion facilities will conservatively account for the potential for complete plugging (with ice and tree trunks) of the diversion tunnel at the gated intake.

Flood routings have been carried out, and indicate that routing effects will be minimal for the diversion flood. Therefore, the diversion facilities will be designed for the peak flood flow.

The criteria for the diversion tunnel intake are shown in Table 10.4-2.

Table 10.4-2. Criteria for the Diversion Tunnel Intake

Diversion tunnel alone (water level below cofferdam spillways)	5-year return period flood
Sluice alone (assumes complete plugging of the diversion tunnel)	50-year return period flood
Tailwater rating	See Figure 10.4-1
Upstream cofferdam freeboard	30 ft. minimum above spill channels
Diversion tunnel Manning's 'n'	0.013
Hydraulic losses	HARZA design guide – DG-112

The diversion tunnel will be sized to convey at least the five-year return period flood (50,500 cfs), considered reasonable protection for the cofferdam construction, the initial foundation excavation tasks (which will be carried out over a period of six months), and the initial RCC placement up to the top level of the cofferdam.

The dam sluice and has been sized to pass the 50-year flood, assuming the diversion tunnel has been completely plugged during spring breakup with ice and woody debris. A consideration in detailing of the tunnel and sluice was that the same gates would be used for closure on both at different times. To facilitate passage of flow to the sluice without associated failure of the cofferdam, an overflow channel will be excavated on both abutments either side of the cofferdam and the channels will be lined with concrete.

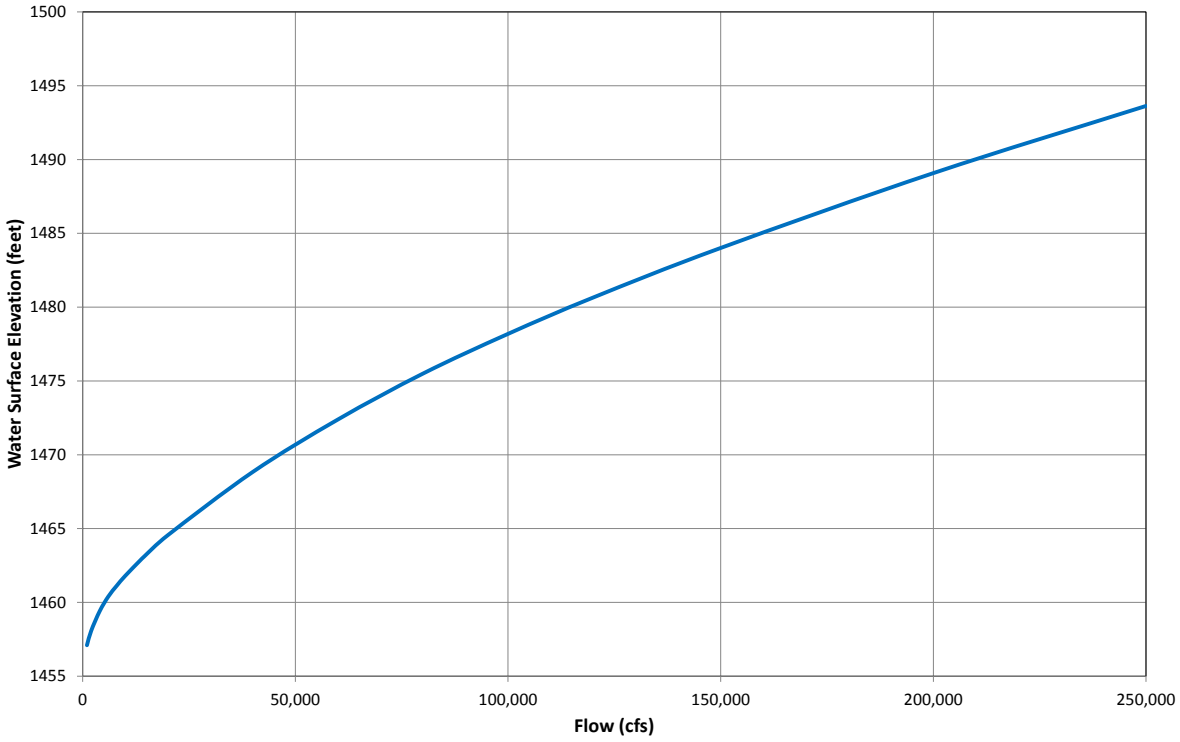

Figure 10.4-1. Tailwater Rating Curve at Dam Site

10.4.3. Analytical Results

Analysis of the hydraulics of the diversion tunnel and sluice were performed for a variety of cross sections, elevations, grades and lengths. The final configuration of the emergency outlet is discussed in Section 10.13. During the development of the design, the sluice length was reduced (because the curvature of the dam allows a steeper downstream face and thus a shorter sluice length).

The locations of the tunnel portals were selected so that rock cover at the crown equal to twice the projected tunnel excavated diameter. The portals will necessitate overburden excavation to facilitate tunneling.

Hydraulic analysis indicated that the tunnel capacity was substantially limited by the size of the intake gates. Consideration was given to an enlarged 44 ft. wide inlet with no piers and then transitioning to the 36 ft. tunnel about 100 ft. downstream from the intake. This alternative was not selected because any jamming would be inaccessible inside the tunnel.

An alternative to assuming plugging of the diversion tunnel would be to construct a larger tunnel that has demonstrated the capability to pass a major spring river ice breakup, such as the 48 ft.

diversion tunnel at Bennett Dam on the Peace River, Canada. However, a 48 ft. diversion tunnel was considered to be uneconomical, and to involve risk at the portals.

The selected tunnel alternative includes an enlarged two gate intake. Compared to the 1985 design, the intake gates were increased from 14 ft. wide to 22 ft. wide to increase the tunnel capacity. During ice breakout heavy equipment could be pre-positioned above the intake to assist in clearing jams. The outlet structures used in the 1985 design was adopted for the analysis.

The size of the total sluice opening through the RCC dam would be 44 ft. by 50 ft., which includes a 6 ft. width allowance for a removable steel central pier. The central pier would not be installed when the sluice was operational – but would be installed when the sluice was to be closed. The same 22 ft. wide gates used on the tunnel could also be used on the sluice.

After the analysis, a selection was made of the features shown in Table 10.4-3.

Table 10.4-3. Diversion Tunnel and Sluice Features

Diversion Tunnel	
Size	36 ft. diameter vertical-sided horseshoe
Gates Inverts	2 each at 22-ft. wide by 36-ft. high
Inlet	El. 1463 ft.
Outlet	El. 1450 ft.
Length	2,060 ft.
Slope	0.64%
Sluice	
Size	44 ft. high x 50 ft. wide (includes 6 ft. of width allowance for a removable central pier)
Inverts	
Inlet	El. 1460 ft.
Outlet	El. 1450 ft.
Length	525 ft.
Slope	10%
Upstream Cofferdam	
Crest elevation	El. 1560 ft.
Top of impervious core	El. 1553 ft.
Overflow spillway elevation	El. 1530 ft.
Overflow spillway length (each)	2 each at 120 ft.
Downstream Cofferdam	
Crest Elevation	El. 1475 ft.

The downstream cofferdam will be designed to wash away if it is substantially overtopped by flow from the sluice.

The resulting river diversion rating curve is shown in Figure 10.4-2. Due to the complexity of the river diversion hydraulics, the river diversion rating curve should be confirmed at a minimum with a 3-D computational fluid dynamics (CFD) model and potentially also with a physical hydraulic model.

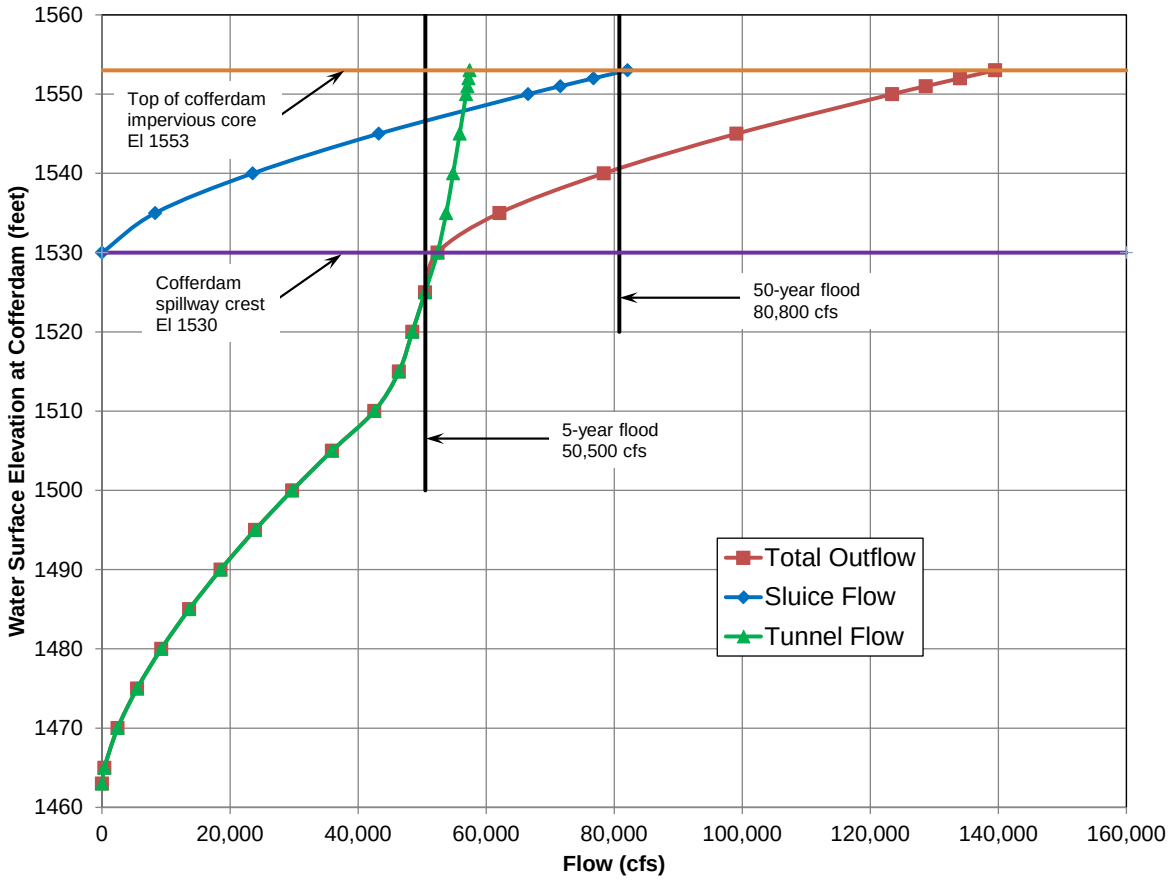

Figure 10.4-2. Derived Diversion Scheme Rating Curve

10.4.4. Operation of Diversion

After diversion, the diversion tunnel capacity will allow the construction area (foundation) within the river to remain dry for all river flows up to 50,500 cfs. At this flow the headwater level at the upstream cofferdam will be at the bypass "weir" crest. The tailwater level will be about three feet below the crest of the downstream cofferdam. This provides protection from the five-year flood.

For floods greater than the five-year return period event – or if the diversion tunnel was blocked by ice or debris – the upstream cofferdam would be bypassed by flow through the overflow bypass (constructed on each abutment of the upstream cofferdam) in a manner such that no damage will occur to the structure.

During the first 13 months of construction operations in the river bed, work could be disrupted by a flood event (or ice breakout) that caused the cofferdam to be bypassed. However after this initial period, the RCC being placed during the summer season would have attained El. 1520 ft. (quickly achieving El. 1529 ft. during the first month of the subsequent season) and the sluice would have been completed allowing bypass through the sluice under all conditions, and thus allowing operations on the dam to continue without further danger of inundation.

Powerhouse substructure concrete will commence at the same time as the RCC and has been scheduled to be completed in 22 months – encompassing two seasons of snowmelt. This would mean that the powerhouse construction could be at danger of inundation, from the downstream side, for 11 months more than the RCC dam construction. During detailed design, the powerhouse concrete design tasks will include a focus on methods for facilitating the construction of the downstream, and south (end) wall between the powerhouse and the spare bay to at least El. 1475.6 ft. (the tailwater elevation for the 50-year flood) so that these walls could be constructed faster – allowing bulkheads to be placed in the stoplog slot and achieving full protection from flooding the powerhouse early.

After the completion of RCC to approximately El. 1540 ft. the upstream cofferdam will not be needed and can be abandoned, and not removed. The downstream cofferdam can be breached after the downstream powerhouse wall has reached El. 1469.5 ft. and will be removed at a convenient time thereafter.

The first closure will be of the diversion tunnel in year nine – which will result in the diversion of the river through the sluice. After completion of the plug, the plug grouting and all the electrical and mechanical works for the emergency outlet, the diversion tunnel gates will be removed from the diversion tunnel and relocated to the sluice to effect final closure – after which the sluice will be filled with concrete and grouted, and minimum flow during reservoir filling will be discharged through the emergency outlet until the reservoir level reaches El. 1850 ft. , after which minimum flow will be released through the low level outlets.

10.5. Dam – Layout Development

10.5.1. General Methodology

Sections 10.5, 10.6, and 10.7 record the development of the dam layout and geometry, using multiple analytical tools. Having selected the type of dam, prior to submission of the Pre-Application Document (PAD), the engineering team recognized that development of the dam geometry to include curvature could benefit the project by reducing the footprint of the project, reducing the volume of concrete and reducing the construction period.

It was decided to perform iterative analysis of different dam configurations, commencing with inexpensive analysis to guide in the selection of further optimizations. It was decided to delay a detailed and expensive FE analysis until configuration had been developed – using relatively inexpensive modeling – that appeared to satisfy the stability and structural criteria.

The intent of the first "preliminary" analyses therefore – described in Section 10.6 – was to determine a dam configuration that will maintain the required stability and safety, while providing the opportunity for minimization of the RCC volume, and thus the shortest construction period. The key factors in the assessment of the viability of the various layouts examined, was the stability per FERC criteria, and the concrete stresses – principally on the upstream face.

During the time that the structural and stability analyses were being performed, ongoing site inspections were in progress and geotechnical analysis were being performed (although these cannot be completed until all boreholes have been completed, all adits constructed, and all rock testing has been carried out). The principal geotechnical data available was drawn from the 1980s reports. In addition, the SSSHA was in progress (but not complete). The PMP/PMF and flood routing studies were in progress during the analyses, as well as the derivation of the proposed seismic design criteria, and the results of these two efforts were incorporated into the structural and stability analyses when available. Sensitivity studies were performed for varying foundation conditions, but these cannot be exhaustive until the results of site investigation studies are available.

An overview of the evolution and logic of the dam configuration studies is shown in a flow chart in Figure 10.5-1 and can be used to aid in understanding the descriptions and sequence of the analyses documented in Sections 10.6 and 10.7 of the report. Availability of external information developed concurrently with the dam layouts and incorporated into the analyses is shown in the rust-colored circles in the figure.

The criteria for stability are clearly defined in FERC guidelines, but the criterion for concrete stress is less well documented. For the preliminary analysis – performed for layouts 2, 3, and 4, a comparison with the allowable tensile stresses in RCC and horizontal joints in RCC was a key factor. For the "Final" modelling described in Section 10.7 – which included mass in the foundation – a comparison was made of the allowable RCC tensile stresses and the predicted stresses at the dam faces during the time history of the selected seismic events that formed the model input.

During future detailed design of the project, after the results of the site investigation (including results from the adits and rock testing) are available to characterize the dam foundation; and the various geological features, the precise orientation of the dam, and a revised foundation excavation profile have been developed, it is expected that the feasibility layout and geometry (of Layout 4 [Modified]) will be refined and adjusted to optimize the complete configuration, and further FE analysis will be performed including mass in the foundation.

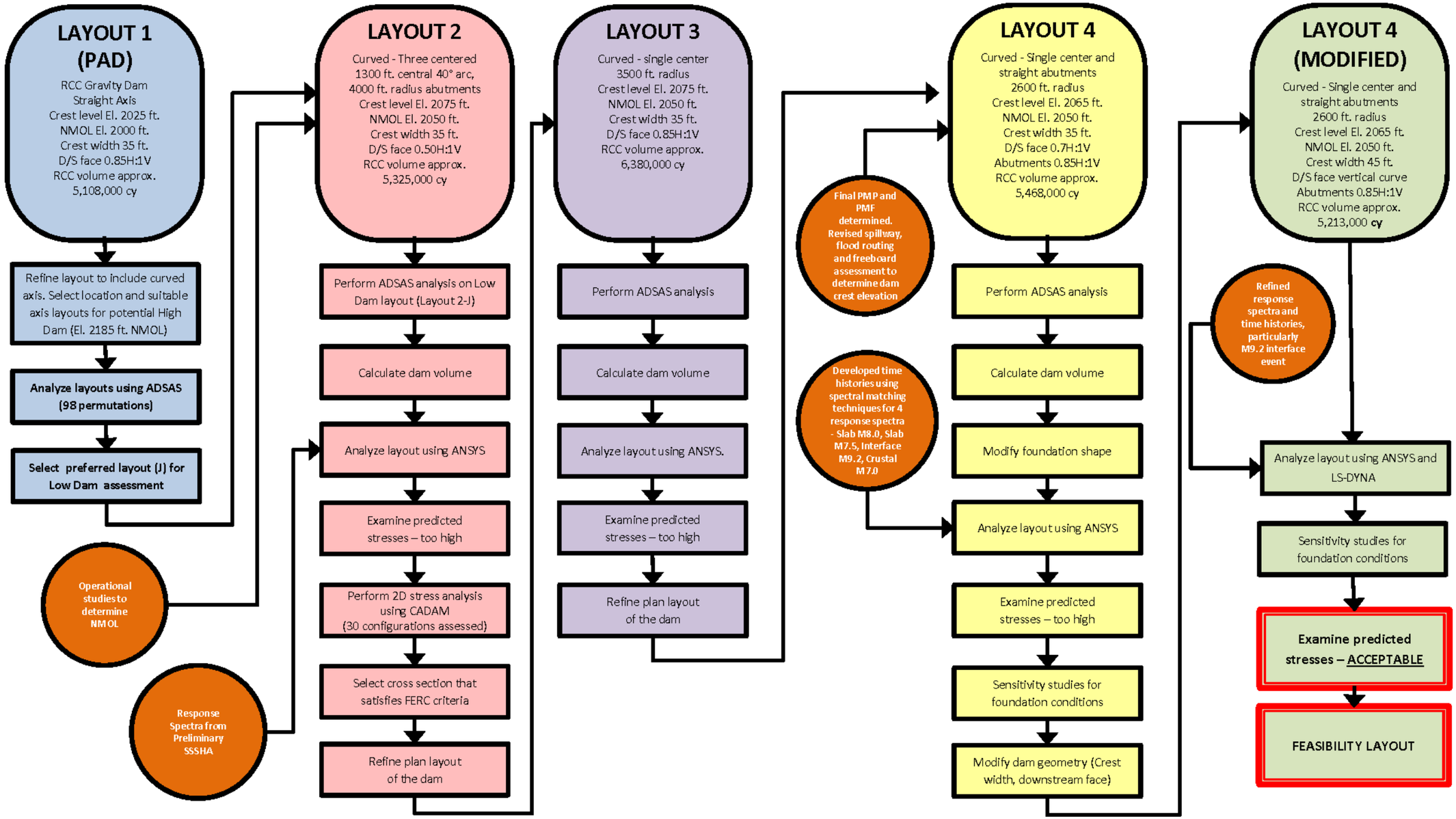

Figure 10.5-1. RCC Dam Configuration Evolution

10.5.2. Pre-application Document (PAD) Dam (Layout 1)

During the preparation of the PAD, three alternative dam types were considered: ECRD, CFRD and RCC. The project layout also considered the location of the powerhouse: surface vs underground. The findings of the assessment of the various layouts based on the various dam types, and described in Section 7, concluded that the most economic arrangement was found to be based on a RCC dam and a surface powerhouse at the toe of the dam. The dam detailed in the PAD had a straight axis with a vertical upstream face and a downstream face sloping at 0.85H:1V (Layout 1). The intakes to the power waterways and low level outlet were located on the upstream face of the dam and the spillway was integral to the dam on the north (right) side of the river channel.

10.5.3. Optimization of Dam Configuration

10.5.3.1. Gravity Dam – Layout Optimization Sequence

Following submission of the PAD the design of the RCC dam was revisited with the aim of optimizing the layout to reap benefits in terms of reduced concrete volume, while maintaining stability and safety, thereby reducing cost and minimizing the construction schedule. The optimization focused on the reduction in concrete volume while ensuring a structurally sound and safe dam.

The optimization of the dam initially focused on steepening the downstream face of the straight axis dam. The straight axis dam solely relied upon the weight of the structure to resist the forces applied by the impounded reservoir.

The examination of possible configurations was performed both using the expected NMOL of the pool and also for a higher dam with a NMOL equivalent to the Stage 3 proposal in the 1980s. The analysis of the higher dam was performed so that any design decisions for the dam proposed in this report would not preclude future raising.

The project site is remote and necessitates a significant investment in infrastructure to enable transportation of materials, plant, and construction workers to and from the site. Any reduction in imported materials could noticeably reduce the capital cost. In addition, the costs of maintaining the construction infrastructure, feeding and housing the workers, and maintaining the required supply chain will be extraordinarily high, so shortening the construction period is paramount. Any reduction in the time for construction would allow generation to commence earlier to commence revenue flows.

The most significant potential optimization of the project is founded on a reduction in the volume of concrete to be placed. Savings could accrue in the direct cost of the cement, fly ash, and the aggregate processing as well as the reduction in the time on site and thus the establishment costs.

The derivation of the proposed configuration is described below and has been an attendant iterative process aimed at selecting a configuration that is safe and (following the applicable optimization and detailed design) will be proven to perform within FERC, and other, guidelines at reasonable cost. The intent in this report is not to finally design all aspects of the dam shape or completely resolve all aspects of the dam shape and performance, so the level of detail of the various analyses is somewhat less than would be undertaken in final, detailed design.

The first challenge in the exercise was the lack of sufficient site investigation focused on the projected dam foundation. Detailed design of an RCC dam will require focused and specific site investigation, including the excavation of adits in the abutments to afford visual examination, mapping and in-situ testing of the rock mass.

Subsequent to the straight axis RCC gravity dam (Layout 1) included in the PAD, three additional configurations have been examined for the dam (Layouts 2, 3, and 4). Each configuration is classified as a curved gravity dam – i.e., the dam relies on its weight for the largest contribution to its stability, but also utilizes some horizontal arch action to enhance the stability and structural performance. Each configuration had a different curvature and slope of the downstream face, and each was located most favorably to the topography and existing rock conditions (e.g., avoiding certain geologic features) as understood at the time each was developed.

10.5.3.2. Three-centered Curved Dam (Layout 2)

To investigate the possibility of further steepening of the downstream face, beyond that for a gravity structure, the introduction of a curve in the dam plan was investigated. The inclusion of a curve in the dam axis would enable transfer of limited loading to the abutments. The configuration of the curved axis was selected assuming (based on the previous investigations) competent bedrock.

Unlike a gravity dam where the structure could be analyzed as a 2-D structure, the assessment of load transfer to the abutments required a 3-D structural analysis.

The configuration was selected based on extensive modeling of 13 possible dam geometrics using the Trial Load Method as described in Section 10.5.3. The computerized version of the Trial Load Method, ADSAS (Arch Dam Stress Analysis System) provides a rapid means of

analyzing the 3-D stress distribution within a dam based on static loads. The 13 possible geometrics comprised a range of radii using different downstream face slopes from 0.3 H:1V to 0.85H:1V. Ninety eight different combinations were examined, including the PAD layout (straight dam) which was designated 'N'. Each run of ADSAS provided upstream and downstream arch, cantilever and principal stresses and a volume of concrete. The most promising arrangement was chosen for a more detailed analysis, using FE analysis for both static and dynamic loading.

The selected geometry comprised a three-centered dam utilizing a downstream slope of 0.5H:1V, a center arc of 40°, and a radius of 1,300 ft., together with flank radii of 4,000 ft. (configuration J).

The preliminary FE analysis procedure is described in Section 10.6 below and the results verified the static results of the ADSAS analysis while recording slightly higher than anticipated stresses during the dynamic loading condition. Following the presentation of the preliminary results to the Board of Consultants in March 2013 it was decided to review the configuration presented to increase the gravity contribution to the stability of the structure.

10.5.3.3. Single Curvature Gravity Dam (Layout 3)

A single curvature gravity dam was developed (Layout 3) to increase the dam's reliance on gravity for stability.

A radius of 3,500 ft. was adopted so that the single curvature structure was positioned symmetrically in the valley and performs predominantly as a gravity structure although with limited benefit realized by load transfer to the abutments. The maximum cross section of the dam was analyzed in 2-D using the Computer Analysis of Dams (CADAM) software to determine the section properties necessary to satisfy FERC stability criteria. CADAM demonstrated that a vertical upstream face and a downstream face sloping at 0.85H:1V was appropriate to satisfy the criteria and was then analyzed using ADSAS and FE analysis.

As noted, the performance of the abutments under load, and the significance of any features in the foundations will be examined more fully following future site investigations.

Layout 3 was considered to be conservative and represents the upper bound of the spectrum of possible configurations, but a reconfiguration from Layout 2 to Layout 3 resulted in approximately one million extra cubic yards of RCC being needed for the dam. Layout 2 is considered the lower bound option of the appropriate dam, so a plot of volume versus height was made for the two configurations (single centered and three centered curves) to indicate a final direction of study for this stage of optimization. These curves are included as Figure 10.5-2 and

show the general range of dam height vs. volume towards which the optimization was then directed.

Using input from the project hydrological studies with respect to the eventual desirable storage, a target volume of RCC of between 5.4 and 5.6 million was selected. With reference to Figure 10.5-2, the maximum crest elevation for the dam would be between El. 2040 ft. for Layout 2 and El. 2075 ft. for the Layout 3 configuration.

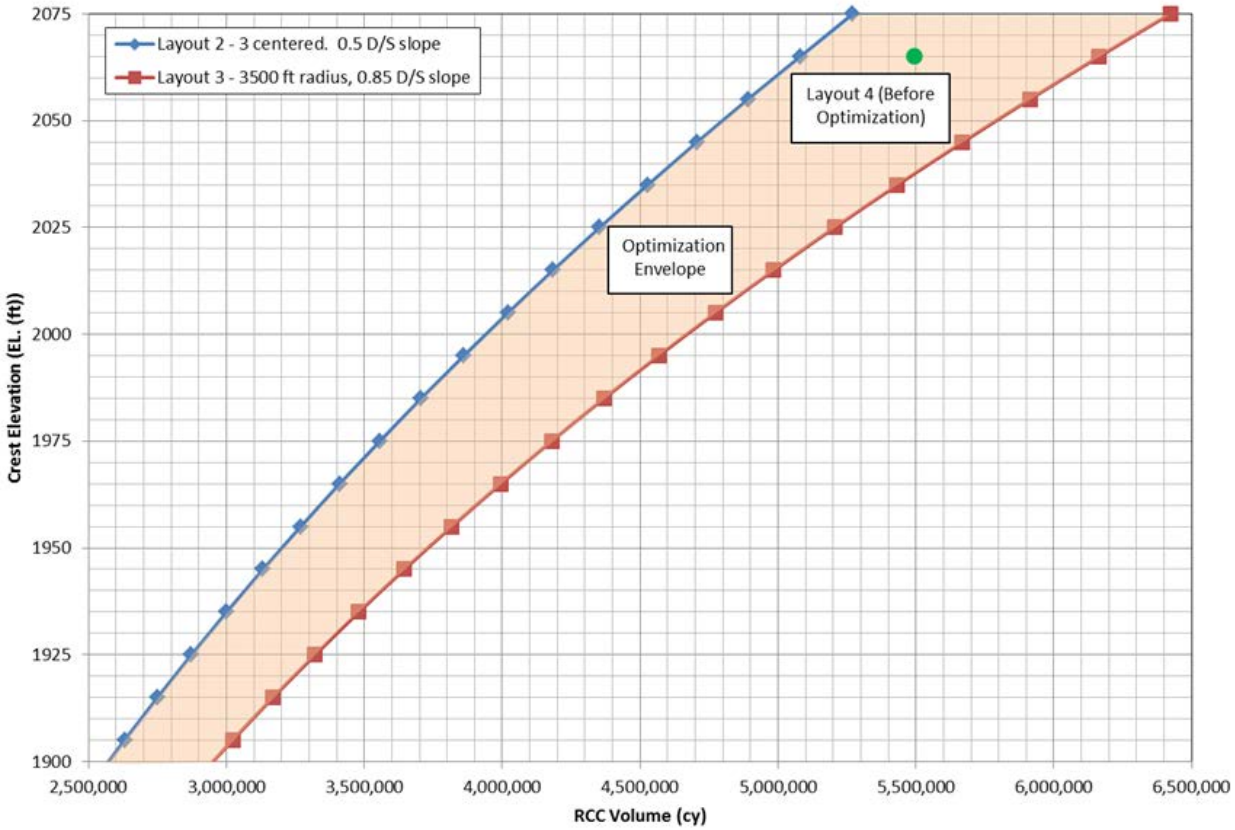

Figure 10.5-2. RCC Volume, Dam Layouts 2 and 3 showing Layout 4 before Optimization

The final selected operational rules for use of the low level outlet – and the surcharge required to pass any selected discharge without opening the gates – are key elements in determining the dam height, as the normal freeboard will be the total of the required surcharge for the use of the low level outlet plus any PMF surcharge. For a NMOL of El. 2050 ft. a total surcharge for both conditions would likely be a maximum of 15 ft. This assumption resulted in a dam crest of El. 2065 ft. being selected.

10.5.3.4. Single Curvature Gravity Dam with Straight Axis Abutments (Layout 4)

Although the construction cost estimate prepared at the end of 2013 included the single radius dam, it was recognized that if the total RCC volume could be reduced to approximately 5.5 million cubic yards or less, then a full season of construction could be eliminated and substantive reductions in project cost achieved. Using the original comparison of volumes for the high dam, a compromise among Dams A, D, and E appeared promising, so a layout was prepared for a single radius for the central part of the dam of 2,600 ft., together with straight gravity sections on either end. By using this combination, the dam foundation footprint remains almost exactly the same as that of Layout 3, and the right abutment location does not change. The left abutment rotates slightly downstream, but is judged to be acceptable – at this level of geotechnical knowledge of the site.

The updated configuration (Layout 4) for the Watana Dam thus comprised a central portion with an axis radius of 2,600 ft. The dam axis changes to a straight line at a tangent point and continues to the abutments.

The crest of the dam is 35 ft. wide, and at El. 2065 ft. is 10 ft. lower than previous iterations. This 10 ft. lowering of the crest level resulted from a reassessment of the flood and freeboard requirements for the dam at the completion of the PMP/PMF studies (which was completed part way through this analysis) and after selection of an acceptable reservoir rise of 15 ft. for the efficient use of the low level outlets and for passage of the PMF. The curved section has a downstream face slope of 0.7H:1V and the straight gravity section includes a 0.85H:1V slope on the downstream face. All portions have a sloping upstream face (0.1H:1V) below El. 1770 ft. transitioning to a vertical face above. The change in downstream face slope reflects the reliance on gravity at the abutments.

10.5.3.5. Single Curvature Gravity Dam with Curved Downstream Face (Layout 4 – Modified)

Following FE analysis of Layout 4 as described in Section 10.6.6.4, the dam configuration was further modified to increase the width of the dam crest to 45 ft., and the downstream face of the curved section of the dam was modified from a straight sloping section to a single radius curve.

The dam geometry selected for the modified Layout 4 is shown in Figures Figure 10.7-2 and Figure 10.7-3.

The inclusion of a single radius curve to the downstream face of the curved portion of the dam results in a further reduction in the volume of RCC required to construct the structure. The

estimated RCC volume for the modified Layout 4 (final) configuration was calculated and the predicted volumes are shown in Table 10.5-1.

Table 10.5-1. RCC Volume (Layout 4 – modified)

Section	RCC Volume (cy)
Left Abutment	595,600
Center	3,706,340
Downstream fill	125,260
Right Abutment	786,750
Total	5,213,950

The Layout 4-modified configuration results in a reduction of more than 254,000 cy of RCC relative to Layout 4; this would result in a one month reduction in the placement schedule.

10.5.4. Curved Alignment Analysis

10.5.4.1. Trial Load Method

Unlike a gravity dam, where the structure could be analyzed as a 2-D structure the assessment of load transfer to the abutments associated with a curved dam requires a 3-D structural analysis. The structural analysis of a curved gravity dam required the use of proprietary modeling software to analyze the distribution of stresses within the body of the dam.

The examination of the benefits of introducing curvature into the dam design was accomplished by the use of the traditional Trial Load Method analysis which allowed a first pass at the optimization of the curvature and downstream slopes of the structure before embarking on a more detailed FE analysis of the structural performance of the selected dam configuration. A FE Model does not readily lend itself to alteration, thus any adjustment (trial and error) in geometry is a time consuming exercise.

The Trial Load Method is a process developed by the Bureau of Reclamation from 1923 to 1935. The analysis was performed using the ADSAS a computerized version of the trial load method approach which utilizes a matrix solution in arriving at the proper division of load between vertical and horizontal elements.

The trial load method assumes that the dam is divided into a system of vertical and horizontal elements with each system occupying the entire volume of the dam and independent of the other. The loads applied to the dam are then divided between these systems in such a way that geometrical continuity is attained throughout the structure. Representative horizontal elements

and vertical elements are selected to be used in the analysis (see Figure 10.5-3). The conditions of deformation for a 3-D structure may then be expressed in terms of three mutually perpendicular linear displacements and three angular displacements.

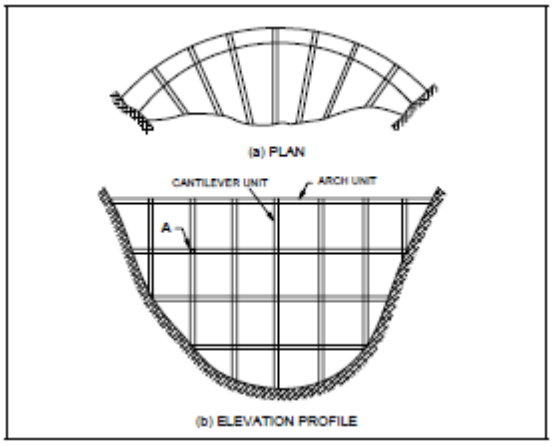

Figure 10.5-3. Typical Elements Used in the Trial Load Method

The requirements for a correct solution of this analysis may be inferred from the Kirchhoff uniqueness theorem in the theory of elasticity. These requirements are:

- The elastic properties of the solid must be completely expressible in terms of two constants: Young's modulus and Poisson's ratio.
- If the volume of the solid in the unstressed state is divided into small elements by passing intersecting surfaces through it, each element must remain in equilibrium.
- Each of these elements must deform as the solid passes into the stressed state so that it will continue to fit with its neighbors on all sides.
- The stresses or displacements at the boundaries of the solid must conform to the stresses or displacements imposed.

The basic assumptions necessary for the method are:

- The concrete of the dam is homogeneous, isotropic, and uniformly elastic material.
- Vertical displacements caused by dead load, shrinkage, and temperature changes prior to joint closure, take place in the cantilever elements before arch action commences, so that no lateral transfer of these effects occurs.
- Stresses calculated from the final load distribution on the selected elements represent the stresses in the dam for the assumed loading.

The 1980s studies had recommended a NMOL of El. 2185 ft. as the ultimate development at the site. In order that any site development option chosen for the current licensing (and construction) would not preclude a future generation from raising the dam, the trial load analysis was initially performed for a NMOL of El. 2185 ft. The results of the analysis were then used to identify a suitable configuration that was then analyzed again with a NMOL of El. 2000 ft. Completion of the power operations modeling studies eventually concluded that the NMOL would be El. 2050 ft.

10.5.4.2. Material Properties and Loads

Material properties used in the ADSAS analysis were:

Sustained modulus of elasticity of concrete:	4,000,000 psi
Poisson's ratio for concrete:	0.25
Unit weight of concrete:	150 pcf
Compressive strength of concrete:	4,500 psi
Deformation modulus of the foundation rock:	4,000,000 psi
Poisson's ratio for rock:	0.33

At this conceptual stage of analysis, dead loads and static water loads were included. Thermal, sediment, ice and seismic loads were not considered, but the examination of the output of the analysis was made with the understanding that the stresses could be somewhat higher than generated (i.e., decisions were taken conservatively).

10.5.5. Analytical Development

The first conceptual layouts developed were based on a single curvature, of 1,800-ft. radius, chosen from experience and with regard to the projected rock contours (from the 1980s investigation) at the dam foundation. The radius was selected with respect to a final crest elevation of approximately El. 2025 ft. from the previous HDR studies. Horizontal angles of intersection between the downstream face of the dam and the contour line of competent rock of 30° or less was used as the guideline for establishing the orientation and abutment conditions. A 1,800-ft. radius ensured angles of contact less than the critical value.

Based on the first ADSAS analysis, unacceptable tensile stresses were evident in the horizontal (arch) elements at the downstream face. To address this unacceptable tensile stress, the radius of curvature was reduced to 1,300 ft. with a transition to a 4,000-ft. radius at each flank. The three-centered arrangement was used in all subsequent runs of ADSAS, with a NMOL of El. 2185 ft.

(and a dam crest elevation of El. 2210 ft.) representing the largest development that could reasonably ever be constructed at the site.

So that the most suitable dam configuration was eventually modeled in the FE analysis, various dam alternatives were assessed. In total 98 alternative configurations were considered (including different downstream slopes) to identify the optimum arrangement.

10.5.6. Preliminary Design Criteria – Structural Analyses

The design parameters used in the analyses for all layouts were selected to be sufficiently conservative that the eventual criteria adopted after a full site investigation (which is yet to be performed), such as foundation conditions, material properties, etc., would not cause substantial reworking of the layout or cross section at the detailed design stage. The material properties and parameters used in the analyses are presented in Table 10.5-2 below. Parameters were revised as the analyses progressed and the dam geometry was refined.

Table 10.5-2. Preliminary Dam Design Parameters for Layout Development

Design Data – Dam	
Crest of dam	El. 2075 ft. (initial)
Crest width	35 ft.
Crest length	3,094 ft.
Upstream face	Vertical
Downstream face (sloping section)	0.5H:1.0V (initial)
Structural height at maximum section	705 ft.
Design Data – Water Surface Elevations	
Normal maximum water level	El. 2050 ft.
Flood surcharge level	El. 2067.1 ft.
Tailwater – Normal	at Foundation Level
Material Properties	
Water	
Unit weight	62.4 pcf

Roller-Compacted Concrete	
Unit weight	150.0 pcf
Unconfined static compressive strength (ASTM C39, C172, C31)	fc' = 5500 psi
Dynamic compressive strength	7150 psi
Static direct tensile strength (ASTM C496)	385 psi
Dynamic tensile strength	580 psi
Friction angle	45°
Static elastic modulus (ASTM C469)	3,000,000 psi
Dynamic elastic modulus	3,900,000 psi
Poisson's ratio	0.25
Coefficient of thermal expansion	0.0000055 / °F
Diffusivity	0.045 sq. ft. / hr.
Foundation Rock	
Unit weight	150 pcf
Static deformation modulus	4,000,000 psi
Dynamic deformation modulus	3,500,000 psi
Friction angle at concrete-rock interface	45°
Cohesion at concrete-rock interface	100 psi
Poisson's ratio	0.25
Unconfined compressive strength (intact rock)	17,750 psi
Tensile strength (intact rock)	1,845 psi
Specific heat	0.20 btu/lb./°F
Thermal conductivity	1.0 btu/lb./°F

Note: ASTM – American Society for Testing and Materials

10.5.7. Two-Dimensional Gravity Analysis

As the dam would predominantly act as a 2-D structure, various cross sections were analyzed using CADAM dam stability analysis software. The software was developed by the research group on dam safety at École Polytechnique, University of Montreal, Canada, for static and seismic stability analysis of concrete gravity dams. The software is based on the gravity method using rigid body equilibrium and beam theory to perform a stress analysis, compute crack lengths, and sliding safety factors. Seismic analysis can be performed using either the pseudostatic or a simplified response spectra method. The analysis was performed to estimate the cross-sectional geometry that would satisfy stability criteria for the usual and unusual load cases required by the FERC Engineering Guidelines for the Evaluation of Hydropower Projects,

Chapter 3, Gravity Dams. The simplified analysis was also used to assess the potential for cracking at the base of the dam as the result of a seismic event.

10.5.8. Finite Element Modeling of Dam

10.5.8.1. Background and Approach

The configurations of the dam determined from preliminary stress analysis were subsequently analyzed using FE methods.

The FE structural and thermal analyses were performed generally in accordance with the FERC *Engineering Guidelines for the Evaluation of Hydropower Projects*, Chapter 11, Arch Dams.

The FE studies performed in the preparation of this report were intended to:

- extend the understanding of the dam performance from the results of the Trial Load Method analysis;
- verify the layout and cross section of the dam throughout configuration development, including seismic loads;
- study the thermal performance in sufficient detail that the construction planning can be completed in greater detail;
- identify the necessity for and extent of the next stage of site investigations of the foundation; and,
- confirm that the selected cross section and layout "does no harm" to any future generations consideration of raising of the dam.

10.5.8.2. Progression of Finite Element Analyses

FE studies performed for Layouts 2, 3 and 4 are described in Sections 10.6 and 10.7. Results from each analysis were used to refine the dam geometry and to further develop the layout for the subsequent analysis.

Dam Layout 2 was analyzed using ANSYS and the linear response spectra method. Layouts 3, 4, and 4(Modified) were analyzed using ANSYS and the nonlinear time history method. Layout 4 (Modified) was then analyzed using the nonlinear time history method and LS-DYNA, including mass in the foundation.

10.6. Dam – Preliminary Analysis

10.6.1. Initial Dam Configuration (Layout 2)

As noted above, multiple alternatives (14 including the straight-axis PAD layout) were first considered and each alternative was analyzed for the potential ultimate development of the dam to a crest level of El. 2190 ft. using ADSAS. Downstream face slopes ranged from 0.3H:1V to 0.85H:1V. Ninety-eight permutations were considered in total. The dam configurations analyzed are described in Table 10.6-1.

Table 10.6-1. Analyzed Dam Plan Configurations for Layout 2 (high dam)

Dam	R_{axis} (Feet)		Center Arc Angle (Degrees)	Crest Length (Feet)
	Middle Section	Outer Sections		
A	1800	Straight	91.3	4543
B	2000	Straight	79.8	4335
C	2200		-	4350
D	2400		-	4251
E	4000		-	3979
F	1300	4000	30	4241
G	1500	4000	30	4171
H	1700	4000	30	4150
I	1800	4000	30	4133
J	1300	4000	40	4426
K	1500	4000	40	4391
L	1700	4000	40	4287
M	1800	4000	40	4252
N*	Straight		-	3805

*Dam N was the straight-axis configuration in the PAD

The ADSAS software cannot model straight axes, so an approximation was made using a radius of 999,999 ft. This technique was used to model the outer portions of the dam for the Dam A, B, and N alternatives.

After the analysis of the "high" dams (a possible ultimate development corresponding to the Stage 3 Watana layout included in the 1980s License Application), configurations F and J were identified as preferred, with a downstream face at 0.5H:1V. A steeper downstream face resulting in a thinner vertical cross section would result in a significant transfer of stresses from the vertical to the horizontal plane which would result in the dam no longer performing completely as a gravity structure. These two alternatives, along with Dam N were then assessed for the low

dam configuration being studied at this time for downstream slopes ranging from 0.4H:1V to 0.6H:1V.

The preliminary stress analysis did not take into account seismic or thermal loads which could affect the stress values negatively. As analyzed, both dams F and J were satisfactory alternatives as analyzed. However, the result of the addition of these extra loads would be less pronounced for Dam J, and it was therefore selected as the configuration for further analysis.

Thus the selection of alternative J for "Layout 2" consists of a central portion with a curved axis of 1,300 ft. radius which changes to a 4,000 ft. radius at a tangent point on the abutments. The downstream face is a uniform slope of 0.5H:1V and the upstream face is vertical. The central portion is defined by a phi angle of 40°. The dam crest for Layout 2 remains at El. 2075 ft.

10.6.1.1. Arch Dam Stress Analysis System (ADSAS)

ADSAS was used in advance of FE analysis to limit the time spent performing multiple seismic analyses at this feasibility stage of design, and the results of the ADSAS analysis provided a level of confidence that the selected dam cross section would be capable of withstanding the expected seismic loads.

The results of the analysis of alternative J (Layout 2) are shown in Figure 10.6-1 for the crown cantilever.

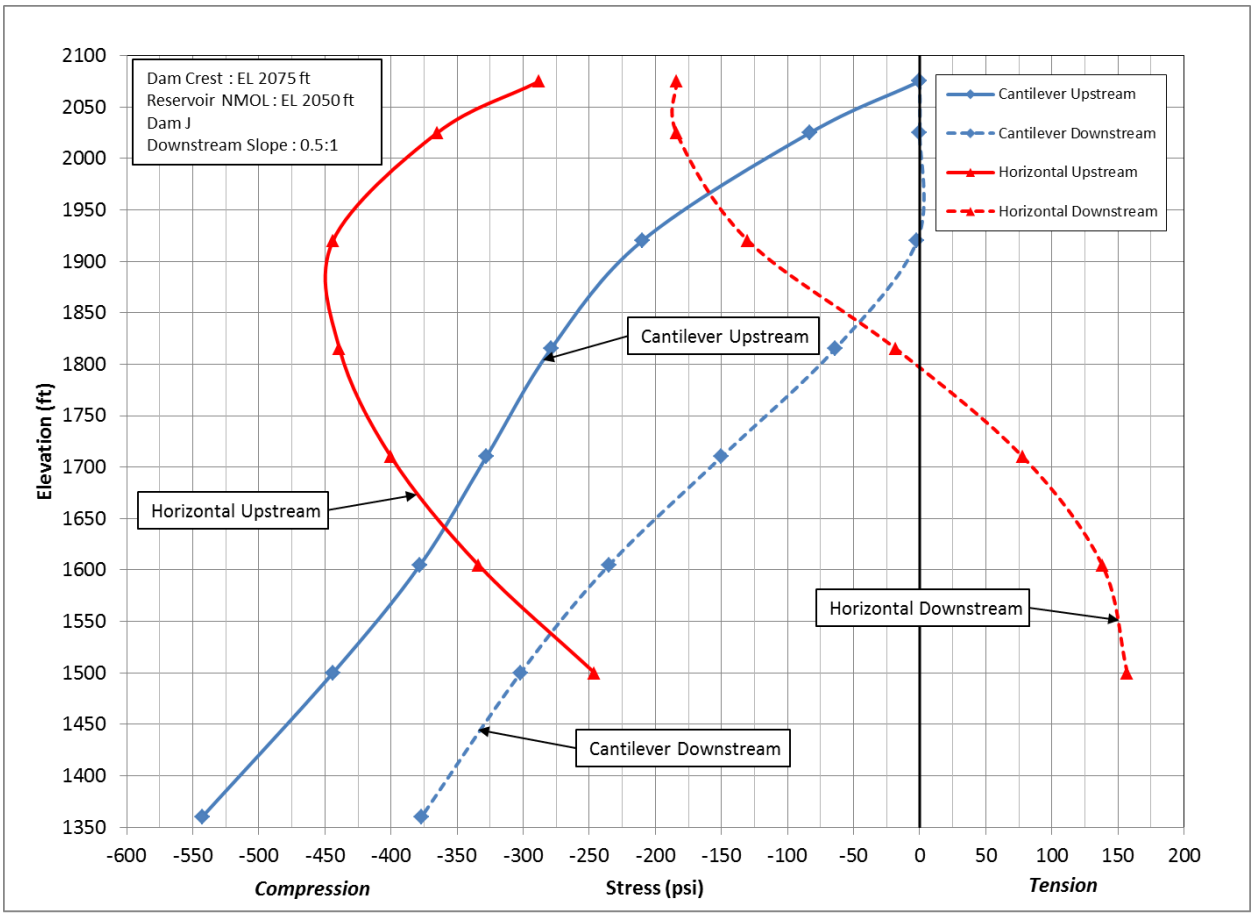

Figure 10.6-1. Layout 2 (Dam J) – Crown Cantilever Stresses

10.6.1.2. FE Structural Analysis

The 3-D static and dynamic FE analyses of Dam Layout 2 were performed using the FE analysis program ANSYS, Version 14. ANSYS is a state-of-the-art commercially available general FE method program, which is widely used as an analytical tool for static and dynamic evaluations of dams.

The ultimate development height of the dam was not dynamically analyzed because it is assumed that the results of the ADSAS calculations give sufficient indication that a safe dam raising is feasible in the future. The only major aspect of the current project that would depend on the requirements for future raising is the distance between the downstream toe of the dam and the powerhouse. It is considered that for the accuracy of the project estimates at this time, the ADSAS analysis was sufficient. During detailed design it is recommended that one analysis be performed of the postulated high dam to verify the required separation of the powerhouse and dam.

A linear FE model was created consisting of 5160 elements and 6658 nodes. Mostly hexagonal ("brick") elements were used, while prism ("wedge") elements were utilized in portions of the model where the geometry was not regular. The dam and rock foundation elements used in the model consisted of 8-node elements, with one node at each corner. Three-dimensional mass elements (added mass) attached to the nodes of the elements on the upstream face of the dam were used to simulate hydrodynamic effects of the reservoir. The weights of the added masses on the dam face were computed as noted below.

The FE method model of the dam comprises four elements in thickness and 20 vertical columns of elements at the crown cantilever. The rock foundation was modeled to a depth equal to the height of the dam, a width equal to three times the dam height and a length equal to the dam height in the upstream and downstream directions. The elements of the dam body are connected directly to the elements of the foundation neglecting any possible separation (opening) at the dam-foundation interface due to applied loadings. This model is shown in Figure 10.6-2 and Figure 10.6-3.

The rock foundation of the FE method model was assigned stiffness in accordance with the review of existing boreholes and engineering properties of rock determined from laboratory testing and similar materials by the project geological engineers – but was assigned no mass. A massless foundation allows for transmission of the seismic ground motion time history from the boundary of the model to the dam foundation. Thus the inertial effects of the foundation mass were not included, leading to a conservative transmission of energy and an overestimate of the seismic force applied to the dam. This was rectified later in subsequent studies when mass was added to the dam foundation as discussed in Section 10.7.

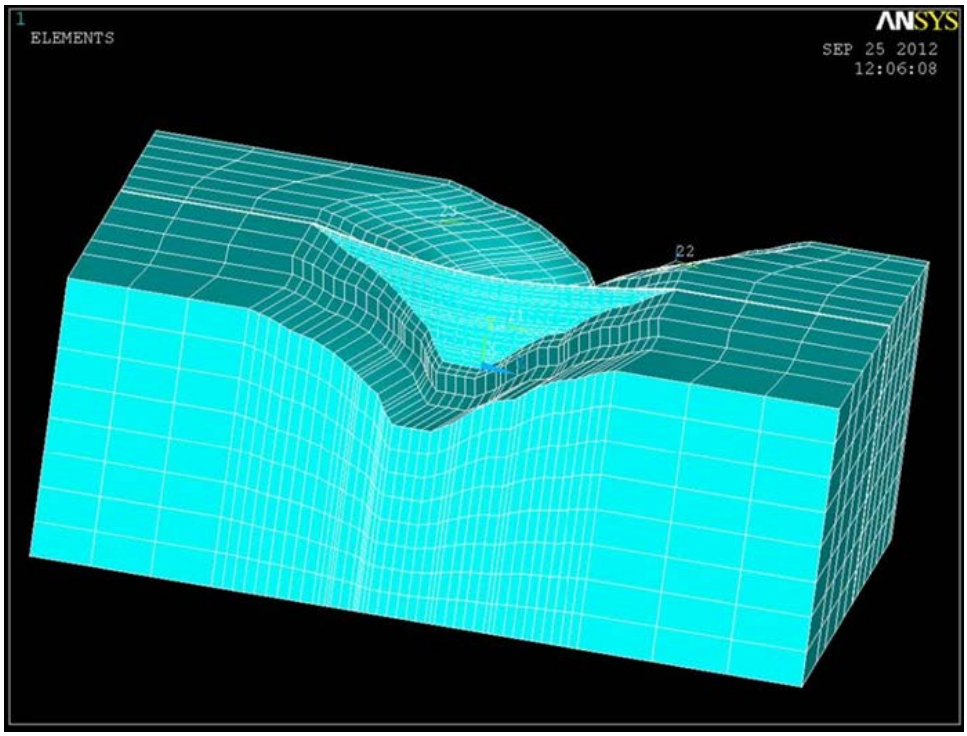

Figure 10.6-2. Finite Element Model Upstream Side (Layout 2)

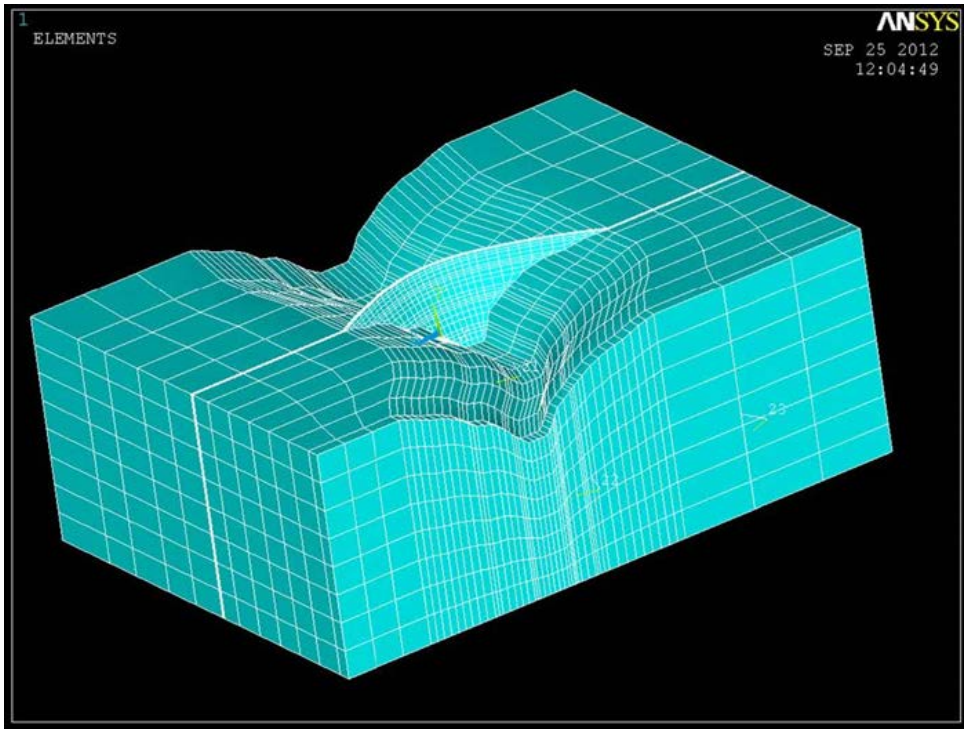

Figure 10.6-3. Finite Element Model Downstream Side (Layout 2)

10.6.1.2.1. Dead Loads

The gravity load was applied as a gravitational acceleration of 32.2 ft./sec^2. The weight of the dam was based on the average density of concrete of 150 lbs./ft^3. Loading due to silt was not considered in the analysis. No gravity loads from the foundation were included, as the foundation elements were assumed to be massless, and simply provided stiffness in the model.

10.6.1.2.2. Hydrostatic Load

The hydrostatic reservoir load was applied in the model as a distributed force load on the dam face based on the maximum normal operating pool reservoir condition of El. 2050 ft. No flood, overtopping, or any other reservoir level fluctuation and resulting load combination was considered in the dynamic analysis.

10.6.1.2.3. Internal Hydrostatic Loads (Uplift)

Uplift pressure at the dam-foundation interface could affect overall stability of the dam but has limited effect on the dam body internal stress distribution being investigated by the FE modeling. In the model for Layout 2 dam elements were continuously attached to the foundation elements and no uplift pressure was considered – although this boundary condition was modified for later configuration modeling.

10.6.1.2.4. Ice Loads

No ice loads were included in the analysis, but will be considered during detailed design.

10.6.1.2.5. Seismic Loads

Concurrently with the development of the FE models, the site specific seismic hazard analysis was in progress, and so the ground motions used for the analysis have been adjusted slightly as the studies progressed. For the initial dynamic analysis of Layout 2 the linear response-spectrum analysis method was used. The horizontal response spectra shown in Figure 10.6-4 were used in the analyses.

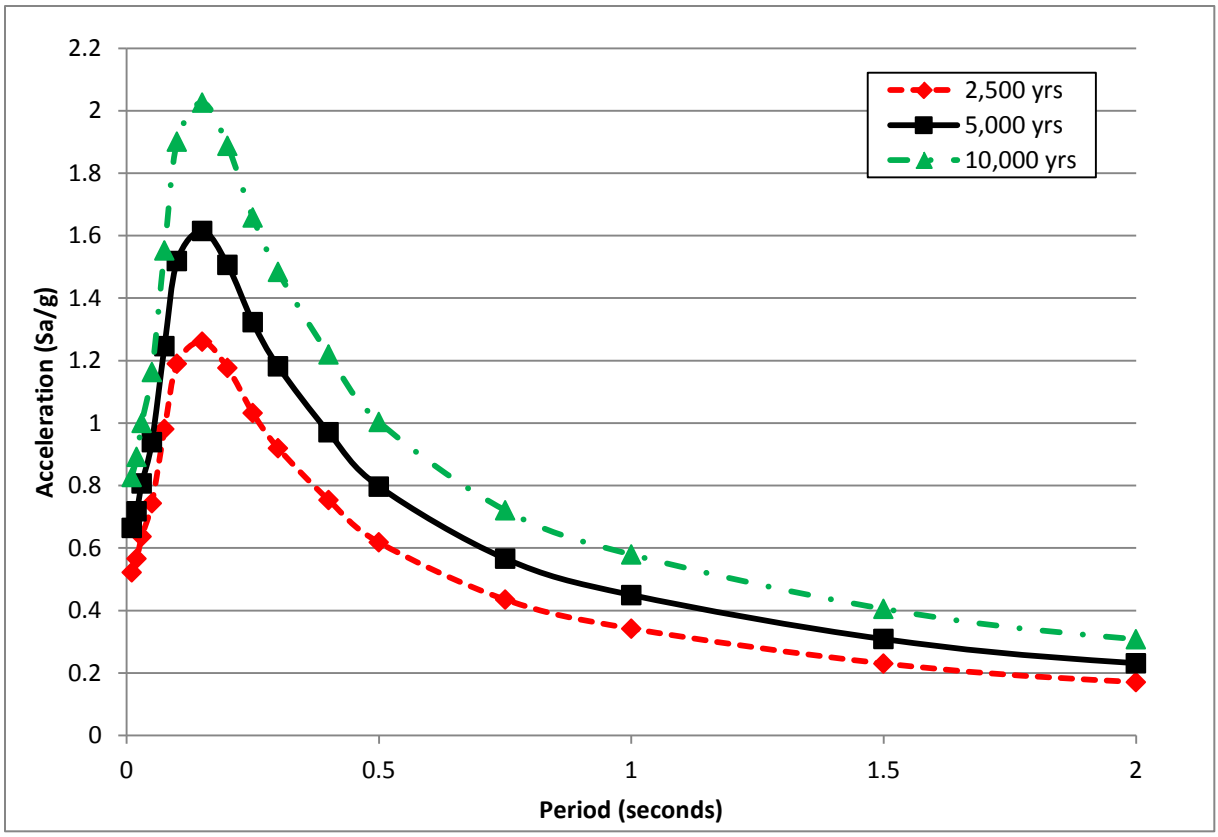

Figure 10.6-4. Response Spectra for Watana Dam Site

An earthquake with 2,500 year return period was adopted as the MCE during the studies performed for Layout 2, with a peak ground acceleration (PGA) of 0.52g. The dam was also analyzed for earthquakes with 0.66g and 0.82g PGA corresponding to the 5,000 yr. and 10,000 yr. event respectively. The return period for the MCE was later modified as the layout development progressed.

10.6.1.2.6. Silt Load

No silt loads were included but will be included in subsequent analysis.

10.6.1.2.7. Hydrodynamic Load

Hydrodynamic reservoir loading on the upstream face of the dam was estimated based on a NMOL of El. 2050 ft. and orientation of each element using the Westergaard method and applied to the model as added masses attached to the upstream nodes for the full reservoir condition.

10.6.1.3. Static Analysis

Analyses using normal static loading were performed and compared with the results of the ADSAS analysis. Some deviations in the stress distribution between the methodologies were observed and were attributed to the way dead load is considered. The trial load method assumes that the dam is built as separate vertical cantilever blocks resulting in the dead load being transferred vertically to the cantilevers with no "arch" action. Elastic FE analysis considers the dam weight as a single block and arch stresses are developed within dam body due to the dam weight. The two-step odd-even cantilever method (described in Section 11-5.2.2 of FERC Engineering Guidelines, Chapter 11 – Arch Dams) was used to analyze the dam for dead loading conditions. The dead load stresses determined using the odd-even cantilever method are in agreement with the ADSAS analysis.

10.6.1.4. Dynamic Analysis

10.6.1.4.1. Modal Analysis

A modal analysis of the dam was performed to calculate the fundamental periods of vibration and mode shapes of the linear model. In response spectra analysis, modal mass is used as an indicator of the number of modes to consider in the analysis. The first twelve natural periods of the dam and respective modal participation mass ratios are shown in Table 10.6-2. The mode shapes for the first six vibration modes are shown in Figure 10.6-5.

Table 10.6-2. Periods of Vibration and Modal Participation Mass Ratio (MPMR) of Dam (Layout 2)

Mode Number	Period	MPMR			Sum of MPMR		
	Sec	U/D	Cross stream	Vertical	U/D	Cross stream	Vertical
1	0.657	0.470	0.002	0.018	0.470	0.002	0.018
2	0.495	0.002	0.074	0.000	0.470	0.076	0.018
3	0.385	0.040	0.000	0.000	0.510	0.076	0.018
4	0.313	0.080	0.005	0.001	0.590	0.081	0.019
5	0.308	0.210	0.010	0.006	0.800	0.090	0.025
6	0.262	0.012	0.003	0.007	0.810	0.094	0.032
7	0.258	0.001	0.700	0.059	0.820	0.790	0.091
8	0.254	0.002	0.061	0.730	0.820	0.850	0.820
9	0.232	0.000	0.001	0.000	0.820	0.850	0.820
10	0.224	0.000	0.001	0.000	0.820	0.850	0.820
11	0.198	0.012	0.000	0.001	0.830	0.850	0.820
12	0.189	0.000	0.000	0.000	0.830	0.860	0.820

Review of the results indicates that the first 12 vibration modes represent more than 80 percent of the total mass of the structure in all directions. Adopting twelve modes in the analysis will adequately approximate the seismic response of the structure at this stage of the design process. More vibration modes would be necessary in final design if this response spectra methodology represented the full extent of simulation, but the use of full time integration (ANSYS and LS-DYNA) – described in section 10.7 – supersedes these calculations.

The fundamental period of the analyzed dam is 0.657 seconds (1.52 cycles/sec.).

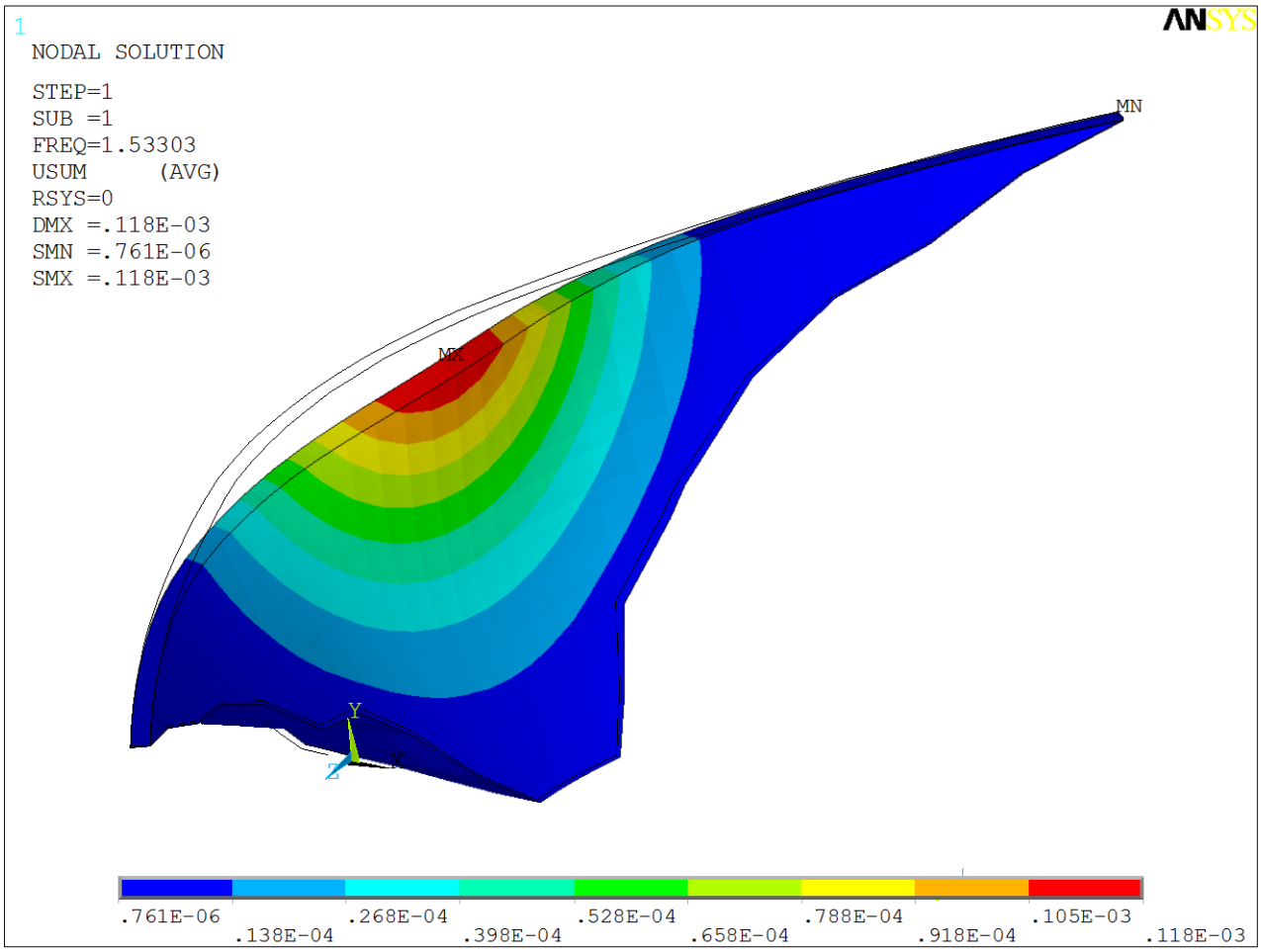

Mode 1

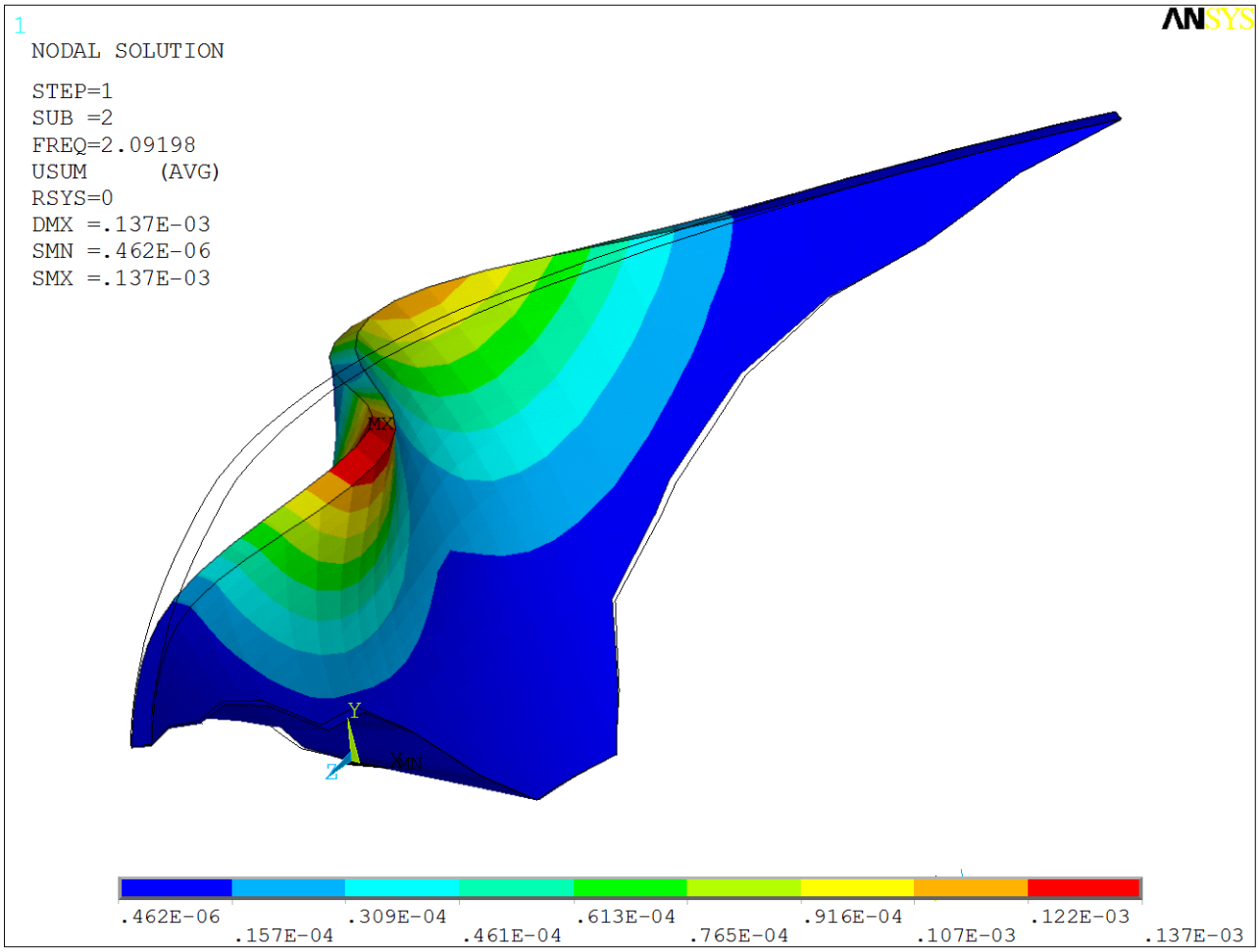
1
NODAL SOLUTION
STEP=1
SUB =2
FREQ=2.09198
USUM (AVG)
RSYS=0
DMX =.137E-03
SMN =.462E-06
SMX =.137E-03
ANSYS
MX
MN
Y
Z
.462E-06
.157E-04
.309E-04
.461E-04
.613E-04
.765E-04
.916E-04
.107E-03
.122E-03
.137E-03

Mode 2

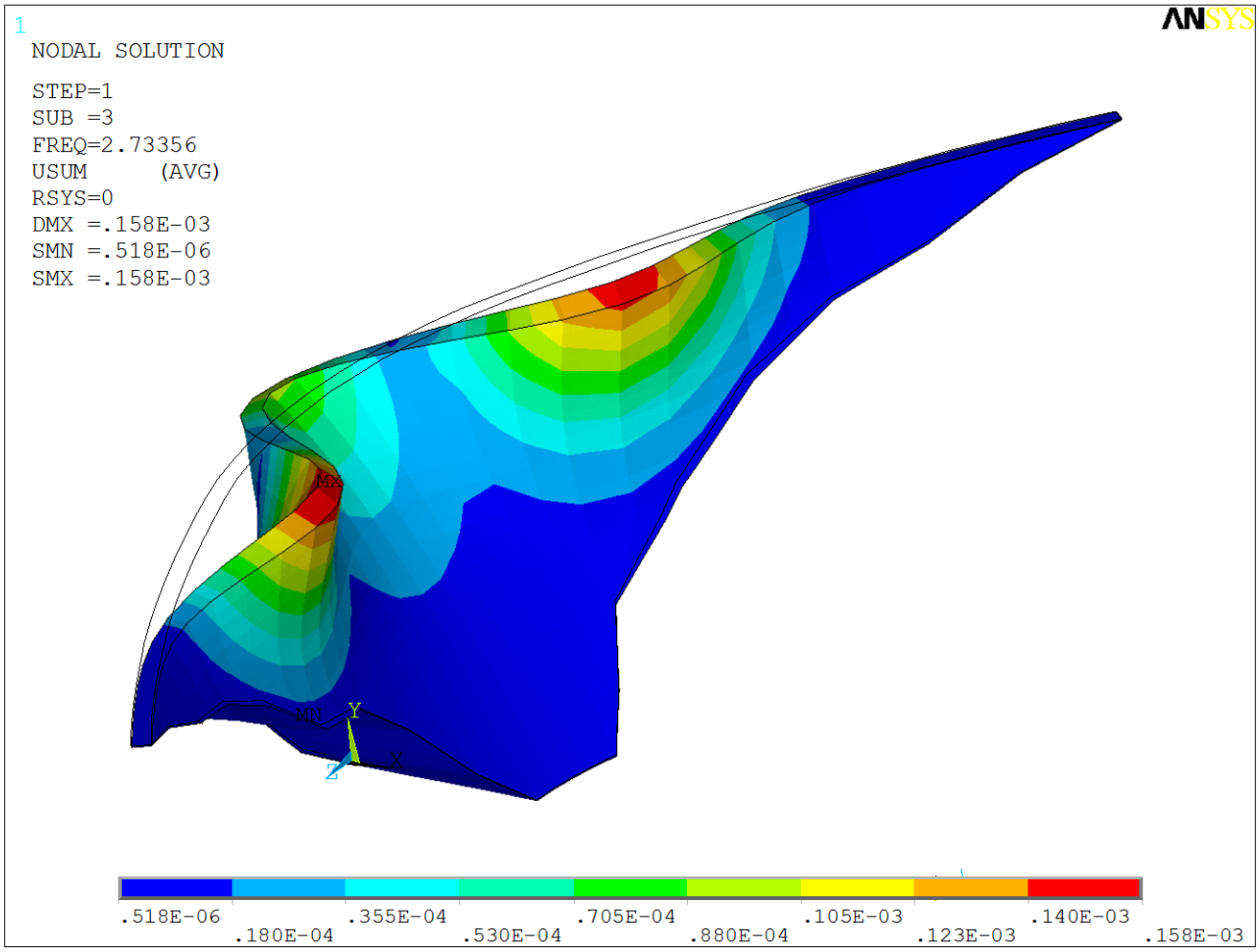
1
NODAL SOLUTION
STEP=1
SUB =3
FREQ=2.73356
USUM (AVG)
RSYS=0
DMX =.158E-03
SMN =.518E-06
SMX =.158E-03
ANSYS
MX
MN
Y
Z
X
.518E-06
.180E-04
.355E-04
.530E-04
.705E-04
.880E-04
.105E-03
.123E-03
.140E-03
.158E-03

Mode 3

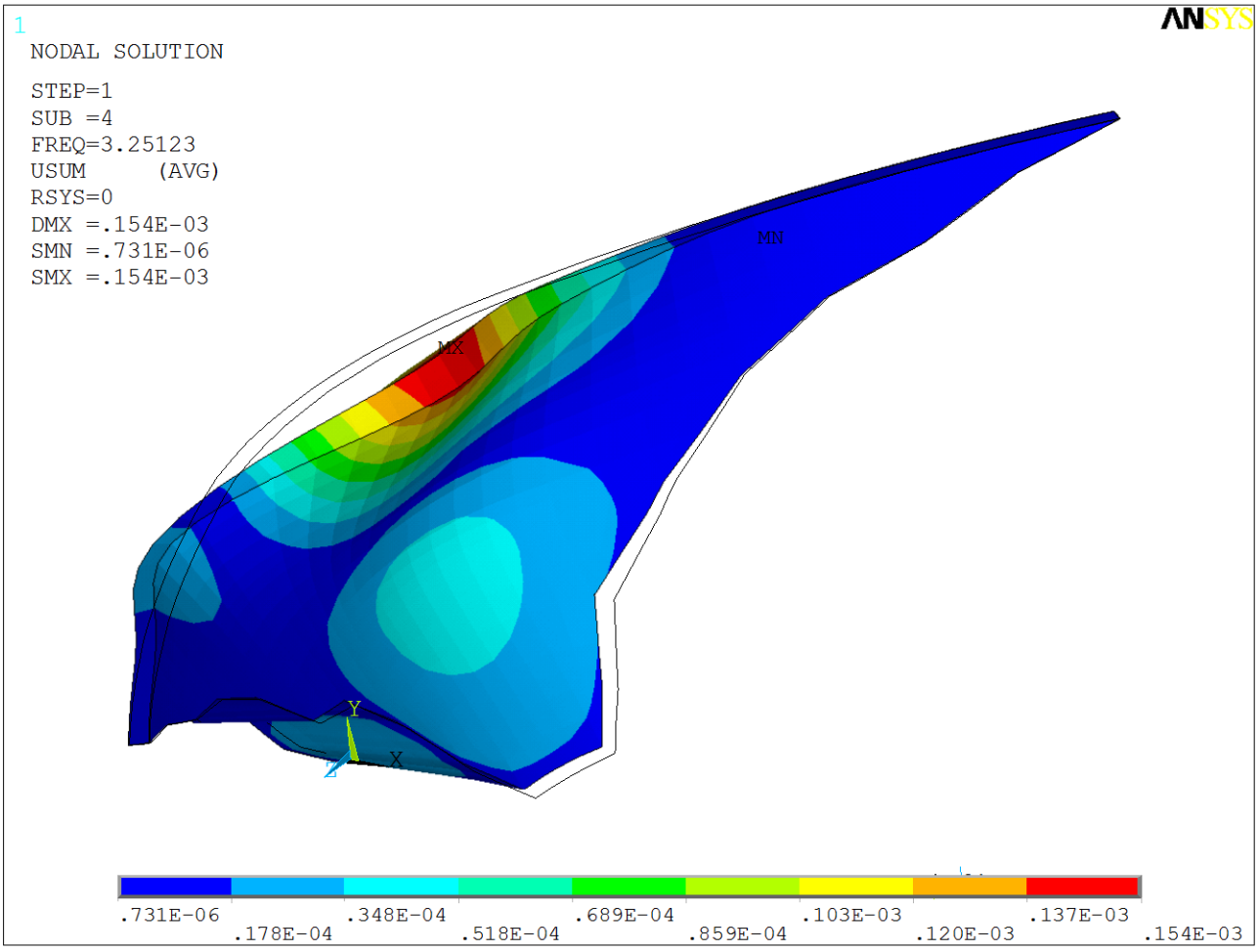
1
NODAL SOLUTION
STEP=1
SUB =4
FREQ=3.25123
USUM (AVG)
RSYS=0
DMX =.154E-03
SMN =.731E-06
SMX =.154E-03
ANSYS
MN
MX
Y
Z
X
.731E-06
.178E-04
.348E-04
.518E-04
.689E-04
.859E-04
.103E-03
.120E-03
.137E-03
.154E-03

Mode 4

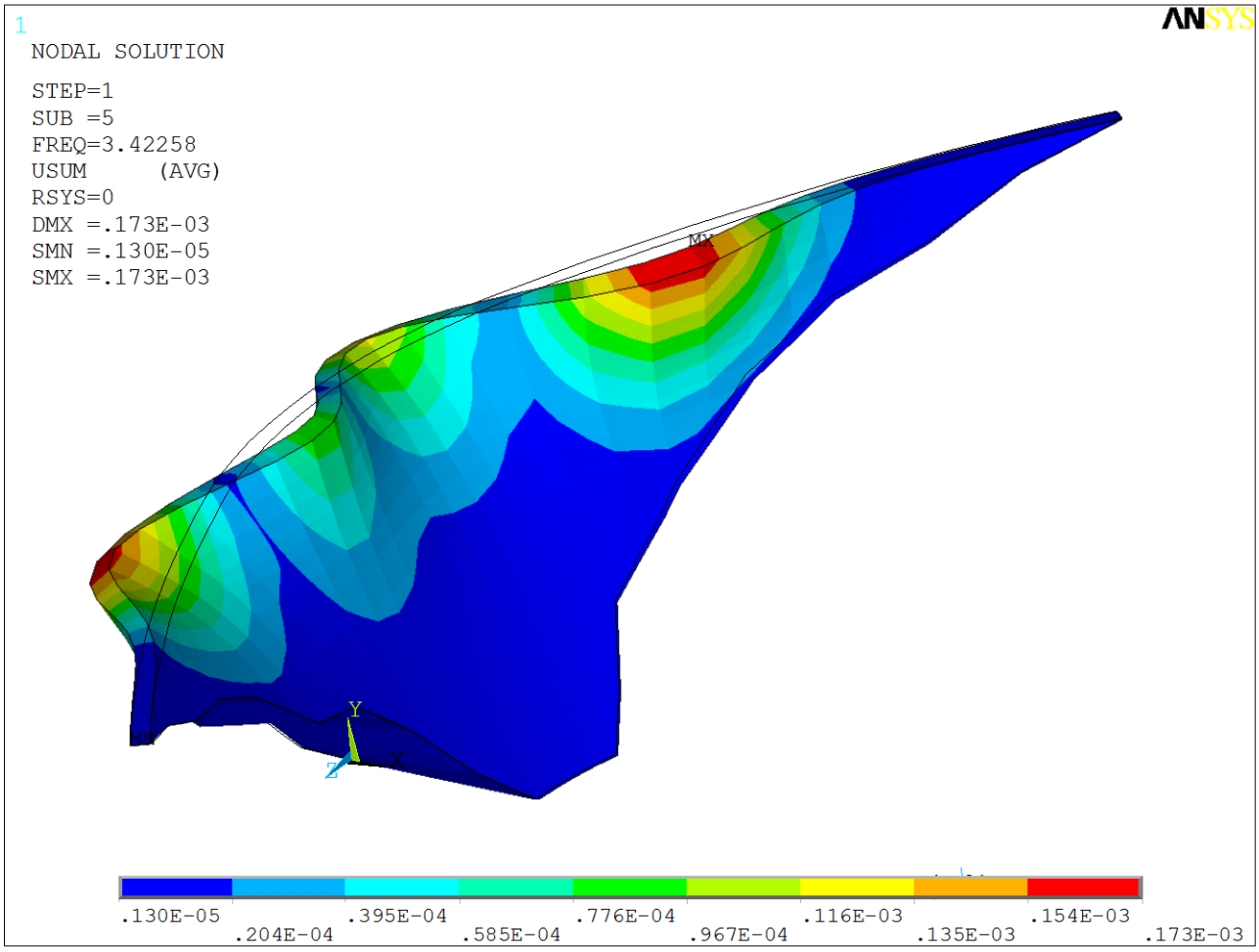
1
NODAL SOLUTION
STEP=1
SUB =5
FREQ=3.42258
USUM (AVG)
RSYS=0
DMX =.173E-03
SMN =.130E-05
SMX =.173E-03
ANSYS
MX
MN
Y
Z
X
.130E-05
.204E-04
.395E-04
.585E-04
.776E-04
.967E-04
.116E-03
.135E-03
.154E-03
.173E-03

Mode 5

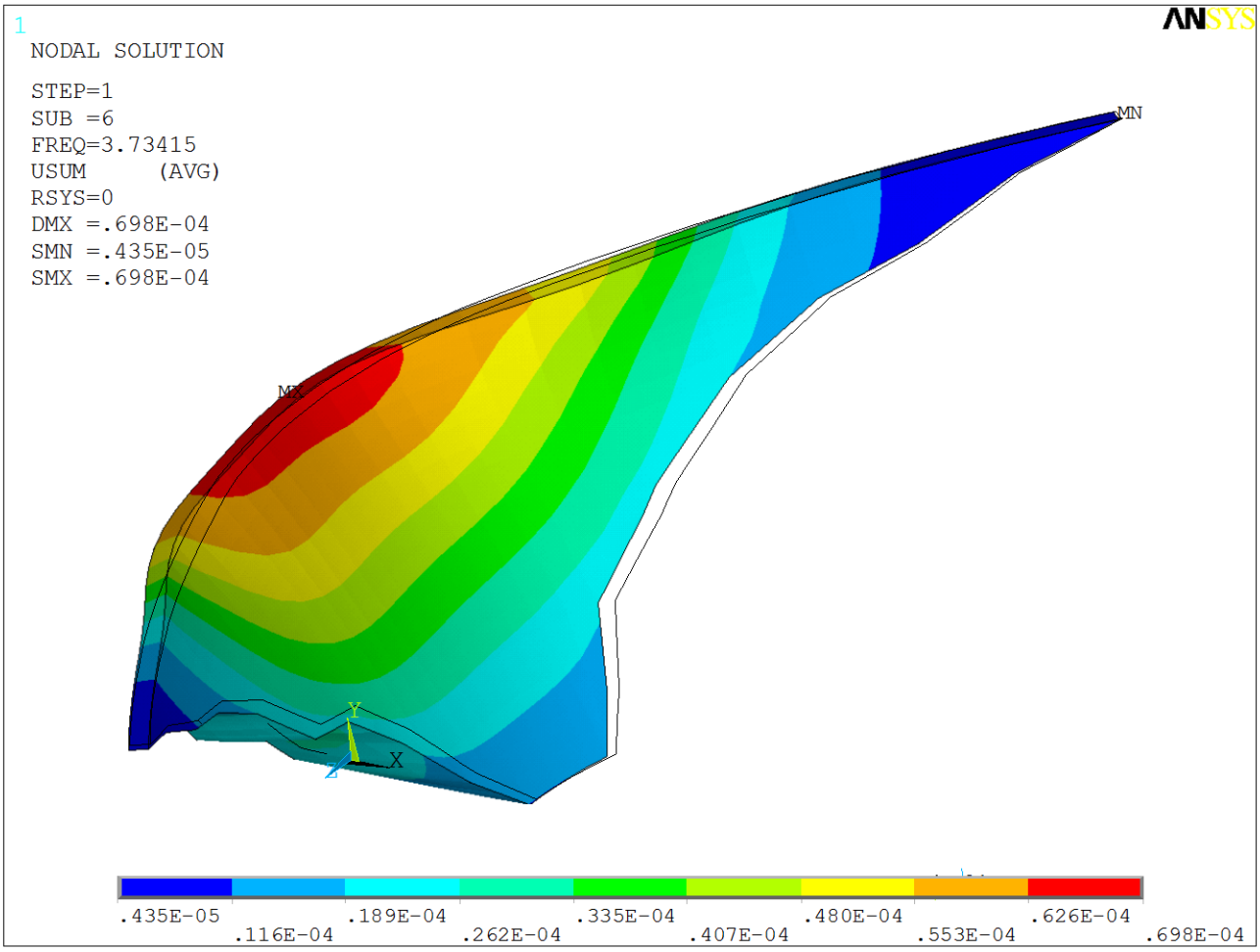

Mode 6

Figure 10.6-5. Mode Shapes – First Six Vibration Modes (Dam Layout 2)

10.6.1.5. Response Spectra Analysis

Elastic dynamic analysis of the dam was performed using response spectra to compute the maximum response of the dam due to earthquake loading. Model input included the two horizontal and the vertical response spectra. The dam was analyzed for three earthquake load scenarios:

- Earthquake with 2,500-year return period with a PGA of 0.522g
- Earthquake with 5,000-year return period with a PGA of 0.664g
- Earthquake with 10,000-year return period with a PGA of 0.827g

The maximum (tensile) and minimum (compressive) horizontal and vertical stresses on the upstream and downstream faces of dam are summarized in Table 10.6-3 and Table 10.6-4. In accordance with ANSYS convention – and for ease of comparison – tensile stresses are positive, and compressive stresses are negative.

Table 10.6-3. Comparison of Seismic Analysis Results – Maximum Tensile Stresses (Layout 2)

Earthquake Return Period	Upstream face		Downstream face	
	Vertical Stress (psi)	Horizontal Stress (psi)	Vertical Stress (psi)	Horizontal Stress (psi)
2,500 yrs.	711	628	663	345
5,000 yrs.	983	909	877	533
10,000 yrs.	1300	1240	1130	752

Table 10.6-4. Comparison of Seismic Analysis Results – Maximum Compressive Stresses (Layout 2)

Earthquake Return Period	Upstream face		Downstream face	
	Vertical Stress (psi)	Horizontal Stress (psi)	Vertical Stress (psi)	Horizontal Stress (psi)
2,500 yrs.	-1132	-1256	-910	-917
5,000 yrs.	-1403	-1538	-1122	-1105
10,000 yrs.	-1721	-1868	-1379	-1324

Current FERC dam safety practice does not judge the seismic safety of the dams based on allowable stress criteria, and limited damage is allowed during the maximum credible earthquake. However, the computed maximum compressive and tensile stresses from a linear elastic analysis remain useful as an indicator of the expected level of damage in a concrete dam. The maximum compressive cantilever stress and compressive horizontal stress are 1,721 psi and 1,868 psi respectively. Therefore the compressive stresses are below the corresponding allowable compressive stress of 2,700 psi for all earthquakes and no compressive damage is to be expected.

The maximum cantilever tensile stress for the 2,500 year return period earthquake is 711 psi, which is in excess of the apparent dynamic tensile strength of RCC. This overstressing is indicated only for a small area on the upstream and downstream face of the dam. The localized nature of the overstress is such that the proposed dam geometry will be acceptably safe against the developed stresses in the dam body during an earthquake with return period of 2,500 yrs. The overstressing will occur for just one or two cycles during the early part of the time history, as discussed in Section 10.7.

The results for the 5,000-yr. and 10,000-yr. events indicate that, should these levels of ground motion be used as criteria there may well be overstress which could cause appreciable damage on the dam body. If more detailed analysis with less conservative criteria still shows overstressing, dam geometry would need to be revised to reduce developed stresses in the dam.

It is also noted that the range of computed tensile stresses at the dam-foundation interface and tensile horizontal stresses between the dam monoliths exceed the tensile capacity of these interfaces. This reinforces the conclusion that linear elastic analyses do not present a realistic seismic response of the dam, and a more sophisticated analysis considering nonlinear contact elements at these locations is more appropriate.

10.6.1.6. RCC Volume

The optimization of RCC volume – while robustly maintaining dam safety – was the crux of the early analyses. The ADSAS program calculates the volume of concrete in the analyzed structure. It should be noted that the concrete volume predicted by ADSAS for the PAD layout (Dam N) is larger than that estimated in December 2011. This difference is due to the spacing between the cantilever sections analyzed in ADSAS. The 2011 estimate was based on sections at every 100 ft. whereas the spacing of sections used in the ADSAS model varied from 95 ft. to 395 ft.

The sections analyzed for the curved dams were all radial from the center of curvature. The base of each vertical element coincided with the end of a horizontal element. The entire base of each vertical element must be founded on rock, so the highest foundation elevation was located at the downstream toe of the dam in several instances. This would generate significant excavation at the foundation as the section would progressively get deeper into the rock abutment as it extended towards the dam's upstream face. This leads to conservative volume estimation. For the purposes of this analysis, however the volume estimations are primarily used for the comparison of the dam alternatives and serve as a measure of the relative scale of the dams. The volumes estimated for a Susitna-Watana high dam with a NMOL of El. 2185 ft. (maximum possible development as determined in the 1980s studies) are listed in Table 10.6-5.

Table 10.6-5. Susitna-Watana High Dam: ADSAS Estimated Dam Volumes (cubic yards)

Dam	Slope of Downstream Face (xH:1V)						
	0.3	0.4	0.5	0.6	0.7	0.8	0.85
A	6,416,000	7,746,000	9,041,000	10,300,000	11,525,000	12,714,000	13,295,000
B	6,416,000	7,767,000	9,086,000	10,372,000	11,626,000	12,847,000	13,446,000
C	6,370,000	7,700,000	9,002,000	10,277,000	11,523,000	12,742,000	13,340,000
D	6,271,000	7,589,000	8,882,000	10,149,000	11,391,000	12,607,000	13,206,000

Dam	Slope of Downstream Face (xH:1V)						
	0.3	0.4	0.5	0.6	0.7	0.8	0.85
E	5,911,000	7,178,000	8,432,000	9,671,000	10,896,000	12,107,000	12,708,000
F	6,341,000	7,655,000	8,932,000	10,174,000	11,380,000	12,550,000	13,121,000
G	6,305,000	7,615,000	8,891,000	10,133,000	11,342,000	12,518,000	13,093,000
H	6,176,000	7,463,000	8,719,000	9,945,000	11,139,000	12,303,000	12,873,000
I	6,261,000	7,574,000	8,856,000	10,108,000	11,330,000	12,521,000	13,105,000
J	6,379,000	7,686,000	8,950,000	10,174,000	11,356,000	12,496,000	13,051,000
K	6,319,000	7,620,000	8,883,000	10,111,000	11,301,000	12,455,000	13,018,000
L	6,233,000	7,523,000	8,780,000	10,003,000	11,193,000	12,350,000	12,916,000
M	6,207,000	7,496,000	8,754,000	9,979,000	11,172,000	12,332,000	12,900,000
N	5,801,000	7,079,000	8,356,000	9,634,000	10,911,000	12,189,000	12,828,000

The volumes for the selected favorable configuration for the lower dam (Layout 2, Alternate J) postulated during these studies were also estimated by the ADSAS program and the results are shown in Table 10.6-6.

Table 10.6-6. Watana Dam (Layout 2): ADSAS Estimated Dam Volumes (cubic yards)

Dam	Slope of Downstream Face (xH:1V)				
	0.4	0.5	0.6	0.7	0.85
J	4,521,000	5,276,000	6,009,000	-	-

10.6.2. Revised Dam Configuration (Layout 3)

10.6.2.1. Configuration Description

After being presented with the results of the FE analysis of the initial configuration (Layout 2, Alternate J), the Board of Consultants suggested that a simple single radius configuration be analyzed, so the team reassessed the work performed to derive the initial configuration with the object to establish an upper envelope of conservatism in the layout. Upon examination of the original ADSAS volume calculations, the most economical of the traditional curved gravity sections was Alternative E with a single axis radius of 4,000 ft., but on examination of the topography, it was found that a radius of 3,500 ft. resulted in a better angle of intersection with the abutment topographic ground contours. This radius was therefore selected for Layout 3, but is not represented in the original volume calculations.

10.6.2.2. Two-Dimensional Gravity Analysis

Using the 3,500-ft single radius layout, 2-D analysis was performed to estimate the cross-sectional geometry that would satisfy stability criteria for the usual and unusual load cases

required by the FERC Guidelines, Chapter 3, Gravity Dams. Multiple cross-sections were analyzed using CADAM, for downstream face slopes ranging from 0.7H:1.0V to 1.0H:1.0V and upstream face batters ranging from vertical to 0.2H:1.0V.

The dam cross-section that satisfied 2-D stability criteria for all load cases – with no tension at the foundation interface (no crack forming at the foundation contact) – had a downstream face slope of 0.85H:1.0V and an upstream face batter of 0.1H:1.0V. The 2-D analysis assumed zero cohesion at the dam foundation interface and included uplift applied on the dam base according to the distribution prescribed by the FERC Guidelines. This cross-section was then further refined and analyzed using ADSAS and FE methods as described in the sections that follow. Post-earthquake stability was also analyzed for comparison to results of the FE analysis done for stability of the cracked dam in a post-seismic condition. As reported in discussion of the FE analysis below, permanent displacement was computed at the base of the crown monolith at the end of the earthquake event; however the dam remained stable for static reservoir loads in the post-seismic condition. Post-seismic uplift pressure distribution on the fully cracked base was assumed to vary linearly from normal headwater pressure at the upstream heel to a reduced level at the drain line and then linearly to full tailwater pressure at the dam toe.

A simplified analysis was also performed at this stage of the dam layout development using PGA of 0.66g and 0.82g for the purpose of estimating the increase in dam volume required for the higher ground motions. For that condition the downstream face of the dam was estimated to require a slope of 1.0H:1V.

10.6.2.3. Arch Dam Stress Analysis System (ADSAS)

In concert with the 2-D gravity analysis, the ADSAS program was again used to perform the analysis of the cross-section with a 0.85H:1.0V downstream face slope and an upstream face batter of 0.1H:1.0V. A dam cross section with a 1.0H:1.0V downstream face slope was also analyzed.

10.6.2.4. ADSAS Results

The stresses calculated by ADSAS for Layout 3 for the cantilever and horizontal elements at the crown cantilever are shown graphically in Figure 10.6-6 and Figure 10.6-7 below.

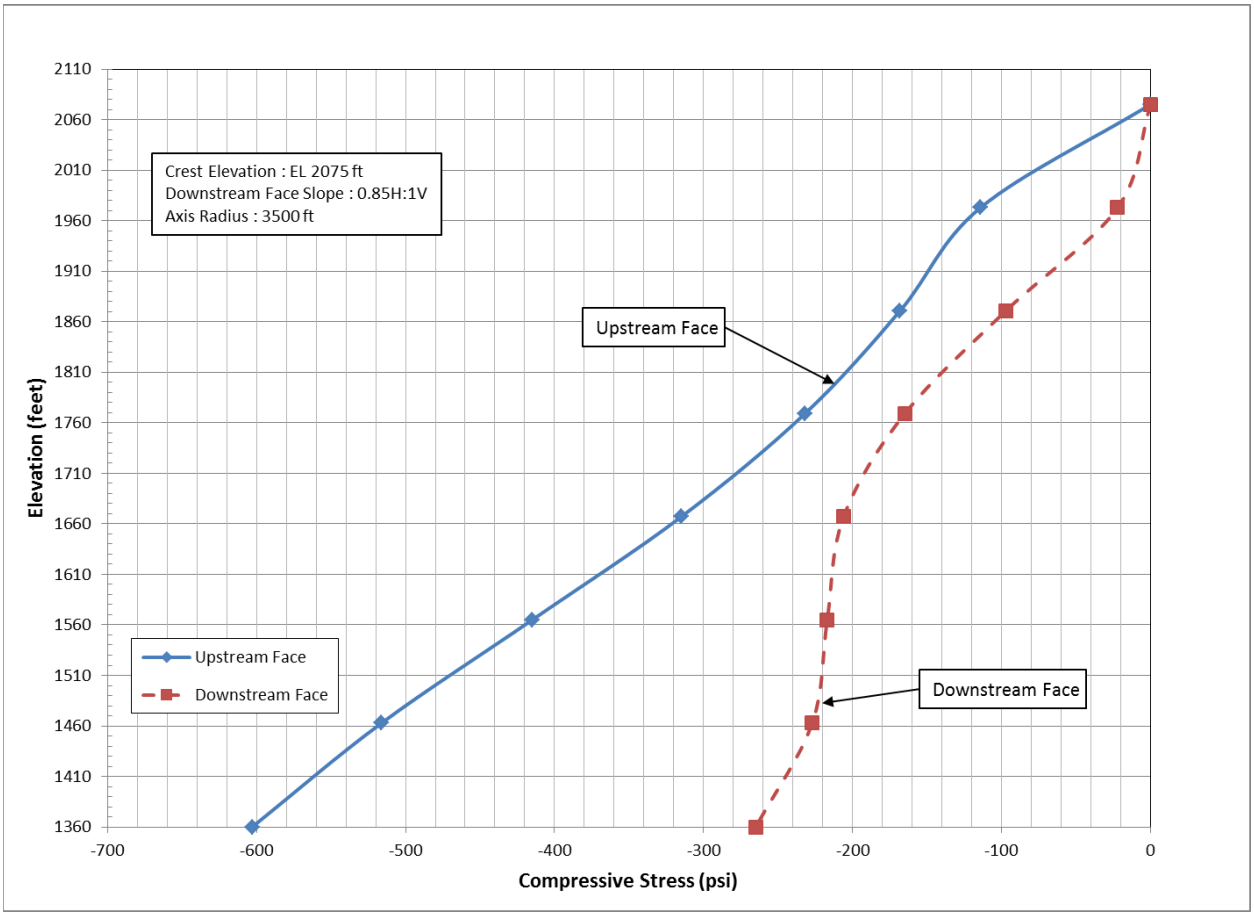

Figure 10.6-6. Layout 3 – Static Loads – Cantilever Stresses at the Crown Cantilever

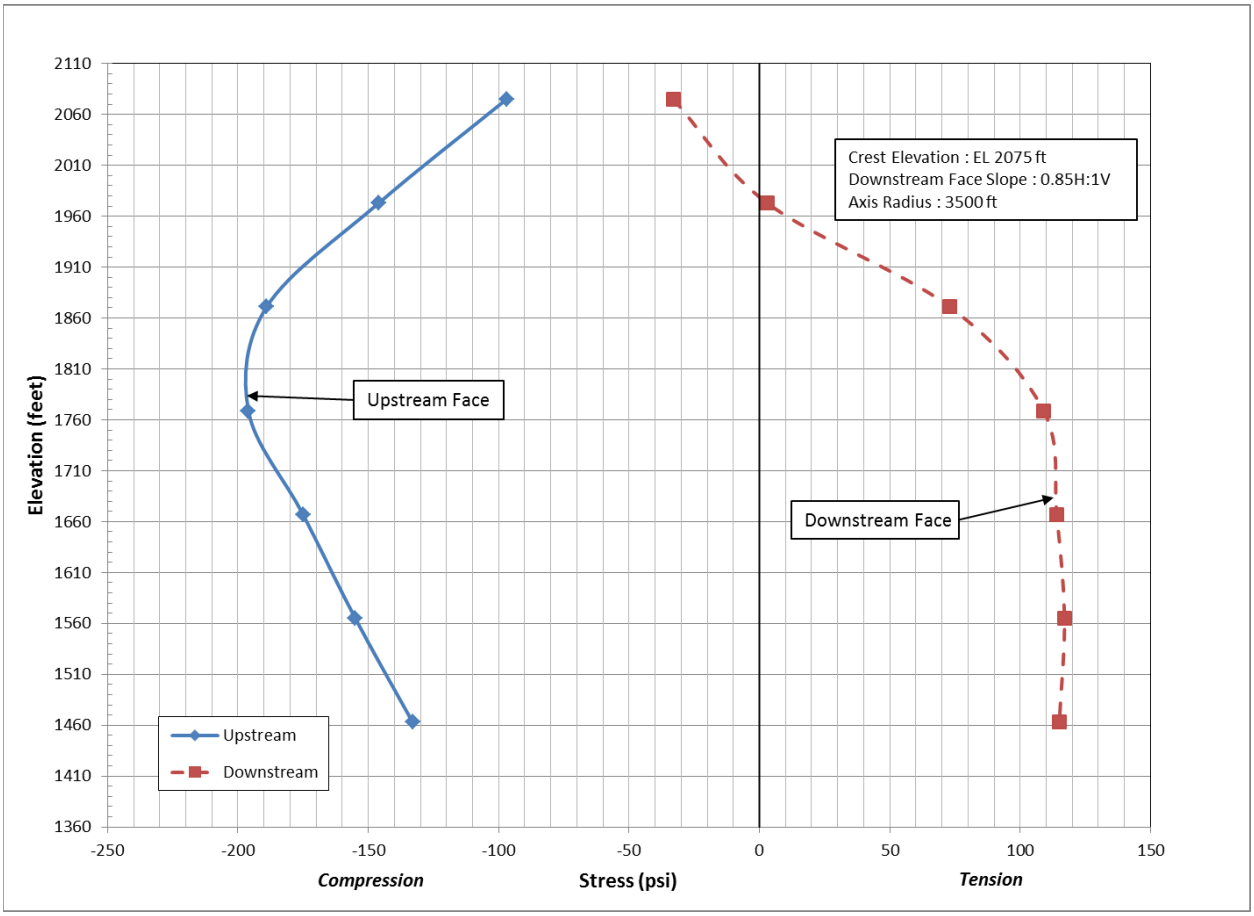

Figure 10.6-7. Layout 3 – Static Loads – Horizontal Stresses at the Crown Cantilever

The ADSAS analysis shows that the vertical cantilever stresses are compressive at the upstream and downstream faces for the entire height of the dam. The maximum vertical compressive stress is less than 37 percent of the allowable compressive stress.

The analysis also shows that there is transfer of some load horizontally to the abutments. This demonstrates that the curved axis reduces the loads carried by cantilevers, and the horizontal "wedge action" resulting from the curvature of the dam increases sliding stability of the dam.

In summary, the Layout 3 configuration is stable under static loading conditions. The Layout 3 cross section was then used for 3-D analysis using FE method software to assess the effect of dynamic loading.

10.6.2.5. FE Structural Analysis

10.6.2.5.1. ANSYS Model

Initially ANSYS Version 14.5 was used for analyzing Layout 3 but subsequent to the first runs, MWH upgraded to Version 15 and also made some adjustments to the foundation of the dam for the analysis of subsequent configuration designated Layout 4. Therefore, to permit reasonable comparison between the various analyses, ANSYS, Version 15.0, was used to perform a re-analysis of Layout 3 which is recorded herein. The geometric model of the dam was created directly within the "Design Modeler" of ANSYS, and subsequently used as the basis for creating the FE method mesh. The FE model consisted of 14,133 elements and 13,236 nodes. The FE model of the dam included 2 elements (thickness) at the dam crest and 16 elements (thickness) at the dam base together with 19 elements along the height of crown cantilever. The maximum element size was thus 40 ft. and further analysis for design development should be undertaken with a significantly (smaller and) more detailed mesh. The rock foundation was modeled to a depth equal to the height of the dam, a width equal to three times the dam height, and a length (in the upstream and downstream directions) equal to the dam height. Three-dimensional mass elements (added mass) attached to the nodes of the elements on the upstream face of the dam were used to simulate hydrodynamic effects of the reservoir. Figure 10.6-8 shows a general 3-D view of the model and a cross section of the crown cantilever.

Taking into account FERC and Board of Consultant observations the following features were included in the FE model:

- Nonlinear frictional contact elements were used to model the contraction joints in the dam body. These contact elements cannot transfer tensile stresses across the interface but can transfer shearing forces based on the coulomb friction criteria. During detailed design the distance between contraction joints will be determined based on a thermal analysis of the dam but is expected to be between 50 to 100 ft. The distance of the contraction joints for this analysis is assumed at 200 ft. to reduce the nonlinear analysis time. A friction coefficient of 1.2 was assumed for these contacts.
- To allow movement on the foundation, nonlinear frictional contact elements, similar to contact elements of dam monoliths, were used to connect the dam body to the foundation. The elements of the dam-foundation contact are connected at the surface of the foundation elements (no embedment, hence no resistance against sliding other than friction). Figure 10.6-8 also shows all the contact elements used in the model. Assuming that the drainage system is 66 percent effective, uplift pressure (with an equivalent triangular distribution) at the base of monoliths was calculated and applied on contact surfaces.

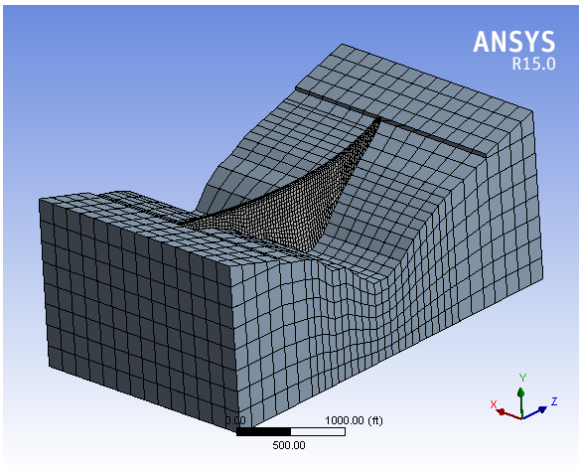

FE U/S view

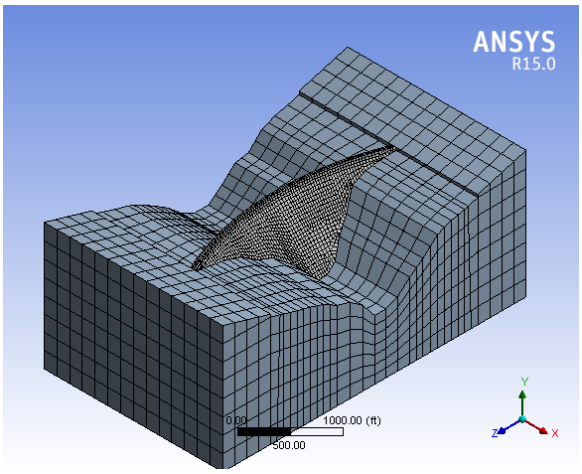

FE D/S View

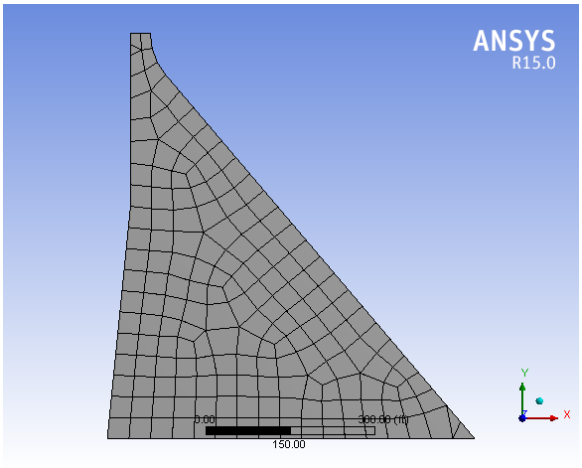

Maximum Cross section of dam model

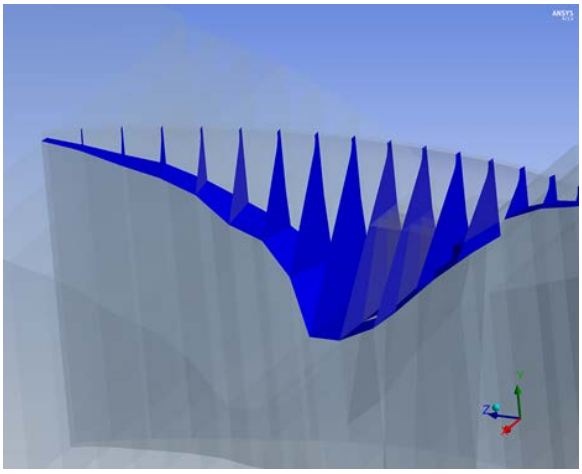

Contact elements in the model

Figure 10.6-8. Finite Element Model of the Dam (Layout 3)

10.6.2.5.2. Static Analysis

The initial analysis included the static loading condition of dead weight, reservoir water and uplift, but without temperature, ice or sediment. Figure 10.6-9 to Figure 10.6-12 graphically show the resulting horizontal and cantilever stress contours in the dam body.

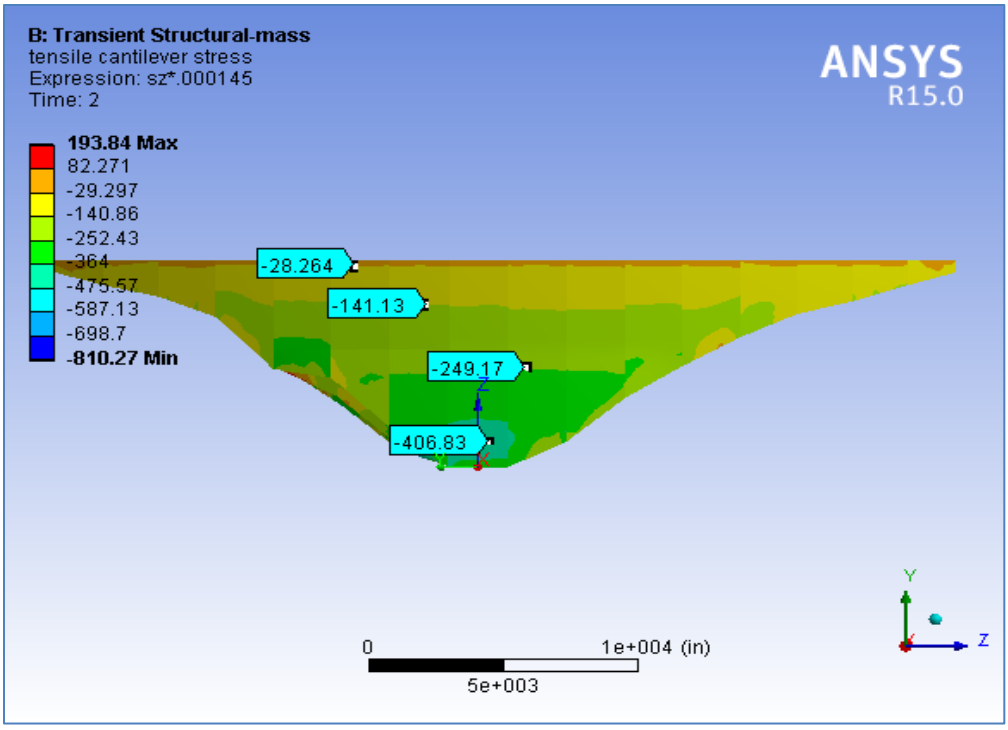

Figure 10.6-9. Vertical Cantilever Stress (psi) – Upstream Face (Layout 3)

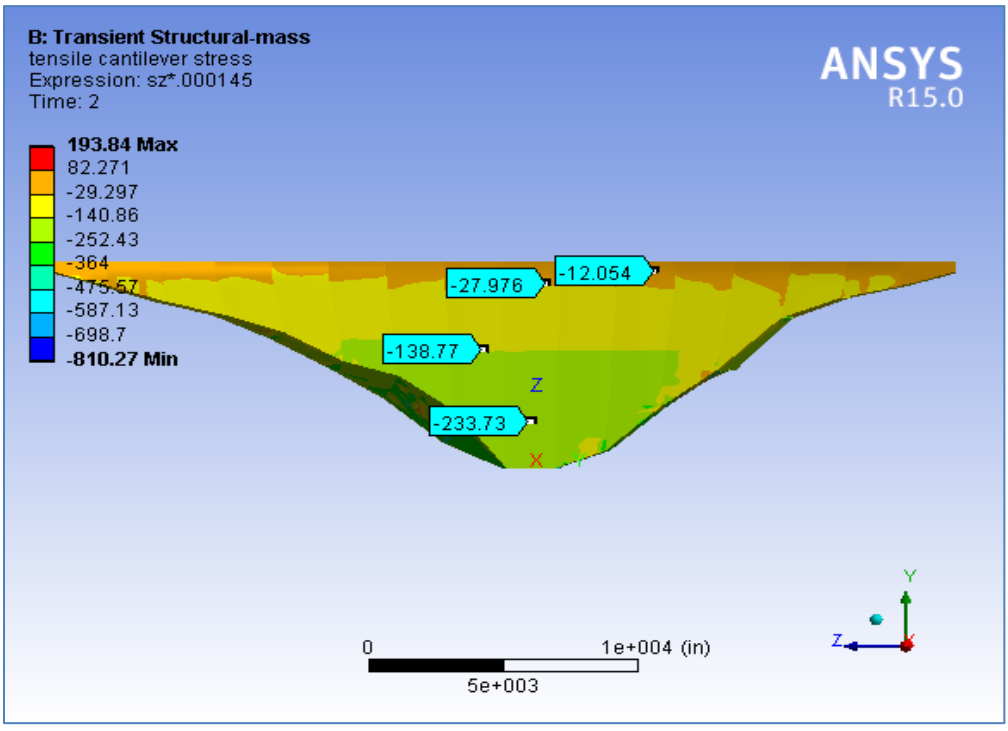

Figure 10.6-10. Vertical Cantilever Stress (psi) – Downstream Face (Layout 3)

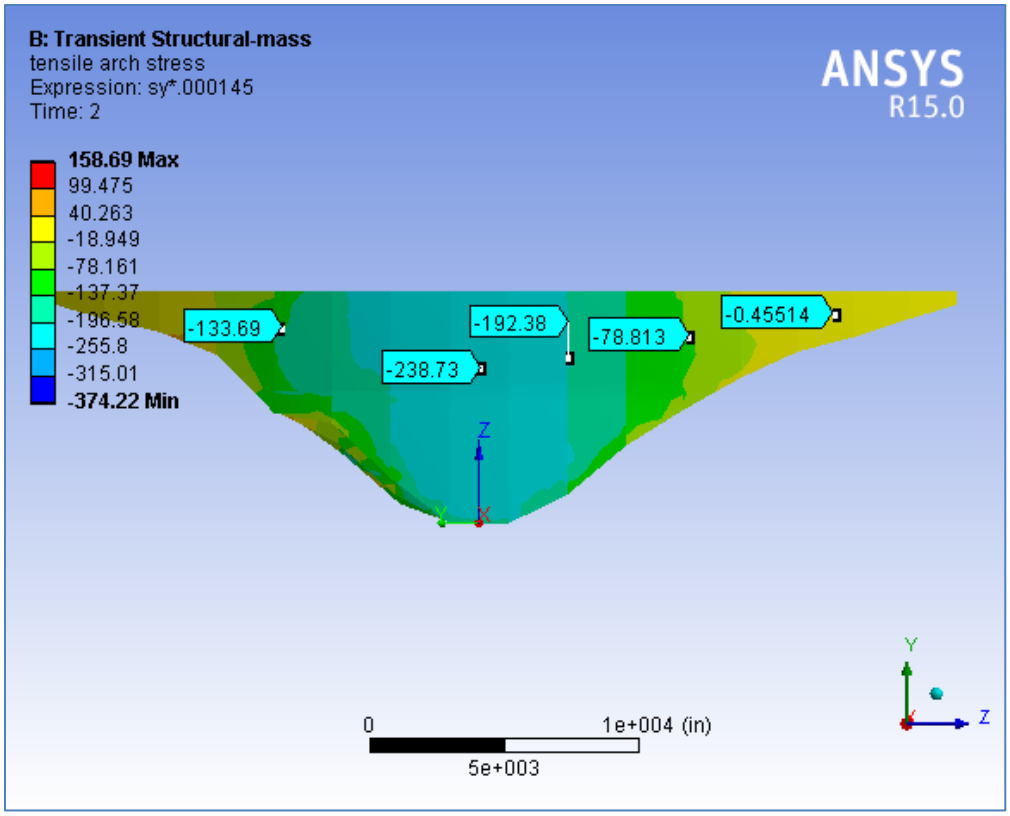

Figure 10.6-11. Horizontal Stress (psi) – Upstream Face (Layout 3)

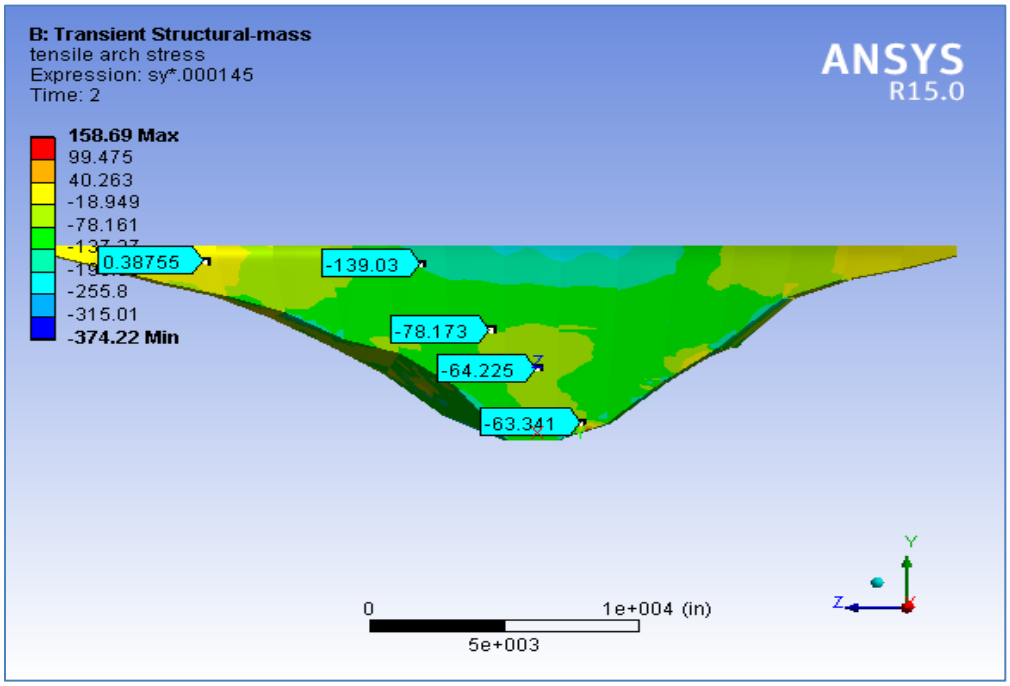

Figure 10.6-12. Horizontal Stress (psi) – Downstream Face (Layout 3)

The FE analysis of Layout 3 indicates that the stresses in the dam body under static conditions are lower than the allowable values. The structure is in a state of compression except for two monoliths on the left and three on the right side with zero horizontal stresses. Because the model includes joints at 200 ft. centers, no tensile stresses developed in the FE model.

The current construction planning anticipates that – to minimize the total project construction schedule – the dam will be constructed in three large monoliths, corresponding to the left abutment, right abutment and central portion of the dam. Therefore the expected response of the dam to dead load would be slightly different from these results. In the detailed design, the dam body will be modeled using three distinct monoliths and additional vertical formed joints – with shear keys – between those monoliths, although "induced" joints normally created during RCC placement will also be included. The model will be analyzed for the weight of the dam by simulating the proposed construction schedule.

10.6.2.5.3. Modal Analysis

A modal analysis of the Layout 3 configuration was performed to calculate the fundamental periods of vibration and mode shapes of the linear model. The first 8 natural frequencies and periods of the dam are shown in Table 10.6-7.

Table 10.6-7. Dam Frequency and Periods of Vibration (Layout 3)

Mode No	1	2	3	4	5	6	7	8
Frequency (Hz)	1.88841	2.58056	3.21403	3.70938	3.83099	3.97313	4.21945	4.44512
Period (sec)	0.52955	0.38751	0.31114	0.26959	0.26103	0.25169	0.23700	0.22497

The fundamental period of vibration is 0.529 second, smaller than the period of 0.657 seconds for dam Layout 2, thus confirming that Layout 3 is stiffer than Layout 2.

Review of the modal analysis results indicates that the first 30 vibration modes represent more than 90 percent of the total mass of the structure in all directions. Rayleigh damping mass coefficient and stiffness coefficient were calculated using the first and 30th circular frequency for an equivalent seven percent damping ratio.

10.6.2.5.4. Transient Analysis

Three acceleration time histories were developed for each type of earthquake events. Two earthquake records from each type of events were used in the analyses. Transient dynamic analyses were performed for a total of eight earthquake records. Developed stresses in the dam body and sliding displacement of dam monoliths are the main parameters to assess the response of the dam against the earthquake. The results indicate that no tensile horizontal stresses develop

in the dam because of the "no tension" behavior of the contact elements. However compressive horizontal stresses develop on the upstream and downstream face of the dam depending on the direction of the earthquake loading.

The envelope of maximum (tension and compression) cantilever stress on the upstream and downstream face of the dam for the (Japan 2011) ITW010 earthquake are shown in Figure 10.6-13 to Figure 10.6-16 (because the figures were drawn directly from ANSYS output, positive values are exceptionally used for compressive stresses only in these figures and care must be taken in interpretation). No tensile cantilever stresses were developed along the dam-foundation interface because of the "no tension" contact elements. High tensile cantilever stresses were developed at the mid-height of the crown cantilever – around 1150 psi.

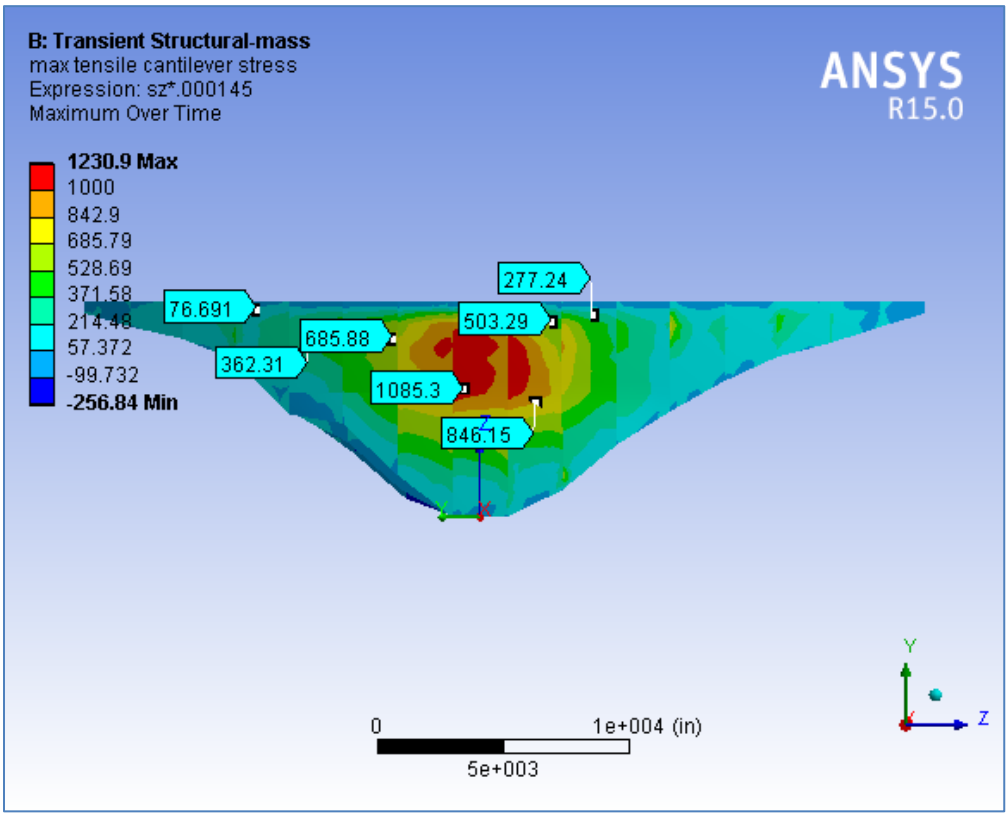

Figure 10.6-13. Envelope of Maximum Tensile Cantilever Stress (psi) due to IWT010 Earthquake – U/S View (Layout 3)

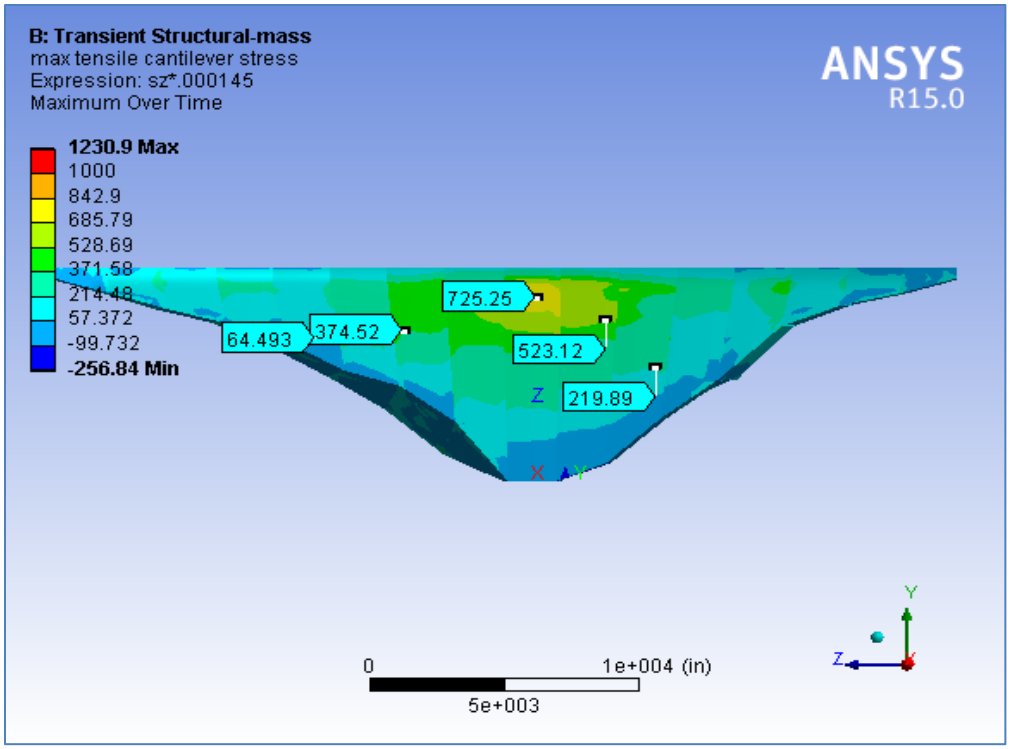

Figure 10.6-14 Envelope of Maximum Tensile Cantilever Stress (psi) due to IWT010 Earthquake – D/S View (Layout 3)

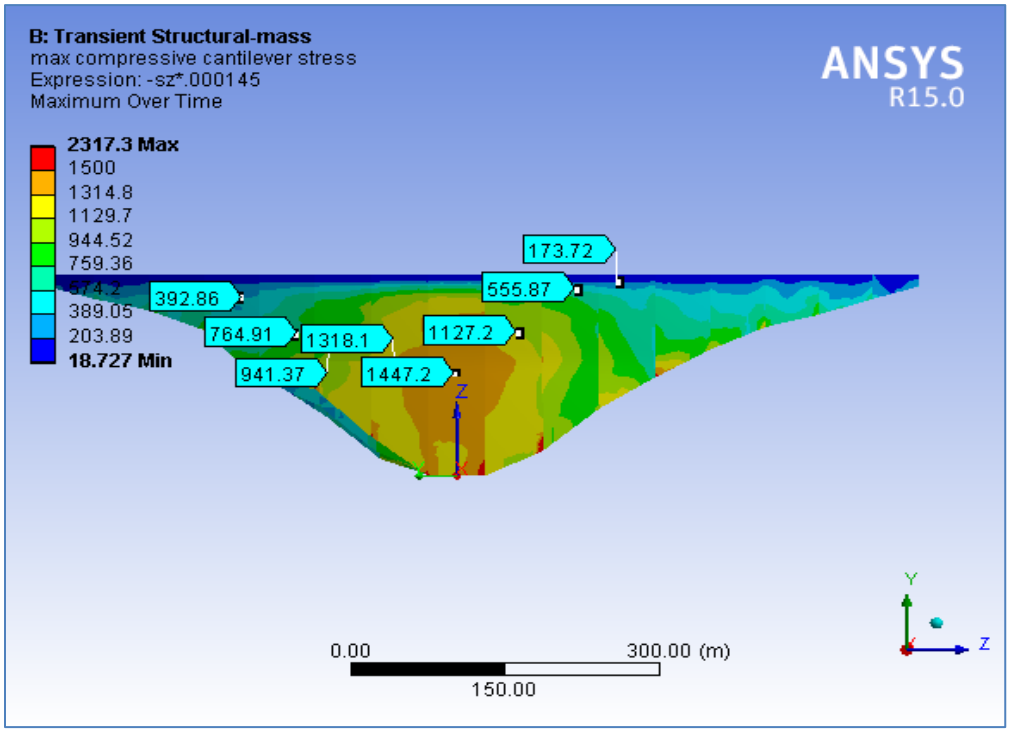

Figure 10.6-15. Envelope of Maximum Compressive Cantilever Stresses (psi) due to IWT010 Earthquake – U/S View (Layout 3)

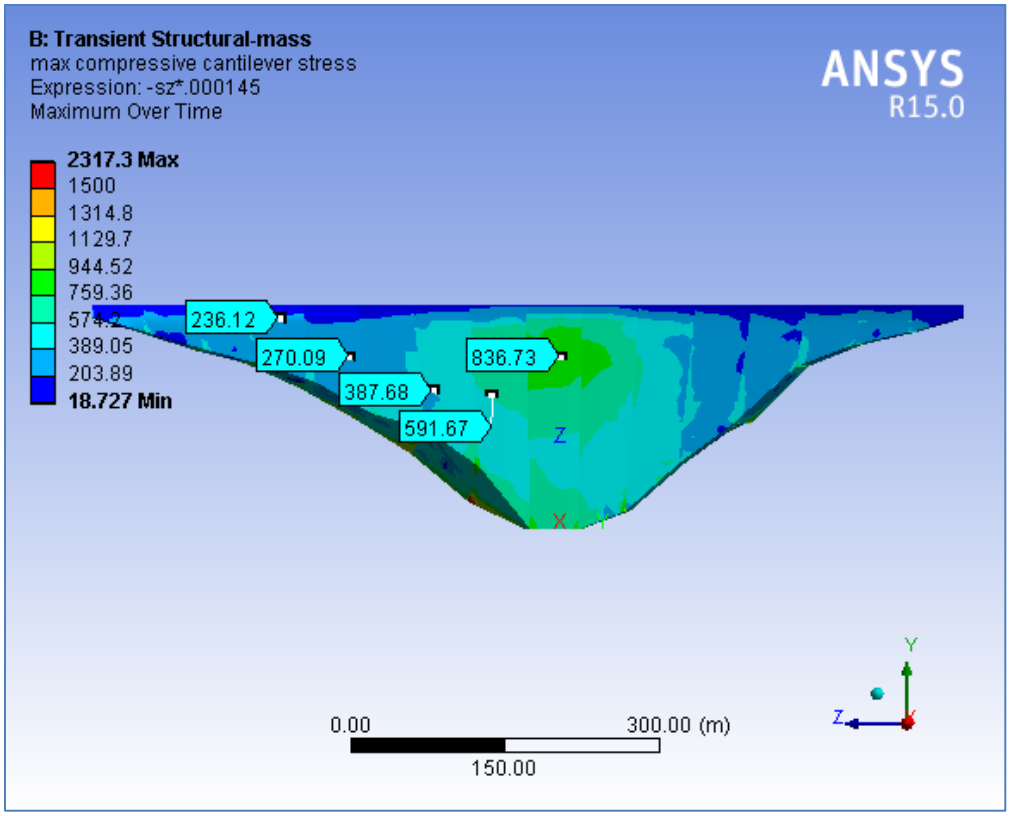

Figure 10.6-16. Envelope of Maximum Compressive Cantilever Stresses (psi) due to IWT010 Earthquake – D/S View (Layout 3)

Figure 10.6-17 shows the residual sliding displacement of the dam monoliths at the end of the, IWI010 earthquake. The maximum sliding exhibited at the base of the crown cantilever is around 1.5 in. The magnitude of the sliding increased for the side monoliths to 2.9 inches and the maximum sliding of five inches occurred on the left side monolith. It is noted that the computed sliding displacement of each monolith is affected by dam-foundation interface geometry, friction coefficient and contact pressure, and state of the contact at the beginning of the earthquake event. Therefore the actual sliding displacements would be expected to be somewhat different from computed values at this stage.

Subsequent, more complex modeling – including foundation mass – described in Section 10.7 provided a more representative estimation of potential displacements for the recommended dam configuration, and in detailed design the final characterization of the foundation, the proposed foundation excavation, any proposed grouting of joints (formed or induced) and the sequence of construction will be taken into account.

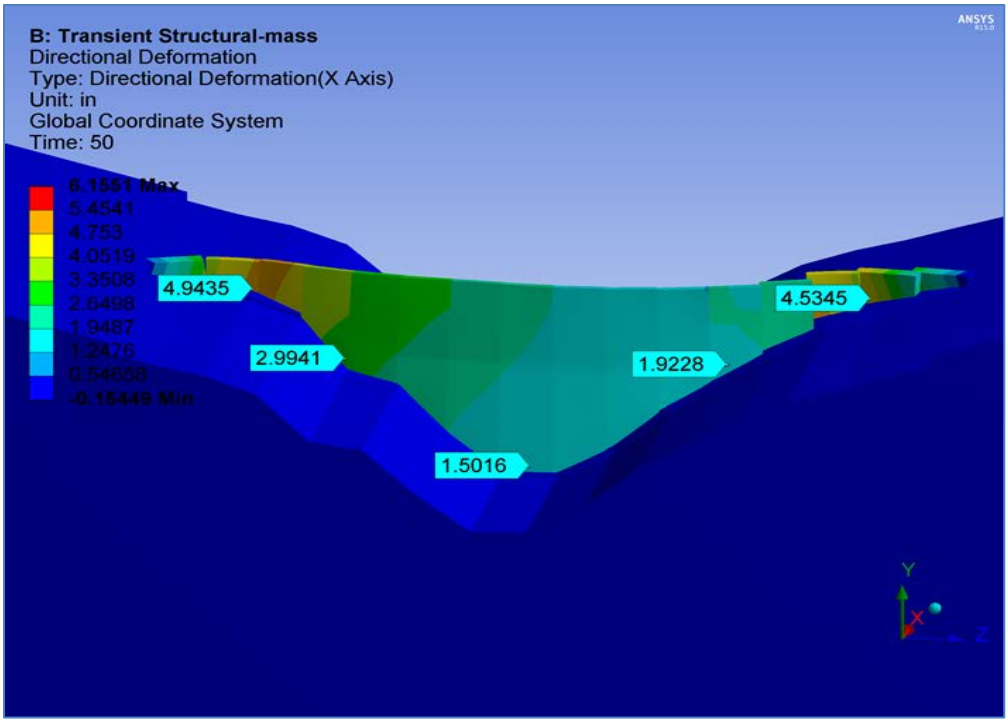

Figure 10.6-17. Residual Sliding Displacement (inches) at the end of IWT010 Earthquake looking d/s (Layout 3)

The basic structural responses of the model to eight earthquake records were similar, but different in magnitude. The detailed stress contours of the dam due to other earthquakes are not shown but the maximum cantilever stress variations along the height of the crown monolith for eight earthquakes are plotted in Figure 10.6-18. The maximum computed stresses in the dam body and permanent displacement of dam monoliths due to the eight earthquakes applied are also summarized in Table 10.6-8.

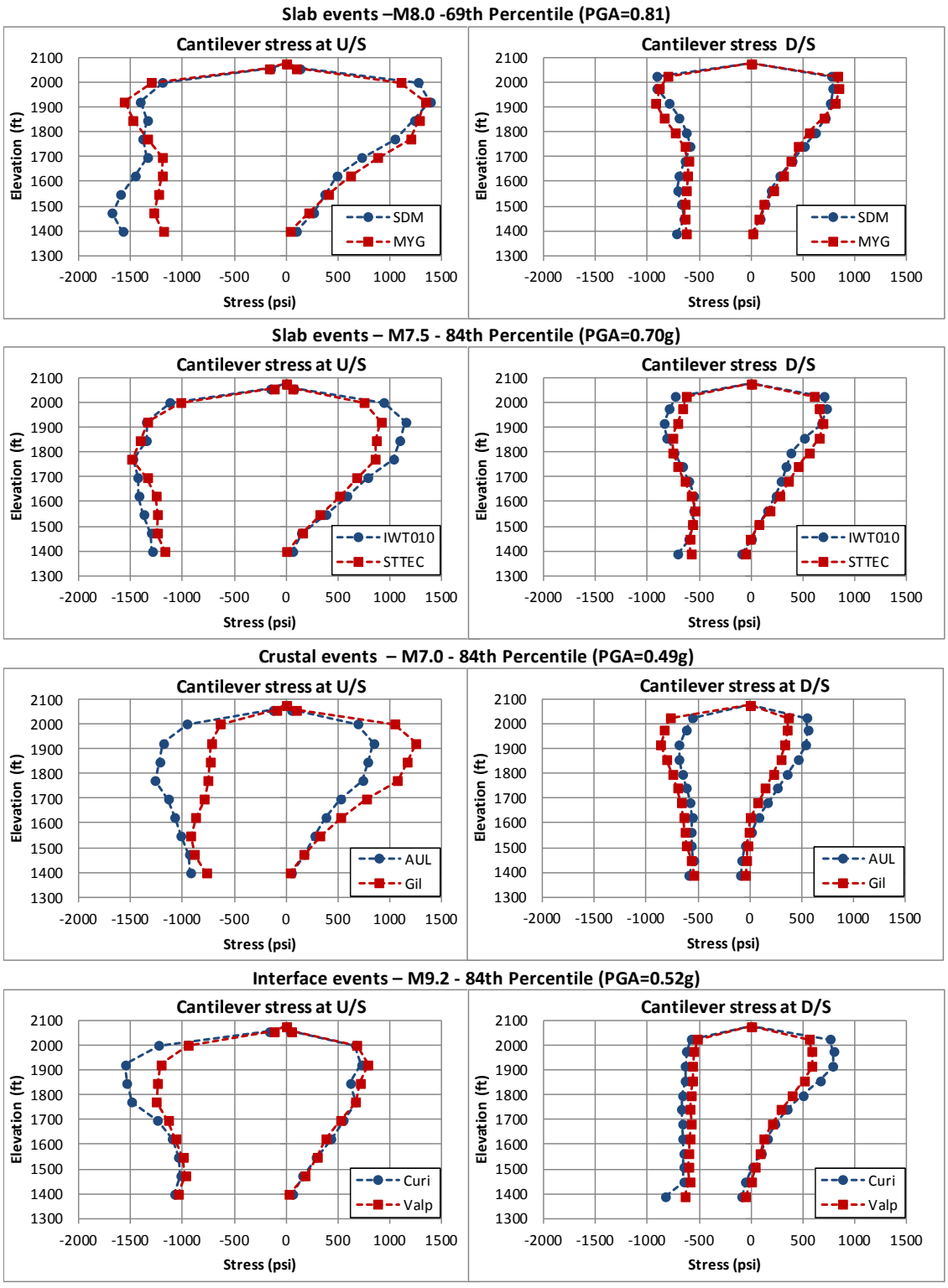

Figure 10.6-18. Envelope of Max. and Min. Cantilever Stresses in Crown Cantilever for Layout 3 for Selected Events

Table 10.6-8. Summary of Dam Layout 3 Response to 8 Earthquake Loadings

Event	Event Station	Stress Location	Horizontal Stress (psi)	Vertical Stress (psi)		Sliding Displacement (in)	
			Compressive	Tensile	Compressive	Crown Monolith	Side Monoliths
Slab events – M8.0 -69th Percentile (PGA=0.81)							
El Salvador 13-Jan-01	SDM	U/S	-1330	1388	-1680	4.1	6.4
		D/S	-1043	788	-909		
Japan 2011 7-Apr-11	MYG009	U/S	-1175	1344	-1558	3.8	4.4
		D/S	-903	848	-919		
Slab events – M7.5 – 84th Percentile (PGA=0.69g)							
El Salvador 13-Jan-01	STTEC	U/S	-794	913	-760	1.8	2.2
		D/S	-596	695	-1330		
Japan 2011 7-Apr-11	IWT010	U/S	-732	1149	-839	1.5	3
		D/S	-721	726	-1346		
Crustal events – M7.0 – 84th Percentile (PGA=0.49g)							
Irpinia, Italy 23-Nov-80	AUL	U/S	-762	841	-1265	0.8	1.2
		D/S	-538	557	-682		
Loma Prieta, California 18-Oct-89	GIL	U/S	-697	1252	-916	0.2	0.5
		D/S	-607	363	-858		
Interface events – M9.2 – 84th Percentile (PGA=0.52g)							
Chile (M 8.8)	CURI	U/S	-969	726	-1552	2.1	2.5
		D/S	-619	797	-634		
Chile (M 8.8)	VALPM	U/S	-630	791	-1250	1.5	2
		D/S	-639	563	-563		

Note:
AUL - Italian Crustal Earthquake Record - November 1980
CURI - Chile Interface Earthquake Record - February 2010
GIL - Lomo Prieta, CA Crustal Earthquake Record - October 1989
VALPM - Chile Interface Earthquake Record - Feb 2010

The maximum tensile cantilever stress of 1,388 psi occurred in the dam body during the El Salvador (SDM) earthquake. However the average of maximum tensile stresses from all selected earthquakes is around 945 psi. This stress is greater than the projected dynamic tensile strength of the RCC, hence cracking of the dam could be expected according to these results. The maximum displacement calculated at the base of the crown monolith is 4.1 in. which occurred during the SDM earthquake – and the average displacement is approximately 2.2 in. These represent permanent displacements at the end of the earthquake event. CADAM was used to analyze the dam with a fully cracked base and uplift distribution per FERC criteria, and the dam

was shown to remain stable for the post-seismic condition. Post-seismic uplift pressure distribution on the fully cracked base was assumed to vary linearly from normal headwater pressure at the upstream heel to a reduced level at the drain line and then linearly to full tailwater pressure at the dam toe. As discussed in other sections, dam and foundation drains will be sized to accommodate potential sliding displacements and to remain effective following movement of the dam during extreme loading.

10.6.2.5.5. RCC Volume

To check the ADSAS volume calculations, the volume of the Layout 3 dam was calculated using an excel spreadsheet in two ways: (1) per one foot elevation; and (2) at five feet increments along the dam crest. The spreadsheet calculated the gross volume of the dam; adjustments were then made to the estimated volume to include the concrete between the powerhouse and the downstream face of the dam and to include volume reductions for inserts including penstocks, spillway and intakes.

The volume estimates are listed in Table 10.6-9. A batter in the upstream direction (0.1H:1V) was included at the upstream face of the dam below El. 1770 ft.

Table 10.6-9. RCC Quantities (Layout 3)

Downstream Face Slope	0.85H:1V
Gross RCC volume	6,831,000 cy
Quantity adjustment	416,000 cy
Net RCC volume	6,415,000 cy

10.6.3. 2nd Revised Dam Configuration (Layout 4)

10.6.3.1. Configuration Description

As described in Section 10.5, the dam configuration for Layout 4 comprised a central portion with an axis radius of 2,600 ft., and straight-axis abutment sections.

The crest of the dam is 35 ft. wide, and at El. 2065 ft. is 10 ft. lower than previous iterations. This 10 ft. lowering of the crest level resulted from a reassessment of the flood and freeboard requirements for the dam at the completion of the PMP/PMF studies (which was completed part way through this analysis) and after selection of an acceptable reservoir rise of 15 ft. for the efficient use of the low level outlets and for passage of the PMF. The curved section has a downstream face slope of 0.7H:1V and the straight gravity section includes a 0.85H:1V slope on the downstream face. All portions have a sloping upstream face (0.1H:1V) below El. 1770 ft.

transitioning to a vertical face above. The change in downstream face slope reflects the reliance on gravity at the abutments.

10.6.3.2. Two-Dimensional Gravity Analysis

A preliminary check of 2-D stability of the 2,600-ft radius dam was performed using CADAM, for the cross-section with a downstream face slope of 0.7H:1.0V and upstream face batter of 0.1H:1.0V. The 2,600-ft radius dam with this center cross-section was then further analyzed using ADSAS and the FE method as discussed below. As reported in the discussion of the FE analysis, permanent displacement was computed at the base of the crown monolith at the end of the earthquake events.

Assuming zero cohesion at the dam base, the simplified analysis showed the dam satisfied stability criteria for the normal static, flood and post-seismic conditions with a cracked base. The resultant location for all forces under the cracked condition fell within the dam base, and sliding factor of safety was adequate using residual friction angle at the dam foundation contact surface. Post-seismic uplift pressure distribution on the fully cracked base was assumed to vary linearly from normal headwater pressure at the upstream heel to a reduced level at the drain line and then linearly to full tailwater pressure at the dam toe.

10.6.3.3. ADSAS

As noted earlier, ADSAS has the capability of analyzing three centered dam configurations including those that include straight sections at both ends – as selected for Layout 4.

Modeling of the curved portion of the Layout 4 dam has been carried out to assess the stresses both vertically and horizontally within the dam. The analysis omitted the straight portions at the abutments as they will perform as gravity sections. The outer sections have been defined with a cross section that is typical for a gravity dam and the stress analysis can be performed using a traditional 2-D analysis approach.

Similar to the previous configuration (Layout 3) the ADSAS analysis shows that the cantilever stresses are compressive at the upstream and downstream faces for the entire height of the dam. The cantilever stresses within the dam are more evenly distributed than Layout 3; the resultant is nearer to the center of dam section and is lower in magnitude.

Cantilever stresses and horizontal stresses are plotted in Figure 10.6-19 and Figure 10.6-20 respectively. The revised configuration results in slightly greater transfer of loading to the arches. The stresses within the arches at the extrados are compressive for the full height of the crown cantilever while the along the intrados the stresses transition from compressive to tensile about 160 ft. below the crest. The analysis shows that the upper section of the dam, where the

arch effect is most noticeable, has a larger compressive component than Layout 3. The stresses are low, relative to the allowable stresses but demonstrate that the dam shape is more efficient in accommodating the applied loads.

The analysis confirmed that the dam cross-section was stable under static loading conditions. This cross section was then used for analysis using FE method software to assess the effect of dynamic loading.

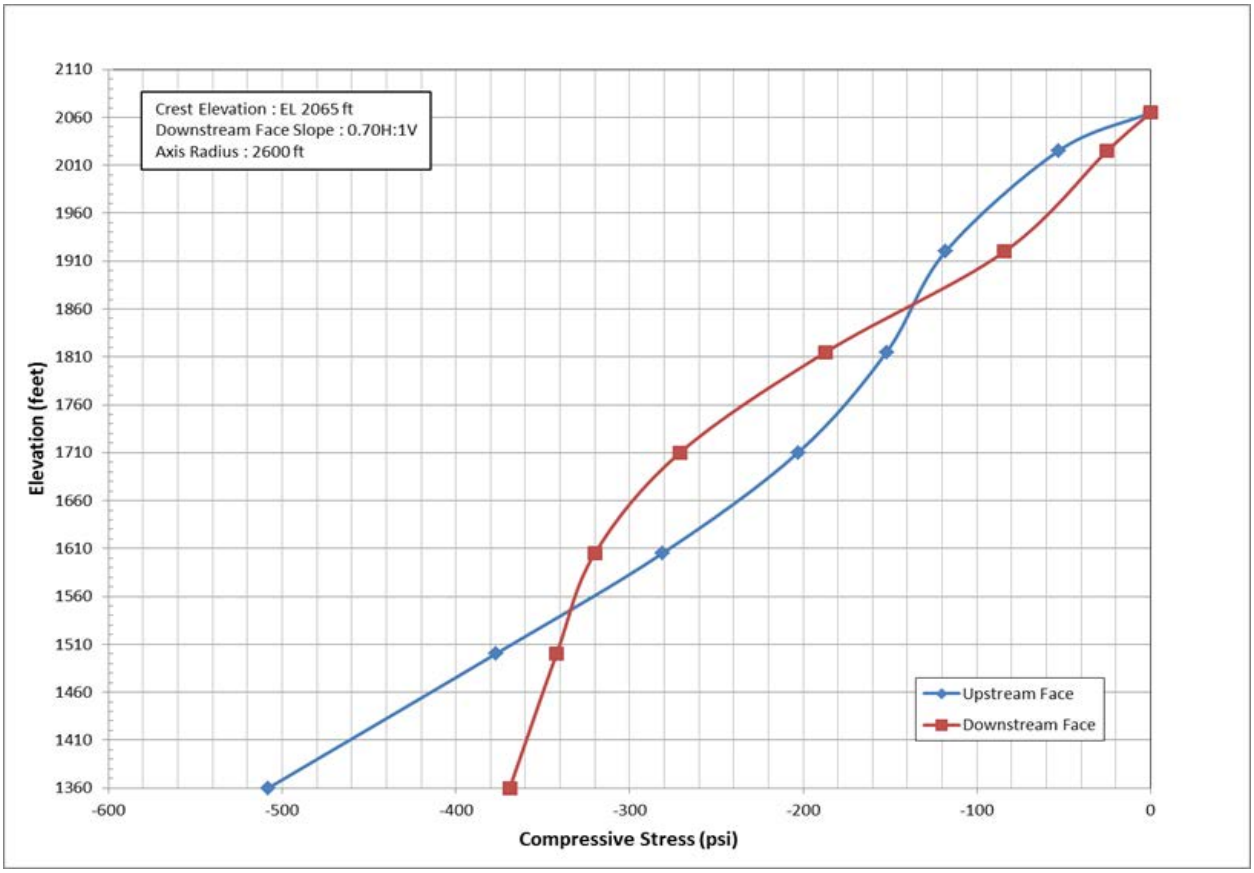

Figure 10.6-19. Cantilever Stresses at the Crown Cantilever (Layout 4)

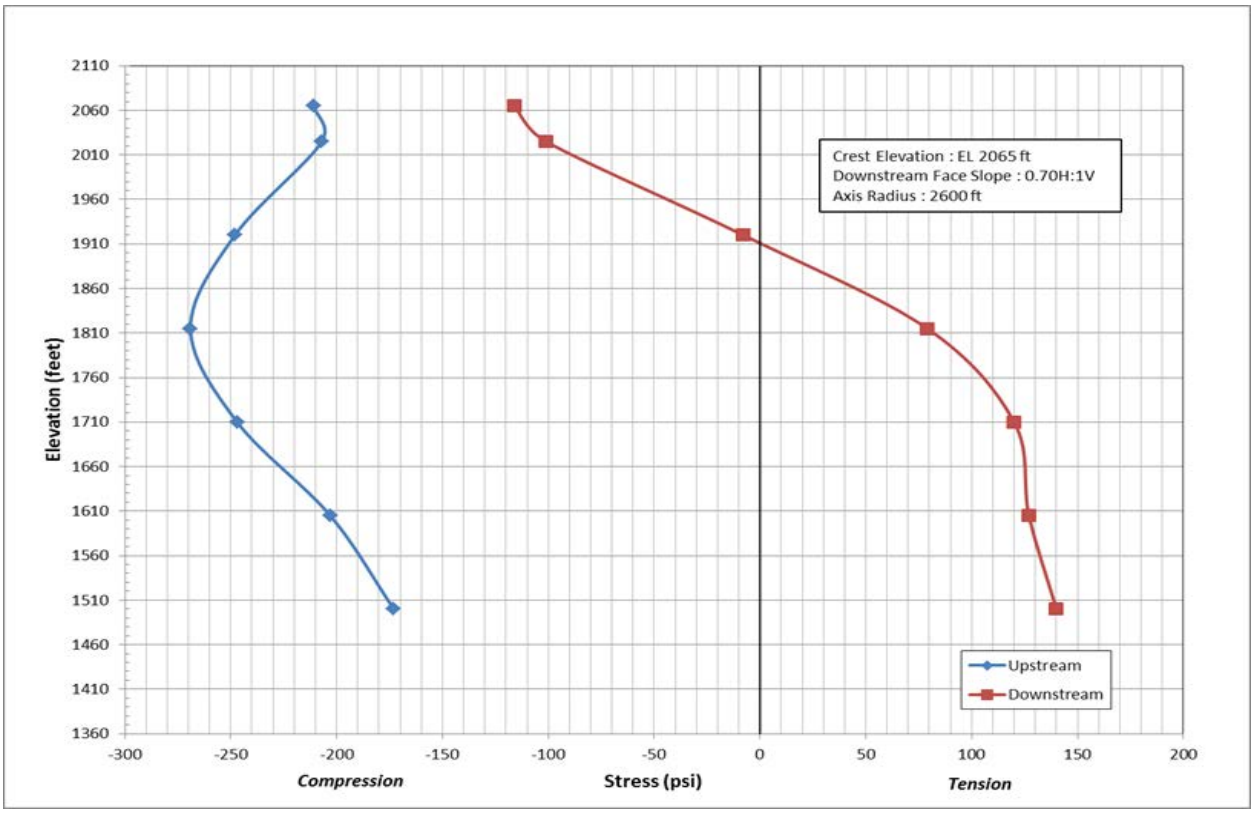

Figure 10.6-20. Horizontal Stresses at the Crown Cantilever (Layout 4)

10.6.3.4. FE Structural Analysis

Structural Analysis was performed using ANSYS v15. A new FE model was developed for this 2nd revised curved dam configuration (Layout 4). The developed FE model is basically similar to the previous model of Layout 3 with the same modeling characteristics but with a new geometry and new FE mesh. Because the foundation surface had to be re-evaluated for the slightly revised geometry, an opportunity was taken to adjust the foundation, and also to use the revised foundation for the Layout 3 as recorded above. Nonlinear frictional contact elements were used between the dam and the foundation and also between dam monoliths in both Layout 3 and 4.

Eight earthquake time histories were used for transient analysis of the dam foundation. For each analysis, dead weight of the dam was applied in first step and hydrostatic and dam base uplift forces were applied in second step, the seismic velocity time history was applied in subsequent steps. Results of Layout 4 analyses indicated higher tensile cantilever stresses on the downstream face at the top of the dam. It has been observed, during the detailed design of other similar dams, that such stresses can be reduced by small geometric adjustments of the dam

profile – which are easy to accommodate in RCC construction. Therefore, the dam cross section was slightly modified for this analysis by increasing the width of the dam cross section at the top. The width of the dam crest was increased by 10 ft. at crest level (to 45 ft.) with no changes at the base of dam. The FE model was revised accordingly and continued analyses were performed using the modified cross section. Figure 10.6-21 shows the FE model for the modified geometry of Layout 4.

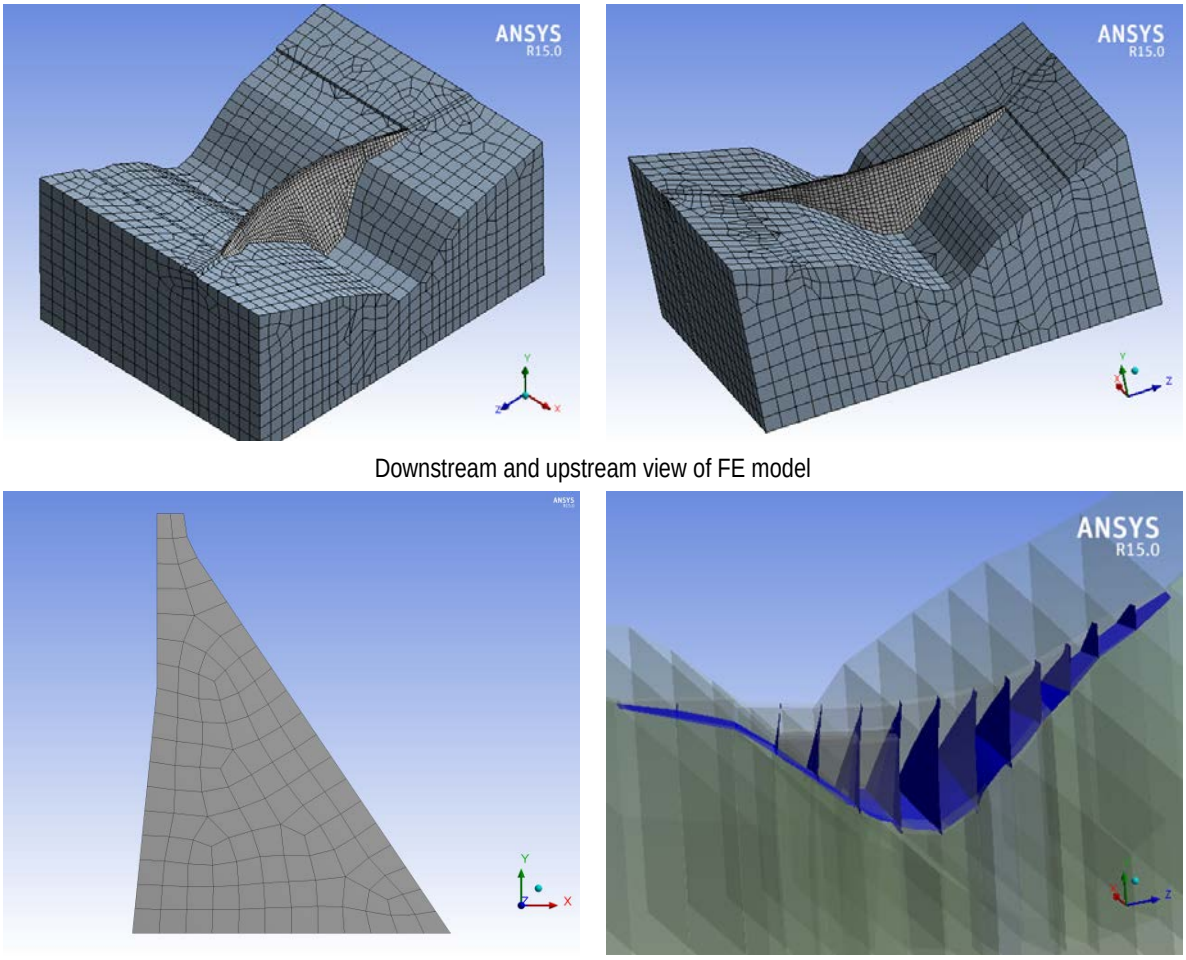

Figure 10.6-21. Finite Element Model of Layout 4

10.6.3.5. Modal Analysis

A modal analysis of the dam was performed and the computed periods of vibration for first 30 free vibration modes of the dam and respective modal mass participation ratios are shown in Table 10.6-10. The mode shapes for the first 4 vibration modes are shown Figure 10.6-22. The fundamental vibration frequency of the Layout 4 dam is just 3 percent smaller than the frequency

of the Layout 3 dam. The Layout 4 dam is thinner and was expected to be more flexible than the Layout 3 dam. However, its smaller radius increases its stiffness resulting in similar vibration frequencies for the two layouts.

Table 10.6-10. Frequencies and Modal Mass Participation Ratio for Layout 4

Mode	Frequency (Hz)	Period (sec)	Mass Participation Ratio			Mass Participation Ratio Cumulative		
			Stream Direction	Cross Stream	Vertical	Stream Direction	Cross Stream	Vertical
1	1.82631	0.54755	4.64E-01	2.06E-04	1.12E-02	0.464	0.000	0.011
2	2.49171	0.40133	1.96E-04	5.05E-03	1.53E-04	0.464	0.005	0.011
3	3.14058	0.31841	4.15E-02	5.75E-05	2.37E-04	0.505	0.005	0.012
4	3.71290	0.26933	2.49E-01	5.61E-03	3.64E-03	0.754	0.011	0.015
5	3.76679	0.26548	1.80E-02	3.34E-03	7.63E-04	0.772	0.014	0.016
6	4.22878	0.23647	1.94E-03	7.81E-01	6.49E-03	0.774	0.795	0.022
7	4.40551	0.22699	1.58E-02	2.13E-05	1.90E-02	0.790	0.795	0.041
8	4.49801	0.22232	2.39E-03	8.53E-03	7.27E-01	0.793	0.804	0.769
9	4.89662	0.20422	5.91E-05	1.21E-02	2.14E-03	0.793	0.816	0.771
10	5.05699	0.19775	3.92E-06	4.81E-05	6.01E-06	0.793	0.816	0.771
11	5.69345	0.17564	7.63E-03	5.94E-05	6.24E-04	0.800	0.816	0.772
12	5.96243	0.16772	2.29E-03	4.01E-04	1.94E-04	0.802	0.816	0.772
13	6.13543	0.16299	5.95E-03	2.34E-02	1.40E-07	0.808	0.840	0.772
14	6.17244	0.16201	8.23E-02	9.30E-04	3.88E-03	0.891	0.841	0.776
15	6.33437	0.15787	4.95E-05	7.23E-05	8.94E-06	0.891	0.841	0.776
16	6.93305	0.14424	1.72E-03	5.19E-06	3.96E-03	0.893	0.841	0.780
17	7.00990	0.14266	2.53E-03	6.62E-04	2.72E-02	0.895	0.842	0.807
18	7.07257	0.14139	1.36E-03	5.52E-05	1.05E-02	0.896	0.842	0.817
19	7.59786	0.13162	8.23E-07	1.40E-03	2.35E-04	0.896	0.843	0.818
20	7.69704	0.12992	1.67E-04	6.42E-05	6.19E-06	0.897	0.843	0.818
21	7.82501	0.12780	3.16E-03	8.64E-05	3.26E-02	0.900	0.843	0.850
22	8.08248	0.12372	5.63E-03	6.96E-09	8.22E-03	0.905	0.843	0.858
23	8.21690	0.12170	5.12E-06	2.71E-04	2.07E-03	0.905	0.843	0.860
24	8.26867	0.12094	8.72E-05	1.42E-02	3.17E-05	0.905	0.858	0.860
25	8.68587	0.11513	2.19E-04	3.43E-05	1.07E-03	0.906	0.858	0.862
26	8.98427	0.11131	2.67E-03	1.84E-03	7.93E-05	0.908	0.859	0.862
27	9.06453	0.11032	1.74E-02	1.25E-04	3.49E-03	0.926	0.860	0.865
28	9.24927	0.10812	4.56E-04	9.18E-04	5.02E-05	0.926	0.861	0.865
29	9.40572	0.10632	7.21E-04	6.17E-03	2.33E-03	0.927	0.867	0.867
30	9.50533	0.10520	2.84E-04	3.17E-02	2.26E-03	0.927	0.898	0.870

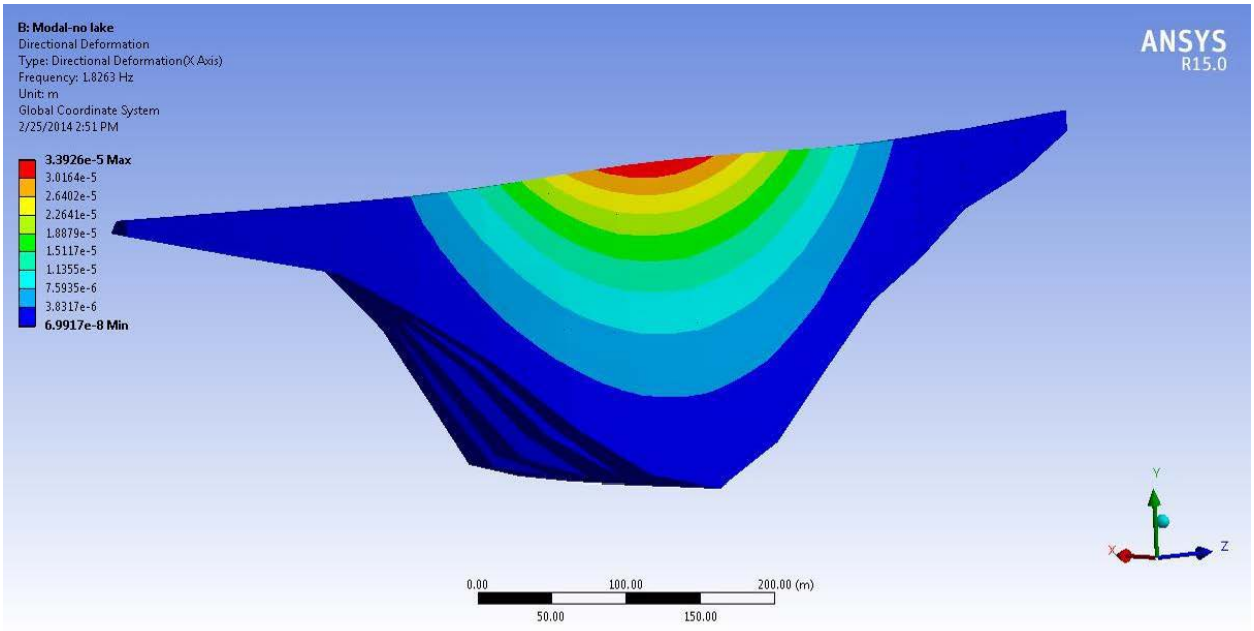
B: Modal-no lake
Directional Deformation
Type: Directional Deformation(X Axis)
Frequency: 1.8263 Hz
Unit: m
Global Coordinate System
2/25/2014 2:51 PM
3.3926e-5 Max
3.0164e-5
2.6402e-5
2.2641e-5
1.8879e-5
1.5117e-5
1.1355e-5
7.5935e-6
3.8317e-6
6.9917e-8 Min
ANSYS
R15.0
0.00
100.00
200.00 (m)
50.00
150.00
Y
X
Z

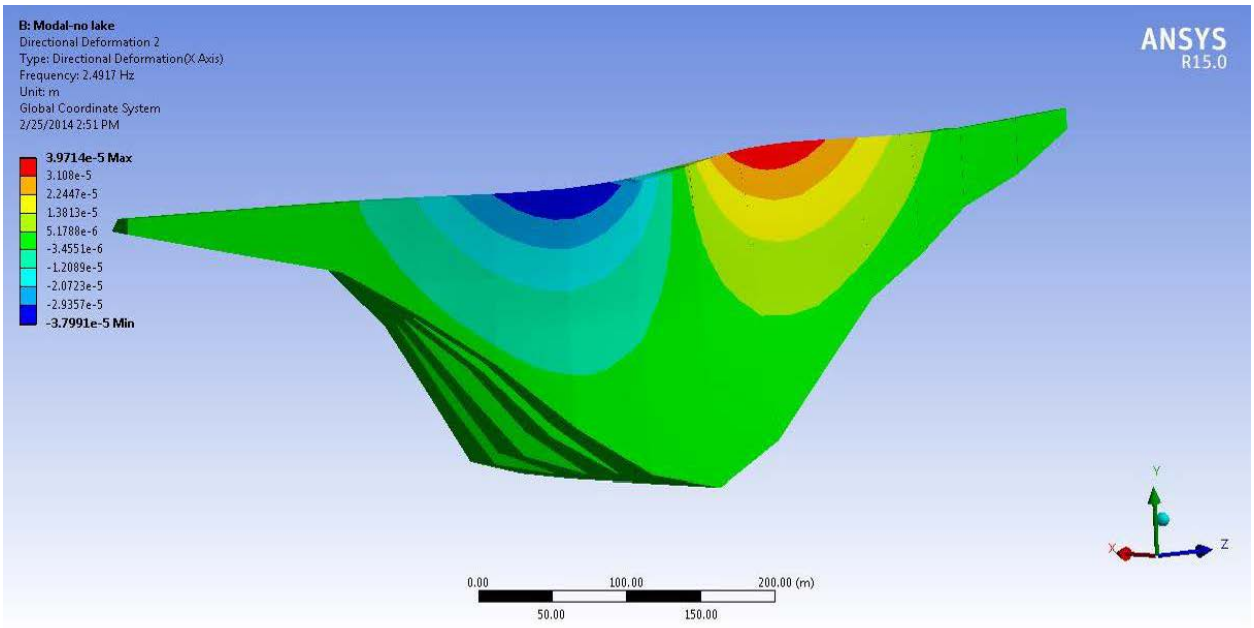
B: Modal-no lake
Directional Deformation 2
Type: Directional Deformation(X Axis)
Frequency: 2.4917 Hz
Unit: m
Global Coordinate System
2/25/2014 2:51 PM
3.9714e-5 Max
3.108e-5
2.2447e-5
1.3813e-5
5.1788e-6
-3.4551e-6
-1.2089e-5
-2.0723e-5
-2.9357e-5
-3.7991e-5 Min
ANSYS
R15.0
0.00
100.00
200.00 (m)
50.00
150.00
Y
X
Z

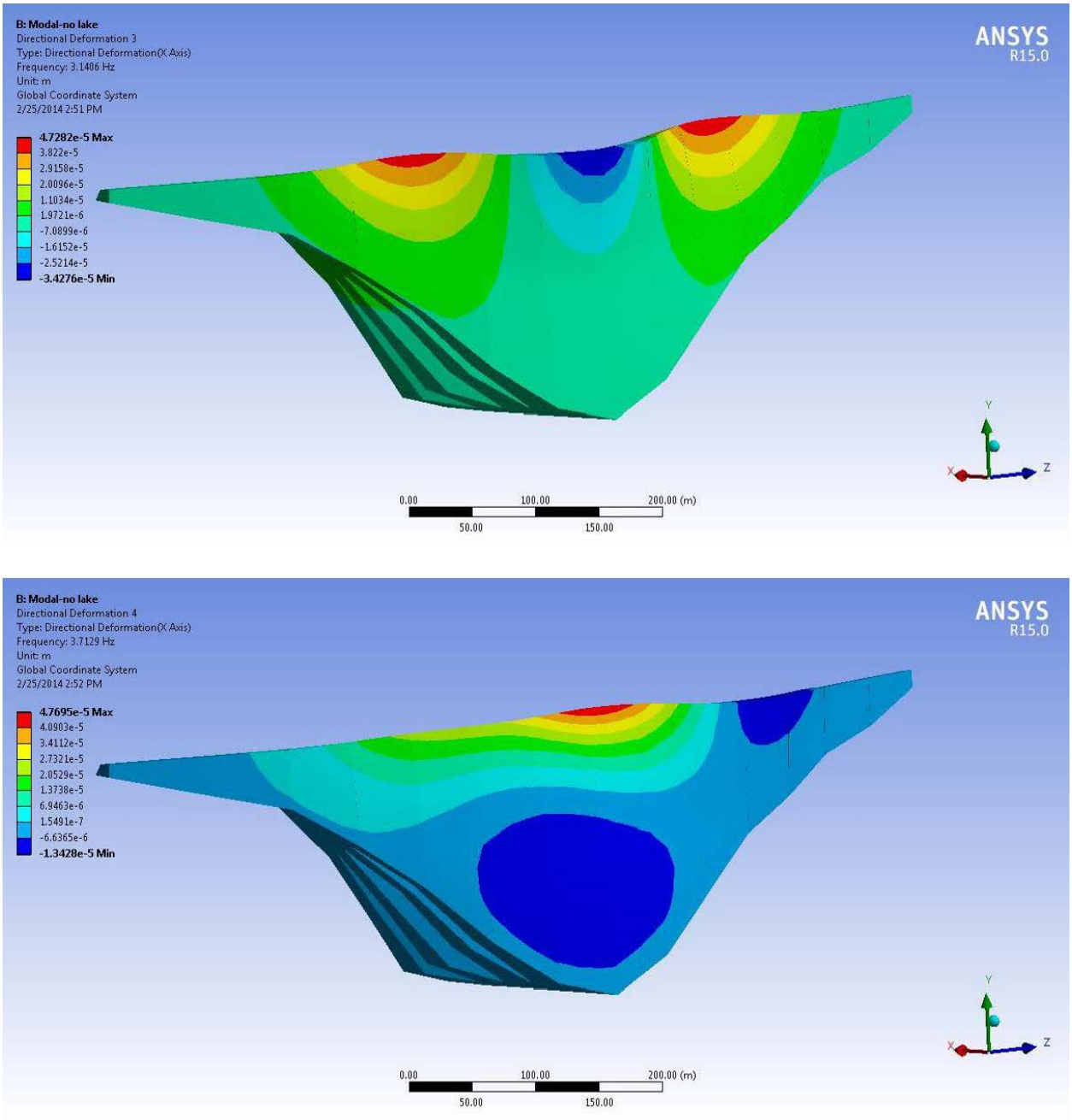

Figure 10.6-22. First Four Vibration Mode Shapes (Dam Layout 4)

10.6.3.6. Transient Analysis Results

Transient dynamic analyses were performed for eight earthquake records (two earthquakes for each selected type of event – Slab M8.0, Slab M7.5, Crustal M7.0, and Interface M9.2).

The envelope of maximum tensile cantilever stress on upstream and downstream face of the dam for IWT010 earthquakes are shown in Figure 10.6-23 and Figure 10.6-24. Figure 10.6-25 shows the residual sliding displacement of the dam monoliths at the end of the (Japan 2011), IWT010 earthquake.

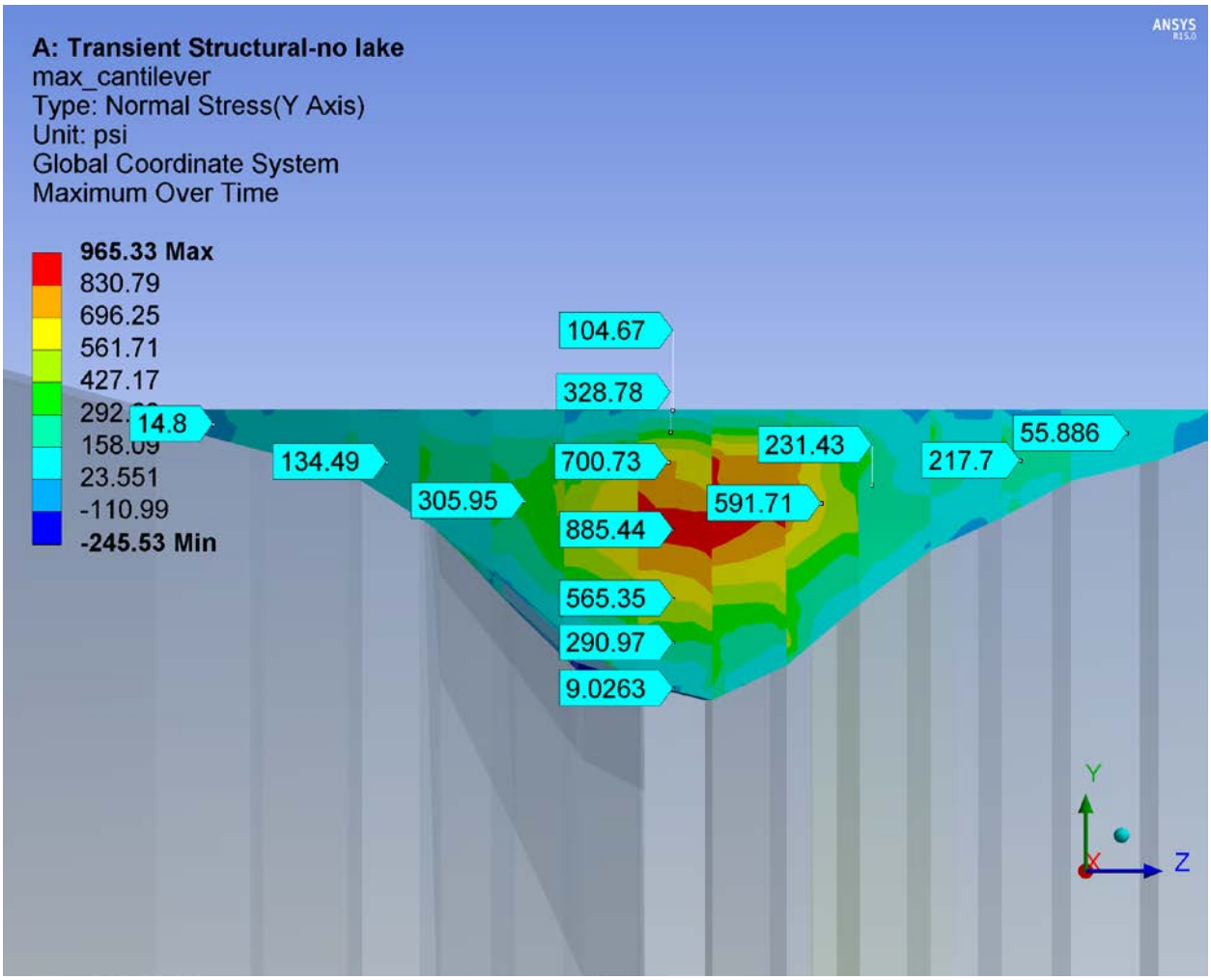

Figure 10.6-23. Envelope of Maximum Tensile Cantilever Stresses (psi) due to IWT010 Event – U/S view (Layout 4)

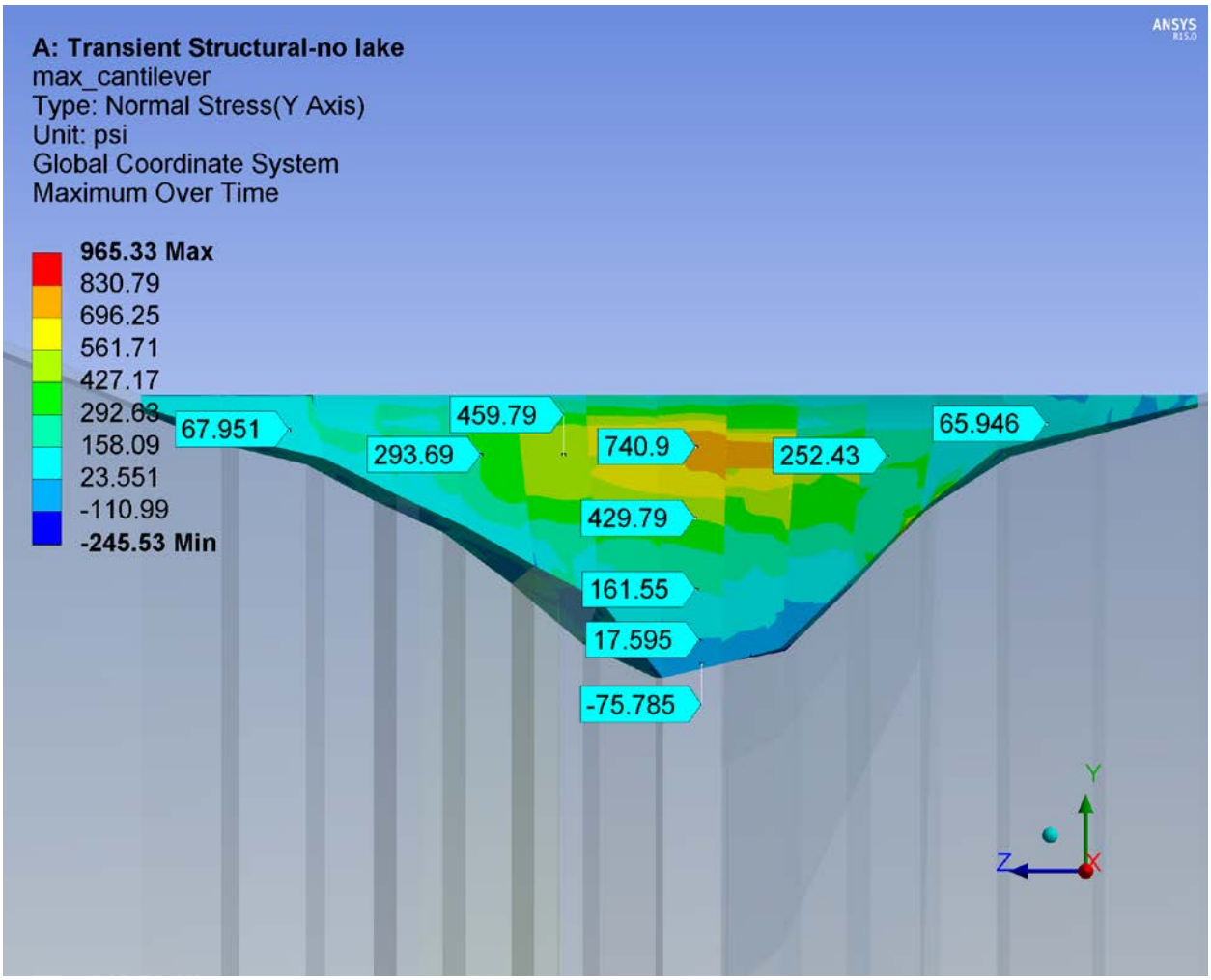

Figure 10.6-24. Envelope of Maximum Tensile Cantilever Stresses (psi) due to IWT010 Event – D/S view (Layout 4)

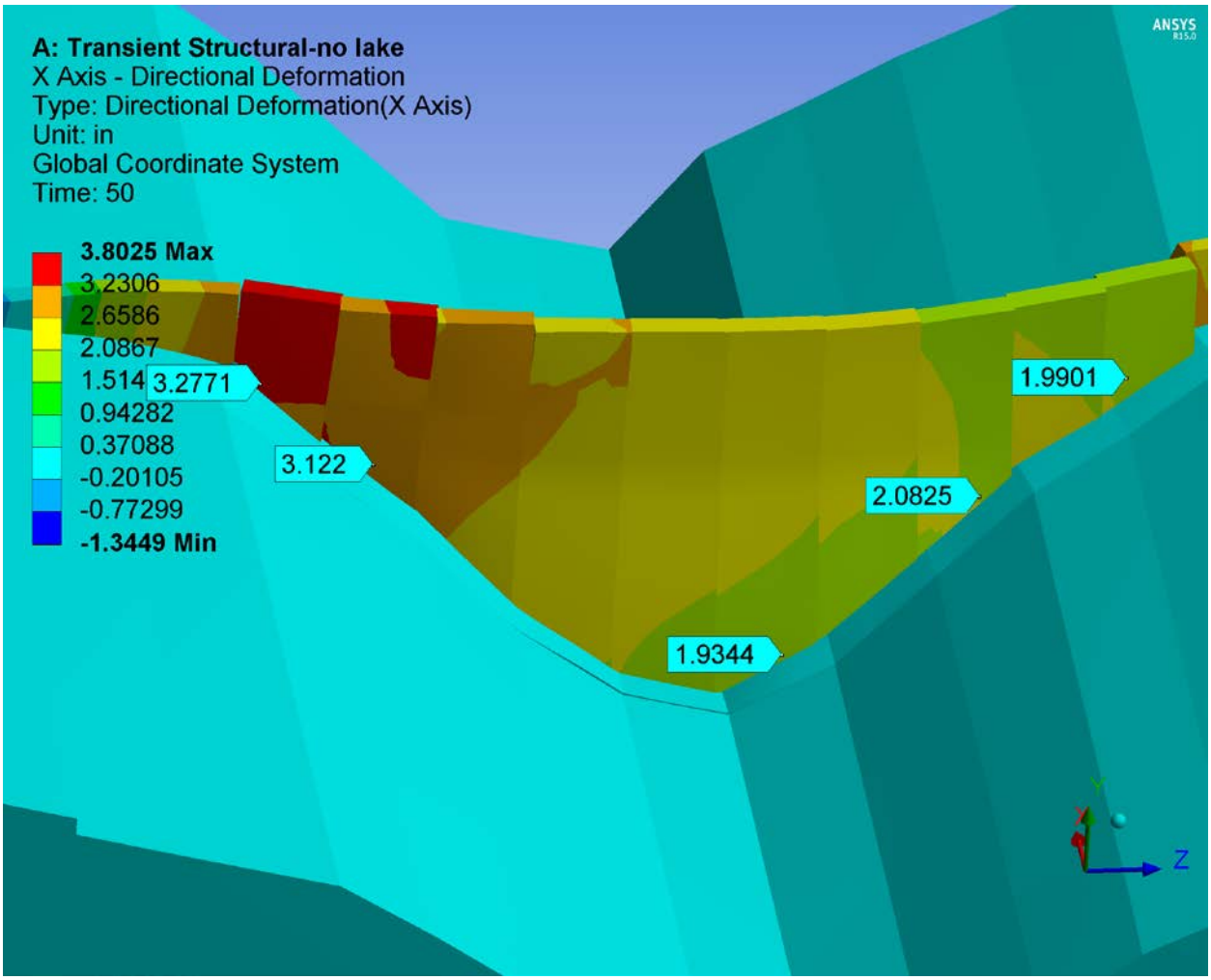

Figure 10.6-25. Residual Sliding Displacement of the Dam (inches) at the End of IWT010 Event looking D/S (Layout 4)

The maximum cantilever stress variations along the height of crown monolith for eight earthquakes are plotted in Figure 10.6-26. The maximum computed stresses in the dam body and permanent displacement of dam monoliths due to eight earthquakes are also summarized in Table 10.6-11 for comparison.

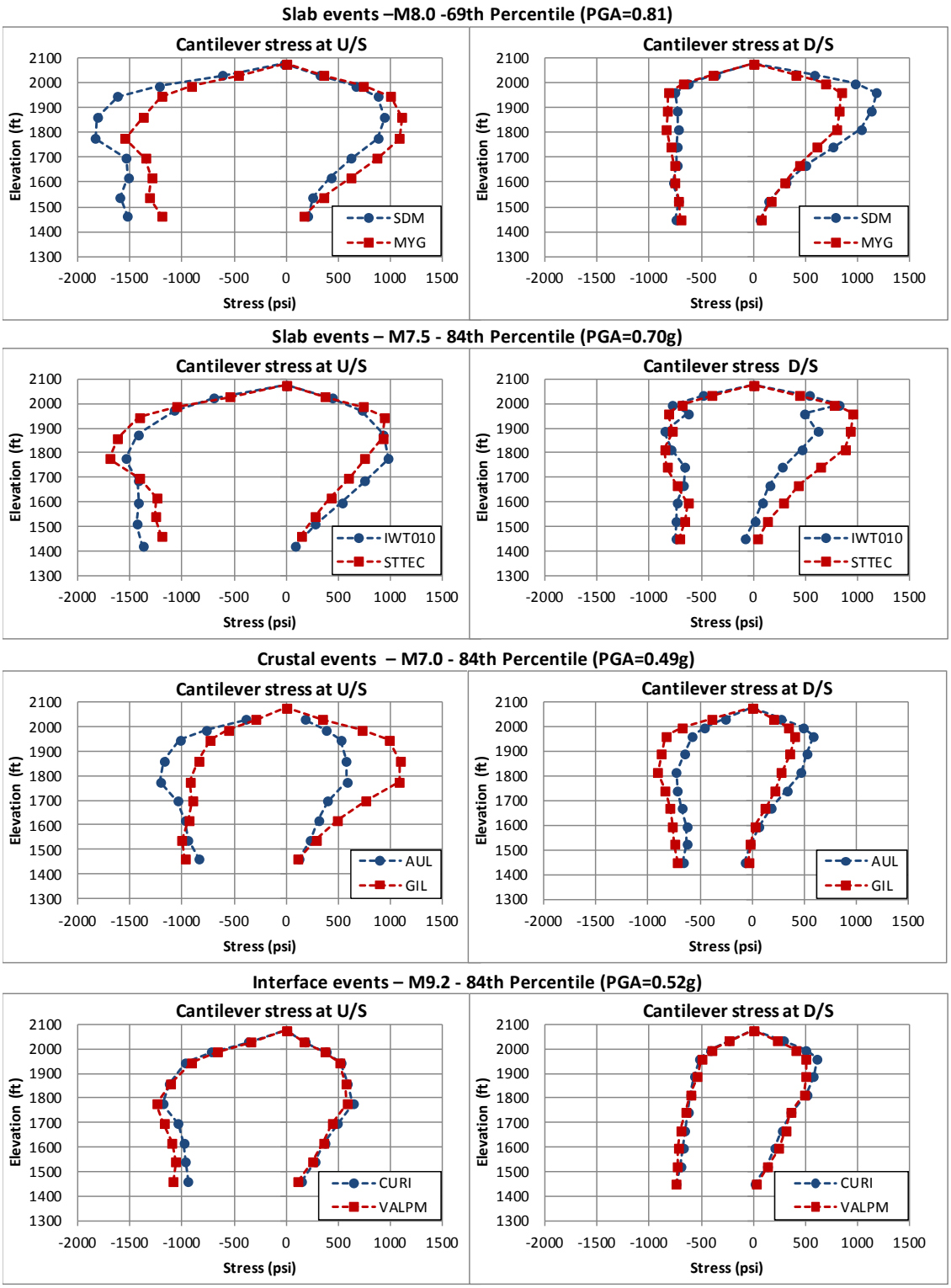

Figure 10.6-26. Envelope of Maximum and Minimum Stresses in Crown Cantilever for Layout 4

Table 10.6-11. Summary of Dam Response to 8 Earthquake Loadings (Layout 4)

Event Title	Event Station	Stress Location	Horizontal Stress Compressive (psi)	Vertical Stress (psi)		Sliding Displacement (in)	
				Tensile	Compressive	Crown Monolith	Side Monoliths
Slab events – M8.0 – 69th Percentile (PGA=0.81)							
El Salvador 13-Jan-01	SDM	U/S	-1278	942	-1830	4.7	6.5
		D/S	-995	1182	-772		
Japan 2011 7-Apr-11	MYG009	U/S	-1277	1109	-1549	4.1	7.7
		D/S	-947	841	-837		
Slab events – M7.5 – 84th Percentile (PGA=0.69g)							
El Salvador 13-Jan-01	STTEC	U/S	-1008	945	-1692	2.4	3.3
		D/S	-698	957	-855		
Japan 2011 7-Apr-11	IWT010	U/S	-867	886	-1581	1.9	2.5
		D/S	-638	772	-821		
Crustal events – M7.0 – 84th Percentile (PGA=0.49g)							
Irpinia, Italy 23-Nov-80	AUL	U/S	-703	584	-1206	1	1.5
		D/S	-573	587	-725.9		
Loma Prieta, California 18-Oct-89	GIL	U/S	-801	1091	-998	1.1	1.6
		D/S	-634	409	-905		
Interface events – M9.2 – 84th Percentile (PGA=0.52g)							
Chile (M 8.8)	CURI	U/S	-877	641	-1181	2.7	3.6
		D/S	-673	611	-741		
Chile (M 8.8)	VALPM	U/S	-730	852	-1245	1.6	2.2
		D/S	-615	507	-741		

Note:
AUL – Italian Crustal Earthquake Record - November 1980
CURI – Chile Interface Earthquake Record - February 2010
GIL – Lomo Prieta, CA Crustal Earthquake Record - October 1989
VALPM – Chile Interface Earthquake Record - Feb 2010

The average stresses and displacements for each of four earthquake events were calculated for dam Layout 4 and Layout 3 and shown in Table 10.6-12. The average of maximum cantilever stresses on the upstream face of dam Layout 4 is generally less than stresses in dam Layout 3 at similar locations. The maximum tensile cantilever stress of 1366 psi in Layout 3 (slab event, PGA=0.81) is reduced to 1021 psi in Layout 4. The contribution of the transfer of horizontal load is higher in Layout 4 – because of the shorter radius and enhanced thickness of the section at the upper part of the dam discussed earlier – compared to Layout 3, resulting in a reduced cantilever action and cantilever tensile stresses. The maximum tensile stress in the downstream

face increases from 818 psi in Layout 3 to 1011 psi in Layout 4 (slab event, PGA=0.81g). However it is still below the maximum tensile stresses on upstream face of the dam.

Table 10.6-12. Comparison of Dam Responses for Dam Layouts 3 and 4

Event Title	Stress Location	Horizontal Stress Compressive (psi)	Vertical Stress (psi)		Sliding Displacement (in)	
			Tensile	Compressive	Crown Monolith	Side Monoliths
Slab events –M8.0 – 69th Percentile (PGA=0.81)						
Layout 3	U/S	-1253	1366	-1619	4.0	5.4
	D/S	-973	818	-914		
Layout 4	U/S	-1277.5	1025.5	-1689.5	4.4	7.1
	D/S	-971	1011.5	-804.5		
Slab events – M7.5 – 84th Percentile (PGA=0.69g)						
Layout 3	U/S	-763	1031	-800	1.7	2.6
	D/S	-659	711	-1338		
Layout 4	U/S	-937.5	915.5	-1636.5	2.15	2.9
	D/S	-668	864.5	-838		
Crustal events – M7.0 – 84th Percentile (PGA=0.49g)						
Layout 3	U/S	-730	1047	-1091	0.5	0.9
	D/S	-573	460	-770		
Layout 4	U/S	-752	837.5	-1102	1.0	1.5
	D/S	-603.5	498	-815.45		
Interface events – M9.2 – 84th Percentile (PGA=0.52g)						
Layout 3	U/S	-800	759	-1401	1.8	2.3
	D/S	-629	680	-600		
Layout 4	U/S	-803.5	746.5	-1213	2.15	2.9
	D/S	-644	559	-741		

The average sliding displacement for Layout 4 in all cases is greater than the sliding displacement of Layout 3. Sliding displacement increased up to 100 percent for crustal events, but remains at about 10 percent for slab (PGA=0.81g) events. Although the sliding displacement is greater for this Layout 4, the dam remains stable during the earthquake events and in the post seismic condition, as discussed in Section 10.6.5.5.4.

10.6.3.7. RCC Volume

Estimation of the RCC volume in the Layout 4 dam was carried out using the same approach as that used for Layout 3. An Excel spreadsheet was used to calculate the dam volume using two

independent methods, by elevation and by station. Adjustments were made to the previous spreadsheet to allow the straight and curved portions to be calculated and for different downstream slopes. The spreadsheet analysis was also refined to include the sloping portion of the upstream face.

The analysis accounts for the RCC fill between the dam and powerhouse and also the reduction in dam RCC volume arising from placement of the penstocks, power intakes, low level outlet intake and pipes, sluice and the spillway crest.

The volume of RCC in Watana Dam for the updated Layout 4 configuration is shown in Table 10.6-13 follows:

Table 10.6-13. RCC Volume (Layout 4)

Section	RCC Volume (cy)
Left Abutment	
Straight portion	80,970
Curved portion	513,810
Center	
Curved portion	3,949,590
Downstream fill	125,260
Right Abutment	
Curved portion	697,010
Straight portion	101,360
Total	5,468,000

As part of the ongoing development, and in preparation for the thermal analysis of the dam, the locations of the vertical construction joints between the abutments and center section have been selected to make certain that the projected first season RCC placement volume could be completely placed while the river diversion was progressed, and also to ensure that the RCC beneath the spillway crest would be at the required finished elevation to facilitate commencement of construction of the spillway crest at the end of the first RCC placement season. The formed vertical joints will include large shear keys, and are also expected to be grouted at the end of dam construction.

The volume-elevation relationship for the updated configuration is shown graphically in Figure 10.6-27 below:

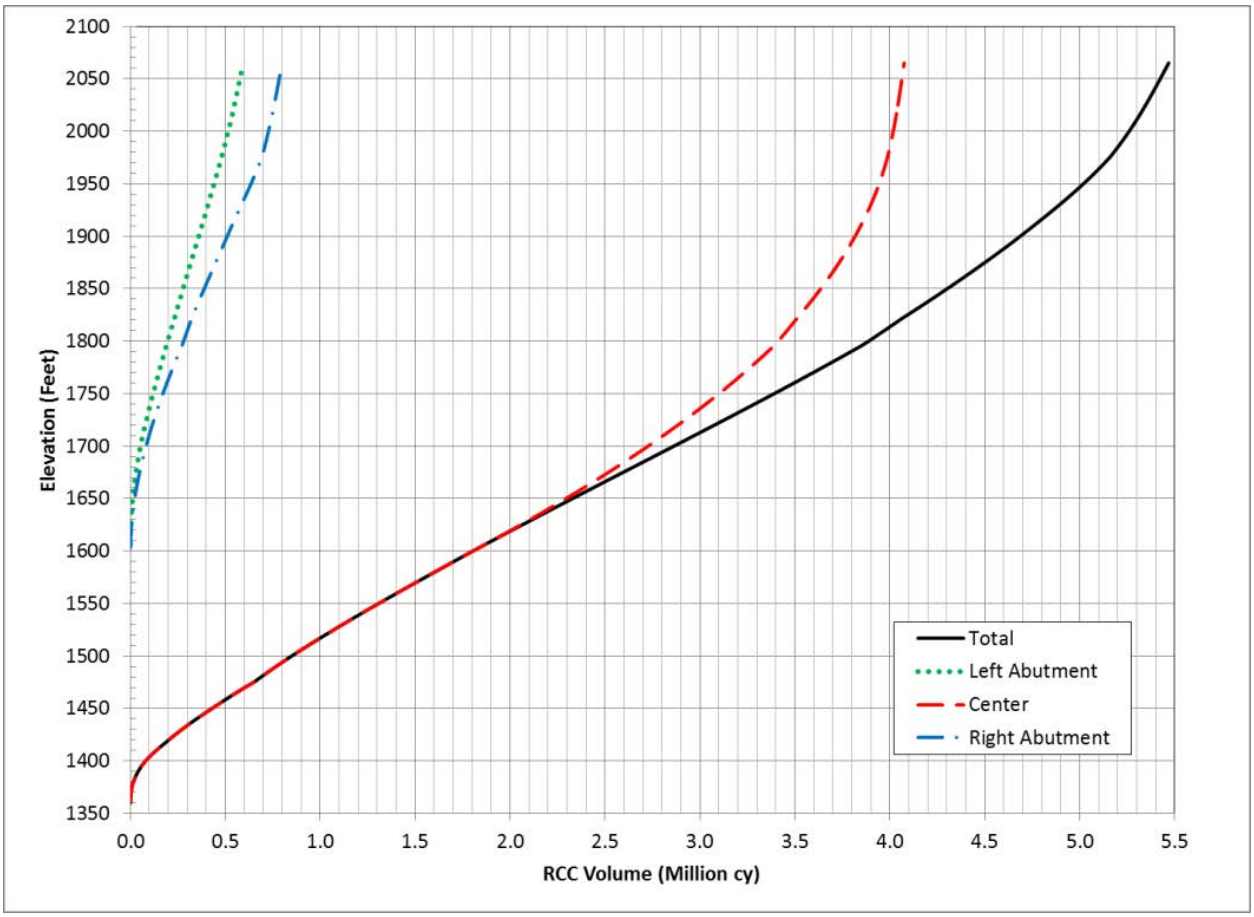

Figure 10.6-27. RCC Volume vs Elevation (Layout 4)

The estimated volume of RCC in the previous configuration was 6,420,000 cy. The updated configuration requires 952,000 cy less RCC to construct and thus can be completed one season earlier than that projected for Layout 3.

10.6.4. Sensitivity to Foundation Conditions

Following the desk review of the foundation conditions – absent any on site verification – the foundation was divided into two zones, and assigned different characteristics. The dynamic analyses performed for Layout 3 and Layout 4 were subject to sensitivity studies based on different characteristics of the foundation. However, the results reported here are for only the sensitivity studies of Layout 4. Two transient analyses of Layout 4 subjected to IWT010 earthquake loading were performed and stress results are shown in Figure 10.6-28. (The results shown are for Layout 4 before the cross section was modified.) In the first analysis the deformation modulus of both zones was doubled ($E=2E_f$) and in the second analysis a value of $E=0.5E_f$ was used.

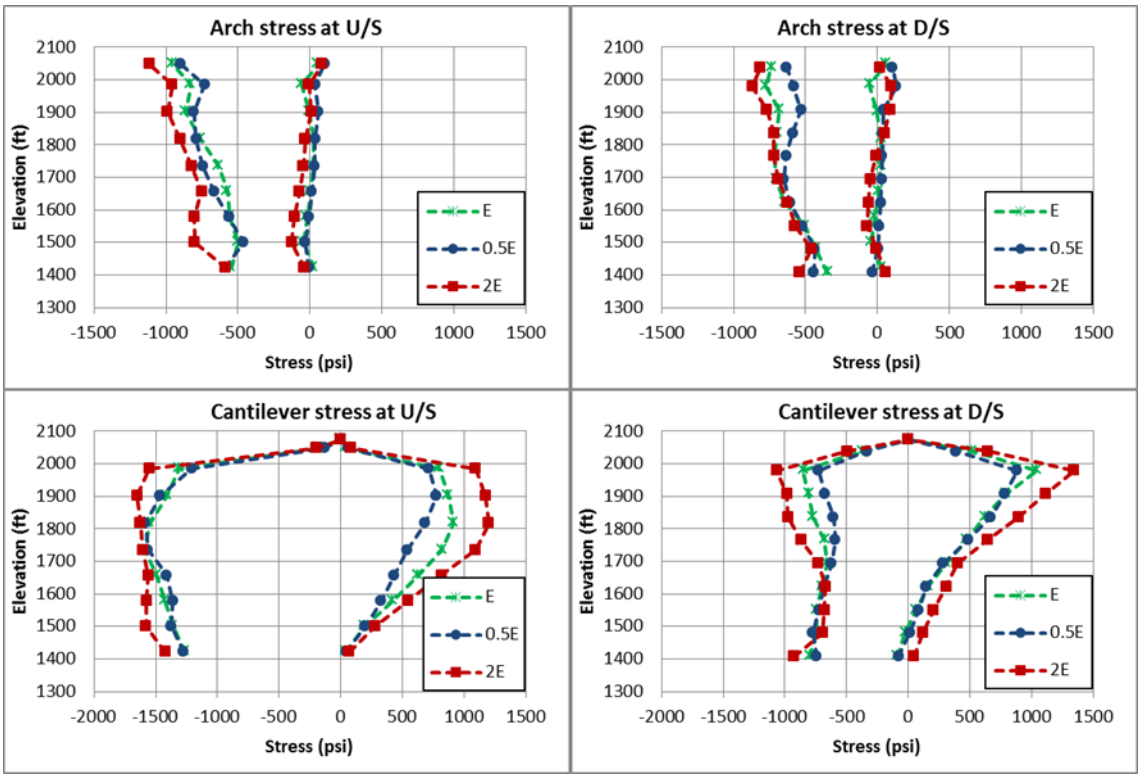

Figure 10.6-28. Effect of Foundation Deformation Modulus on Maximum/Minimum Stresses (Layout 4)

The variability between foundation blocks was not subject to sensitivity analyses because the softer area of the foundation did not extend over more than one monolith or two for the size of elements detailed in the model. Future analyses in which a greater numbers of elements are modeled should consider the variability in foundation conditions.

Results of the sensitivity studies show that lower deformation modulus of the foundation has negligible effect on the stress distribution in the dam. However, increasing the deformation modulus of the foundation by 100 percent will increase the maximum tensile stresses in the dam around 25 to 30 percent. The magnitude of the foundation deformation modulus has some effect on the developed stress and requires in situ testing from the proposed adits and laboratory testing of the dam foundation rock to verify rock properties.

10.6.5. Discussion on Analysis without Foundation Mass

10.6.5.1. Review of Preliminary Analysis

The results of the analysis presented in Section 10.6 were for the purposes of defining – at feasibility level – the proposed configuration of the dam structure. It was an iterative process, and has been organized so that realistic feasibility design progress can be made in the absence of

robust site investigation data, but taking into account the input of external parties such as the Board of Consultants. At this feasibility level of design, the focus has been comparison of various dam geometries rather than an excessively detailing of structural elements of the dam.

Thus the stability and dynamic analysis has been targeted at realizing the most promising arrangement rather than defining the final geometric solution. Together with the current appreciation of the geological features of the site, the selected dam configuration will define the site investigation and adit location – the results from which will allow more accurate and representative analysis to be carried out together with more complete sensitivity analysis.

An RCC dam that includes curvature represents the optimum arrangement – utilizing a substantial component of gravity action, but that redistributes loads horizontally in a manner that enhances stability. RCC construction is a methodology that allows easy accommodation of somewhat complex shapes such as the three centered dam originally postulated as a possible layout. Layout 2 was postulated as the most aggressive layout in terms of achieving a safe project while minimizing concrete – and was recognized as one bound of the envelope of possible solutions. Layout 3 – including a gravity section while maintaining a "traditional" gravity cross section with a 0.85 downstream slope – is considered to be the most conservative of the options studied, but carries a penalty of one million extra yards of RCC and one year extra construction period. Layout 4 provides a compromise, well within the envelope of safe and reasonable solutions but with the benefit of the reduction of 920,000 yds^3.

Comparison of the 2-D analysis shows that – assuming zero cohesion at the base – Layout 3 performed in accordance with FERC stability criteria, but could suffer a cracked base at higher ground motions. For Layout 4 – also assuming zero cohesion at the dam base – the simplified analysis showed the dam satisfied FERC stability criteria for the normal static, flood and post-seismic conditions with a cracked base. The resultant location for Layout 4 for all forces under the post-seismic cracked condition fell within the dam base, and sliding factor of safety was adequate.

With respect to the results of the nonlinear FE analysis using a massless foundation, the results for Layout 3 and Layout 4 were similar, with all compressive stresses within the limits of expected RCC design strengths. With regard to tensile cantilever stresses, Layout 4 exhibited a better response compared to Layout 3. The maximum tensile stresses on the upstream face of the dam is reduced from 1366 psi in Layout 3 to 1,025 psi in Layout 4 (slab event, PGA=0.81) and the average reduction in upstream vertical stresses is around 15 percent for all earthquake events. Although the computed tensile stresses on the downstream face of Layout 4 are slightly higher than the similar stresses in Layout 3, the maximum developed tensile stress on the downstream face is still smaller than the maximum tensile stress on the upstream face. Sliding displacements

predicted for each layout can be managed through design – generally being under two inches for the crown cantilever, but sometimes over four inches for the side monoliths. Dam and foundation drains will be sized to accommodate potential sliding displacements and to remain effective following movement of the dam during extreme loading.

In reviewing the results – even though the ongoing site specific seismic hazard analysis and the PMP/PMF studies have resulted in modifications to the required dam criteria – it is evident that the 2-D stability requirements can be achieved by Layouts 3 and 4 but the FE analysis (using simplistic assumptions) have shown calculated tensile stresses that are above those projected for well mixed and placed RCC – but which can be reduced to acceptable levels by shaping of the upper part of the dam, and by more refined FE analysis.

RCC produced and placed by a competent contractor – even in the strenuous conditions in Alaska can be expected to exhibit compressive strength of 6,000 psi, and tensile strength of up to 400 psi, based on strength of parent material and lift joints measured at existing RCC dams. Under seismic loads a tensile strength of 580 psi on the lift joints can be assumed, based on experience at Olivenhain and San Vicente dams. Based on the static and dynamic analyses presented for Layout 4 it is clear that nonlinear analysis, with massless foundation, indicates stress values that exceed the expected tensile strength of the RCC.

However, the main factors that influence the 3-D analysis of curved dams have been identified by several researchers (Chopra 2008, USBR 2006). The current state of the art in seismic analysis and evaluation of concrete dams is to carefully consider these factors in the numerical simulation, to avoid over-conservative or under-conservative design. More careful modeling of the fluid structure interaction considering the compressibility of the water; and foundation rock inertia and damping are major factors which have been identified as contributing to a more representative and accurate model of the stresses in the structure.

According to a series of example analyses, it was demonstrated that (Chopra 2008):

- By neglecting water compressibility, stresses may be significantly overestimated for some dams or underestimated for others.
- By neglecting foundation-rock mass and damping, the stresses may be overestimated by a factor of two or three.

In the analyses described above water compressibility has been neglected and the foundation has been assumed to be massless – in the interests of speed of analysis. To more accurately estimate the performance of the structure, further analytical development of the selected alternative was performed including Chopra's recommendations.

10.6.6. Modeling of Fluid Structure Interaction

Water compressibility effect can be considered by performing a Fluid Structure Interaction (FSI) analysis using acoustic elements to model the dam reservoir.

ANSYS Acoustic elements, fluid 30, were used to add the reservoir to the FE model.

However, transient analysis of the model using acoustic elements (Fluid30) and nonlinear elements did not converge. After discussion with ANSYS technical support team, Fluid 80 element was identified as an appropriate substitute for Fluid30 element. Satisfactory results were obtained by conducting an example benchmark.

Subsequently, Fluid 80 elements were used for FSI analysis of Watana Dam Layout 4 and the model is shown in Figure 10.6-29. Absorbing boundary conditions were considered at the far end boundary of the reservoir to absorb the outgoing pressure waves in the reservoir.

Using FSI analysis the computed dam sliding was reduced about 50–100 percent compared to the similar results from the previous added mass model. The maximum tensile stresses of the concrete derived from the two analyses appeared to be close and it is concluded that the compressibility of the water does not affect the maximum tensile stresses for the model although the stress distribution was changed.

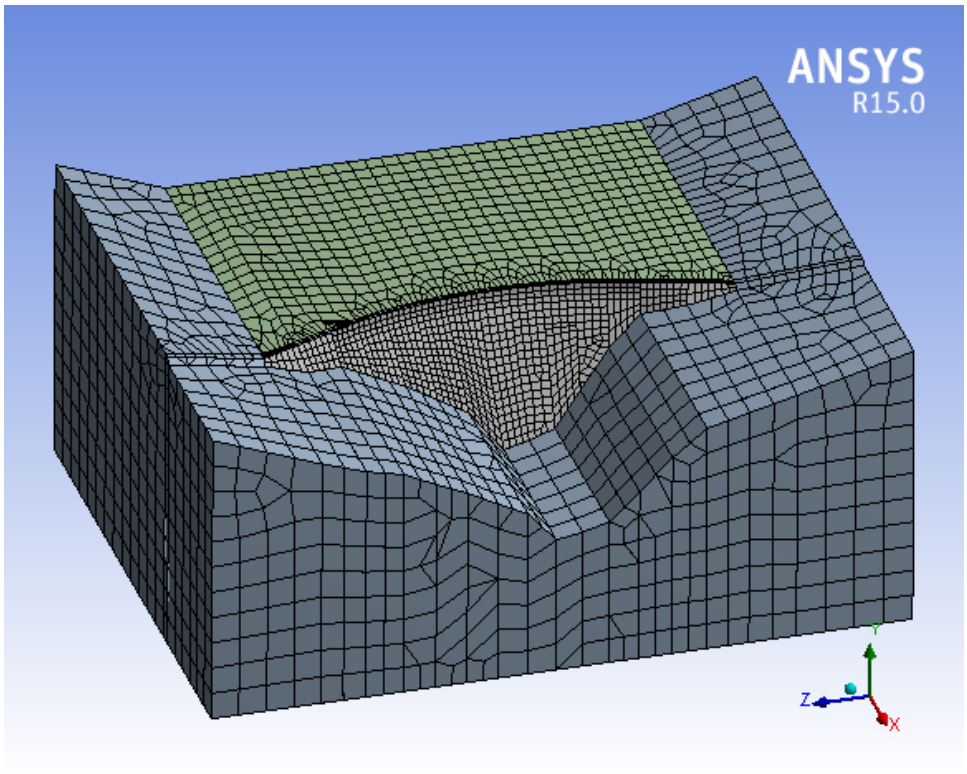

Figure 10.6-29. FE Model of Dam Layout 4 with Fluid 80 Acoustical Elements to represent Reservoir

10.7. Dam – Final Modeling including FSI, Foundation Mass and Damping

10.7.1. Final Dam Layout (Layout 4 – Modified)

For final feasibility analysis, the model of the Layout 4 configuration was modified to increase the width of the dam crest to 45 ft., and instead of a straight downstream face, the downstream face of the curved section of the dam was modified to a single radius curve.

The dam geometry selected for the modified Layout 4 is shown in Figure 10.7-1 and Figure 10.7-2.

10.7.2. LS-DYNA Analysis Software

As discussed above, a more realistic FE analysis of dams can be performed by including Fluid Structure interaction, and adding mass (and damping) to the foundations. Incorporating these aspects, a significant reduction in the calculated tensile stresses can be expected, compared to the simple analysis without mass in the foundations. The proposed configuration – developed as a result of the analyses described in Section 10.6 was therefore analyzed using LS-DYNA to

include the mass of the foundation. LS-DYNA is a commercialized version (by Livermore Software Technology Corporation [LSTC]) of computer program DYNA developed at Lawrence Livermore National Laboratory. It is a highly nonlinear transient dynamic FE code using explicit solutions. It can model mass in the foundation, model the reservoir with fluid elements, model contraction joints and foundation discontinuities, and has non-reflecting boundaries at the foundation and reservoir extents. LS-DYNA has been successfully used by the Bureau of Reclamation, US Army Corps of Engineers, the California Department of Water Resources, and many private consulting firms in several seismic dam-reservoir-foundation simulations.

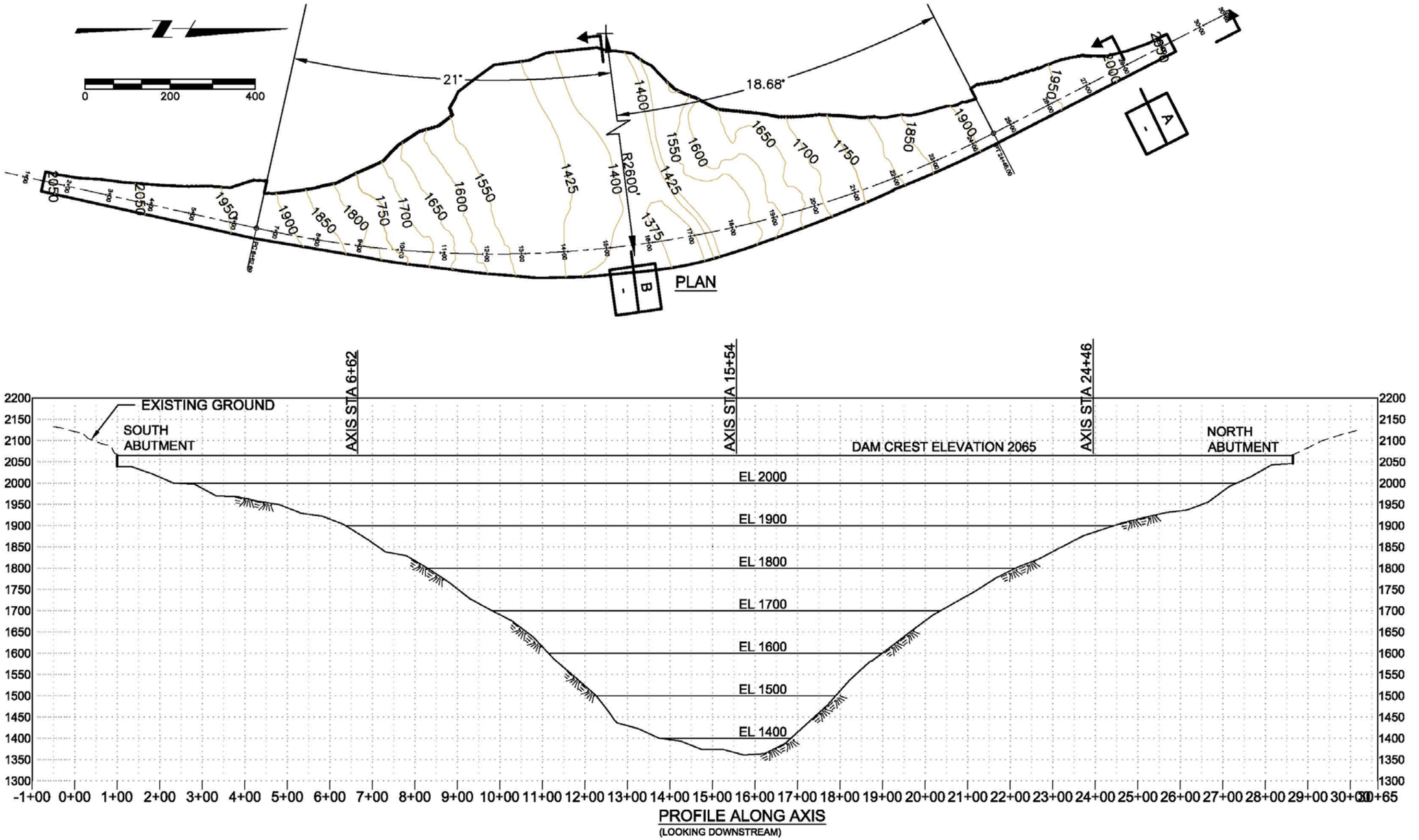

Figure 10.7-1. Plan and Elevation of Dam Layout 4 – Modified

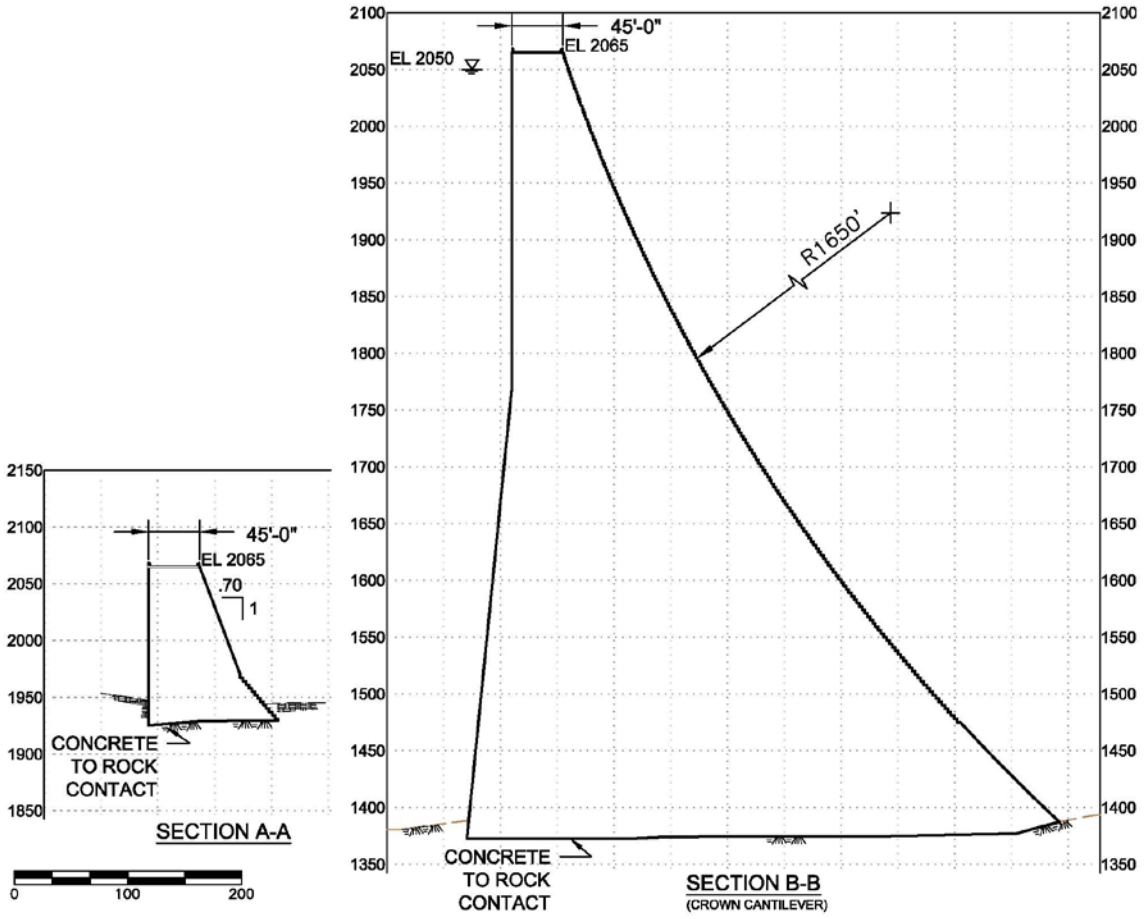

Figure 10.7-2. Sections of Layout 4 – Modified

10.7.3. Selection of Time Histories for Final Modeling

The selection of seismic criteria for the final modeling was reviewed as described in this section to include – in the modeling – the regional seismic data obtained during the feasibility studies to date.

10.7.3.1. Approach

Response spectra were developed from a deterministic seismic hazard analysis for each design event. After the design response spectra were developed representative earthquake records were selected and spectrally matched. The following sections include additional discussion on the development of design response spectra, selection of time histories, spectral matching technique and earthquake record parameters before and after spectral matching. Plots of the acceleration,

velocity, displacement, Arias intensity and Fourier amplitude spectra are included in Appendix B6.

10.7.3.2. Development of Design Response Spectra

Based on the Preliminary SSSHA Report (Fugro 2012), the seismic hazard at the dam site encompasses contributions from three different sources: the subduction zone events – interface and intraslab (also referred to as the slab), and crustal events. Time histories were developed for each type of event to evaluate the difference in frequency content.

Guidance furnished by FERC, Evaluation of Earthquake Ground Motions, was followed and a deterministic spectra was used (Idriss & Archuleta 2007). Table 10.7-1 contains the deterministic parameters for each of the selected events, and Figure 10.7-3 illustrates the response spectrum. The 2,500, 5,000, and 10,000 year return period uniform hazard spectra are also included on Figure 10.7-3; this data is from the SHA Report (Fugro 2012). It should be noted that the V_{S30} used in the probabilistic seismic hazard assessment is 800 m/s.

The 84th percentile or above was used for all of the events, except the magnitude 8.0 event for the slab, where the 69th percentile is used. Additional discussion regarding the selection of the 69th percentile forms Appendix B7. The interface event was scaled up at the fundamental period of the dam (0.55 seconds) to match the 5,000 year return period, resulting in the 88th percentile, see Figure 10.7-3. In contrast to the results of the probabilistic seismic hazard, current field data indicate a V_{S30} of 1,100 m/s which was used, as provided in Draft Revised Intraslab Model and PSHA Sensitivity Results (Fugro 2014). The increase in V_{S30} will decrease the ground motions; therefore, it should be noted that the uniform hazard spectra will be slightly higher compared to the deterministic spectra.

Table 10.7-1. Deterministic Seismic Input Parameters

CASE	Crustal	Interface	Intraslab	
	Fog Lake	Alaskan Subduction Zone		
Magnitude	7.0	9.2	7.5	8.0
Hypocentral distance (km)	-	-	50	
R_{RUP} (km)	7.0 (R_{JB}=3.5)	78	-	
V_{S30} (m/s)	1,100 m/s			
Type of faulting	Normal	Reverse	Normal	
Dip (degrees)	80	-	-	
Seismogenic Depth (km)	20	-	-	
Width (km)	20.3	-	-	
$Z_{1.0}$ (km)				

CASE	Crustal	Interface	Intraslab	
	Fog Lake	Alaskan Subduction Zone		
$Z_{2.5}$ (km)				
Z_{TOR} (km)	0.5			
Hanging Wall	YES	-	YES	YES
PGA(g) [percentile]	0.49 [84th]	0.58 [88th]	0.69 [84th]	0.81 [69th]
Ground Motion Prediction Equation [weight]	BA08 [0.25] CY08 [0.25] CB08 [0.25] AS08 [0.25]	BCH11 [0.5] ZH06 [0.25] AM09 [0.25]	BCH11 [0.5] ZH06 [0.25] AB03 [0.25]	

Note:
km – kilometer(s)
Source: Deterministic Seismic Hazard Analysis; Fugro 2013
Acronyms: BA08= Boore and Atkinson 2008; CY08=Chiou and Youngs 2008; CB08=Campbell and Bozorgnia 2008; AS08=Abrahamson and Silva 2008; BCH11=BC Hydro 2012; ZH06= Zhao 2006; AM09=Atkinson and Macias 2009, AB03=Atkinson and Boore 2003

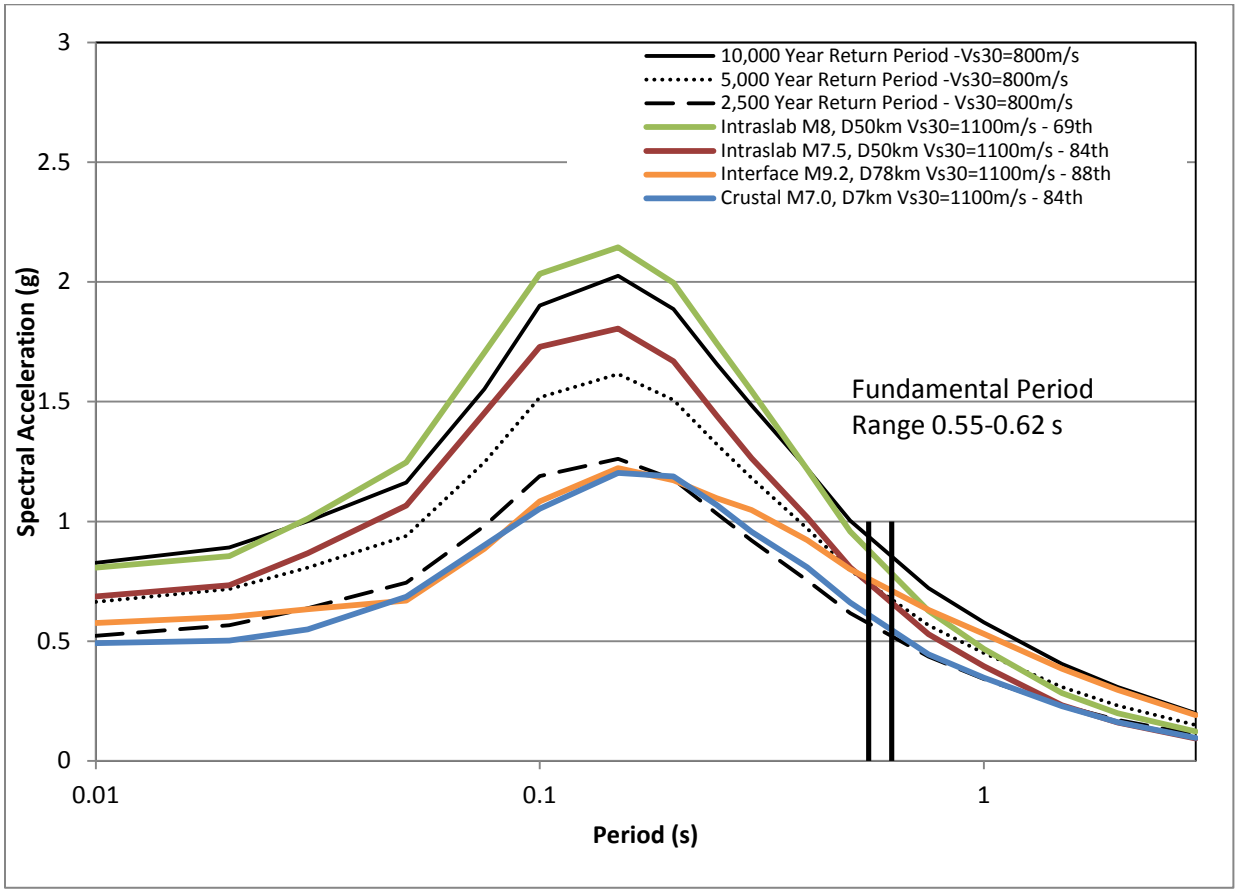

Figure 10.7-3. Design Response Spectra

A vertical response spectrum was developed by computing a vertical to horizontal ratio following the guidance of Gülerce and Abrahamson (2011). The applicability to subduction zone events was based on the work performed by Gregor et al. (2012). The magnitude and distance pair used for the deterministic analysis was used as the input parameters to develop the vertical to horizontal ratios. The ratios correspond to median values and are presented in Table 10.7-2. The vertical and horizontal response spectra are shown in Table 10.7-3 through Table 10.7-5 for each event type together with plots shown in Figure 10.7-4 through Figure 10.7-6.

Table 10.7-2. Median Vertical / Horizontal Ratios

Period (s)	Slab M8.0	Slab M7.5	Interface	Crustal
0.010	0.658	0.652	0.579	0.728
0.020	0.659	0.652	0.579	0.728
0.030	0.715	0.708	0.600	0.791
0.050	0.719	0.710	0.582	0.902
0.075	0.695	0.684	0.642	0.921
0.100	0.670	0.657	0.638	0.798
0.150	0.652	0.640	0.634	0.660
0.200	0.656	0.647	0.648	0.597
0.250	0.668	0.661	0.656	0.586
0.300	0.683	0.678	0.669	0.590
0.400	0.713	0.713	0.696	0.597
0.500	0.729	0.732	0.709	0.596
0.750	0.838	0.842	0.802	0.655
1.000	0.825	0.829	0.776	0.634
1.500	0.820	0.824	0.794	0.648
2.000	0.791	0.795	0.782	0.639
3.000	0.773	0.777	0.787	0.643
4.000	0.805	0.808	0.836	0.683
5.000	0.816	0.820	0.848	0.693
7.500	0.816	0.820	0.848	0.693
10.00	0.816	0.820	0.848	0.693

Table 10.7-3. Horizontal and Vertical Design Response Spectra for Intraslab Events

Period	M8.0 69th Percentile		M7.5 84th Percentile	
T (s)	Horizontal Acceleration (g)	Vertical Acceleration (g)	Horizontal Acceleration (g)	Vertical Acceleration (g)
0.01	0.8075	0.531	0.6870	0.4479
0.02	0.8553	0.564	0.7337	0.4784
0.03	1.0121	0.724	0.8675	0.6142
0.05	1.2464	0.896	1.0668	0.7574
0.075	1.7055	1.185	1.4522	0.9933
0.1	2.0342	1.363	1.7286	1.1357
0.15	2.1449	1.398	1.8046	1.1549
0.2	1.9965	1.310	1.6686	1.0796
0.25	1.7432	1.164	1.4413	0.9527
0.3	1.5443	1.055	1.2646	0.8574
0.4	1.2174	0.868	1.0162	0.7246
0.5	0.9581	0.698	0.8078	0.5913
0.75	0.6262	0.525	0.5289	0.4453
1	0.4679	0.386	0.3960	0.3283
1.5	0.2835	0.232	0.2326	0.1917
2	0.1986	0.157	0.1603	0.1274
3	0.1226	0.095	0.0935	0.0726

Note: Deterministic Inputs shown in Table 10.7-1.

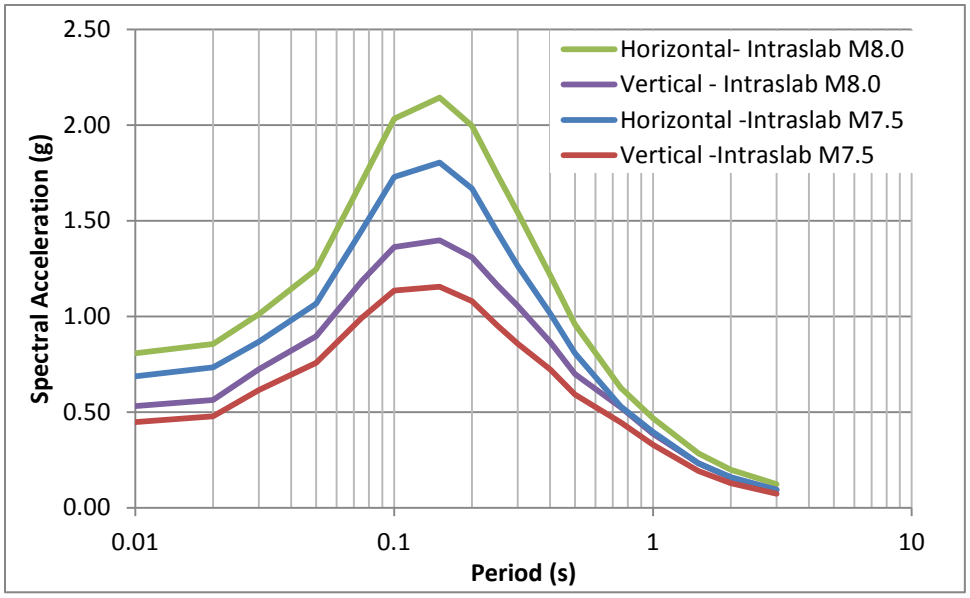

Figure 10.7-4. Intraslab M8.0 – 69th Percentile Design Response Spectra and Intraslab M7.5 – 84th Percentile Design Response Spectra

Table 10.7-4. Horizontal and Vertical Design response Spectra for Interface Events

Period	M9.2 88h Percentile	
T (s)	Horizontal Acceleration (g)	Vertical Acceleration (g)
0.01	0.5754	0.3332
0.02	0.6011	0.3481
0.03	0.6328	0.3797
0.05	0.6697	0.3898
0.08	0.8857	0.5686
0.10	1.0832	0.6911
0.15	1.2221	0.7748
0.20	1.1724	0.7597
0.25	1.0975	0.7199
0.30	1.0472	0.7005
0.40	0.9222	0.6419
0.50	0.8005	0.5675
0.75	0.6308	0.5059
1.00	0.5298	0.4111
1.50	0.3848	0.3056
2.00	0.2964	0.2318
3.00	0.1914	0.1506

Note: Deterministic Inputs shown in Table 10.7-1.

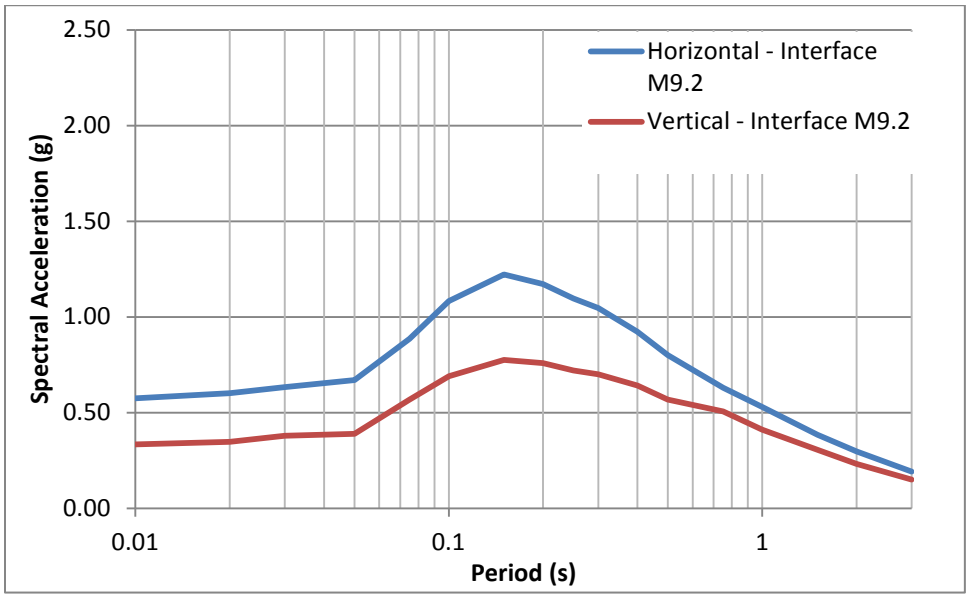

Figure 10.7-5. Interface M9.3 – 88th Percentile Design Response Spectra

Table 10.7-5. Horizontal and Vertical Design Response Spectra for Crustal Events

Period	M7.0 84h Percentile	
T (s)	Horizontal Acceleration (g)	Vertical Acceleration (g)
0.01	0.4910	0.3574
0.02	0.5022	0.3656
0.03	0.5487	0.4340
0.05	0.6859	0.6187
0.08	0.9005	0.8294
0.10	1.0523	0.8397
0.15	1.2028	0.7938
0.20	1.1882	0.7094
0.25	1.0686	0.6262
0.30	0.9567	0.5645
0.40	0.8077	0.4822
0.50	0.6615	0.3943
0.75	0.4455	0.2918
1.00	0.3476	0.2204
1.50	0.2289	0.1483
2.00	0.1611	0.1029
3.00	0.0965	0.0620

Note: Deterministic Inputs shown in Table 10.7-1.

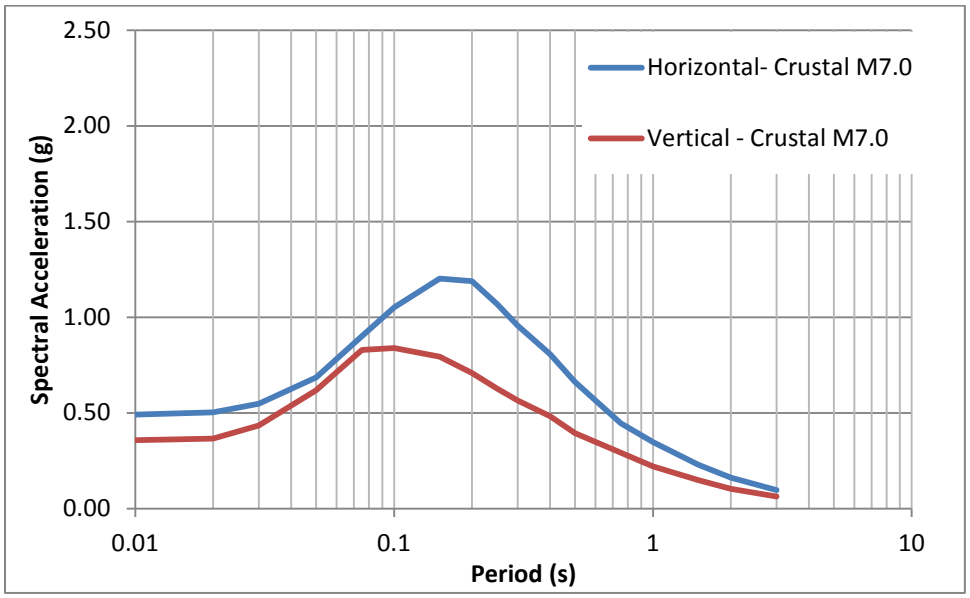

Figure 10.7-6. Crustal M7.0 – 84th Percentile Design Response Spectra

10.7.3.3. Selection of Time Histories

Pre-selection of time histories was completed by searching COSMOS, PEER, K-NET (Japanese Earthquake Database), and a database run by the University of Chile and the Chile Ministry of the Interior and Public Safety for ground motions that had magnitude, distance and record properties similar to the controlling events.

Ideally, the selected time histories should have the same source, style-of-faulting, magnitude, distance, site conditions and directivity condition as the event for which the evaluation is being performed. However, in practice, it is not always possible to find a perfect match.

The criteria used to select the events are discussed below.

10.7.3.3.1. Intraslab

The catalog search for slab events included motions recorded during the El Salvador 2001 M7.6 event (14 recordings), Japan 2003 M7.1 event (412 of recorded motions), Chile 2005 M7.9 event (10 recordings) and available records for the Japan 2011 M7.0 event (504 recordings).

The number of slab ground motions considered was then narrowed down to those events that had a recording distance from 50 to 115 kilometers (km) and included all three components. The design distance was 50 km and it was initially chosen to select those events that fell between +/- 50 km, however this limited the database to a total of 28 events. By increasing the maximum distance to 115 km and additional 24 events were able to be included. The closest event distance was 72 km away, so the distance range was revised to 72-115 km. Chile M7.9 events were not able to be used because no records fell within 115 km; the closest distance was recorded to be 135 km. This narrowed down the database to 52 events, 21 from the 2003 M7.1 Japan event, 20 from the 2011 M7.0 Japan event and 11 from the El Salvador event. Those 52 events were then visually compared to the design response spectra and those with similar spectral shapes were spectrally matched. By putting together a catalog of those strong motion events that occurred on the slab, it is believed that the ground motion parameters (e.g., duration and equivalent number of cycles) should be representative of the target slab scenario. Currently, there is a very limited amount of earthquake events, and strong motions, available that can be comparable to the large slab scenario (i.e. M8.0), which leads to high scaling factors. If the selection of time histories includes the record properties of the scaled ground motions, then the time histories could be scaled by large factors without affecting the average response (Watson-Lamprey & Abrahamson 2005). In addition, large scaling factors do not lead to a bias in median nonlinear structural response if, after scaling, the ground motions have similar target spectral acceleration, magnitude and the closest distance (Luco & Bazzurro 2007).

10.7.3.3.2. Interface

The catalog search for interface events included motions recorded during Japan 2011 M9.0 event (1400 of recorded motions) and available records for the Chile 2010 M8.8 event (55 recordings). The design distance is 92 km and it was chosen to select those events that fell between +/- 50 km (42-142 km). This narrowed down the database to 148 events; 138 from the 2011 M9.0 Japan event and 10 from the 2010 M8.8 Chile event. Those 148 events were then visually compared to the design response spectra and those with similar spectral shapes were spectrally matched. By putting together a catalog of those strong motion events greater than M8.8 that occurred on the interface, it is believed that the ground motion parameters (e.g., duration and equivalent number of cycles) should be representative of the target slab scenario.

10.7.3.3.3. Crustal

The search for the crustal time history was performed using the PEER NGA West 1 Database for those events having a magnitude ranging between 6.5 and 7.5 at distances of 0 to 15 km, contained all three components and a V_{S30} greater than or equal to 400 m/s. After using the search criteria the time histories were then narrowed down to those motions that had similar spectral shape.

10.7.3.3.4. Selected Events

Once the ground motions with similar spectral shape were complied, then selected recorded strong motions were synthetically modified to match the target spectra. The record parameters for the seed events are presented for the slab, interface and crustal events in Table 10.7-6 through Table 10.7-9.

Table 10.7-6. Record Parameters for Selected Slab Time Histories – M8.0 -69th Percentile (PGA=0.81)

Event Title	Station		Arias Intensity (m/s)	Predominate Period (sec)	Predominate Freq. (Hz)	Significant Duration (s)		No. Cycles
						5–95%	5–75%	
Japan (M7.1) 05/26/2003 Rrup=107km	MYG009EW	Seed	0.19	1.53	0.65	33.8	12.8	83
		Spectrally Matched	16.05	0.22	4.46	33.5	12.6	79
	MYG009NS	Seed	0.18	0.22	4.53	39.7	13.7	91
		Spectrally Matched	16.06	0.23	4.34	36.6	14.6	87
	MYG009UD	Seed	0.08	0.71	1.40	36.0	16.1	135
		Spectrally Matched	8.12	0.21	4.72	36.1	16.6	118
El Salvador (M7.6) 01/13/2001 Rrup=112km	MONTEW	Seed	1.12	0.57	1.77	17.3	10.4	44
		Spectrally Matched	9.10	0.57	1.77	20.6	11.2	39
	MONTNS	Seed	1.14	0.25	3.95	18.2	11.2	33
		Spectrally Matched	9.41	0.25	3.95	20.0	12.9	40
	MONTUD	Seed	0.77	0.25	3.95	19.6	14.1	79
		Spectrally Matched	5.67	0.25	3.95	24.6	16.0	55
El Salvador (M7.6) 01/13/2001 Rrup=114km	STTEC090	Seed	7.71	0.29	3.43	10.8	5.5	36
		Spectrally Matched	6.98	0.29	3.43	11.7	6.7	27
	STTEC180	Seed	6.54	0.16	6.16	14.3	6.9	52
		Spectrally Matched	9.15	0.16	6.08	17.6	8.9	49
	STTECUP	Seed	2.80	0.31	3.19	15.8	11.3	47
		Spectrally Matched	3.64	0.10	9.87	15.9	11.6	47

Table 10.7-7. Record Parameters for Selected Slab Time Histories – M7.5 -84th Percentile (PGA=0.69)

Event Title	Station		Arias Intensity (m/s)	Predominate Period (sec)	Predominate Freq. (Hz)	Significant Duration (s)		No. Cycles
						5–95%	5–75%	
Japan (M7.1) 05/26/2003 Rrup=107km	MYG009EW	Seed	0.19	1.53	0.65	33.8	12.8	83
		Spectrally Matched	11.50	0.37	2.71	34.1	12.8	72
	MYG009NS	Seed	0.18	0.22	4.53	39.7	13.7	91
		Spectrally Matched	11.07	0.26	3.90	36.6	14.1	92
	MYG009UD	Seed	0.08	0.71	1.40	36.0	16.1	135
		Spectrally Matched	5.89	0.13	7.79	36.0	16.5	120
El Salvador (M7.6) 01/13/2001 Rrup=112km	MONTEW	Seed	1.12	0.57	1.77	17.3	10.4	44
		Spectrally Matched	6.60	0.24	4.12	21.3	11.8	45
	MONTNS	Seed	1.14	0.25	3.95	18.2	11.2	33
		Spectrally Matched	6.85	0.20	4.99	20.3	12.9	32
	MONTUD	Seed	0.77	0.25	3.95	19.6	14.1	79
		Spectrally Matched	4.06	0.25	4.04	25.6	16.1	60
El Salvador (M7.6) 01/13/2001 Rrup=114km	STTEC090	Seed	7.71	0.29	3.43	10.8	5.5	36
		Spectrally Matched	4.76	0.20	4.94	12.6	6.9	27
	STTEC180	Seed	6.54	0.16	6.16	14.3	6.9	52
		Spectrally Matched	6.79	0.15	6.79	17.8	9.4	46
	STTECUP	Seed	2.80	0.31	3.19	15.8	11.3	47
		Spectrally Matched	2.54	0.10	9.87	16.8	11.8	44

Table 10.7-8. Record Parameters for Selected Interface Time Histories – M9.2 -88th Percentile (PGA=0.58)

Event Title	Station		Arias Intensity (m/s)	Predominate Period (sec)	Predominate Freq. (Hz)	Significant Duration (s)		No. Cycles
						5–95%	5–75%	
Chile (M8.8) 02/27/2010 Rrup=85km	CURIEW	Seed	10.55	1.45	0.69	49.3	37.0	102
		Spectrally Matched	13.06	0.23	4.35	51.1	37.3	76
	CURINS	Seed	2.85	0.73	1.37	53.1	40.1	277
		Spectrally Matched	17.11	0.55	1.83	57.3	43.0	175
	CURIUD	Seed	10.88	0.42	2.40	50.7	38.2	134
		Spectrally Matched	6.06	0.42	2.40	51.8	38.9	128
Japan (M9.0) 03/11/2011 Rrup=105km	ATK023EW	Seed	0.39	1.09	0.92	93.8	57.0	87
		Spectrally Matched	15.2	1.09	0.92	100.3	59.8	83
	ATK023NS	Seed	0.49	0.78	1.28	94.3	56.8	129
		Spectrally Matched	19.09	0.54	1.84	102.2	61.8	106
	ATK023UD	Seed	0.23	0.43	2.35	95.2	61.3	130
		Spectrally Matched	7.47	0.43	2.35	95.1	61.6	139
Japan (M9.0) 03/11/2011 Rrup=130km	CHB012EW	Seed	2.03	0.27	3.66	62.6	35.6	58
		Spectrally Matched	10.27	1.35	0.74	72.8	45.8	46
	CHB012NS	Seed	2.63	0.34	2.94	57.7	33.0	86
		Spectrally Matched	12.05	0.30	3.38	73.1	43.5	47
	CHB012UD	Seed	0.62	4.88	0.21	66.0	36.3	84
		Spectrally Matched	4.68	4.88	0.21	69.2	40.3	89

Note:
ATK023 - Japanese Interface Earthquake Record – March 2011
CHB012 - Japanese Interface Earthquake Record – March 2011

Table 10.7-9. Record Parameters for Selected Crustal Time Histories – M7.0 -84th Percentile (PGA=0.49)

Event Title	Station		Arias Intensity (m/s)	Predominate Period (sec)	Predominate Freq. (Hz)	Significant Duration (s)		No. Cycles
						5–95%	5–75%	
California Loma Prieta (M6.93) 10/18/89 Rrup=9.2km	GIL067	Seed	0.90	0.37	2.68	5.0	1.6	20
		Spectrally Matched	1.36	0.22	4.56	5.8	2.0	30
	GIL337	Seed	0.70	0.37	2.71	4.8	1.3	18
		Spectrally Matched	1.34	0.45	2.23	5.5	1.8	23
	GILUP	Seed	0.17	0.44	2.28	7.5	2.8	22
		Spectrally Matched	0.71	0.30	3.38	7.1	3.3	27
Iran Dayhooh (M7.1) 09/16/1978 Rrup=13.9km	AUL000	Seed	0.06	0.59	1.69	19.0	12.7	36
		Spectrally Matched	3.67	0.48	2.10	19.6	13.9	35
	AUL270	Seed	0.07	0.36	2.80	19.2	13.1	34
		Spectrally Matched	3.47	0.32	3.15	19.9	13.6	27
	AUL-UP	Seed	0.02	0.44	2.28	19.3	13.1	30
		Spectrally Matched	1.65	0.45	2.22	19.0	13.6	30
Italy Irpinia (M6.9) 11/23/1980 Rrup=9.5km	DAYLN	Seed	1.42	0.39	2.56	12.3	6.7	35
		Spectrally Matched	2.56	0.95	1.05	13.6	7.5	32
	DAYTR	Seed	1.36	0.43	2.31	12.4	6.9	15
		Spectrally Matched	2.05	0.77	1.30	11.9	6.4	24
	DAYUP	Seed	0.65	0.18	5.54	14.8	8.3	68
		Spectrally Matched	1.93	0.18	5.55	15.2	8.9	56

10.7.3.3.5. Spectral Matching Approach

Time histories were developed using spectral matching techniques. The spectral matching approach uses a time domain approach (RSPMatch, Abrahamson 2012) with the goal of modifying a given time history to be spectrum compatible with a given target spectrum but without any significant modification to the non-stationary characteristic of the original time history.

Spectral matching adjusts the time series in the time domain by adding wavelets to the initial time series. A formal optimization procedure for this type of time domain spectral matching was first proposed by Kaul (1978) and was extended to simultaneously match spectra at multiple damping values by Lilhanand and Tseng (1987, 1988). While this procedure is more complicated than the frequency domain approach, it has good convergence properties and in most cases preserves the non-stationary character of the reference time history.

Several passes were performed using the RSPMatch program until the fit to both the spectral shape and displacement time history were acceptable.

10.7.3.4. Results – Selected Ground Motions

The ground motions selected for the intraslab, crustal and interface events are presented in Table 10.7-6 through Table 10.7-9. The record properties for the seed and output time history are also summarized in the tables.

The Arias intensity for the crustal events was calculated using empirical correlations developed from the NGA West 1 dataset (N. Abrahamson, personal communication 2014). Equally weighting the five ground motion prediction equations resulted in a median Arias intensity of 0.65 m/s and an 84th percentile Arias intensity of 1.48 m/s. The Arias Intensity for the horizontal components of the spectrally matched crustal time histories range from approximately 1.34 to 3.67 m/s.

The Brookhaven Model (Silva et. al. 1996) was used to estimate the significant duration between 5 and 75 percent for each of the four response spectra. The rupture distance was used as input to the Brookhaven Model for the crustal and interface events, and the hypocentral distance was used for the intraslab event (N. Gregor, personal communication, August 29, 2014). The Brookhaven Model was originally developed for crustal events, but has been shown to work adequately for the interface and is the best model available for the intraslab (N. Abrahamson, personal communication 2014). The results are summarized in Table 10.7-10.

Table 10.7-10. Estimate of Significant Duration using the Brookhaven Model

Event	Horizontal Duration (5-75%), seconds		Vertical Duration (5-75%), seconds	
	16th percentile	84th percentile	16th percentile	84th percentile
Intraslab M_w 7.5	6.7	20.9	7.8	20.4
Intraslab M_w 8.0	9.6	29.8	9.7	25.3
Crustal M_w 7.0	3.4	10.6	3.7	9.6
Interface M_w 9.2	25.6	79.3	19.7	53.3

Overall, the durations of both the seed and spectrally matched time histories generally fall within the 16th to 84th percentile predicted by the Brookhaven Model. The exceptions are the vertical interface motion recorded at station AKT023 and both horizontal motions for the M8 intraslab event recorded at station STTEC. The spectrally matched vertical motion at station AKT023 had a higher significant duration of 61.6 seconds (5-75 percent) compared to the 84th percentile from the Brookhaven Model of 53.3 seconds. The spectrally matched horizontals from station STTEC intraslab motion were 6.7 seconds and 8.9 seconds which are slightly lower than the 16th percentile predicted value of 9.6 seconds.

Appendix B6 contains the earthquake records plots. In Appendix B6, Figure 1 through Figure 5 show plots of acceleration, velocity, normalized displacement, response spectra, Husid plots, and Fourier amplitude spectra for each time history component before and after spectral matching. Each motion has two horizontal components and one vertical component.

Acceleration, velocity, and normalized displacement are plotted in Appendix B6, Figure 1 in blue (labeled SEED) for the first horizontal component. The spectrally matched acceleration, velocity, and normalized displacement time histories are shown in Appendix B6, Figure 1 in red. The plots of acceleration, velocity, and normalized displacement are overlaid so that they can easily be compared. The purpose of these plots is to confirm that the spectrally matched time history remains similar to the original input motion and that extraneous wavelets are not being added to the motion. Appendix B6, Figure 2 is a plot of the acceleration, velocity, and displacement for the SEED motion and Appendix B6, Figure 3 is the same for the spectrally matched motion.

Appendix B6, Figure 4 illustrates the match to the horizontal design spectrum (black line labeled TARGET), with the recorded motion shown in blue and the spectrally matched motion shown in red. The overall goal of spectral matching is to achieve a fit as close as possible to the design response spectrum. It is important to note that the fit to the lower periods (0.01s to ~0.02s) for some events has more variability about the target spectrum; this result is limited by the sampling rate of 100-200 samples per second and has little impact on the structure, as most dams are impacted by periods greater than 0.1 seconds.

The Arias normalized intensity (also called a Husid plot) for the initial and spectrally matched acceleration time history is plotted at the top in Appendix B6, Figure 5; the bottom plot in Appendix B6, Figure 5 is the Fourier amplitude spectra. Again, the blue line is the seed or initial motion and the red line is the spectrally matched motion. These plots show that the Arias intensity is not significantly different from the original input motion. The Fourier amplitude spectra plot illustrates that the frequency content was not significantly modified in the frequency range of 0.1 to 10 Hz (period range of 0.1 to 10 seconds).

The same presentation order is followed for each component and motion – acceleration, velocity, and normalized displacement; SEED acceleration, velocity, and displacement; spectrally Matched acceleration, velocity, and displacement; response spectra; and Husid plot (top), Fourier amplitude spectra (bottom).

Twelve sets of three component spectrum compatible time histories were developed: three sets were developed for the intraslab event M8.0-69th percentile, three sets were developed for the intraslab event M7.5-84th percentile, three sets for the M9.2-Interface-84th percentile, and three sets for the crustal M7.0-84th percentile.

10.7.3.5. Time Histories Used in the Analysis

For the feasibility analysis, one spectrally matched time history was selected from each of the design events (two intraslab, one interface and one crustal). Two events were selected from the intraslab to represent the different magnitude levels, 7.5 or 8.0; as this part of the seismic hazard assessment is still in progress.

In total, four sets of time histories containing three records each have been developed for the slab, interface and crustal events using spectral matching techniques. All of the ground motions are based on the deterministic analyses using a V_{S30} of 1,100 m/s. The intraslab event utilized two different earthquake records, one was from the El Salvador M_w7.6 and the other was from the Japan M_w7.0.

For the MCE, the following time histories shown in Table 10.7-11 have been used:

Table 10.7-11. Selected Time Histories for Feasibility Analysis– Intraslab and Crustal

El Salvador (M 7.6)	STTEC	M_w 7.5 – 84th percentile	Intraslab
Japan 2011 (M 7.0)	MYG 009	M_w 8.0 – 69th percentile	Intraslab
Loma Prieta, California (M 6.93)	GIL	M_w 7.0 – 84th percentile	Crustal

Based on comments received from the Board of Consultants to increase the response spectra, the following response spectra for the interface event in Table 10.7-12 was also used for the analysis:

Table 10.7-12. Selected Time Histories for Feasibility Analysis – Interface

Chile 2010	CURI	M_w 9.2 – 88th percentile	Interface

The ground motions selected for the slab, interface and crustal events are presented in Table 10.7-6 through Table 10.7-9. The record properties for the seed and output time history are also summarized in the tables. Plots are included in Appendix B6.

According to the published guidelines (ICOLD, FEMA, Alaska Dam Safety, and USACE) the normal choice of operating basis earthquake (OBE) would be the earthquake that can reasonably be expected to occur within the service life of the project, that is, with a 50 percent probability of exceedance during the service life. (This corresponds to a return period of 144 years for a project with a service life of 100 years.) For Susitna-Watana, such an event would equate to a PGA of the order of 0.16g, which could be regarded as unacceptably low by the general public who are not conversant with civil and structural design guidelines. The following Table 10.7-13 shows the PGAs for selected return periods:

Table 10.7-13. PGAs for Selected Return Periods

Return Period, years	PGA
100	0.13g
150	0.16g
500	0.27g
1000	0.37g

MWH recommends that the OBE be selected as the 500 year event, equating to a PGA of 0.27g. The dam structure will be evaluated under this event and from a structural perspective all facilities will be able to continue to operate without interruption or significant repair.

10.7.3.5.1. OBE Time History

For the purposes of the feasibility level design only one event was run for the OBE case. The crustal motion, GIL, was scaled by 0.61 to match the 500 year return period from the Probabilistic Seismic Hazard Analysis. The geometric mean of the horizontal components from the Crustal GIL motion was also computed. Figure 10.7-7 plots the 500 year return period (OBE), the geometric mean from the GIL horizontal components with a factor of 0.61 applied and the crustal response spectrum scaled to 500 year return period event for comparison.

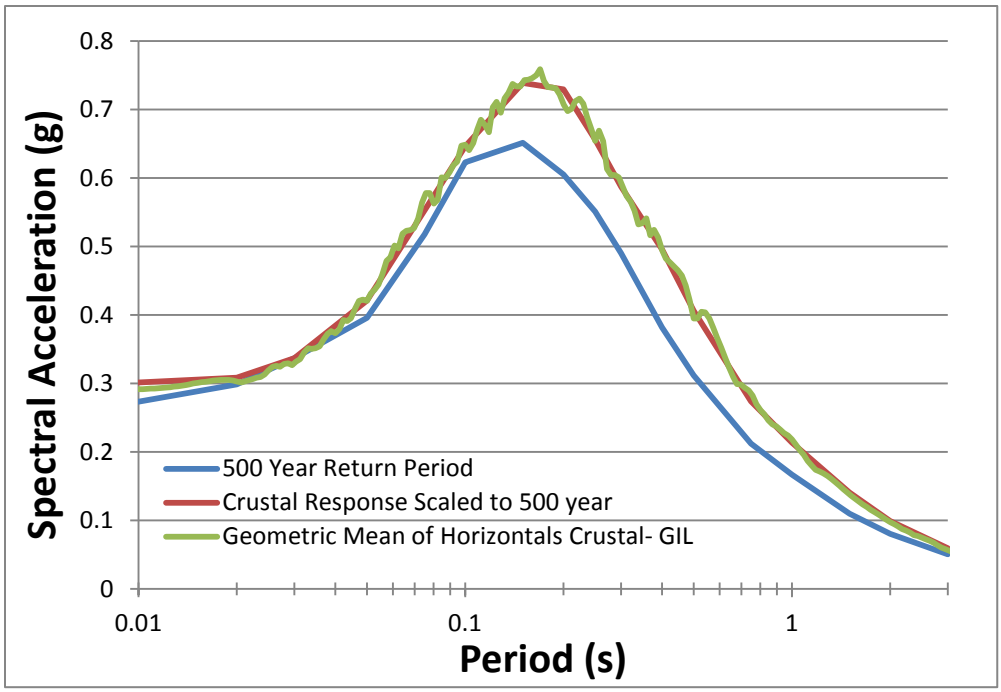

Figure 10.7-7. OBE Response Spectra and Scaled Crustal Event

10.7.4. Methodology of Structural Analysis

Considering mass of the foundation and compressibility of the reservoir in nonlinear transient analysis of a dam-foundation-reservoir system is a complicated analysis. It includes a series of analyses performed in steps, the result of each step being used as input for the subsequent analysis.

The complexity requires that each analysis be performed with caution and the results of each step verified by performing some simple bench mark tests.

Thus the procedure adopted was to initially model the structure in 2-D to develop and verify the analysis method and steps. After the 2-D modeling had been completed satisfactorily, the 3-D model of the structure was developed and final analyses were performed.

Both ANSYS and LS-DYNA software were used in parallel to develop and verify the procedure for transient analysis of the dam-foundation-reservoir system. It is noted that the LS-DYNA has several advantages over ANSYS Mechanical for performing analysis; however ANSYS is more powerful and user friendly for developing the model geometry and preparing the mesh. ANSYS Mechanical and ANSYS Design Modeler were used for developing the geometry and meshing the model, using the Inventor model of the dam provided by the design team.

LS-DYNA has "built in" absorbing boundaries; however, defining these types of boundaries in ANSYS requires significant extra effort. Moreover LS-DYNA has available wide varieties of the required contact elements and its explicit solver with relatively short time steps is reliable for capturing the nonlinear response (opening/closing and sliding of contacts) of the dam during the earthquake.

ANSYS Explicit export was used to export the LS-DYNA input data file (.k File). The LS-DYNA input data file was revised and additional commands added according to the type of analysis. After performing the analysis with LS-DYNA, output results were post processed with LS-PrePost.

To accelerate the process, cloud computing services were engaged to allow the software to run on multiple computer cores.

After performing all the basic analytical runs, various sensitivity runs were performed as described below.

10.7.4.1. Two-Dimensional Analysis

Nonlinear transient seismic analysis of the dam-reservoir-foundation system with LS-DYNA includes several individual analysis steps. The analysis steps include static analysis, deconvolution analysis, and non-linear time history. Implementation of these steps in LS-DYNA was first verified by a 2-D model to ensure that procedure was being applied properly and considering mass of foundation can reduce the tensile stresses in the dam body. A 2-D model of the dam-foundation and reservoir (section through crown cantilever monolith) was developed and extruded 10 ft. in perpendicular direction to create a simple 3-D model. While this model represents a simplified 2-D behavior of the dam cross section it had the advantage of utilizing 3-D elements of the LS-DYNA which were used in the final 3-D modeling of the dam. It provided a simple and fast way for developing and verifying analytical steps. These steps are:

1. Re-convolution analysis: This analysis was performed to correctly apply the ground motions at depth in the foundation and to allow the seismic motions to propagate up through the foundation and around the canyon – essentially producing a spatially varying, and more realistic seismic loading. The following steps were followed to make sure the applied ground motions at depth produced the surface motions postulated by the seismologists:

    a. Compute the minimum FE size to properly transmit the seismic wave through the FE model. The element size is based on the P-wave of the foundation rock and the largest frequency expected to be captured in the model. The ground motion is

normally applied along a horizontal layer of element faces at least 10 (finite) elements beneath the ground surface. The nonreflecting boundaries are then three (finite) elements beneath this layer and at the sides of the box. The horizontal extent of the foundation box normally needs to extend at least three dam heights away from the dam, and have a length to depth ratio of at least 4:1.

b. Build the box shaped foundation model with the same horizontal dimensions as the final model that will include the dam, canyon, and reservoir. The top of the box is located at the elevation of mid-height of the dam. The flat box model allows for application of the ground motion at depth, capture of the computed motion at the ground (top) surface, verification of how well it matches the free-field (target) motion provided by the seismologist, and determination of any scaling factors, if needed, to apply to the ground motions at depth. Comparisons by the Bureau of Reclamation have shown that scaling factors vary very little whether the top of the flat box is positioned at the elevation of base, mid-height, or top of the dam.

c. Deconvolute the three components for the ground motion to the level the ground motion is to be applied at depth (accounting for damping in the model) in units of velocity. This step was overlooked in feasibility study because the rock material has high deformation modulus and low damping and hence minor filtering/amplification effect is expected. Hence the free field motions were implemented at the base of the model in the next step.

d. Compute constant values to apply to the velocity records to convert the velocities into stress-based on the compressional wave speed, shear wave speed, modulus of elasticity, and shear modulus.

e. Run a dynamic analysis with only the box model and capture acceleration or velocity time histories at the top surface of the box.

f. Compare the acceleration response spectra of the computed surface motions to the target response spectra. Accelerations of various nodal points along the top surface of the flat box model were not compared. The sides of the foundation model were positioned considerable distance from the dam model to minimize the influence of the non-reflective boundaries near the dam. Acceleration from a node point at the center of the top surface (where the dam would be in the topographic dam-reservoir-foundation model) was used to compare with the target response spectra. Calculate applicable scaling factors for the three

components. Rerun the box model and check again the computed motions against the target motions.

2. Static run for static loadings:

    a. Build the dam-reservoir-foundation model and restrain the foundation and reservoir extents.

    b. Apply gravity loads to the dam and reservoir and uplift forces over five second solution time.

    c. Capture the reaction forces at all the nodal points of the restrained boundary.

3. Transient run for the rerun static and applied seismic loads:

    a. Replace the restraints on the nodal points along the foundation and reservoir extents with nonreflecting boundaries and the reaction forces captured in 2c.

    b. Repeat the static analysis over five seconds and add an additional five-second "quiet" time to let the model stabilize.

    c. Apply the ground motions at depth on the foundation as traction stresses along a horizontal layer of element faces, from 10 seconds to the end of the earthquake.

Detailed discussion of the implementation of the analytical steps in LS-DYNA is presented in Appendix B8. The results of the analysis showed that considering mass of the foundation and compressibility of water could reduce the maximum normal stress in the dam up to 40 percent which is in line with other investigators (USBR 2006, Chopra 2008). It is noted that the degree of reduction varies with the geometry of structure or applied earthquake loading.

Thus the 2-D analysis confirmed the assumption that running a full 3-D model of the Watana Dam considering the mass of foundation and compressibility of the water is beneficial and would likely predict lower dam stresses compared to the stresses calculated by a massless foundation model.

10.7.4.2. Three-Dimensional Analysis

A 3-D geometric model of the dam had been previously developed in AutoDesk Inventor and is shown in Figure 10.7-8. In a similar manner a 3-D model of the dam-foundation-reservoir was developed. The overall dimensions of the dam-foundation-reservoir model were chosen based on guidance from the U.S. Bureau of Reclamation's Design of Gravity Dams (USBR 1976), and were 1,500 ft. vertical, 4,000 ft. upstream-downstream, and 5,000 ft. cross stream. 3-D views of the developed model are shown in Figure 10.7-8, Figure 10.7-9, and Figure 10.7-10. The dam-foundation interfaces were simplified compared to the proposed foundation excavation to facilitate modeling and meshing of the dam and to limit computational time. This simplification is acceptable – particularly in view of the limited site investigation of the rock foundation of the dam. In the future, when more detailed site investigation results are available, and more informed analytical design can be implemented, the proposed foundation will be re-evaluated, and the final chosen surface can be included in updated FE analysis.

According to the current proposed excavation plan the dam foundation (in the upstream/ downstream direction) is horizontal in most areas except two locations on the left and right abutments. It is sloping upstream in some parts of the right abutment and it is stepped in some parts of the left abutment to eliminate the assumed natural downstream slope of the rock surface. To create a regular and simple FE mesh the complex interface geometry was replaced with horizontal interfaces under all dam monoliths in the 3-D model. This assumption may well create conservative results for the sliding displacement along the right abutment.

The developed Inventor 3-D model was imported into ANSYS Design Modeler. This software was used to modify the model as required so that ANSYS Mechanical was able to be used to develop the FE mesh. Standard eight node elements were used to mesh the dam, foundation and reservoir. Element sizes were chosen based on the limitation of the explicit solution method for capturing wave propagations in the model. A maximum element size of 60 was used for foundation and reservoir; however a smaller element size was used in the dam body for more accurate stress calculation in the dam body.

The FE model consisted of 722,796 elements and 777,823 nodes.

Figure 10.7-8. AutoCAD Inventor Model – simplified for use in Finite Element Analysis

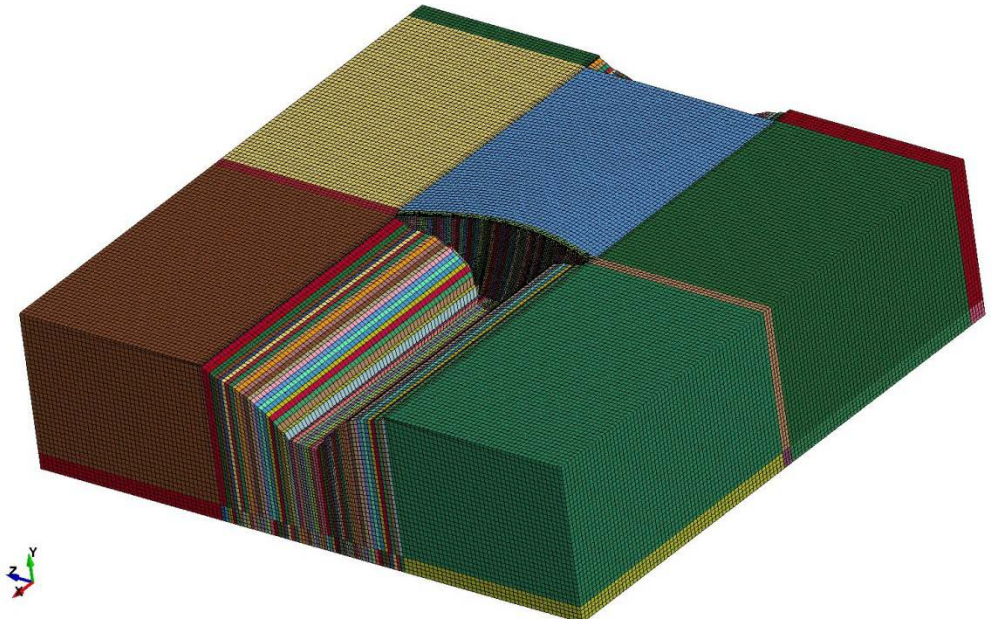

Figure 10.7-9. 3-D View of Model Developed in LS-DYNA

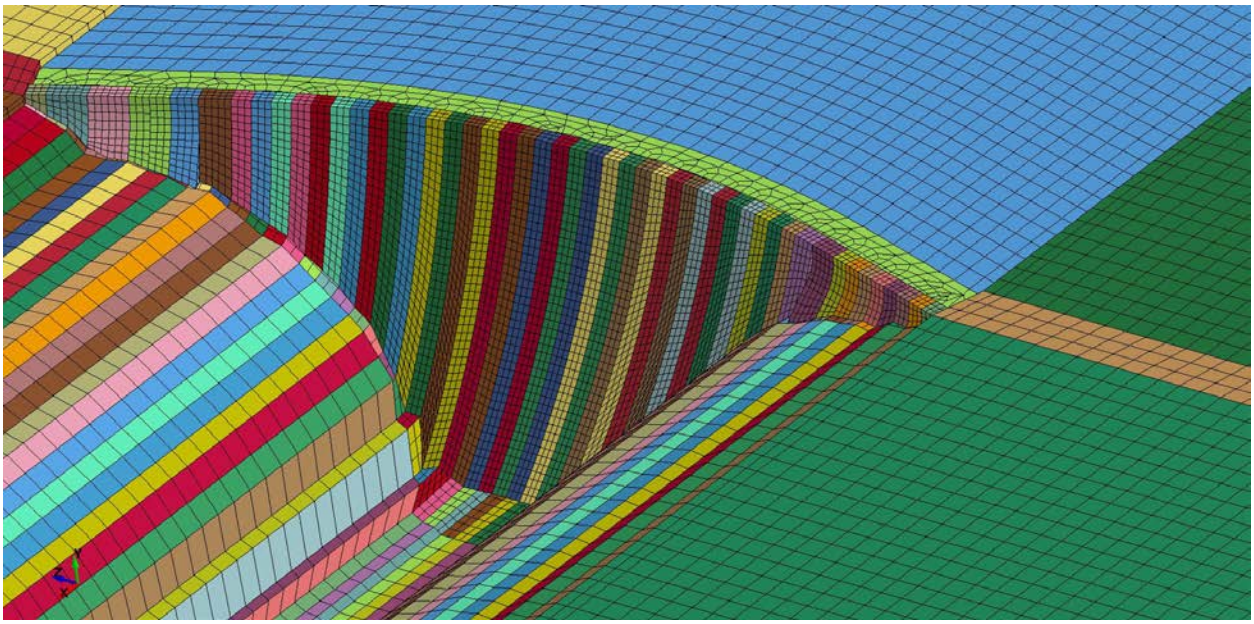

Figure 10.7-10. Enlarged 3-D View of LS-DYNA Model

10.7.4.2.1. Material Properties

Table 10.7-14 summarizes the material properties used in the LS-DYNA model.

Table 10.7-14. Foundation and Dam Material Properties used in LS-DYNA

Material	Mass Density	Deformation Modulus	Poisson's Ratio
	(pcf)	E (psi)	
Foundation	170	3.5E+6	0.25
Concrete	150	3.9E+6	0.25
Water	62.4	3.1E+05 (Bulk Modulus)	

The fluid elements in LS-DYNA are 3-D solid elements with water material properties. The formulation also incorporates an Equation of State that minimizes the shear in the fluid. In accordance with expected construction practice, the FE model included vertical (unformed) contraction joints between dam monoliths at every 50 ft. along the dam axis. Contraction joints were modeled as frictional contact surfaces with no tensile capacity. Frictional contact surfaces were also used to model the interface between the dam and foundation. A total of 161 contact surfaces were included in the model. Each contact surface consists of a master list of 3-D planar elements forming a surface and a slave list of 3-D planar elements forming a surface. The nodes of the master surface are independent from the nodes of the slave surface so the surfaces can slide and come apart, but not penetrate one another.

10.7.4.2.2. Static Analysis

In LS-DYNA the static loading is applied like a dynamic ramped load over a time period (larger than the natural period of vibration of structure). An additional quiet time (while holding the static loading constant) is also required to stabilize the model at the end of the analysis.

Weight of the dam and reservoir and uplift pressure at the contact between the dam and foundation contact were applied as static load in the analysis. These forces were ramped from zero to five seconds and kept constant for five seconds to achieve steady state conditions at the end. During the static analysis the sides and base of the foundation and the extent of the reservoir were constrained against movement perpendicular to their faces. The nodal traction forces along the constrained boundary conditions were recorded at the end of analysis for use in the next step of transient analysis.

The results of the static analysis were verified by performing a separate static analysis of the model in ANSYS Mechanical. Distribution of the vertical stresses in the dam body and horizontal displacement at the dam crest from the two separate analyses were examined and

found to be identical. The existing hydrostatic pressure in the reservoir elements at the end of the "quiet time" was also verified through manual calculations.

10.7.4.2.3. Deconvolution Analysis

Seismic records must be implemented in the analysis as traction loads along a horizontal layer of element faces in the foundation model. These tractions in each direction were calculated as the product of the corresponding earthquake velocity and a damping coefficient. Lysmer dampers were used as initial estimation. A deconvolution analysis was performed to update the Lysmer damper values for the foundation geometry and mesh that was used in the simulations.

The tangential (c_t) and normal (c_n) Lysmer dampers (per unit area) were calculated based on shear wave and longitudinal wave velocities,

$$c_t = \rho . S_t = 18.89\ psi.sec/in$$

$$c_n = \rho . S_n = 32.71\ psi.sec/in$$

where S_t and S_n are the shear wave and longitudinal wave velocities calculated using the foundation material properties,

$$G = E/2(1+\nu) = 1400\ ksi$$

$$\lambda = E.\nu/(1+\nu)(1-2\nu) = 1400\ ksi$$

$$S_t = \sqrt{G/\rho} = 6177.2\ ft/sec$$

$$S_n = \sqrt{(\lambda + 2G)/\rho} = 10698.8\ ft/sec$$

The following Table 10.7-15 summarizes the Lysmer damper values for the foundation.

Table 10.7-15. Foundation Rock Material Properties and the Corresponding Wave Velocities and Lysmer Damper Coefficients

Mass Density	Deformation Modulus	Poisson's Ratio	Shear Wave Velocity	Longitudinal Wave Velocity	Lysmer Damper - Tangential	Lysmer Damper - Normal
P (pcf)	E (psi)	**v**	V_S (ft./sec.)	V_L (ft./sec.)	c_t (psi/in./sec.)	c_n (psi/in./sec.)
170	3.5E+06	0.25	6177.2	10698.8	18.89	32.71

A 3-D box model of the foundation was prepared with similar geometry, mesh size and damping as the complete model and absorbing boundary conditions were applied to the base and sides of the model. In addition, tractions were implemented in three directions at the base of the model. These tractions were calculated as the product of Lysmer damper (tangential for shear directions and normal for vertical direction) and the corresponding velocities.

A simulation was performed and three components of acceleration at the top of foundation were captured. Acceleration response spectra were computed for the three components which were compared with the corresponding response spectra of the free-field motion. The damping factors were adjusted so that the responses were identical at the natural frequency of the dam.

This numerical analysis was performed for the Gil and MYG earthquakes and resulted in comparable values for the damping factors. As a result, the adjusted damping coefficients, shown in Table 10.7-16, were used for the transient analysis of the complete model.

Table 10.7-16. Scaled Damper Coefficients used in Three Directions as a Result of Deconvolution

Stream Direction	Cross Valley Direction	Vertical Direction
c_x (psi/in./sec.)	c_z (psi/in./sec.)	c_y (psi/in./sec.)
17.10	17.88	36.14

10.7.4.2.4. Transient Analysis

For the transient analysis, the constrained boundaries in the 3-D model of dam-foundation-reservoir were replaced with non-reflecting boundaries and static and seismic loadings were applied to the model. Ramped static loading was applied for the first 10 seconds to the model along with the computed reaction forces from static analysis as static initialization boundary forces. The computed earthquake traction loadings from the earthquake velocity records and the damper coefficients were applied to the foundation.

Explicit analyses are conditionally stable based on the solution time step. LS-DYNA computes an initial stable time step based on the smallest element size, the wave speed of the material (which is based on modulus and mass density), and the damping. As sliding occurs, or contraction joints open and close, nonlinearities are introduced into the model that may require a smaller solution time step. The computed time step can be scaled down to attempt to reach convergence based on the response of the model. In addition to analysis with the calculated time step, two additional analyses were performed using time steps of 5 and 10 times smaller than the calculated time step. It was determined that using a five times smaller time step ($\Delta t=2.4e^{-5}$ seconds) gave acceptable results for this case.

Transient seismic analyses were performed for four MCE cases and one OBE case as described in Section 10.7.3.5 and the results are summarized below:

MCE Loading Cases

The maximum tensile vertical stresses on the upstream and downstream faces of the dam and the maximum principal stress on the downstream face of the dam are shown in Figure 10.7-11 to Figure 10.7-13. The maximum stresses were extracted from these figures and are presented in Table 10.7-17 for comparison. The maximum tensile vertical stress on the upstream face of the dam was determined to be 662 psi and occurred at El. 1770 ft. (peak stress point) during the MYG earthquake. The maximum tensile vertical stress and maximum tensile principal stress on down face of the dam was determined to be 745 psi and 929 psi respectively, both occurring at elevation 1930 during the MYG earthquakes.

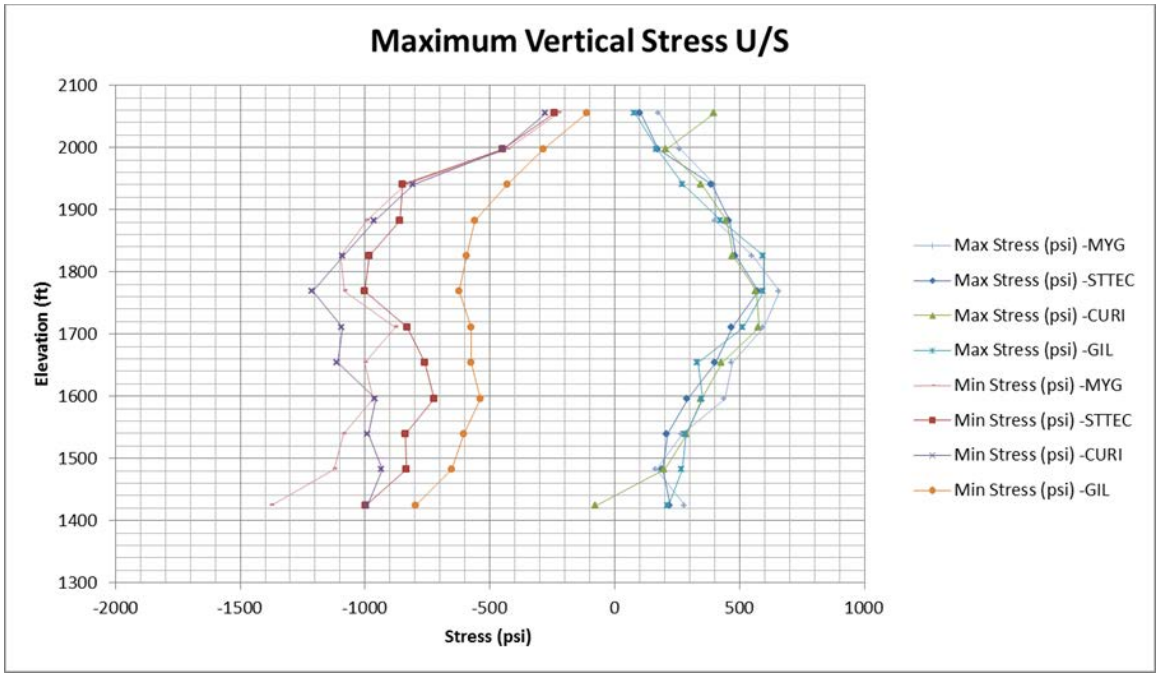

Figure 10.7-11. Maximum Vertical Stresses in U/S Face of Crown Cantilever Monolith During MCE

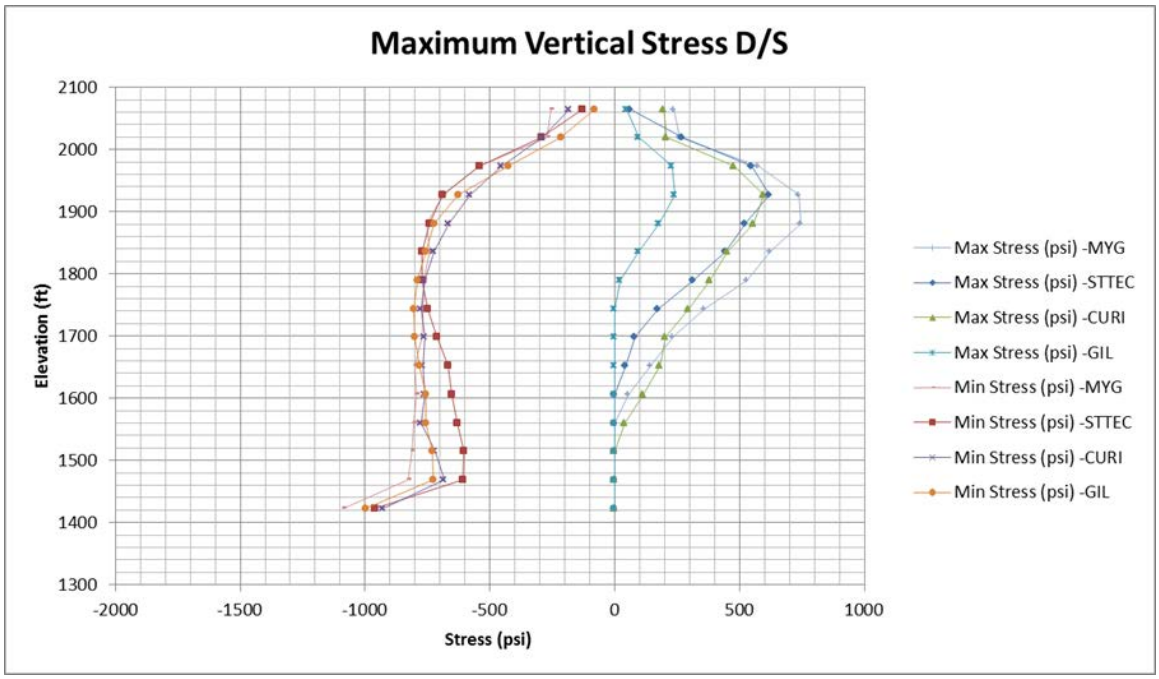

Figure 10.7-12. Maximum Vertical Stresses in D/S Face of Crown Cantilever Monolith During MCE

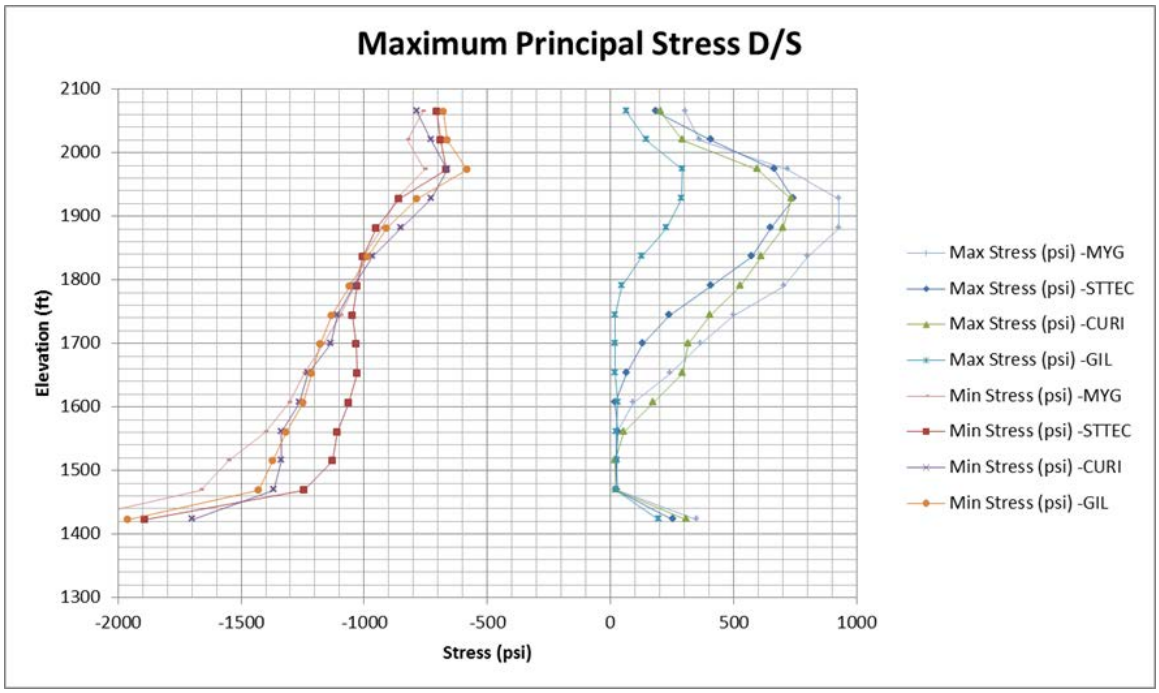

Figure 10.7-13. Maximum Principal Stresses in D/S Face of Crown Cantilever Monolith During MCE

Table 10.7-17. Maximum Tensile Stresses for MCE Events

Earthquake Type	Event Name	Vertical Tensile Stress (Psi)		Principal Tensile Stress (Psi)
		Upstream	Downstream	Downstream
Intraslab M8 (PGA=0.81)	MYG	662	745	929
Intraslab M7.5 (PGA=0.70)	STTEC	576	621	743
Interface M9.2 (PGA=0.58)	CURI	580	597	738
Crustal, M7.0 (PGA=0.48)	Gil	597	240	293

Using RCC with approximately 600 psi of dynamic tensile strength between RCC lifts would be enough to prevent cracking along the RCC lift joints on the upstream face of the dam during the MYG event. The maximum tensile stress on the upstream face of the dam was determined to be smaller for all other cases except the MYG earthquake. Even with the MYG event the number of and duration of overstressing is very short, as shown in Figure 10.7-14, and the extent is limited to a small area on the upstream face of the dam as shown in Figure 10.7-15. These conditions are unlikely to create any significant damage to the dam structure.

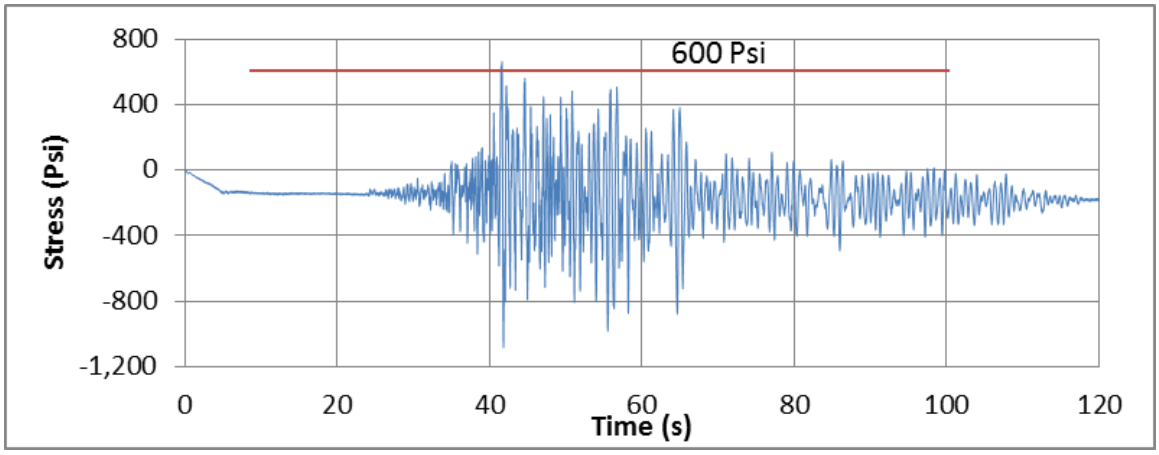

Figure 10.7-14. Time History of Normal Stress at the Peak Stress Point in U/S Face During MYG Event

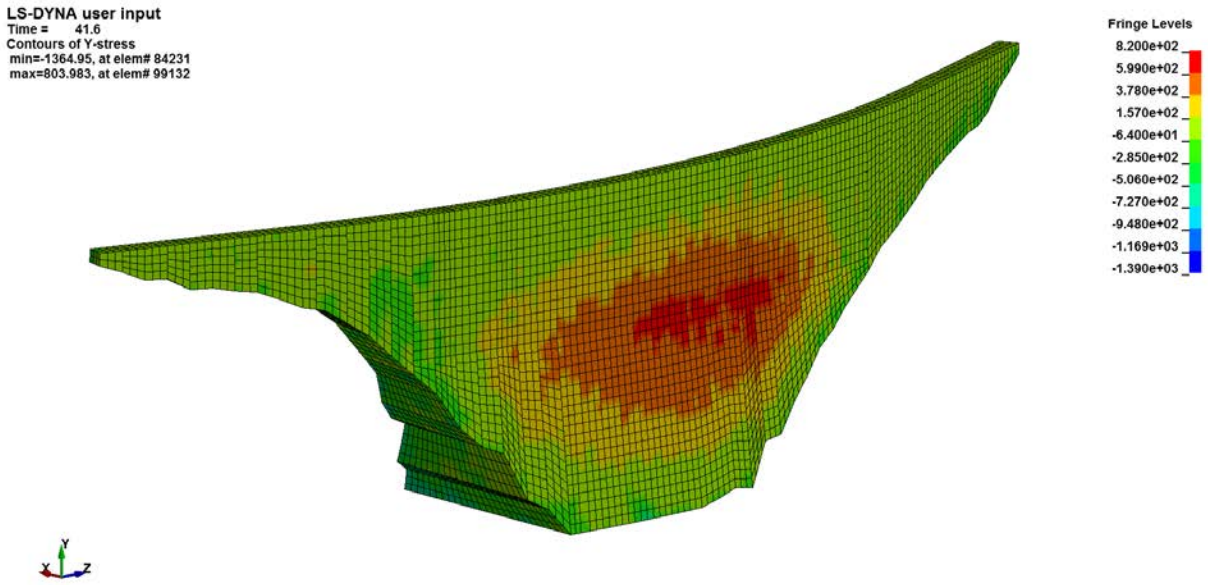

Figure 10.7-15. Maximum Vertical Tensile Stress on Upstream Face of the Dam during MYG Event (red area shows tensile stress >600 psi)

On the downstream face of the dam, the vertical tensile stresses should be compared with the tensile strength of RCC lifts, while the principal stresses should be compared with the tensile strength of the parent concrete of RCC as the acceleration is horizontal. To prevent cracking on the downstream face of the dam, at least 750 psi of tensile strength on the RCC lift joints and 900 psi of tensile strength in the parent RCC is required. If the constructed RCC strength is lower than these values cracking may occur on the downstream face during the event. However, industry accepted design guidelines allow cracking as long as the structure remains stable during, and after, the event.

Figure 10.7-16 shows the variations of the principal tensile stress at the peak stress point on the downstream face of the dam, if a tensile strength of 600 psi for parent RCC is achieved. There is a single overstressing during the MYG earthquake while there are two or three during the STTEC and CURI earthquakes. The extent of the overstressed area on the downstream face of the dam and on the crown cantilever monolith (as shown in Figure 10.7-17 for MYG earthquake) shows that estimated cracking will be very limited. For a crack to create instability in a large structure such as Watana Dam, it has to be substantially through the dam body and the duration of overstressing must be long. As shown, the computed overstressed area is very small and does not extend through the dam body, and the duration of overstress is restricted to a few hundredths of a second. These two factors show the dam is stable during and after a major seismic event with only minor damage and not enough time to cause any movement in the body of the dam.

During detailed design, more refinements to the dam configuration will be explored and more FE analysis undertaken to further reduce the magnitude of projected tensile stresses.

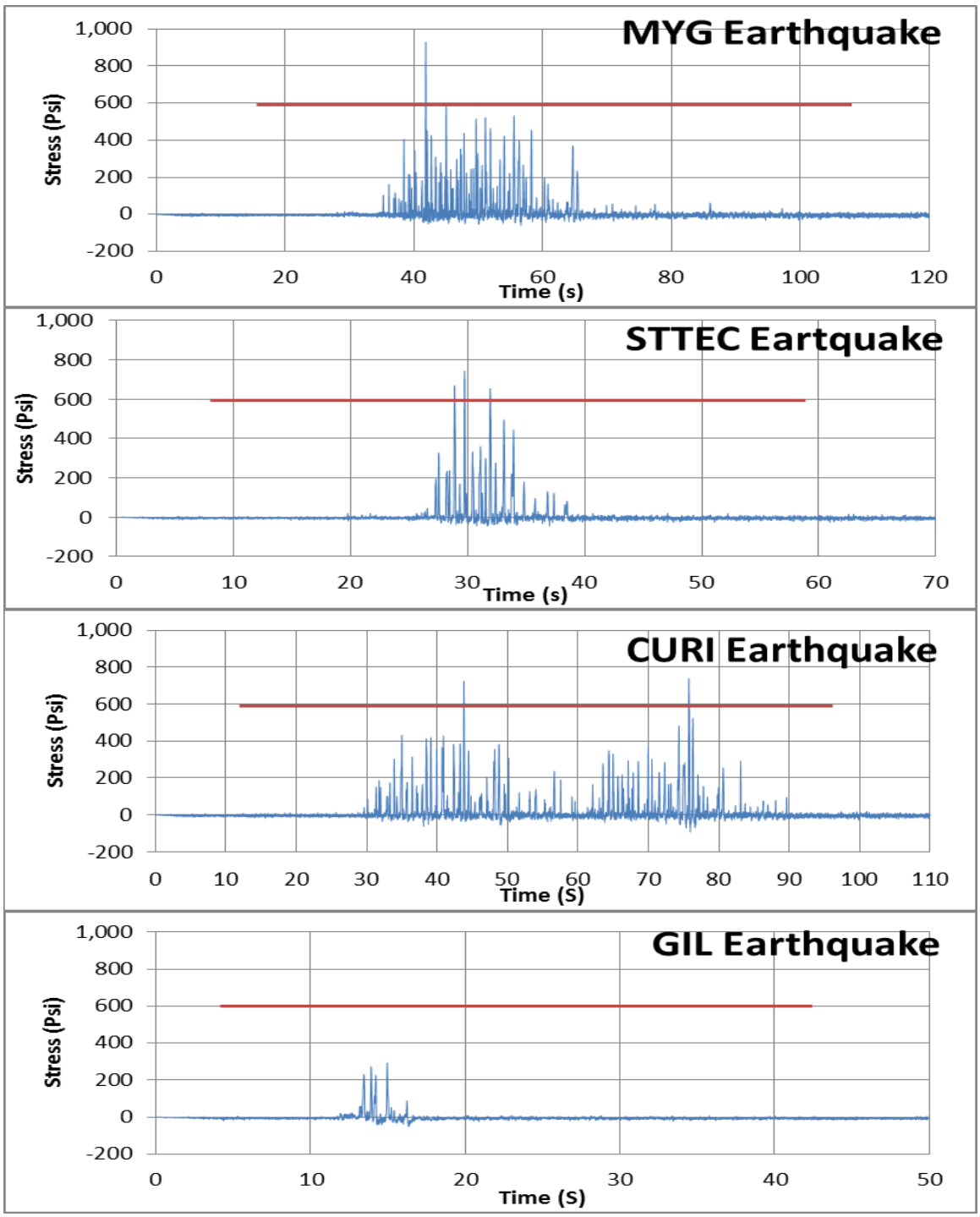

Figure 10.7-16. Time History of Principal Stress at the Peak Stress Point in D/S Face During Four MCE Events

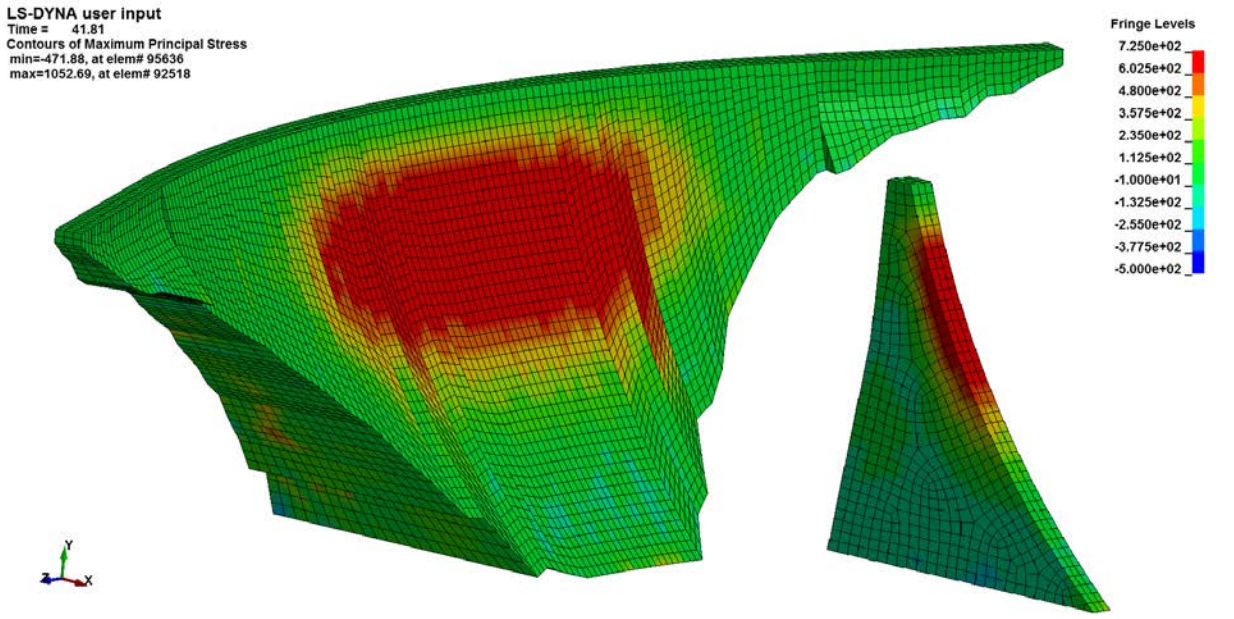

Figure 10.7-17. Maximum Principal Tensile Stress on Downstream Face and Crown Cantilever Monolith of the During MYG Event (red area shows tensile stress >600 psi)

A 2-D model of the crown cantilever with a horizontal cracked section (at the level of peak stress points) was developed. This crack was modeled as a continuous sliding surface. Analysis results showed that a maximum of four inches downstream sliding could happen during the GIL earthquake. Much smaller sliding displacements are expected at this interim joint in the monoliths because of the 3-D behavior and tapering geometry of individual monoliths.

Sliding Displacements

Results of the analyses have shown that the dam monoliths will slide during the earthquake in the absence of consideration for cohesion at the dam/foundation contact. The modeled sliding displacements along five typical monoliths – as shown in Figure 10.7-18 – are presented in Table 10.7-18 as the maximum sliding along the base of the monoliths at the end of four different MCE events, and as a function of time in Figure 10.7-19 through Figure 10.7-22.

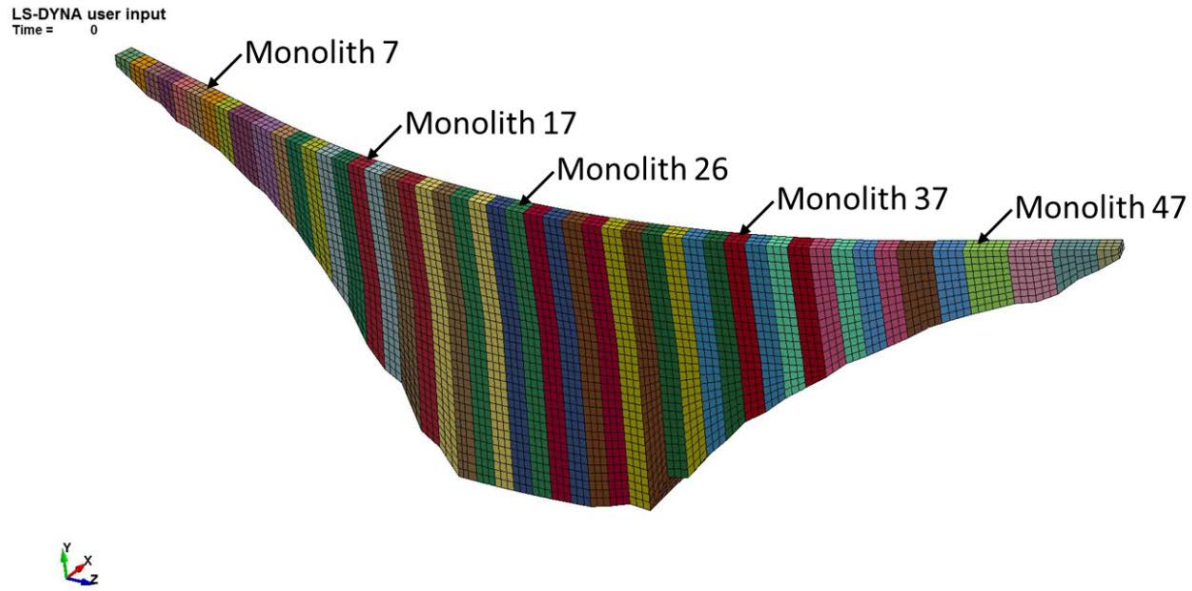

Figure 10.7-18. Monoliths Numbering

The maximum sliding displacement of 3.9 inches projected by the analysis occurs at monolith 37 (right abutment) during the CURI event while the sliding at the center of dam is approximately 2.2 inches. As noted above, the proposed dam foundation interface will slope upstream at the right abutment, but is modeled as horizontal in the current analysis for simplicity. Hence, sliding of the right abutment would be expected to be less than the computed value of 3.9 inches.

Moreover, the assumed 1.2 friction coefficient (friction angle of 55 degrees) used in the non-linear analysis is regarded as a conservative assumption. A greater friction coefficient (1.4 to 1.5) is expected, due to the character of the foundation rock, strength of the RCC, and the additional sliding resistance that would be realized from the powerhouse and mass concrete at the toe of the dam. For comparison, analysis using a friction coefficient of 1.48 (friction angle of 56 degrees) was performed for the CURI earthquake. The results, presented in Table 10.7-18 show 20 percent reduction in sliding displacement compared to the similar case with a friction coefficient of 1.2.

Table 10.7-18. Maximum Sliding on Selected Monoliths

Earthquake Event	Monolith 7 (inches)	Monolith 17 (inches)	Monolith 26 (inches)	Monolith 37 (inches)	Monolith 47 (inches)
MYG (friction coeff.=1.2)	3.7	2.8	2.2	3.3	3.9
STTEC (friction coeff.=1.2)	1.3	1.2	1.2	2.9	2.6
CURI (friction coeff.=1.2)	3.0	2.6	2.2	3.9	3.0
GIL (friction coeff.=1.2)	0.3	0.9	0.9	0.7	0.9
CURI (friction coeff=1.48)	2.5	2.2	1.7	3.2	2.4

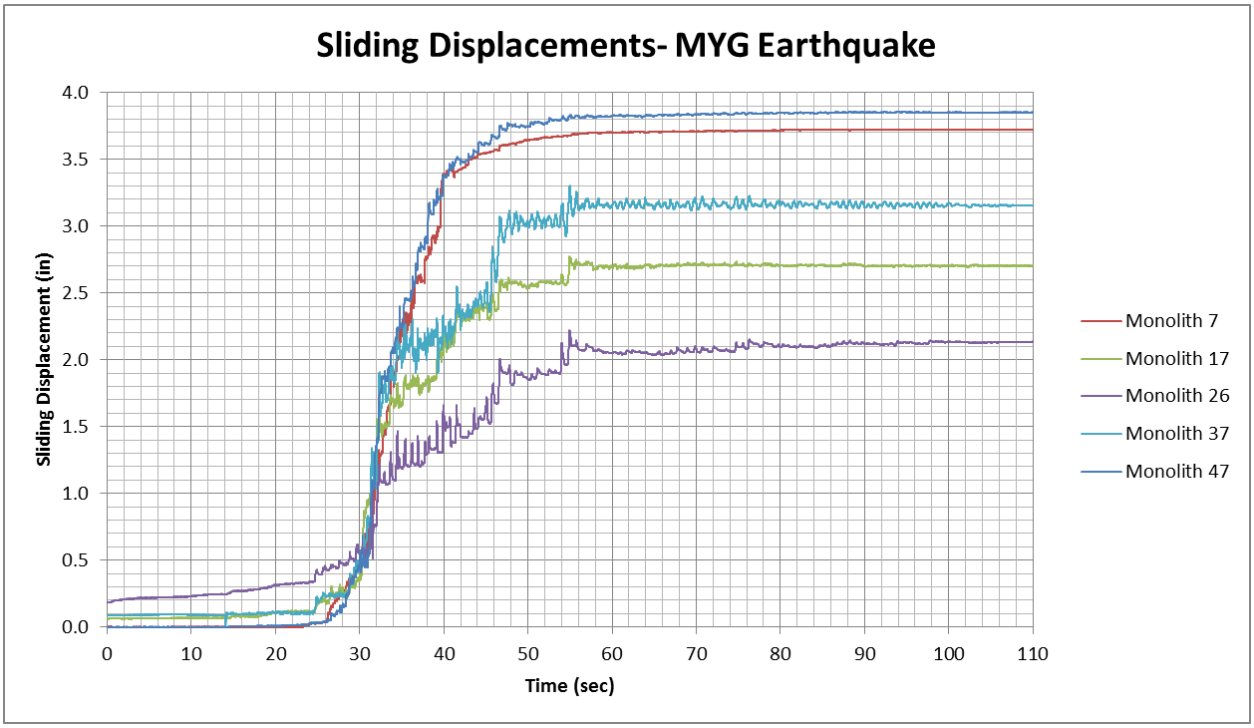

Figure 10.7-19. Dam Base Sliding Displacement During MYG Earthquake

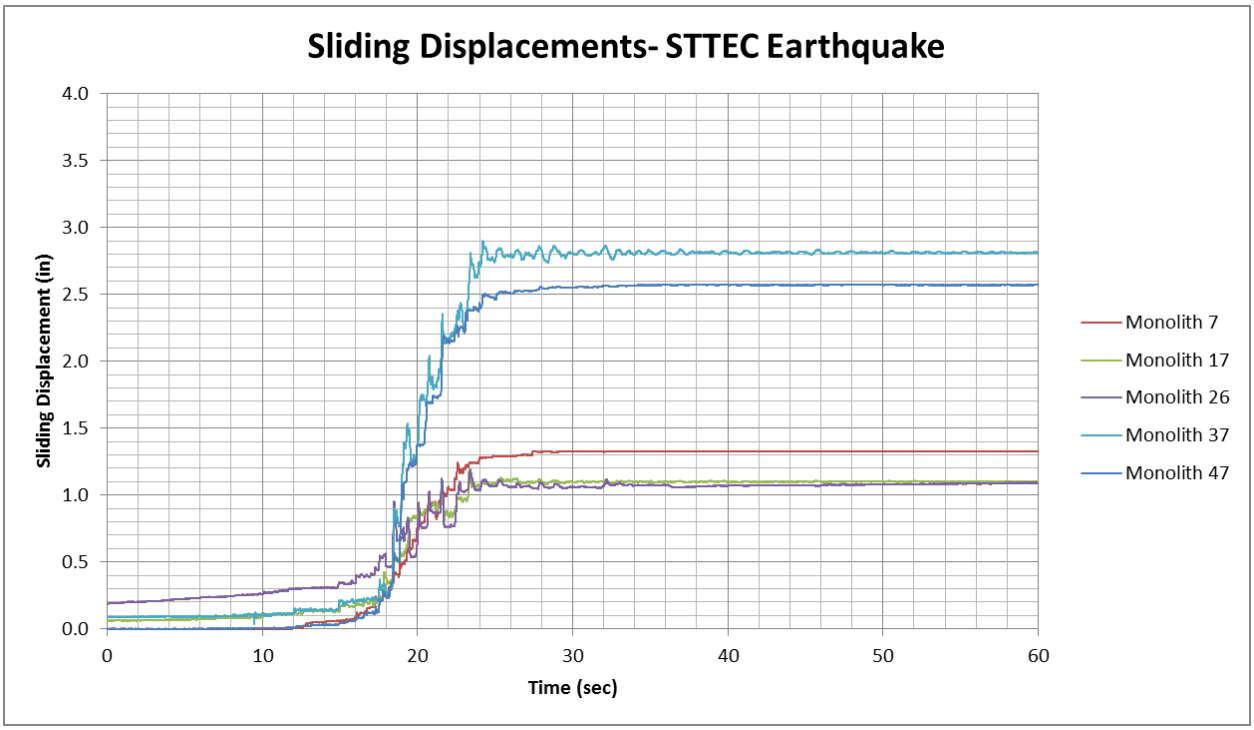

Figure 10.7-20. Dam Base Sliding Displacement During STTEC Earthquake

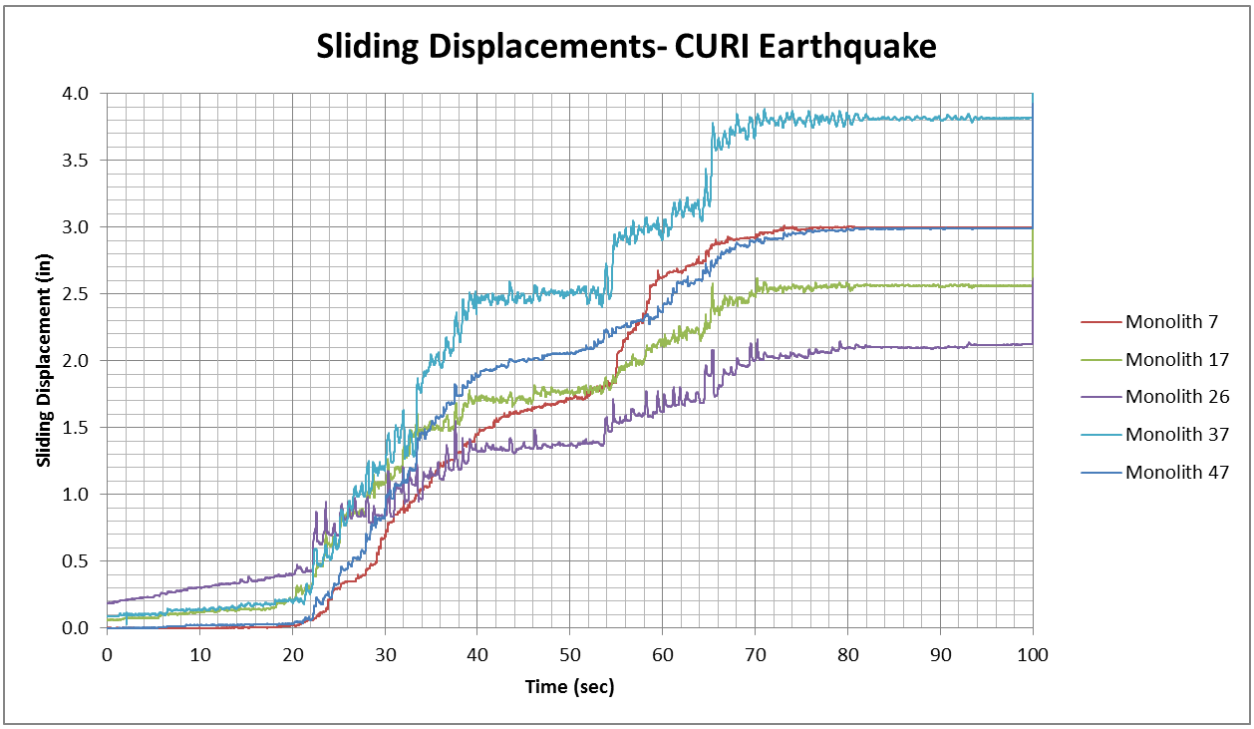

Figure 10.7-21. Dam Base Sliding Displacement During CURI Earthquake

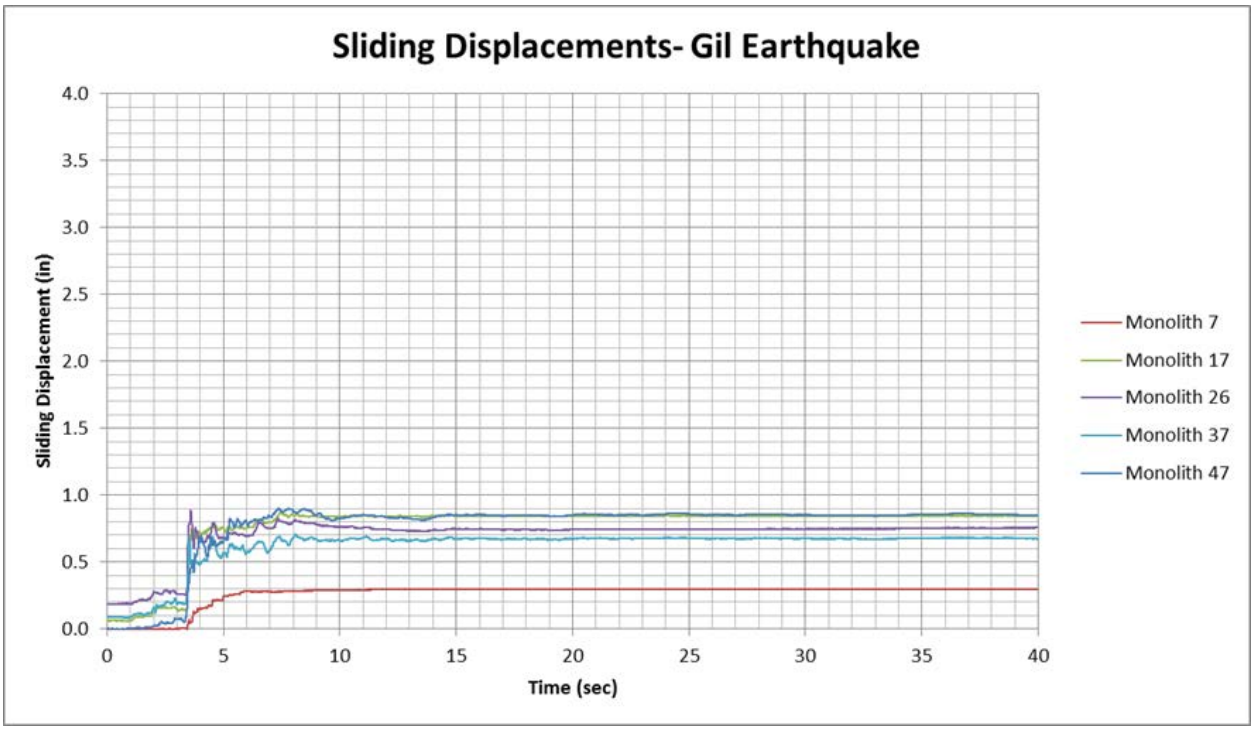

Figure 10.7-22. Dam Base Sliding Displacement During GIL Earthquake

The estimated sliding displacements of two to four inches can be accommodated by the appropriate design of the vertical drains to minimize the effects. Dam and foundation drains will be sized to remain effective following movement of the dam during extreme loading.

OBE Loading Cases

The developed OBE record as explained in section 10.7.2.5.1 was used to perform seismic analysis and assess the response of the dam for the operational basis earthquake. The summary of the results including developed tensile stresses and sliding displacements are shown in Table 10.7-19 and Table 10.7-20.

The maximum tensile normal stress is 240 psi equating to about 80 percent of the static tensile strength of RCC. No cracking in the dam body, or between the RCC lifts is expected during OBE event. Maximum of 0.55 inches of sliding displacement along the base of dam model is very small. These small displacements are probably initial adjustments along the contact surfaces in the model and can be neglected.

Table 10.7-19. Maximum Tensile Stress in the Dam during OBE Events

Earthquake Type	Event Name	Vertical Tensile Stress (Psi)		Principal Tensile Stress (Psi)
		US	DS	DS
Crustal, 500 yrs.	Gil	0	194	240

Table 10.7-20. Maximum Sliding during OBE Events

Earthquake Event	Monolith 7	Monolith 17	Monolith 26	Monolith 37	Monolith 47
GIL	0.05	0.45	0.55	0.35	0.2

10.7.4.3. Sensitivity Studies – Non-homogeneous Foundation

The foundation conditions are not yet fully characterized by site investigation. It was therefore important to perform sensitivity analyses to account for potential variations from the assumed conditions.

Three analyses were performed to investigate the sensitivity of the computed results to the foundation material properties, and in each case the STTEC event was used for these analyses.

During excavation of any dam foundation, it is possible to "overblast" the foundation and – although careful blasting will be specified and consolidation grouting will be performed over the whole foundation to create an excellent foundation against which to place RCC – it is prudent to examine the effect, should there be a thin disturbed layer at the top of the foundation. Two analyses were performed for this condition – first including a layer exhibiting a deformation modulus of E=2.8e6 psi; and second a similar analysis assuming a deformation modulus of E=2.0e6. The stresses and sliding displacements computed from these analyses are shown in Table 10.7-21 and Table 10.7-22. Comparing these results with those of the previous analyses that included a homogeneous foundation shows that the presence of a thin layer under the dam base of lower deformation modulus does not significantly affect the results.

The reinterpretation of the characterization of the foundation recorded in Section 6 has significantly reduced the postulated widths, number and continuity of the geological features first identified in the Acres reports of the 1980s. This recent reinterpretation – which became available in December 2014 late in the feasibility study – was unable to be incorporated into the completed FE analyses. For the determination of the zones of lower modulus used in the sensitivity studies, the rock mass assessments from the 1980s information were therefore used – as discussed in Section 10.3.3.3.1 – which indicated much larger areas of potentially lower quality foundation than are now indicated.

The sensitivity analysis results are shown in Table 10.7-21 and Table 10.7-22. The tensile stresses in the dam body (both upstream and downstream) decreased as a result of the assumed foundation properties; however, greater sliding displacements (25 percent increase) were computed for monoliths on the right abutment. It will be very important in the ongoing mapping and site investigation to fully characterize the geologic features so that FE analyses during detailed design can be undertaken using more informed foundation properties, and any required foundation treatment of geological features can therefore be correctly assessed. However, the 2014 reinterpretation of the foundation character shows that the assumptions made for the 2013 ANSYS sensitivity analyses were very conservative, and the width of the geologic features is such that they will likely be treated by normal over excavation – and filling with conventional concrete – and are likely to have minor influence on the overall behavior of the structure.

Table 10.7-21. Maximum Tensile Stress Sensitivity to Foundation Properties

Foundation Property	Vertical Tensile Stress (psi)		Principal Tensile Stress (psi)
	US	DS	DS
Homogeneous foundation	576	621	743
Weak Layer (E=2.8e6)	605	644	776
Weak Layer (E=2.0e6)	584	657	792
Weak Right Abutment	559	567	670

Table 10.7-22. Maximum Sliding Displacement Sensitivity to Foundation Properties

Foundation Property	Monolith 7 (inches)	Monolith 17 (inches)	Monolith 26 (inches)	Monolith 37 (inches)	Monolith 47 (inches)
Homogeneous foundation	1.3	1.2	1.2	2.9	2.6
Weak Layer (E=2.8e6)	1.4	1.2	1.2	3.0	2.7
Weak Layer (E=2.0e6)	1.4	1.3	1.3	3.1	3.0
Weak Right Abutment	1.3	1.3	1.3	3.7	2.6

10.7.5. Conclusions

Results of FE analyses considering mass of the foundation and compressibility of the reservoir water shows that computed stresses and sliding displacements of the dam were reduced 30 to 40 percent on average compared to analysis without foundation mass. The comparison is shown in Table 10.7-23.

Table 10.7-23. Comparison of Results of Massed Foundation Model with Massless Foundation Model

Earthquake Event	Normal Stress (psi)					
	Massed Foundation		Massless Foundation		Reduction (%)	
	Upstream	Downstream	Upstream	Downstream	Upstream	Downstream
MYG	662	745	1109	841	40%	11%
STTEC	576	621	945	957	39%	35%
CURI	580	597	641	611	10%	2%
Gil	587	240	1097	409	46%	41%
Earthquake Event	Sliding Displacement (in)					
	Massed Foundation		Massless Foundation		Reduction (%)	
	Crown Monolith	Side Monoliths	Crown Monolith	Side Monoliths	Crown Monolith	Side Monoliths
MYG	2.2	3.9	4.1	7.7	46%	49%
STTEC	1.2	2.6	2.4	3.3	50%	21%
CURI	2.2	3	2.7	3.5	19%	14%
Gil	0.9	0.9	1.1	1.6	18%	44%

For the OBE events the results of analyses showed that the computed tensile stresses on the upstream or downstream face of the dam were less than the allowable stresses. The computed sliding displacements were small along the base of the dam. The displacements are interpreted as the minimum required to engage the contact along the dam-foundation interface and can be neglected. No cracking or damage in the dam body or along the dam-foundation interface is expected during the OBE events and the dam would remain completely operational after an OBE event.

For the MCE events, the developed tensile stresses on the downstream face of the dam are higher than the tensile strength of the RCC and limited cracking of the dam would likely occur at the top of the dam. However, the overstressed area and the total time of overstressing are limited. The probable damage in the dam body would be limited. The separate 2-D analysis investigated the response of the damaged (cracked) dam during the earthquake. Results show that no instability or uncontrolled release of water can be expected.

Hence, Dam Layout 4 (Modified) would remain fully operational after the OBE event. During the MCE event the dynamic analysis shows that there may be some cracking at the upper elevations of the dam, and sliding displacement at the foundation but post earthquake analysis using FERC criteria and CADAM indicates no instability or uncontrolled release of water is expected. The dam is estimated to remain stable for static reservoir loads with a cracked base and uplift applied to the foundation. Dam and foundation drains will be sized to accommodate potential sliding displacements and to remain effective following movement of the dam during

extreme loading. During detailed design, more refinements to the dam configuration will be investigated and additional FE analysis will be performed to verify expected reductions in tensile stresses and estimated sliding displacement.

10.8. RCC Placement

10.8.1. RCC and Aggregate Quantities / Production

The volume of the dam was calculated in vertical intervals for use in developing production rates for various zones of RCC placement.

Placement of RCC will be carried out using the sloping layer method. The sloping layer method was first used in 1997 on the Jiangya Dam (China) and has been used successfully at numerous RCC dams including Murum Dam, Kinta Dam (both Malaysia) and Al Wehdah (Jordan) – and on nearly all Chinese constructed RCC dams.

The technique has advantages of creating an upper surface that is of such size as to enable the subsequent layer to be placed while the previously placed surface is still "green" avoiding the need for special treatment of the surface. This creates homogeneous monolithic RCC across lift joints, an important feature for a dam of the height planned at Watana Dam. At Murum, for example core has been drilled through the placed RCC and continuous core of up to 70 ft. has been recovered. The technique reduces the number of horizontal construction lift joints by up to 90 percent. The technique also reduces the area of "fresh" RCC that could be exposed to rainfall or subject to freezing.

The RCC placement analysis calculated the dam volume on one foot thick layers. Ten layers were combined to estimate the duration of placement for a sloping layer zone. The dam will be constructed with two defined construction joints, and additional transverse vertical induced contraction joints spaced at approximately 50 ft. intervals created as RCC placement progresses. The joints will extend the full thickness of the dam cross section, and as noted consideration will be given during detailed design to incorporating facilities within the joints – or some of the joints – to enable post contraction grouting to enable full arch action to be developed by the reservoir under reservoir loading. The proposed construction schedule attached in Appendix B10 sets out the planned duration and placement quantity of RCC in each season. These durations and volumes are summarized in Table 10.8-1 below.

Table 10.8-1. RCC Production Schedule

Season	Days	Start	RCC Quantity (Theoretical) (cy)	Placement Rate (cy/hr.)
1	150	May 08	1,000,000	335.6
2	150	April 23	1,000,000	335.6
3	150	April 27	1,000,000	335.6
4	150	May 02	1,214,000	407.4
5	150	May 07	1,000,000	335.6

*Based on a 20 hr. working day

10.8.2. RCC Placement Sequencing

Sequencing of the seasonal RCC placement is described below. The placement locations and estimated volumes are shown in Table 10.8-2 and the placement sequence is shown in Figure 10.8-1.

Table 10.8-2. RCC Placement Locations

Season	Location	Volume (cy)	
		Location	Season
1	Right Abutment	562,750	
	Left Abutment	435,500	998,250
2	Middle & Downstream Platform	1, 006,850	1,006,850
3	Middle	1,000,300	1,000,300
4	Middle	1,231,850	1,231,850
5	Middle	610,600	
	Left Abutment	160,100	
	Right Abutment	224,000	994,700
Total			5,213,950

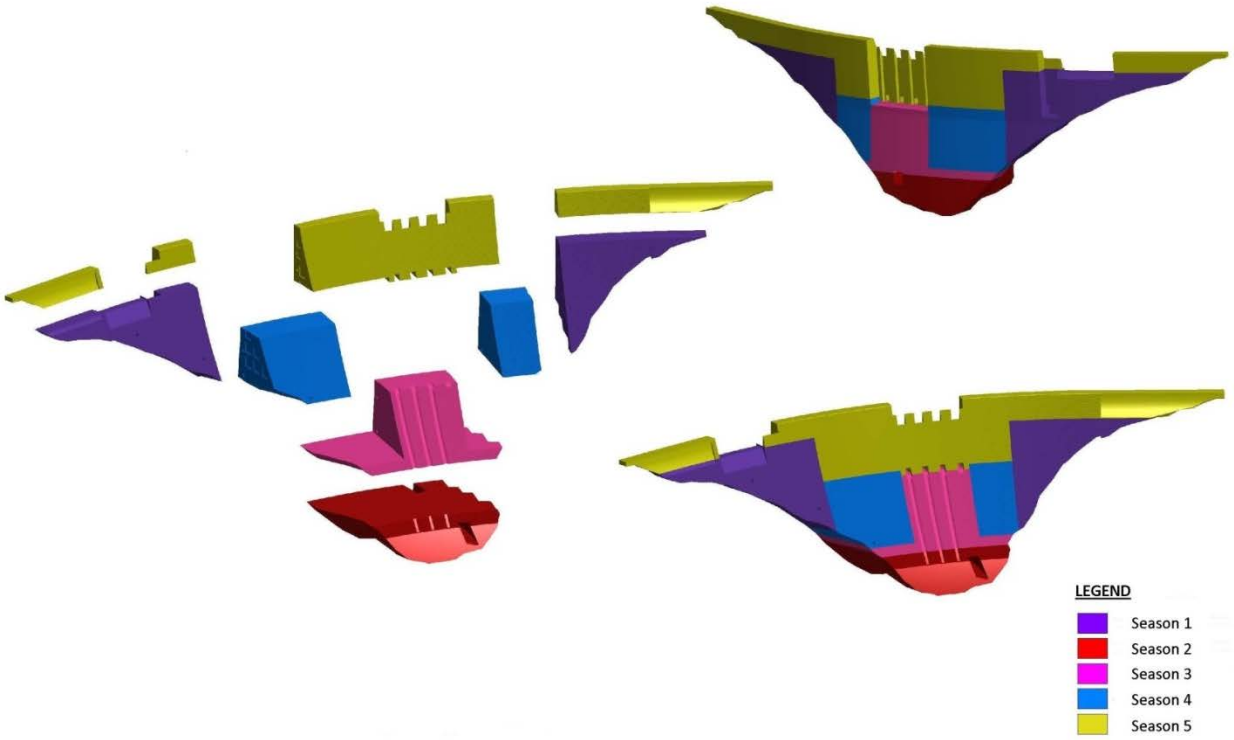

Figure 10.8-1. Seasonal Sequence of RCC Placement

10.8.2.1. Season 1 of RCC

Season 1 of RCC placement will focus RCC placement at both abutments. Placement will begin at the right abutment and about 563,000 cy of material will be placed. This will enable the construction of the intake to the elevations of the low level outlet and the spillway crest to commence in the first construction year. Placement at the right abutment will be completed by about August, and will take about 84 days. The finished surface of the RCC will generally be completed to El. 1985 ft. apart from beneath the footprint of the intake to the low level outlet pipes.

Construction will then move to the left abutment where about 435,500 cy will be placed over an approximately 65 days. At the end of the placement season, the left abutment will be constructed to El. 1968 ft.

Placement rates are shown in Figure 10.8-2 and Figure 10.8-3.

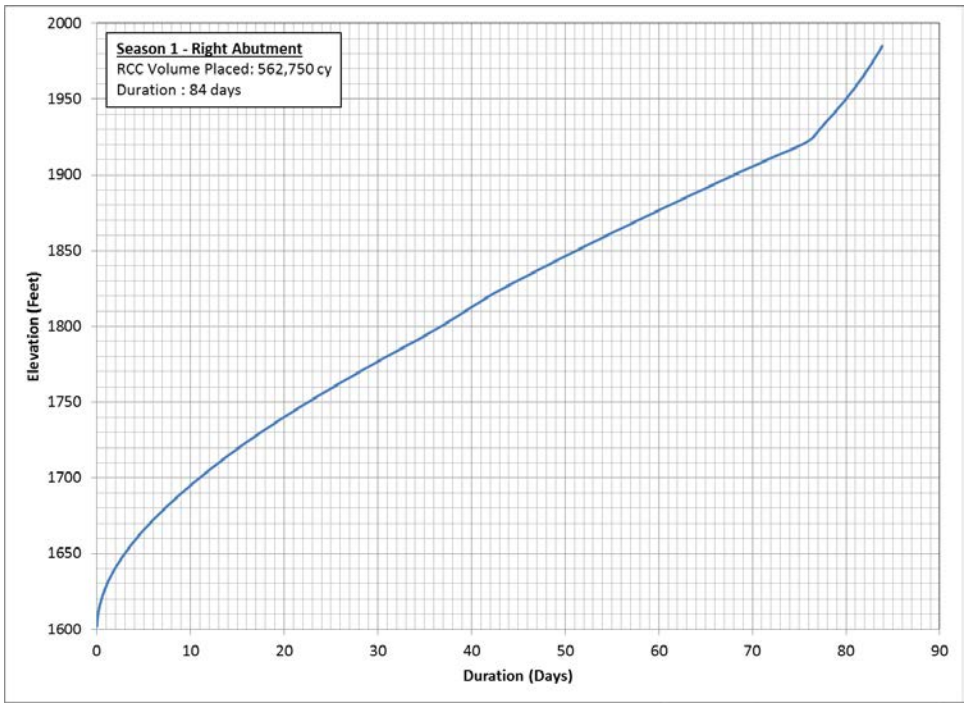

Figure 10.8-2. Season 1 RCC Placement : Right Abutment

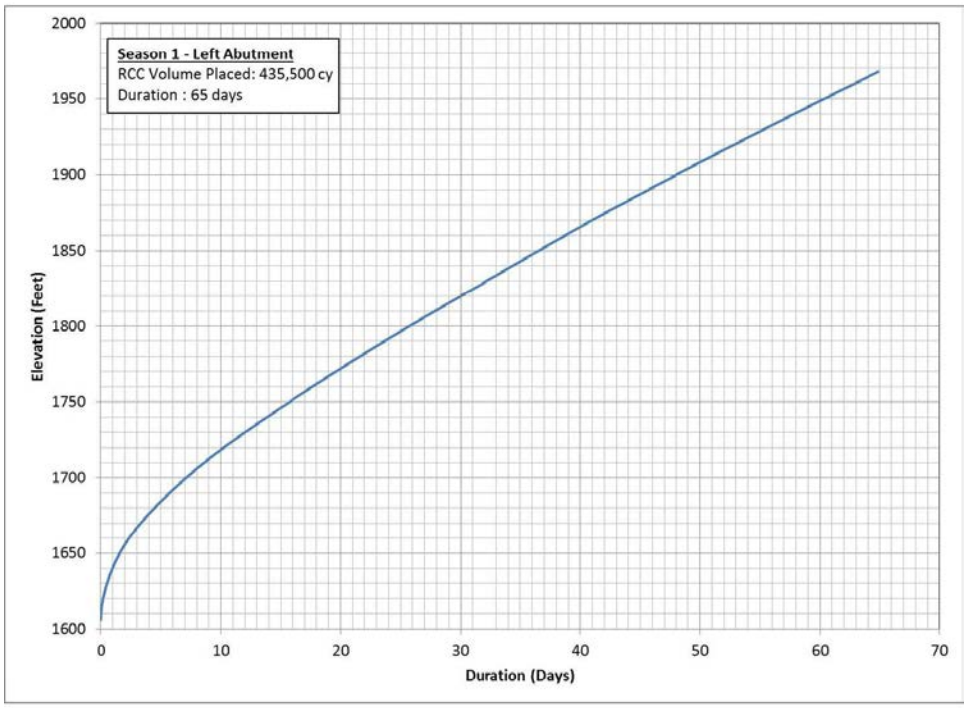

Figure 10.8-3. Season 1 RCC Placement : Left Abutment

10.8.2.2. Season 2 of RCC

The second season will focus on placement of RCC in the riverbed at the bottom of the valley. The river diversion tunnel will have been completed, the diversion of the river implemented and foundation excavation completed – in advance of the start of the second season of RCC placement. The season will involve placement of RCC across the entire width of the valley floor.

A key goal for the season is to place RCC such that the finished surface level – at least at the upstream part – is at least five feet above the elevation of the top of the sluice as soon as possible during the season, so that the upstream cofferdam can be allowed to be overtopped in the event that the diversion tunnel is blocked or overwhelmed. The early placement during the season will have a crest width of about 45 ft. and the downstream face formed at a slope of 0.85H:1V. At the end of the season, the fill between the dam and powerhouse will be completed; the finished surface of the dam will be at El. 1520 ft. or more at the upstream portion. The relationship between elevation and volume for the season is shown in Figure 10.8-4.

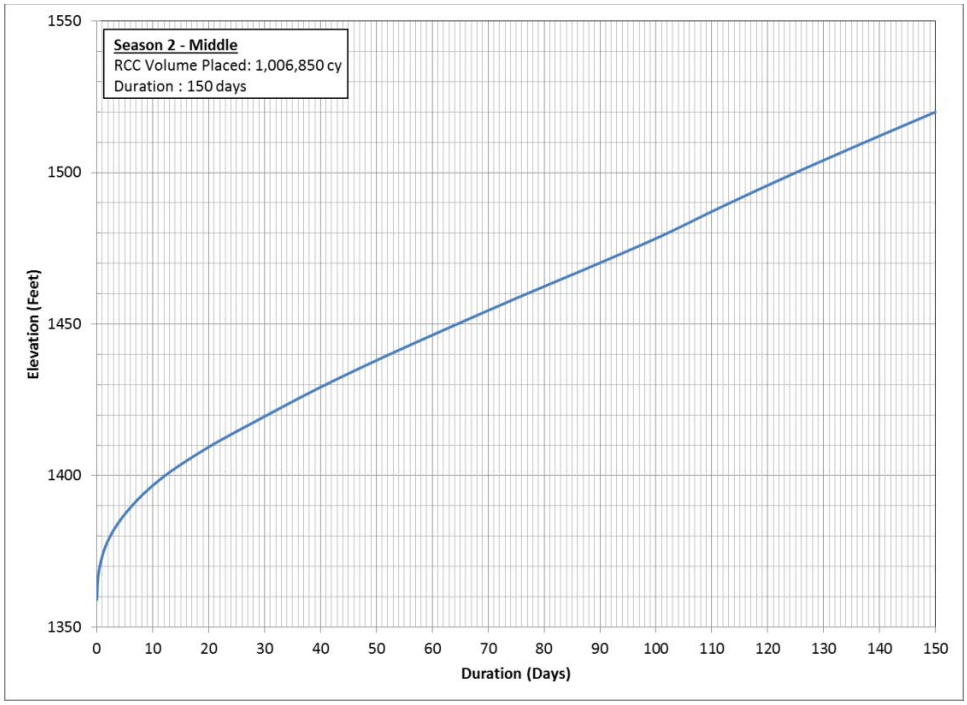

Figure 10.8-4. Season 2 RCC Placement : Middle Dam Section

10.8.2.3. Seasons 3 and 4 of RCC

Seasons 3 and 4 will focus on RCC placement within the middle section of the dam. Placement rates will be the highest during the fourth season. Figure 10.8-5 shows the relationship of

elevation and layer volume and indicates that the largest layer is at El. 1604 ft. with a volume of approximately 9,330 cy.

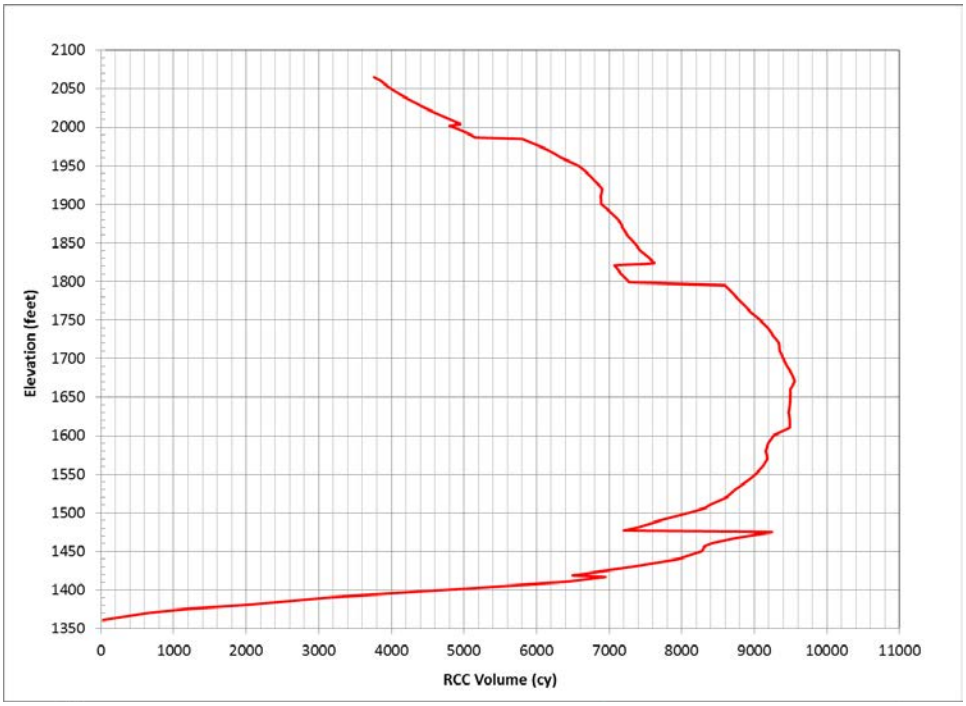

Figure 10.8-5. RCC Layer Volume vs Elevation

During Season 3, all RCC will be placed beneath the power intakes and penstock footprints, to allow construction of the power intakes to commence as soon as possible as shown in Figure 10.8-6. RCC layer elevations at the end of Seasons 3 and 4 are shown in Table 10.8-3.

Table 10.8-3. End of Season Elevations: Middle Section

Season	RCC Layer Elevation
3	El. 1555 ft. with the portion beneath the penstocks and power intakes at El. 1795 ft.
4	El. 1816 ft. either side of the previously placed Power Intake footprint RCC.

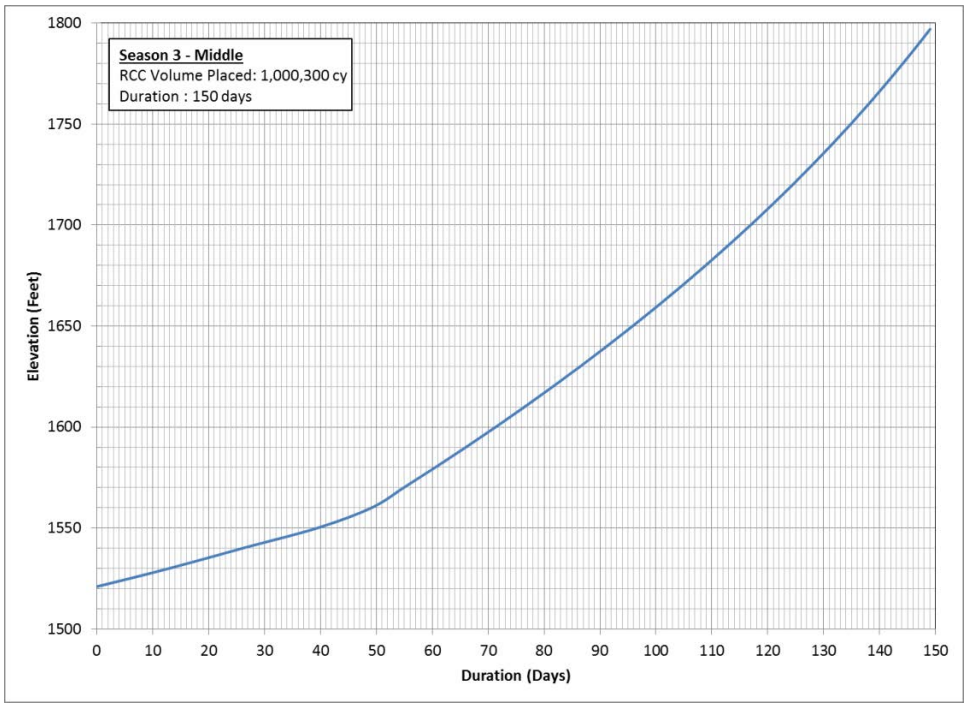

Figure 10.8-6. Season 3 RCC Placement : Middle Dam Section (Beneath Power Intakes Footprint)

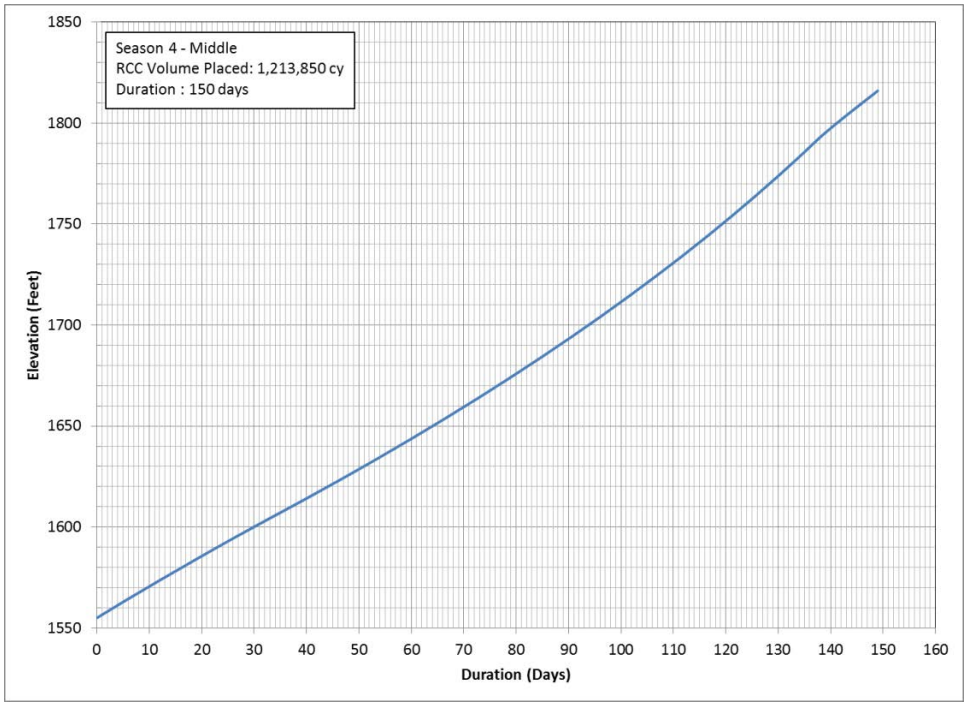

Figure 10.8-7. Season 4 RCC Placement : Middle Dam Section

10.8.2.4. Season 5 of RCC

The fifth and final season will encompass the completion of the RCC – which will be done while the reservoir fills. The middle portion of the dam will be completed first, followed by the right abutment. The left abutment will be the final portion of the dam to be completed. Elevation-volume relationships are shown in Figure 10.8-8 through Figure 10.8-10.

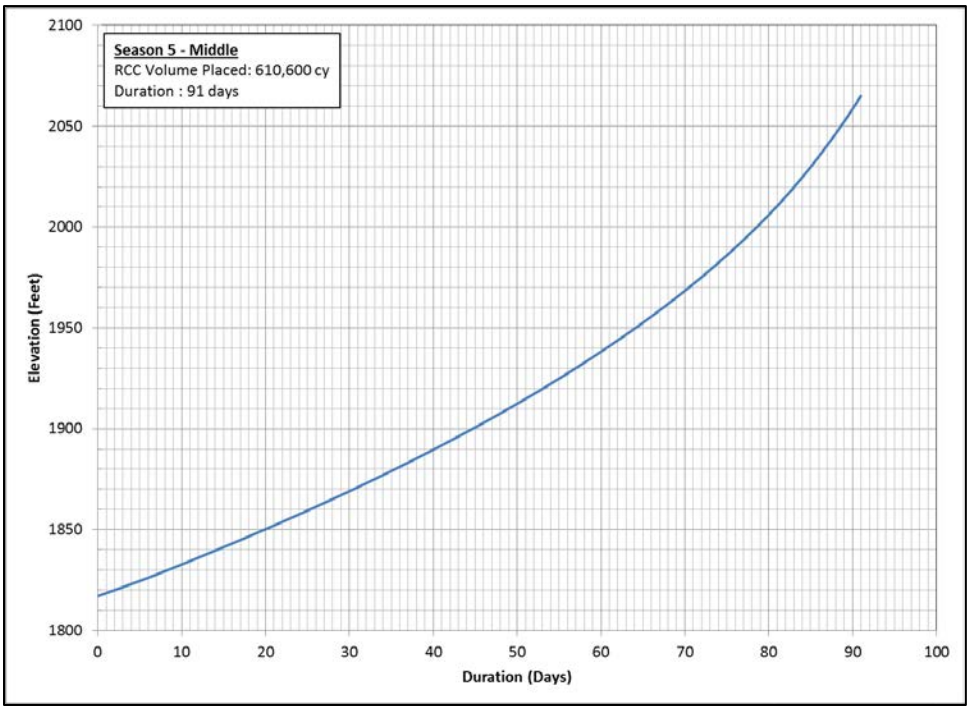

Figure 10.8-8. Season 5 RCC Placement : Middle Dam Section

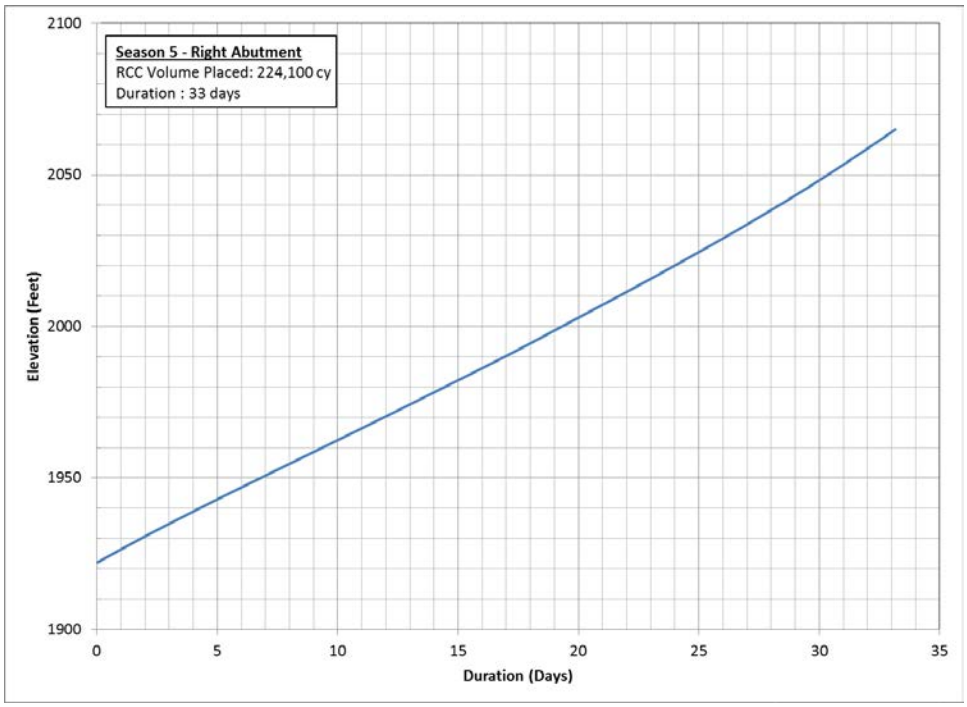

Figure 10.8-9. Season 5 RCC Placement : Right Abutment

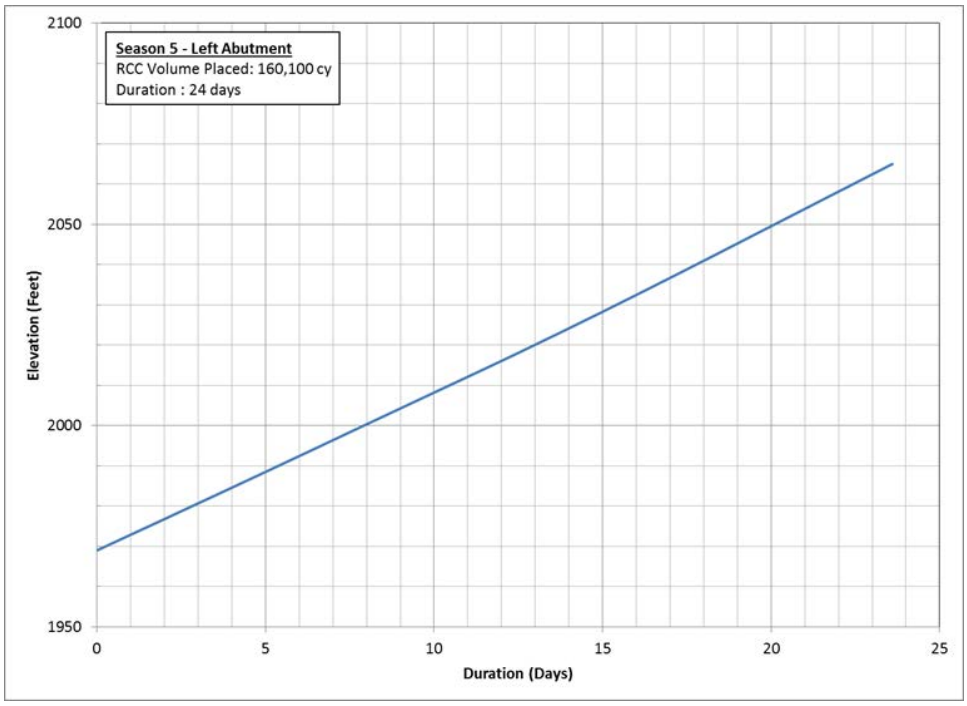

Figure 10.8-10. Season 5 RCC Placement : Left Abutment

10.9. Dam – Thermal Considerations

10.9.1. General

Thermal behavior will be an important aspect to consider in the final design of the Watana Dam, for reasons that include, but are not limited to:

- For RCC, external considerations – such as cooling on the large areas of RCC (or thermal gain from the sun) – are often more significant than the hydration of cement;
- Because of the speed of construction, there can be significant thermal gradients between the mass of RCC and the open faces;
- The seasonal nature of construction at the Watana site will require very careful attention to the "cold joints" between seasons;
- The curved axis of the dam will result in some arch action which will be mobilized after the shrinkage of the structure;
- The abutments of the dam are cool – and possibly below 32°F on much of the left abutment – and provisions must be made to avoid thermal shock during initial covering of the foundation.

A full thermal analysis to address all issues has not been carried out at this stage, but a detailed analysis – taking into account the placement sequence shown in Section 13.3.6; proposals for insulation; the selected mix design; projections of mixing and placement temperatures; and the proposed abutment preparation – will be performed, and planning of the whole sequence of placement made, prior to finalizing the contract specifications.

This section describes the topics that will need to be addressed in the detailed design and construction planning related to thermal performance as well as a simplified analysis that has been made of the dam section.

10.9.2. Transverse Joints

Temperature induced cracks are to be expected in a RCC gravity section, and current practice is to induce a transverse crack/joint at approximately every 50 ft. along the axis of the dam. It should be noted that the proposed design of Watana Dam includes two formed joints – with shear keys – which have been included to facilitate, during the seasons prior to river diversion, the construction of the upper sections of the dam on each abutment.

The formed joints and the induced joints will all be constructed with double waterstops at the upstream face, and a large diameter vertical drain between them. If the dam stability relied

solely on gravity action, there would be no consideration of further treatment of the joints, but there is expected to be some mobilization of "arch action" during a seismic event. Detailed design may indicate that the formed joints incorporate facilities for grouting (and regrouting) at, or near, the end of construction – thus allowing "arch action" to be mobilized. In addition, the inclusion of grout pipes in some or all of the induced joints will be investigated if the detailed design analyses show benefit from such post construction grouting. It may be that few (or no) areas of the dam will need such post placement grouting – for example the RCC placed in season 2 will be heavily restrained by the bedrock foundation, while the central area (to facilitate early construction of the intakes), placed in season 3 is effectively unconstrained. It is envisaged that the RCC placed in season 4 – between the previously placed abutment sections and the central section placed in season 3 – will be the main candidate for grouting of induced joints. Grouting of induced joints has been practiced at Shapai in China, among other curved RCC dams.

10.9.3. Abutment Temperature

The bedrock at the left abutment – in at least some areas – has a stable temperature at or below 32°F. No concrete is to be placed against frozen surfaces (formwork, rock etc.) and the rock surfaces will therefore need to be covered and heated to the RCC placing temperature or higher for a minimum period of 24 hours before placing. It is assumed that this can be achieved using heating pads, or by drilling short holes and circulating hot water or steam through them (as discussed in Section 10.3). Once the RCC is placed, the abutment will act as a heat sink, and the heat of hydration will establish a steady state condition such that the interface between the rock and concrete will be at an acceptable temperature. This will be checked by thermal modeling during detailed design and will be monitored post construction.

10.9.4. Insulation Requirements

Mean ambient temperatures at the site fall below 32°F throughout the winter, so at the end of each placing season all exposed RCC will have to be covered with insulation materials. Heavy insulation will be needed on the top surface during the winter period to protect the RCC against "curling".

In addition, it is expected that it will be in the interest of the contractor to extend the RCC placement season as much as possible. The extension of the placing season in the fall will be more straightforward than starting earlier in the year, so a contractor intent on beating the overall schedule will wish to extend the end of each season as much as possible. It is expected that season extension by two or three weeks might be achieved by the establishment of insulation above each 10 ft. layer of RCC, so that as the sloped layers are placed, the insulation is removed and immediately replaced. The possibilities for such methodology and the insulation requirements will be investigated using sophisticated thermal modeling during detailed design.

10.9.5. Control of Mixing and Placing Temperatures

As noted, the monthly mean ambient temperature during the placing season is no higher than 52°F and at the shoulder seasons it is approximately 40°. It is therefore seen to be straightforward to limit the RCC placing temperature to 40°F by using river water (which is above 50°F only in June and July, when some ice can be added). The passing of river water through the stockpiles early and late in the season, together with use of ice during the middle of the season should maintain a constant and acceptable placing temperature without the need for cooling of the structure. However, it is foreseen that heating and insulation of the stockpiles will be needed throughout the winter, and it is prudent to cover and insulate the conveyor belts (both to move aggregate and to deliver RCC) – particularly at the shoulder seasons.

10.9.6. Preliminary Simplified Thermal Analysis

Although a complex thermal analysis, taking into account all the variables discussed above is beyond the scope of the feasibility study, a simplified study was performed to investigate the behavior of the suggested cross section of the dam. Preliminary thermal calculations showed that surface cracking of the RCC would likely occur during construction of the dam. Cracking can be prevented by providing insulation until the RCC has gained sufficient strength and the thermal stresses are relieved due to cooling of the dam interior body. The time required for insulation can be optimized by carrying out parametric studies on the initial placing temperature of RCC.

The current analysis has been based on typical RCC thermal properties derived from similar projects. Final analysis will require properties determined from the actual RCC mix that will be used on the project.

The developed model did not include the openings for the power or low level outlet intakes or spillway. The effect of the conventional concrete portions of these elements on the thermal response of the dam was not analyzed. These geometric anomalies are more susceptible to thermal cracking and will need to be investigated in the subsequent design phase. Final thermal analysis would consider the effect of all geometric features in the dam's thermal response.

Parametric studies on the initial placing temperature and insulation time would be required to control the cracking and to optimize the construction cost.

A detailed 3-D model of the dam can be developed to include stage construction, all openings and construction features of the dam. This model can be used for analysis and determining the overall thermal response of the dam. The stresses for inclusion in the final structural FE analysis of the operating dam can also be derived from this model.

10.9.6.1. Design Criteria

10.9.6.1.1. Climatological Properties

10.9.6.1.1.1. Ambient Temperature

The monthly ambient temperature values used in the simplified analysis were taken from the Acres feasibility study dated 1982. The values are reproduced below in Table 10.9-1.

Table 10.9-1. Susitna Project Site Monthly Temperature Data

	Max	Min	Mean	Max	Min	Mean
	ºF			ºC		
January	8	-4.8	1.6	-13.4	-20.4	-16.9
February	13.5	-0.4	6.6	-10.3	-18.0	-14.1
March	19.4	3	11.2	-7.0	-16.1	-11.6
April	32.9	14.2	23.5	0.5	-9.9	-4.7
May	45.7	29.1	37.4	7.6	-1.6	3.0
June	58	39.9	49	14.4	4.4	9.4
July	60.2	43.8	52	15.7	6.6	11.1
August	56	41.1	48.6	13.3	5.1	9.2
September	47.1	32.6	39.9	8.4	0.3	4.4
October	30.4	17.5	24	-0.9	-8.1	-4.4
November	15.7	3.7	9.7	-9.1	-15.7	-12.4
December	9.2	-3.4	2.9	-12.7	-19.7	-16.2

10.9.6.1.1.2. Water Temperature

The USGS publication titled “Sediment Discharge Data for Selected Sites in the Susitna River Basin, Alaska, October 1982 to February 1984”, records water temperature readings taken in the Susitna River at Gold Creek and near Talkeetna. An average of the readings has been collated and is listed in Figure 10.9-1 and Table 10.9-2 below.

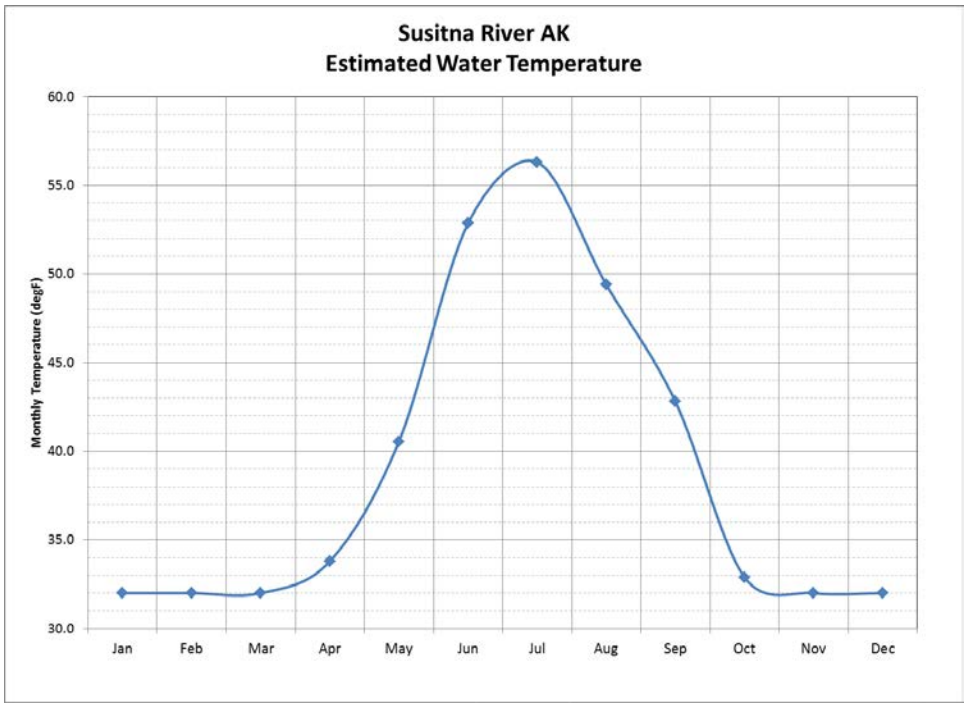

Figure 10.9-1. Susitna River Estimated Mean Monthly Water Temperature near Gold Creek

Table 10.9-2. Susitna River Mean Monthly Water Temperature near Gold Creek

Month	Water Temperature	
	(°F)	(°C)
January	32.0	0.0
February	32.0	0.0
March	32.0	0.0
April	33.8	1.0
May	40.6	4.8
June	52.9	11.6
July	56.3	13.5
August	49.4	9.7
September	42.8	6.0
October	32.9	0.5
November	32.0	0.0
December	32.0	0.0

10.9.6.1.2. Thermal Properties of RCC

Thermal properties of RCC were selected from similar projects and references with sufficient conservatism required for the feasibility level analysis. The thermal properties of RCC and foundation rock used in the analysis are presented in Table 10.9-3 below.

Table 10.9-3. Foundation and RCC Thermal Properties (used in analysis)

RCC	
Unit weight	150 pcf
Heat of Hydration of cement	150 to 175 Btu/lb. @ 28 days
Adiabatic temperature rise of RCC	59°F @ five days and 68°F @ 28 days
RCC mix contains (per cubic yard)	125 pounds of cement; and 200 pounds of fly ash
Coefficient of Thermal Expansion	4.8 E-6/°F
Specific Heat	0.22 Btu/lb.°F
Thermal Conductivity	1.25 Btu ft./(hr. ft^2 °F)
Placement Temperature (minimum)	50°F
Foundation Rock	
Unit weight	170 pcf
Specific Heat	0.21 Btu /lb.°F
Thermal Conductivity	1.15 Btu ft./(hr. ft^2 °F)
Foundation Temperature	Left abutment 30°F
	Right abutment 32°F

The thermal convective (or heat transfer) coefficient of the RCC surface in contact with air was calculated based on the wind velocity of 6 mph. The thermal convective coefficient for RCC with no formwork was calculated to be 2.91 Btu/(hr. ft^2 °F) and for RCC with no formwork to be 0.80 Btu/(hr./ft^2 °F).

10.9.6.2. Finite Element Method

ANSYS Version 15 was used for thermal analysis of the dam to evaluate the developed temperature field in the dam body during construction. A 3-D FE model was created representing dam Layout 4 (but not the modified Layout 4) as shown in Figure 10.9-2, and a 2-D FE model was created representing the dam cross section as shown in Figure 10.9-3. Eight node solid elements with thermal conductivity capacity and the material properties presented above were used to model the dam. The model included 10 ft. high elements to simulate the expected RCC lifts between "cold" joints. The "death and birth" of elements option, available in ANSYS, was used to simulate the construction of dam layers in a simple manner – not in the staged construction method that will ultimately be developed in accordance with Figure 10.8-1.

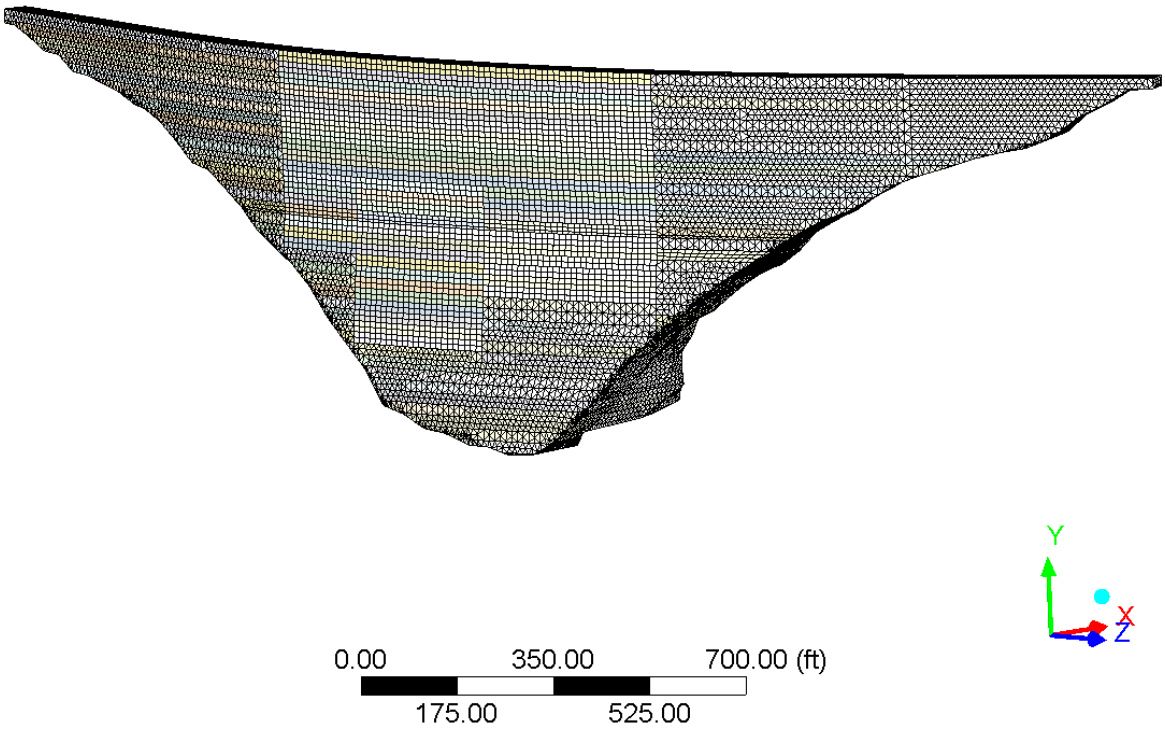

Figure 10.9-2. 3-D Finite Element Model of the Dam for Simplified Thermal Analysis

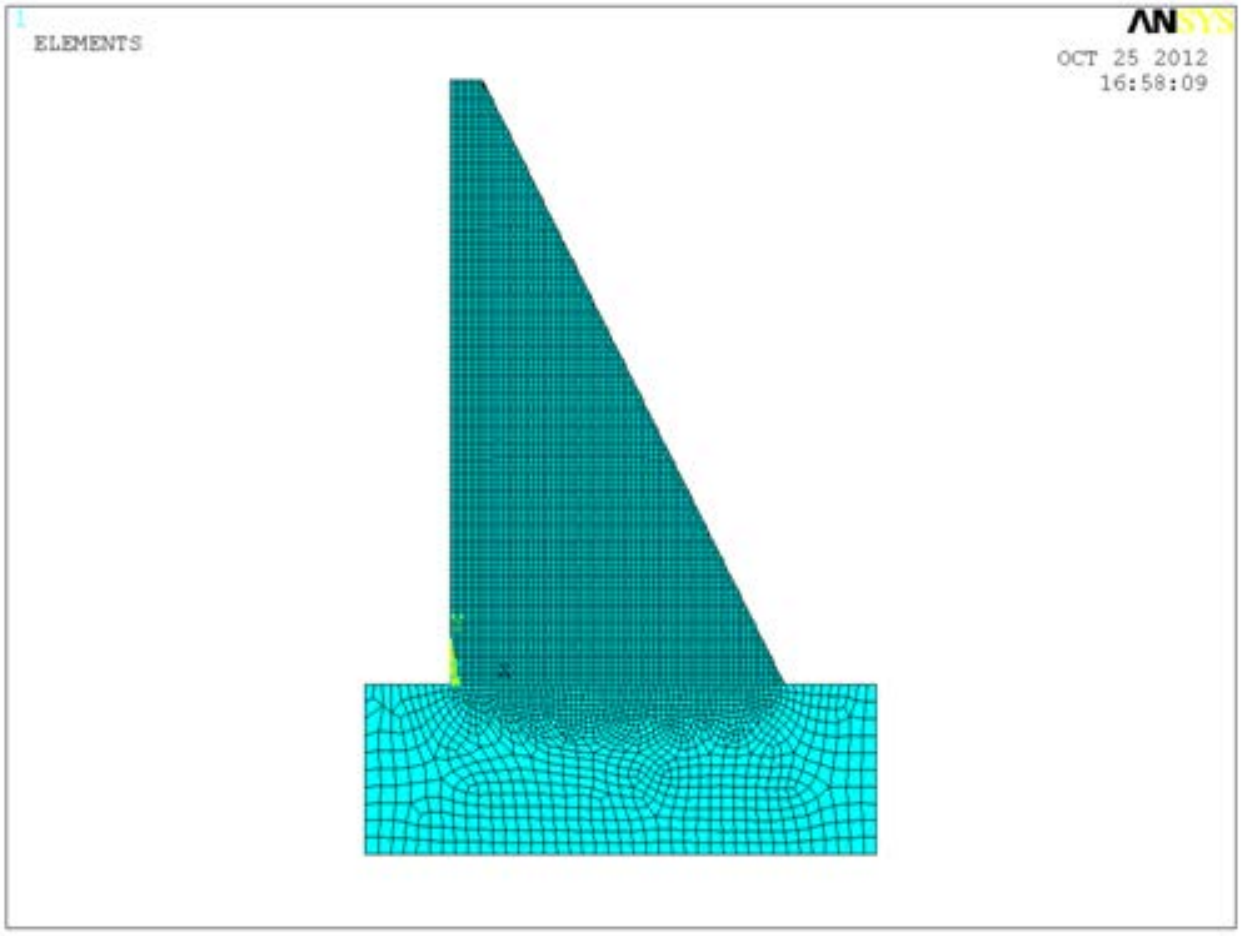

Figure 10.9-3. 2-D Finite Element Model of the Dam for Simplified Thermal Analysis

Analysis results show that the temperature in the dam body can reach 77°F during construction. Results from the thermal analyses were used to compute strains in the dam body in accordance with ACI 207.2R, where peak temperatures and temperature drop computed in the FE model were used to evaluate the potential for thermally induced cracking.

10.9.6.2.1. Surface Gradient Cracking Analysis

A surface gradient strain evaluation was performed. The surface gradient evaluation considered the potential for development of surface cracks during the critical period in the days immediately after placement when the surface of the concrete cools and contracts more rapidly than the warmer interior mass concrete.

Calculations were performed across the center of lift 55 as shown in Figure 10.9-4. Figure 10.9-5 shows the computed temperature across the center of lift 55 for different ages of the lift. The surface gradient strains were evaluated based on the difference between actual temperatures

throughout the cross section and the concrete placement temperature. The critical point in surface gradient strain evaluations required determining where stress in the concrete is zero, or where it switched from tension (at the surface) to compression (beneath the surface). By plotting balanced temperature differences through the cross section, the depth at which this transition occurred was determined.

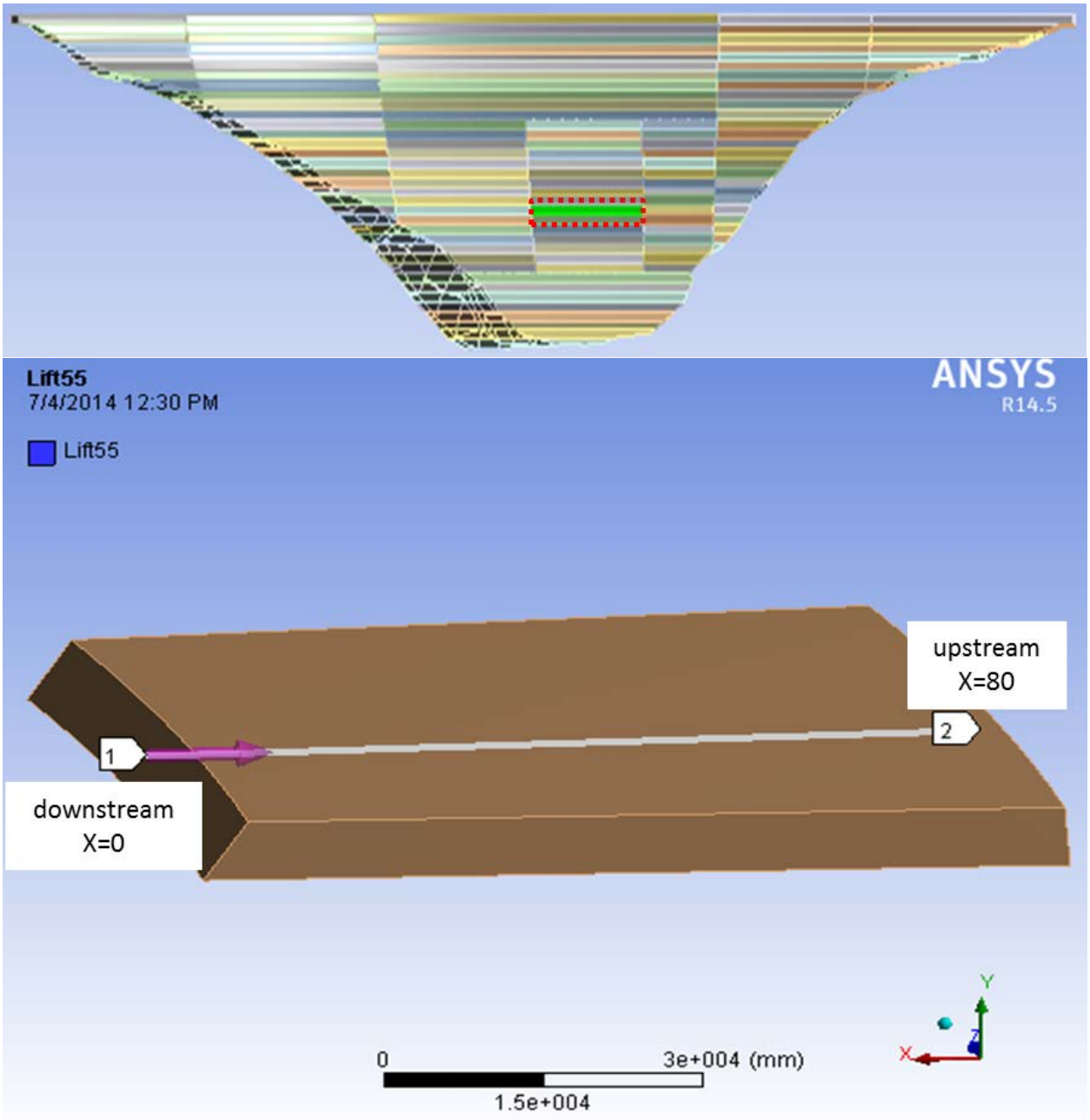

Figure 10.9-4. Location of LIFT 55 Used for Surface Cracking Calculations

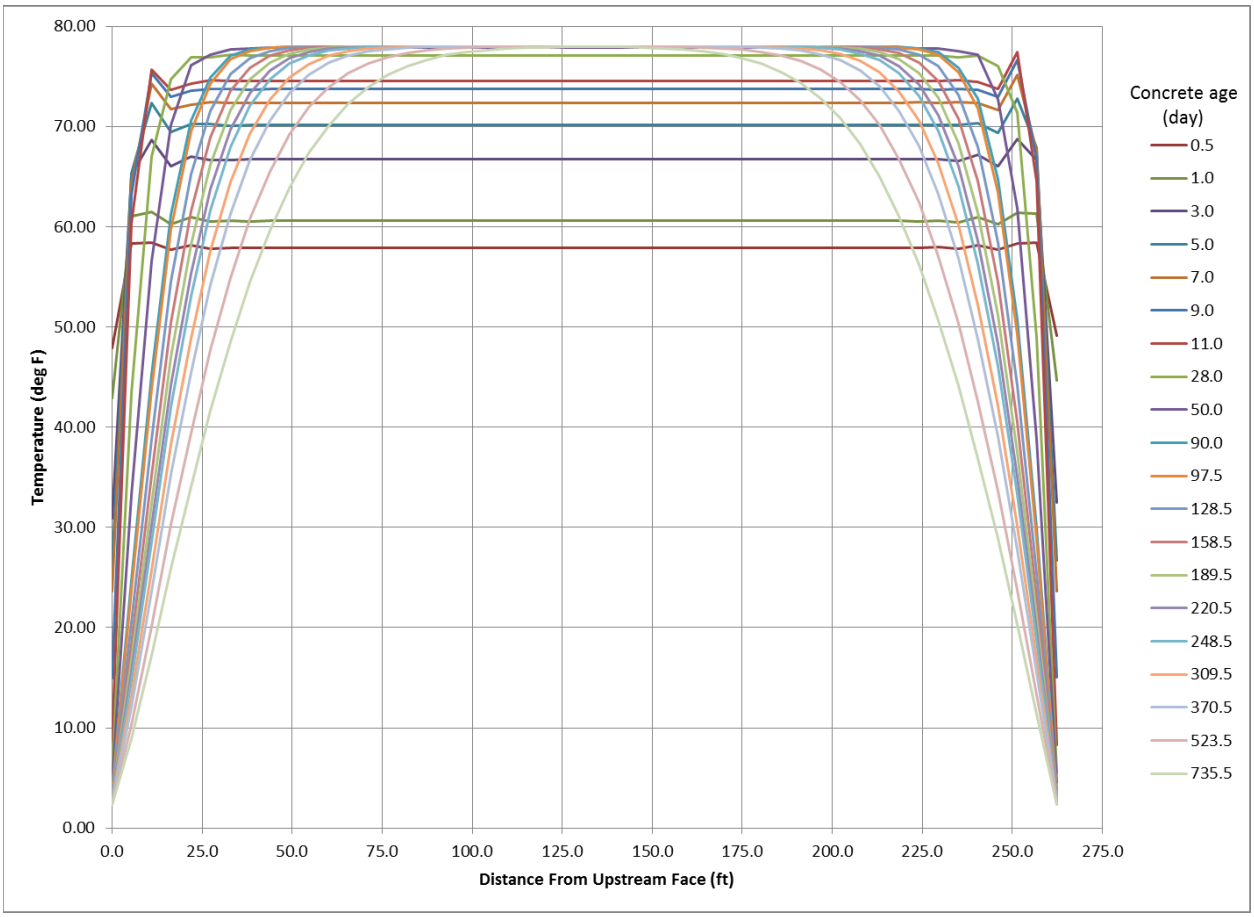

Figure 10.9-5. LIFT 55 Temperature Profile

This depth was subsequently used to calculate the strain modification factor, K_R. for input into strain computations as defined in ACI 207.2R. For the surface gradient evaluation, age of the concrete during the curing process was used to determine the time dependent material properties for input into the calculation of strain capacity.

A summary of calculations and the possibility of surface cracking are shown in Table 10.9-4. Analysis results shows that surface cracking of the RCC may develop during the first 28 to 50 days of RCC placement. Therefore insulation is recommended.

Table 10.9-4. Surface Tensile Stress Gradient Calculations

	Concrete age Lift 55											
Hours	24	72	120	168	216	264	672	1200	2160	2339	3083	3803
Days	1	3	5	7	9	11	28	50	90	97	128	158
	Depth of the Tension Block (ft.)											
X =	5.35	7.81	8.96	9.58	9.81	10.10	15.88	19.62	20.05	24.74	26.80	28.81
H(downstream)	5.35	7.81	8.96	9.58	9.81	10.10	15.88	19.62	20.05	24.74	26.80	28.81
X =	257.15	256.69	254.72	253.84	253.51	253.15	248.16	244.98	240.75	234.00	237.2	235.53
H(upstream)	5.18	5.68	7.64	8.53	8.83	9.19	14.17	17.36	21.62	22.38	25.16	26.81
	Effective Temperature Differences at Surface (°F)											
ΔT(downstream)	-4.47	-14.19	-18.19	-20.38	-25.89	-29.43	-31.69	-32.07	-31.81	-31.73	-31.41	-31.09
ΔT(upstream)	-3.89	-13.85	-18.82	-21.62	-26.95	-30.99	-33.22	-33.53	-33.17	-33.08	-32.72	-32.37
	Restraint Factors K_R at Surfaces											
K_R(downstream)	0.74	0.64	0.60	0.57	0.56	0.55	0.35	0.24	0.11	0.11	0.09	0.08
K_R(upstream)	0.75	0.73	0.65	0.61	0.60	0.59	0.41	0.30	0.18	0.16	0.10	0.09
	Surface Tensile Strain $x10^{-6}$ corrected for internal restraint (K_R)											
ε(downstream)	27.0	77.4	94.6	102.7	127.6	142.7	97.6	66.4	31.2	29.8	25.9	22.5
ε(upstream)	25.1	87.0	104.8	113.8	139.0	156.1	115.9	87.5	51.1	45.2	29.4	26.2
εmax.	27.0	87.0	104.8	113.8	139.0	156.1	115.9	87.5	51.1	45.2	29.4	26.2
	Slow Load Tensile Strain Capacity $x10^{-6}$ vs Concrete age											
Concrete age	1	3	5	7	9	11	28	50	90	97	128	158
Slow load TSC	40.0	56.0	66.0	74.0	78.0	81.0	90.0	96.0	100.0	100.0	100.0	100.0
	Checking											
Cracking	NO!	YES!	YES!	YES!	YES!	YES!	YES!	NO!	NO!	NO!	NO!	NO!

10.10. Instrumentation

10.10.1. General

Chapter 9, Instrumentation and Monitoring of the Engineering Guidelines for the Evaluation of Hydropower Projects (FERC, undated) sets out minimum instrumentation recommendations for new dams. The recommendations vary depending upon the type of dam and the hazard classification of the structure. Watana Dam will be a High Hazard potential structure, and the recommended project parameters to be monitored are as follows:

- Reservoir level;
- Tailwater level;
- Drain flow, seepage and leakage;

- Pore/Uplift pressure, under dam foundation and downstream;
- Surface alignment;
- Internal movement;
- Stress and strain;
- Joint displacement;
- Thermal profile in the RCC and in abutment rock;
- Foundation movement; and,
- Seismic motion in the dam body and foundation.

As well as the dam, there will need to be careful measurement of rock slopes in the vicinity of the dam, and the groundwater conditions in the Relict Channel.

As far as possible, the instrumentation shall be set up for real time monitoring remotely, or for ease of downloading data. Also the instrumentation design shall as far as possible include redundancy and the possibility of checking the real time conditions in at least two ways.

10.10.2. Dam

10.10.2.1. Reservoir and Tailwater Level

Water level measurement can be accomplished using simple devices that are also inexpensive.

A staff gauge will be fixed to the upstream face of the dam which would be manually measured by reading the gage either at the dam, or remotely by CCTV cameras that could be trained onto the gage. This will be a secondary, failsafe method of monitoring the reservoir water surface elevation.

The reservoir water level will fluctuate by up to 200 ft. each year. At lower water surface elevations the reading of the gage would be difficult. A gage located at the upstream face, near the spillway would provide a useful means of monitoring the reservoir surface elevation during periods of spillway operation.

Automated water level measurement options comprise float type water level gage, ultrasonic sensor or a bubbler installation. A bubbler level sensor will be installed which determines water/ liquid level by measuring backpressure of a gas bubbler system. An advantage of this technique of level measurement is that the electronics are remote from the water, ensuring long term reliability and accuracy. Bubbler systems capable of operating to the full operational range of the reservoir are commercially available.

10.10.2.2. Drain Flow, Seepage and Leakage

The drainage system installed in the foundation downstream of the grout curtain will relieve uplift pressures beneath the dam that may arise from the seepage of water beneath or through the grout curtain. Any flow through the drains will discharge into the drainage gallery/adit and be conveyed along a capture channel to a sump that will be located at the lowest point in the gallery system.

Measurement of the flow within the capture channel will be achieved by weirs or Parshall flumes. Ultrasonic sensors could be placed at the weir locations to allow automated real-time measurement of the seepage flows. The capture channel system will be divided into discreet sections, with weirs installed at the downstream end of each section. In the event of unusual or unexpected changes in the amount of seepage, the section of grout curtain in question can be quickly isolated for further investigation.

Vertical drains will also be drilled from each of the upstream galleries both upwards and downwards, at appropriate regular intervals so that all potential leakage through the RCC is captured and measured by weirs at various levels within the access and drainage galleries.

10.10.2.3. Pore / Uplift Pressure

Pore pressure and uplift pressure in the dam foundation will be monitored by vibrating wire piezometers. Vibrating wire piezometers are insensitive to freezing conditions, and automated results can be transmitted over long distances. This type of piezometer has a very short lag time, allowing real-time monitoring of the pore pressures.

The location and number of piezometers will be selected to allow an understanding of the uplift pressure distribution beneath the dam. Five lines of piezometers, radially aligned will be installed, one along the highest section of the dam, one line near to the edge of the river bed, one beneath the spillway section, one within the right flank section, and one within the left flank section. The line at the highest dam position will comprise four boreholes, each with two piezometers at defined elevations; the other lines will comprise three boreholes as shown on the same figure. Four boreholes are planned at the highest dam location; the furthest downstream borehole will provide data on uplift pressures beneath the concrete fill between the dam and the powerhouse and also for future monitoring in the event the dam is raised.

10.10.2.4. Surface Alignment

Survey measurement of the dam (crest and downstream face) is necessary to monitor the movement of the structure. To monitor the dam's movement, a triangulation network will be necessary. The network will consist of a series of monuments embedded into the crest of

Watana Dam, targets located on the downstream face and at least six theodolite piers located on the sides of the valley downstream of the dam, three on each side of the river. The targets on the downstream face of the dam will be positioned to correspond with the location of the plumb lines.

10.10.2.5. Internal Movement

Inclinometers or plumb lines are the most common types of instrumentation that are installed to measure internal movement. Plumb lines are considered to be the most accurate device (ICOLD 2005). Three plumb lines will be installed within the dam body, one at the maximum section of the dam (the crown cantilever) and one at the midpoint to each abutment. The cross sectional profile of the dam will enable a single plumb line to extend from the dam crest down to the drainage gallery. As necessary, inverted plumb lines will also be installed in the dam.

10.10.2.6. Strain

Strain gages will be installed to monitor load distribution within the dam. Clusters of strain meters (12 per cluster) will be installed at strategic locations in the dam.

10.10.2.7. Joint Displacement

The two construction joints formed during RCC placement will be monitored to observe their performance arising from reservoir level fluctuation and ambient temperature changes. The joint meters will be located to monitor vertical and horizontal joint performance. All induced contraction joints daylighting in galleries – and any observed cracks in galleries – will have 3-D joint movement monitors mounted at them. Additional joint meters will be installed at the junction of the powerhouse and the adjacent upstream concrete pad. These will be used to monitor the relative position of the dam and powerhouse.

10.10.2.8. Foundation Movement

To complement the plumb lines within the dam, inverted plumb lines will continue into the foundation. Inclinometers will also be installed within the foundation and will enable information to be obtained of areas of interest within the foundation during construction and operation of the project. Inverted plumb lines will also be included in the foundation of both abutment blocks.

Extensometers, installed within boreholes in the foundation will also provide measurement information on the foundation. Early installation will enable the characteristics of the foundation to be monitored during construction of the dam and powerhouse. The location of the

extensometers will coincide with the other instrument groups. The total length of each extensometer will be between 25 percent and 50 percent of the dam height.

10.10.2.9. Seismic Response

The effects of an earthquake will be monitored using accelerometers. An accelerometer will be installed on the dam crest and another installed within the drainage gallery near the dam foundation. These will allow the damping effect of the structure to be measured.

10.10.2.10. Temperature

In addition to ambient temperature, the water temperature and internal body temperature of the dam will be monitored. These parameters, in conjunction with water level and movement data can be used to verify the expected performance of the dam calculated during the design process.

Internal dam temperature measurement will be carried out using thermometers embedded in the concrete during construction. Thermometers are the preferred instrument as they have been found to be more dependable are more precise and are simple in their operation.

Four rows of thermometers are proposed. The number of thermometers in each row will vary depending on the thickness of the dam. Temperature sensors will also be installed on the upstream face of the dam, at the same elevations as the internal sensors. The external sensors will provide information on the temperature profile within the reservoir and allow the temperature profile within the dam body to be monitored.

10.10.3. Rock Slopes and Abutments

In addition to the use of instrumentation to monitor the performance of the dam, the performance of various rock slopes – in particular the dam abutments – will need to be monitored.

Rock slope monitoring requirements are normally determined by inspection during construction, and comprise survey targets fixed onto the face of the rock slope (monitored using the same survey monitoring monuments as installed for monitoring of the dam stability); extensometers often installed in subhorizontal boreholes in the slopes and particularly near the base of any identified rock wedges; and vibrating wire piezometers to assess groundwater conditions. Typically instrumentation is installed early – as soon as a potential rock instability is noticed – so that monitoring can be performed while construction occurs and thereafter during the operation of the project.

The abutments of the dam will require more comprehensive instrumentation. Any significant rock wedges identified during the design of the dam will be monitored using an array of

instrumentation. Extensometers, monitors and vibrating wire piezometers will also be used, and if appropriate, the grouting galleries accessible from the dam galleries will be extended to enable extensometers and piezometers to be placed at the most appropriate locations and angles. Abutment temperature will be measured both during construction and operation to determine the condition of any frozen joint materials.

As with all instrumentation, the instruments will be installed early in the construction period so that monitoring can be performed while construction occurs and thereafter during the operation of the project.

To the extent that it is possible, all data recorded will be relayed in real time to a central monitoring station for analysis.

10.10.4. Relict Channel

The groundwater conditions within the relict channel must be monitored during the project operation – together with ground temperature. It may be appropriate to also measure any leakage into Tsusena Creek using open drains and weirs.

10.11. Freeboard

The freeboard required for a particular dam is influenced by the water level increase during the design flood event, wave run-up and wind set-up.

The analysis followed procedures contained in the U.S. Department of the Interior Bureau of Reclamation (USBR) publication ACER Technical Memorandum No. 2 (ACER TM No. 2).

10.11.1. Analysis

The magnitude of wave run-up and wave set-up is directly related to wind speed and fetch length.

The fetch length is the maximum uninterrupted straight-line length over water for a particular wind direction. ACER TM No. 2 sets out the approach to be followed in calculating the effective fetch, described later.

Wave run-up refers to the maximum vertical height attained by a wave running up a dam face relative to the stillwater level. Run-up is a complex phenomenon that depends on the local water level, the incident wave properties and the nature of the face being run-up (slope, height, reflectivity, roughness and permeability).

Wave set-up is the result of wind stresses which results in water levels increasing at the downwind end, and subsequently decreasing at the upwind end of the reservoir. This is most noticeable for reservoirs that are straight and long.

10.11.2. Wind Speed

10.11.2.1. Wind Data

The wave height and run-up at Watana Dam was estimated by Acres in the 1982 feasibility report. The report used wind data recorded at Summit Station which was considered representative of wind conditions at the dam site.

Additional wind speed data was obtained for the Summit Station. Hourly wind speed data was obtained for the period 1948 through 1982 from the National Oceanic and Atmospheric Administration, National Climatic Data Center website. Summit station stopped recording climatological data in 1984.

The data was used to calculate the hourly recorded wind speeds for the months of June, July and August of each year. These months were focused upon as they correspond to when the reservoir is predicted to be the fullest and therefore the least amount freeboard would be available.

A statistical analysis was performed to determine the wind speed exceedance distribution. The results of the analysis are summarized in Table 10.11-1 and Figure 10.11-1.

Table 10.11-1. Wind Speed Frequency

Percentage Exceeded	Wind Speed mph
1	20.21
2	18.65
5	16.51
10	14.62
20	12.21
30	10.59
40	9.06
50	7.85
60	6.47
70	5.13
80	3.79
90	1.56
95	0.53
98	0.15

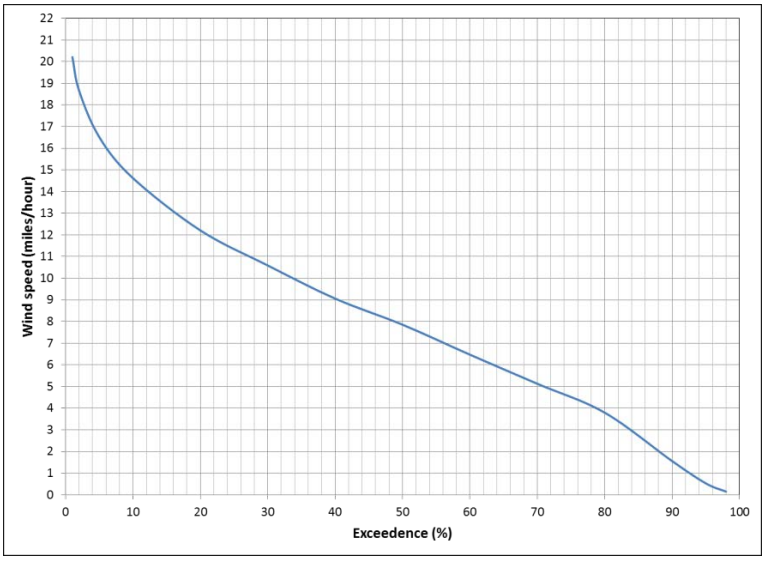

Figure 10.11-1. Wind Speed Frequency

10.11.2.2. Wind Speed Frequency

The available data was analyzed using the Pearson and Gumbel methods to arrive at return period wind speeds. The two methods are commonly adopted methods in determining flood frequency relationships and can be applied to perform similar statistical analyses of wind data. For return periods exceeding 1000 years the methodologies display a divergence in the estimated wind speeds due to uncertainties in the extrapolation methods. The estimated wind speeds are summarized in Table 10.11-2 and Figure 10.11-2 shows the divergence between the two methods.

Table 10.11-2. Return Period Wind Speeds

Return Period	Wind speed (mph)	
	Pearson Type III	Gumbel
1	19	16
2	25	26
5	31	27
10	35	32
20	39	35
50	45	39
100	50	44
200	55	47
500	62	51
1000	68	56
10000	89	59
100000	109	71
1000000	129	82

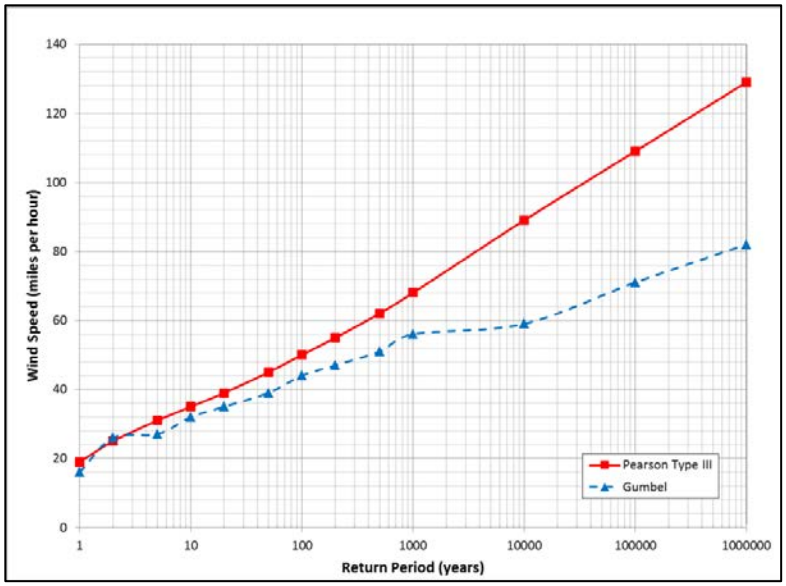

Figure 10.11-2. Return Period Wind Speeds

10.11.3. Wave Run Up and Set Up

10.11.3.1. Effective Fetch

The ACER TM No. 2 sets out a method to estimate fetch that involves constructing nine radials from the point of interest at 3° intervals. The length of each radial is measured and arithmetically averaged. Figure 10.11-3 shows the nine radials selected in determining the effective fetch for Watana Reservoir. The effective fetch length is 2.87 miles.

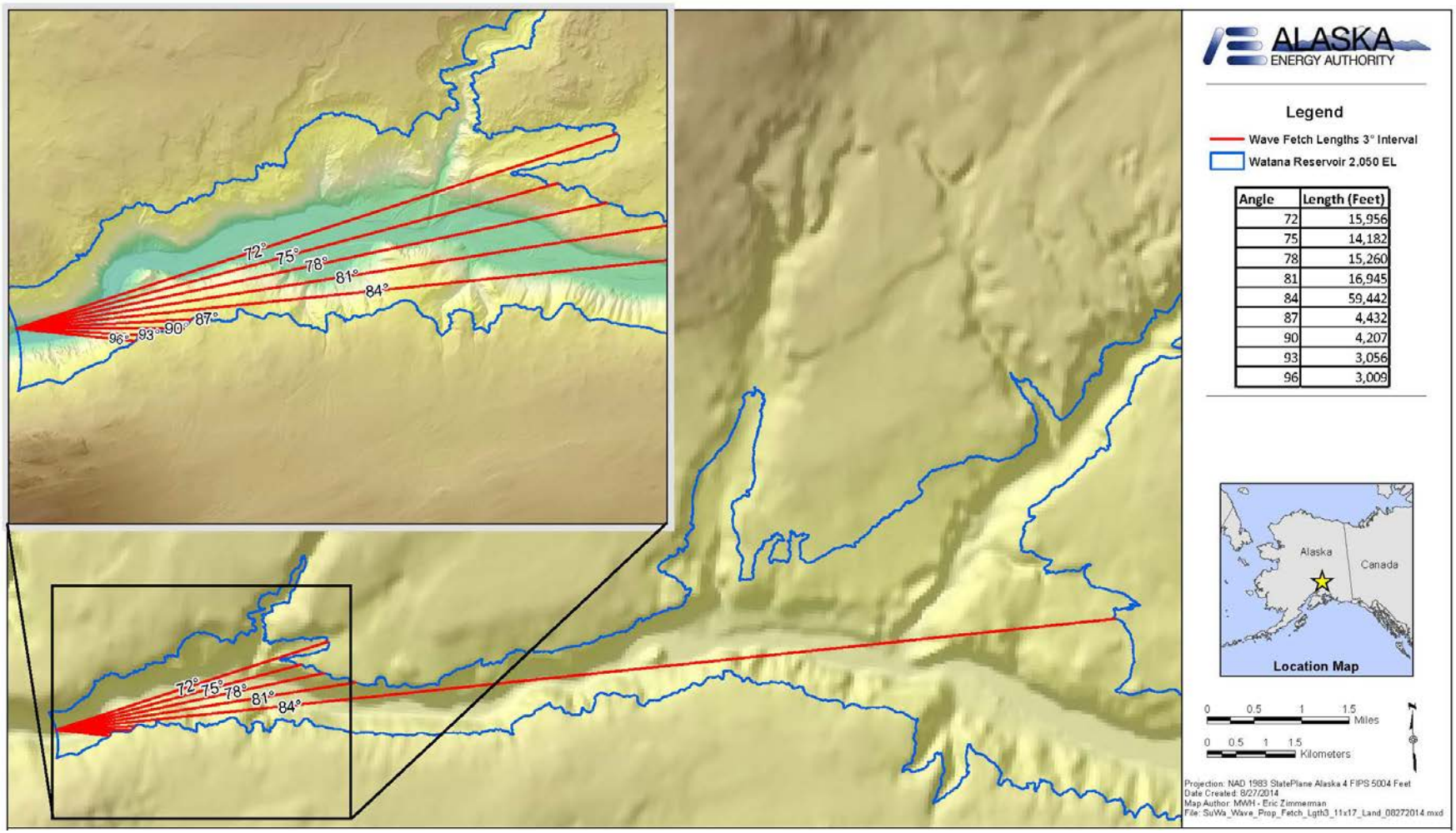

Figure 10.11-3. Effective Fetch Calculation

10.11.3.2. Wind Set Up

For deep reservoirs, wind set up is commonly calculated using the Zeider Zee equation. The equation is expressed as:

$$S = \frac{U^2 F}{1400d}$$

where:

S = wind setup (feet) above the undisturbed water level

U = average wind velocity (miles per hour) over the fetch

F = fetch length (miles)

d = average depth (feet) of water generally along the fetch line

10.11.3.3. Wave Run Up

Two methods of calculating the wave run-up are presented. Both methodologies use the same techniques to estimate the wave properties (height, length, and period) but digress when estimating the actual wave run-up.

Estimation of wave run up is calculated by following the steps described below:

1. Calculate the significant wave height: H_s (feet)

$$H_s = 0.0177(V)^{1.23}(F)^{0.5}$$

2. Calculate wave period: T (seconds)

$$T = 0.559\left(0.589(V)^{1.23}(F)\right)^{0.33}$$

3. Determine deep water wavelength: L (feet)

$$L_o = 5.12T^2$$

4. Check relative depth (depth of water/wavelength) if relative depth >2, no need to modify the results to reflect shallow water conditions.

10.11.3.3.1. Shoreline Protection Manual

The methodology recognized and accepted in the U.S. is that defined in the U.S. Army Corps of Engineers EM-1110-2-1100 – *Coastal Engineering Manual* (USACE 2002) encompassing the methodology described in the *Shoreline Protection Manual (SPM)*.

Once the wave properties have been calculated, the next step is to calculate $H'_o / (g * T_o^2)$. H'$_o$ is the equivalent deep-water wave height and T_o is the deep-water wave period. This value is used to estimate the wave run-up, R, at the dam. Figures 7-8 through 7-12 in SPM Vol. II show the relationships between R/H'_o and slope of upstream face of the dam (reservoir side) for a series of d_s/H'_o values. Figure 7-12 (SPM) is the most relevant to the situation at the Watana Dam. For a vertical upstream face the slope is zero and depending upon the value of $H'_o / (g * T_o^2)$, the relationship R/H'_o is estimated.

Based on the value determined from Figure 7-12 (SPM), the wave run-up is determined. However the wave run-up values predicted by Figure 7-12 (SPM) are expected to be smaller than the wave run-up on the prototype structure because of the inability to scale roughness effects in small-scale laboratory tests (reference SPM Vol. II). The wave run-up values are therefore adjusted for scale effects by using Figure 7-13 (SPM). The upstream face of the dam will be vertical at the dam crest and therefore the scaling effects are not significant. Figure 7-13 (SPM) indicates that the scaling effect will be zero.

10.11.3.3.2. Clapotis (Standing Wave) Method

For a deep reservoir impounded by a dam with a vertical upstream face, a standing wave or clapotis is established adjacent to the structure. The interaction between the clapotis and dam is shown in Figure 10.11-4. The actual wave run-up is the summation of the raised water surface level (h_0) and the wave height.

The raised water surface level of the standing wave (h_0) is calculated using the following equation:

$$h_0 = \frac{\pi H^2}{L} cotanh\left(\frac{2\pi d}{L}\right)$$

where:

L = deep water wave length (feet)

d = depth from Stillwater level (feet)

H = height of free wave (feet)

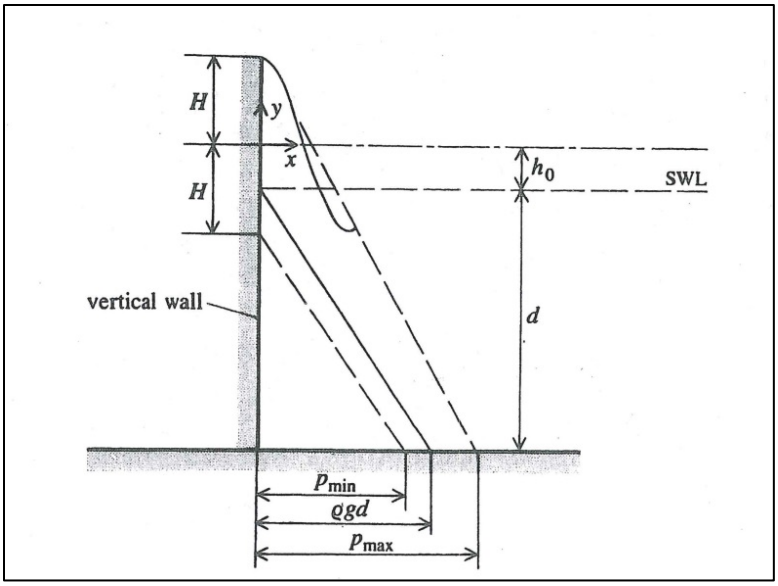

Figure 10.11-4. Effect of a Clapotis Adjacent to a Vertical Face (Novak)

The wave run-up and set-up values have been estimated using both methodologies for the return period wind speeds as determined by the Pearson and Gumbel methods. The results are presented in Table 10.11-3 and Figure 10.11-5.

Table 10.11-3. Wave Run-up and Set-up Values

Return Period	Wind Speed (miles per hour)		Wave run-up + set-up (feet)			
			SPM		Standing Wave	
	Pearson	Gumbel	Pearson	Gumbel	Pearson	Gumbel
1	19	16	1.24	1.00	1.28	1.03
2	25	26	1.73	1.82	1.83	1.92
5	31	27	2.26	1.90	2.41	2.02
10	35	32	2.62	2.35	2.82	2.51
20	39	35	2.99	2.62	3.25	2.82
50	45	39	3.57	2.99	3.91	3.25
100	50	44	4.07	3.47	4.49	3.80
200	55	47	4.57	3.77	5.08	4.14
500	62	51	5.30	4.17	5.94	4.60
1000	68	56	5.94	4.67	6.71	5.20
10000	89	59	8.27	4.98	9.56	5.57
100000	109	71	10.62	6.26	12.51	7.10
1000000	129	82	13.07	7.48	15.65	8.58

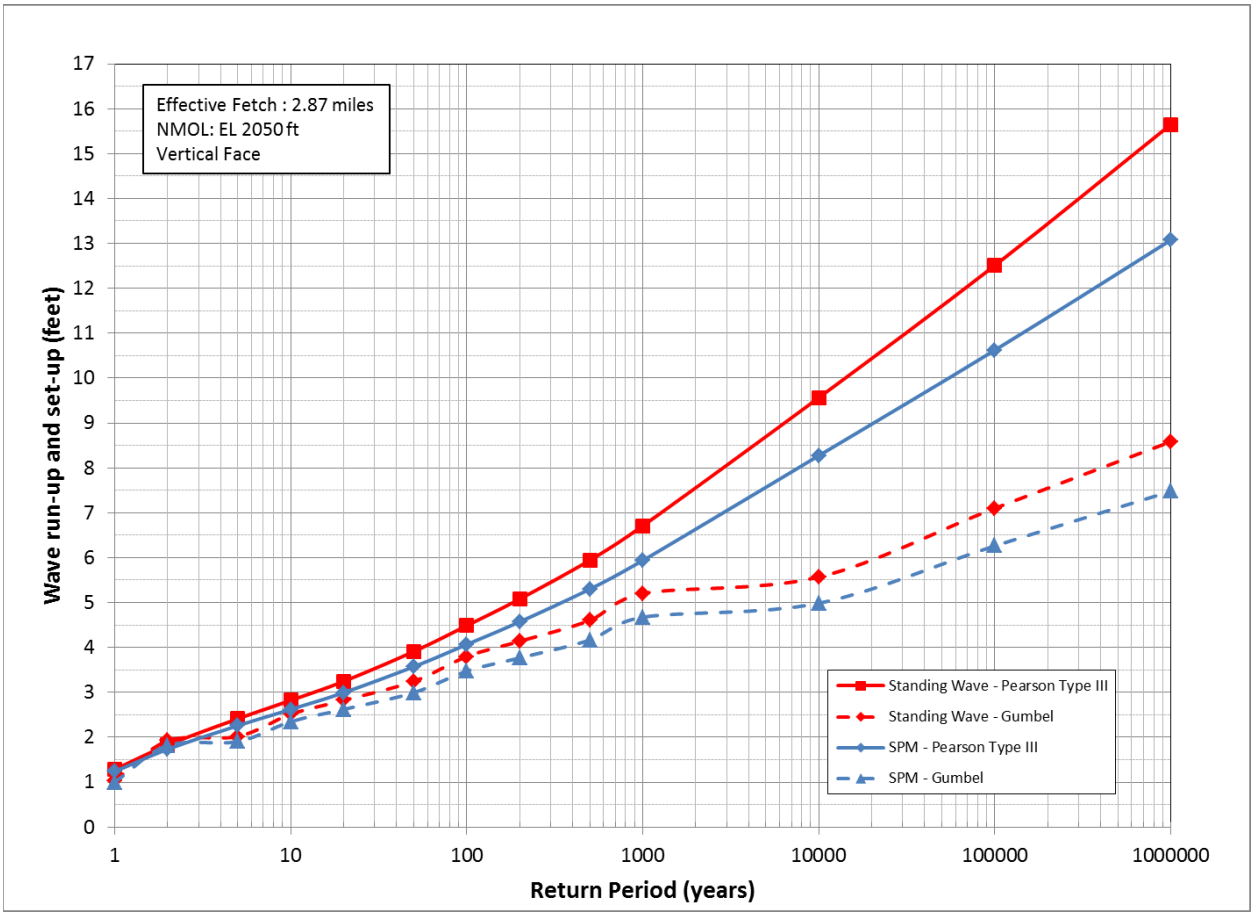

Figure 10.11-5. Wave Run-up and Set-up and Wind Speed Frequency

10.11.3.4. Freeboard Assessment

ACER TM No. 2 recommends that the adequacy of the proposed freeboard is assessed using a design wind speed of *100 miles per hour* with the reservoir at the NMOL. This wind speed equates to a return period of approximately 33,000 years based on the Pearson Type III analysis; the Gumbel method equates to a return period wind in excess of 1,000,000 years.

A second check is recommended in the *USBR Design of Small Dams* where the freeboard is assessed using a *50 miles per hour* wind with the reservoir at the NMOL. The Pearson type III method estimates that this wind speed would be a 1 in 100 year event while the Gumbel analysis estimates the wind speed would equate to a 1 in 400 years return period event.

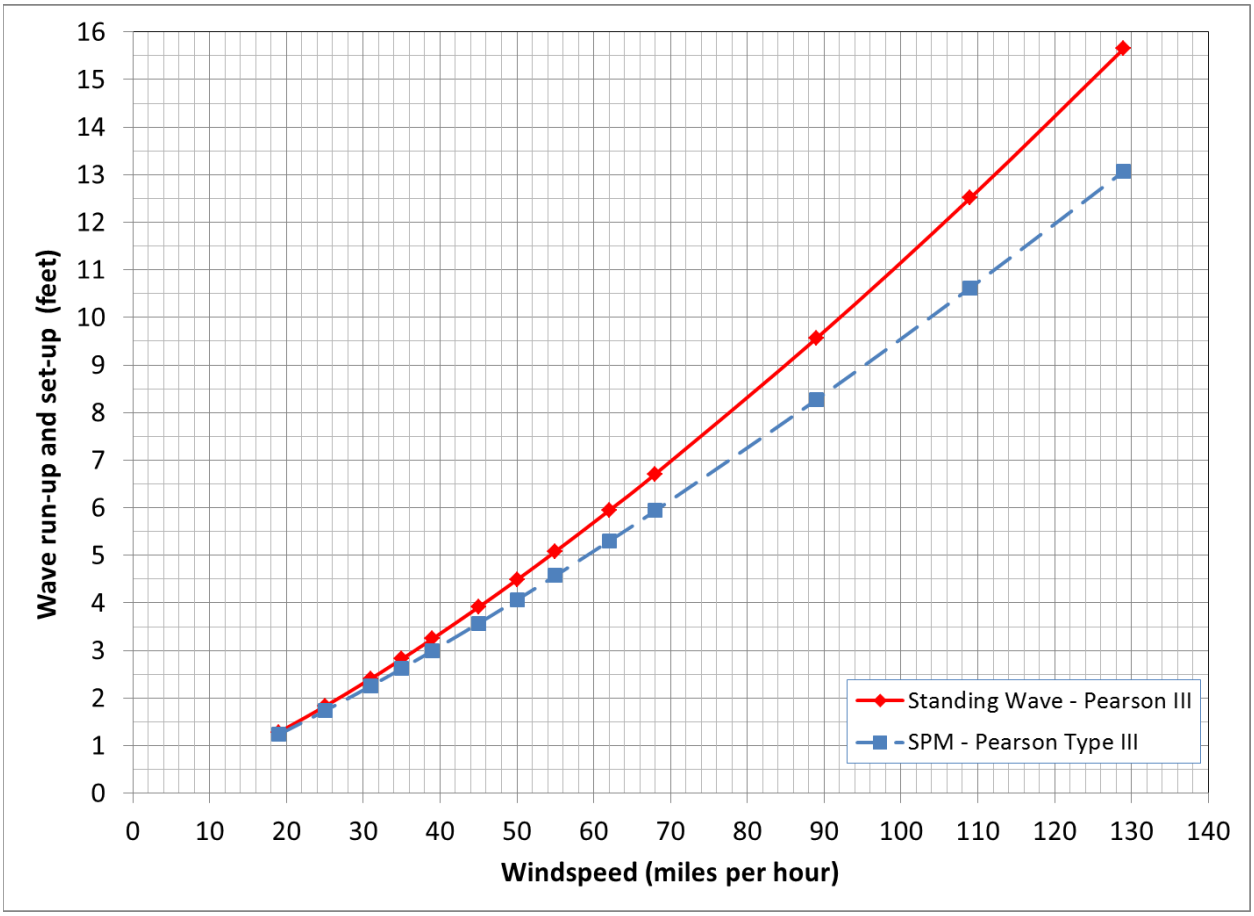

Figure 10.11-6. Wave Run-up and Set-up and Wind Speed Relationship

The relationship between wind speed and wave run-up and set-up is shown in Figure 10.11-6 based on the Pearson Type III analysis. Inspection of the curves shows that the wind setup and wave run up for the two design wind speeds are as follows in Table 10.11-4:

Table 10.11-4. Adopted Wind Set up and Wave Run-up Values

Design Wind Speed (mph)	SPM	Standing Wave
50	4.07	4.49
100	9.55	11.16

Thus using the most conservative value the required freeboard for the NMOL is 11.16 ft., which requires a dam crest of El. 2061.16 ft. However the necessary crest elevation for the PMF is El. 2065 ft. which satisfies the freeboard criteria.

10.12. Spillway

At the commencement of this feasibility study, for the purposes of examining the various dam types and selection of the preferred configuration, the spillway configuration derived in the 1980s was used – which comprised an ogee weir with three radial gates, and a spillway approximately 164 ft. wide. However, while the comparison of layouts was in progress, during 2012 (and encouraged by FERC), a site specific PMP study was initiated, which has led to a revised calculation of the PMF inflow and routed outflow, and thus a reanalysis of an optimized spillway configuration and crest elevation of the dam. The final derived PMF – as documented in Section 9 together with the PMP study – is close to that originally conceived for the 1980s studies, although there is a slight reduction.

To provide flushing flows, the Project will include the capacity to discharge a substantial release from low level outlets, without opening the spillway gates. Initially, the design called for six valves, but during design development, as noted above, this was increased to eight.

The design criteria adopted was for the discharge of the 50-year-flood without opening of the gates, and it was discovered, by examining and estimating the cost of different configurations, that this could be achieved, reasonably, by including an ability to surcharge the reservoir by 7.5 ft. (to El. 2057.5 ft.).

The initial feasibility study spillway configuration (similar to the 1980s studies) included three spillway bays, and gates of a height of 64 ft. Radial gates of this height have been used relatively often around the world, but the Board of Consultants suggested that a reduction in pier height would be beneficial as a response to cross valley seismic waves. When the various flood routings were performed for the PMF – based on the first part of the flood being passed by the low level outlet without gate opening – one of the options checked was a spillway with four gates, and lower piers. Of the options examined, such an arrangement, incorporating four gates, was found attractive, and a final configuration was chosen including an ogee weir crest level of El. 2010 ft., with gates suitable to hold the surcharge at El. 2057.5 ft. as discussed above.

The chosen arrangement allows for the routed passage of the PMF with a top water level of El. 2064.5 ft., and four gates 42 ft. wide and 50.5 ft. high. A further check was performed, and the 10,000-year-flood can be routed through the project – without overtopping the dam – with one gate inoperative. Divided by a center wall, each spillway chute is 82 ft. wide. Optimization is possible and depending upon bedrock level the chute floors can be at different elevations.

The chute spillway is located on the right abutment and founded on bedrock and on the RCC of the dam. During detailed design, the joint between the convention concrete of the spillway and

the RCC of the dam will be carefully considered and the stability of the spillway chute on the right abutment will be verified.

Overtopping of an embankment dam due to wave run up can be a serious matter of dam safety, but criteria adopted by various authorities around the world (including USBR) allow for zero freeboard for concrete dams during the PMF event. Therefore, as described elsewhere, the crest elevation of the Watana Dam has been selected as El. 2065 ft. A solid concrete parapet wall will be constructed, however, on the upstream side of the crest with a top level of El. 2068 ft., which will provide for some protection against oversplash. On the downstream side of the crest there will be guard rails and/or an "open" barrier so that water can drain downstream, and snow can be blown or plowed off the crest.

As the number of gates has been increased to an even number (four) the opportunity was taken to include a concrete wall between the two identical halves of the spillway. This arrangement will allow the spillway to be used under low flood conditions, even if there are repairs being carried out on one side of the chute. For the purposes of feasibility design, it has been assumed that a flow of 60,000 cfs must be passed while repairs are carried out on one half of the spillway, and therefore under such flow conditions water must not spill over the center wall.

CFD modeling has been performed for the various spillway configurations investigated – both three gates with an ogee crest level of El. 2000 ft., and four gates with an ogee crest elevation of El. 2010 ft. – allowing spillway parameters to be confirmed. Typical output from the CFD modeling is shown in Figure 10.12-1 through Figure 10.12-4 for the critical spillway discharges, and has been used to derive the proposed location of aeration, to verify the general spillway configuration, verify the wall heights of the side walls and center wall and to verify the flip angle and impact for plunge pool stability.

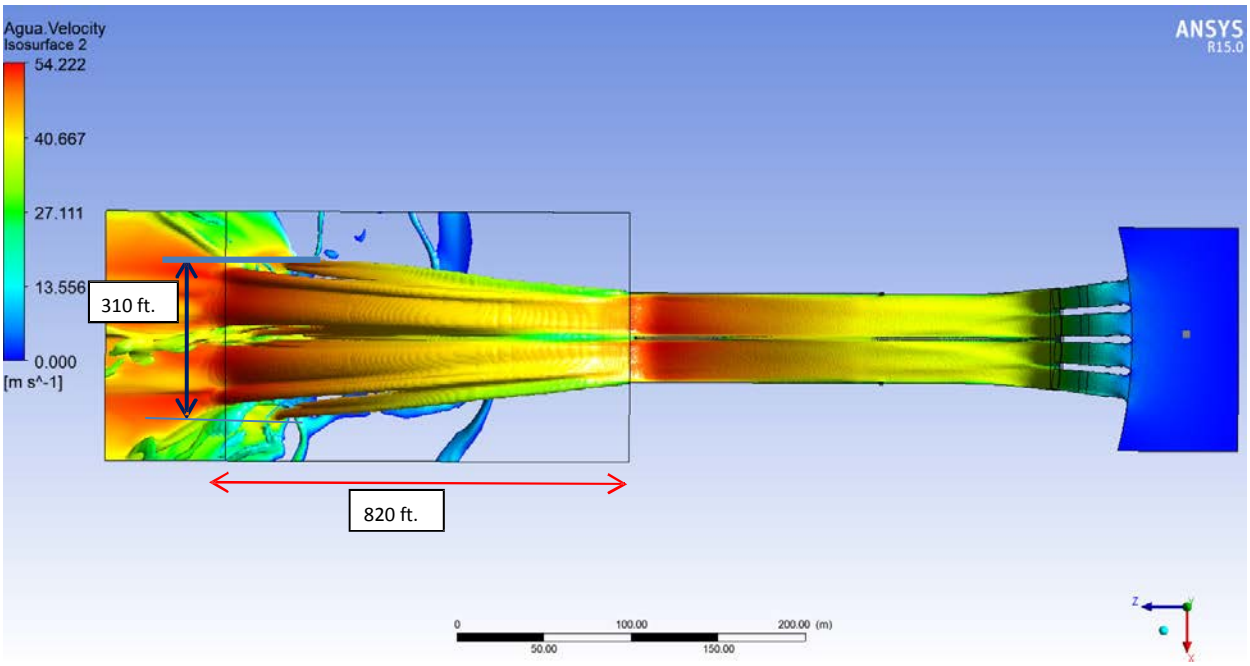

Figure 10.12-1. Routed PMF Flow through Four Fully Open Gates – Plunge Pool Location 1

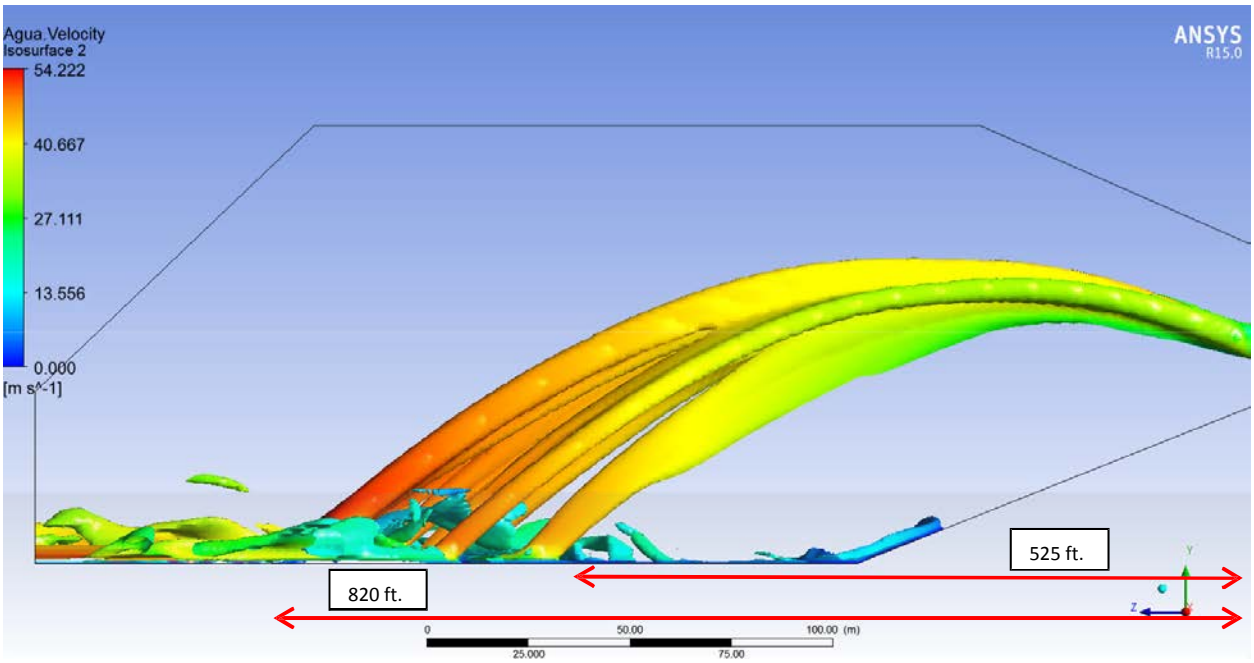

Figure 10.12-2. Routed PMF Flow through Four Fully Open Gates – Plunge Pool Location 2

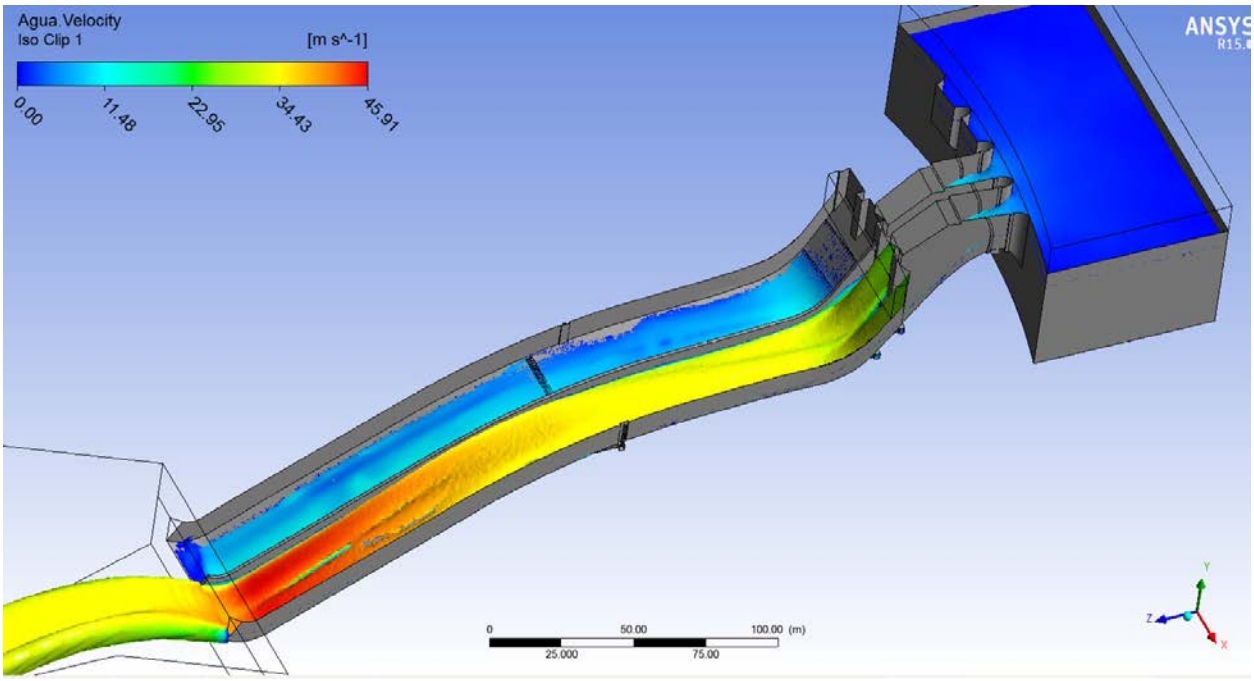

Figure 10.12-3. Two Gates Open – Discharging 60,000 cfs – Center Wall Height Determination

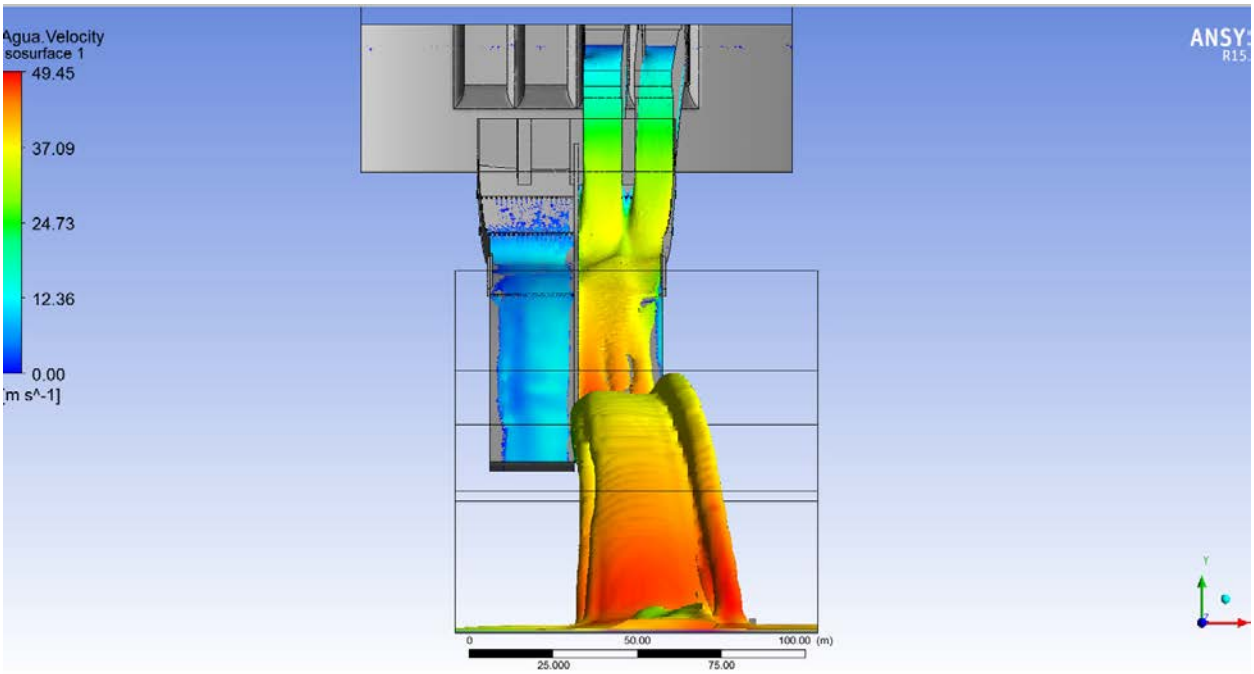

Figure 10.12-4. Two Gates Open – Discharging 60,000 cfs – Unbalanced Flow

The spillway shown in the drawings will perform satisfactorily, but the CFD results show that it will need slight optimization during detailed design to address the upper shape of the chute walls, which lead to the slight unbalanced flow shown in Figure 10.12-4.

CFD modelling indicated the locations at which air should be introduced into the spillway flow. Aeration slots have been indicated at three locations and consist of a gallery through the base of the spillway and three air entry towers through the spillway walls. The design of the top of the towers will stop snow being introduced into the system.

The soffit of the spillway bridge beams will be set to El. 2062.3 ft. to allow the passage of floating debris under the bridge without damage during a PMF event. This will require that the spillway bridge deck and pier top surface level be above crest level requiring a ramp from the general crest level of El. 2065 ft.

During detailed design, consideration could usefully be given to an alternative form of spillway used on the 360 ft. high Theodore Roosevelt Dam in Arizona, amongst others. At Roosevelt Dam, two rectangular submerged orifice spillways were used – controlled by top sealing radial gates – sufficient to pass a flow of 150,000 cfs. Depending on the final orientation of the Watana Dam – chosen after the full site investigations are complete – an arrangement similar to the Roosevelt Dam might offer the following advantages:

- Smaller, and less expensive spillway chute; and,
- Better accommodation of horizontal stresses in the dam.

However, the passage of any debris such as logs is more complicated in such an arrangement (possibly leading to a requirement to clear the whole reservoir), and the stoplogs necessary to be able to service and maintain the radial gates are more complex and bigger than required for a normal chute spillway.

10.12.1. Radial Gates and Operators

Four radial type spillway gates will be provided to control the water flow through the spillway structure. Radial gates will also retain the reservoir between the spillway crest at El. 2010 ft. and the top of the gates El. 2058.5 ft. The gate system will include an independently operated, hydraulically operated, 42 ft. wide by 50.5 ft. high radial gates, located at each of the spillway bays. In general, design of the radial gates and operators will be identical for all four spillway bays except that at least two radial gates will include a flap gate for ice and debris removal (passage).

The structural arrangement of each gate will include a skin plate supported by a system of vertical curved ribs carried on horizontal beams. The horizontal beams will be supported by vertical girders framed on to two sloped radial arms joining at the trunnion. Each trunnion assembly will consist of a hub which will connect to the radial arms and rotate approximately 43 degrees on a trunnion pin. Each side of the gate will be equipped with four guide rollers that will be mounted on the gate horizontal girders for convenient lifting and lowering of the gate in spillway bay. In addition, rubber seals will be provided on sides and bottom of the gate and will seal against the embedded stainless steel sealing surfaces, of which the side plates will be heated.

Each gate will be operated by two hydraulic hoists, mounted on the sides of the piers downstream of the gate skins. Each cylinder operator will be of approximately 125 tons rated capacity and maximum of 42 ft. stroke length. The location of the mounting of the hydraulic cylinders on the spillway piers will need to be optimized during detailed design to minimize the stroke length of the cylinders, and the response of the cylinders to seismic loads. Excessive stroke is detrimental to the life of the cylinder rod end seal and bearings because of the side load caused by bending of the rod when it is inclined to the vertical. Each gate will be provided with an individual hydraulic power unit located on the spillway pier. The gates will be capable of being operated automatically and from a pushbutton control station located in the remote control room or from a control station located on the spillway pier.

A diesel-powered standby generator will be located in an alcove in the powerhouse access tunnel, close to the spillway for operation of the gates during complete power failure. The power and control cables will be routed to minimize the potential for damage, through a vertical shaft drilled from the spillway structure down to the powerhouse access tunnel, and within the spillway concrete and in the shaft without any exposure to the elements.

10.12.2. Spillway Bulkheads

One set of bulkheads will be provided to permit maintenance of the spillway radial gates. Bulkhead guides will be installed upstream of the each of the spillway gates. The bulkheads will be designed to withstand the full differential head.

The spillway bulkhead will be deep enough to extend from the seal plate at the ogee crest up to El. 2060 ft. The bulkhead will be sectionalized into sections for the ease of transportation to the site. Each section will be the full width of the spillway bay. The sections will seal on the downstream side and the transfer of the hydrostatic load from the two end posts of the leaf to the supporting structure will be through bearing pads mounted on the end posts. Bulkhead sections will be installed and removed with a semi-automatic lifting beam connected to a spillway gantry crane. They will be installed and removed under balanced head and a manual fill valve will be provided in the lowest bulkhead section to fill the space between the bulkhead and radial gate.

There will be convenient storage within the coverage area of the spillway gantry crane.

10.12.3. Spillway Gantry Crane

A 75-ton capacity electrical travelling gantry crane will be provided at El. 2065 ft. to facilitate handling and maintenance of the bulkhead and gate equipment for both the spillway gates and the low level outlet facilities. The gantry crane will have sufficient travel, and extra outrigger booms (if necessary) to facilitate maintenance and handling of both water passage equipment.

10.13. Emergency Release Facilities

The diversion tunnel will be converted to a permanent emergency release facility upon completion of dam construction. These facilities will be used initially to pass the required minimum discharge during the reservoir filling period (until the reservoir level reaches El. 1850 ft.) and will also be used to assist in draining the reservoir in an emergency. The discharge criteria (based on the 1980s planning criteria) selected is the discharge of 30,000 cfs at a pool elevation of El. 1850 ft. – which assumes that the reservoir can be drawn down from the operating level to the minimum operating level using the powerhouse flow in conjunction with the spillway, and then the low level outlet.

The facilities first analyzed during this study were those presented at the end of the 1980s study, and included in the PAD, which it is understood were based on a physical model of the facilities proposed at that time for Mica Dam in BC. The facilities included the enlargement of the diversion tunnel to a 45-ft. diameter concrete lined tunnel for a length of about 820 ft. Two concrete plugs would have been installed, one near the upstream end of the enlarged tunnel and the second 340 ft. downstream of the first plug. Each plug was to contain three steel lined water passages controlled by bonneted high pressure slide gates.

From published papers at the time (1980s) it was evidently intended that during operation, energy would be partially dissipated within the energy dissipating expansion chamber. Computational Fluid Dynamics (CFD) modeling was performed for this proposed arrangement, and stable flow was not able to be achieved without pressurization of the chamber between the two plugs, and without highly unstable pulse flows throughout the system. The PAD design was therefore abandoned. It was also discovered that the Mica project abandoned the original design before construction.

A revised arrangement was investigated using CFD numerical modeling software. Nine iterations were performed to achieve a stable emergency discharge of 30,000 cfs at minimum operating level.

Stable discharge can be achieved by constructing a stilling chamber downstream of the plug, so that all energy can be dissipated and the flow in the rest of the diversion tunnel can be sub critical.

Enlargement of a tunnel by excavation of the floor is the safest and easiest way of enlarging the cross section, so after the plug is installed in the diversion tunnel, a stilling basin will be excavated in the floor of the tunnel some 46 ft. deep and 520 ft. long.

Within the plug will be two steel lined conduits, with flow controlled by bonneted gates, approximately 16 ft. high by 7 ft. wide. The gates will be protected by isolation valves allowing the main gates to be maintained. An air vent will be installed at the downstream side of the gates.

The tunnel downstream of the stilling basin will be sized so that there is open channel flow with sufficient space above so that there will always be air above the flow.

Figure 10.13-1 shows a section of the stilling basin and the result of the CFD analysis for the maximum flow that will pass through the system. The feasibility level analysis shows that the design should be able to be developed into a safe arrangement.

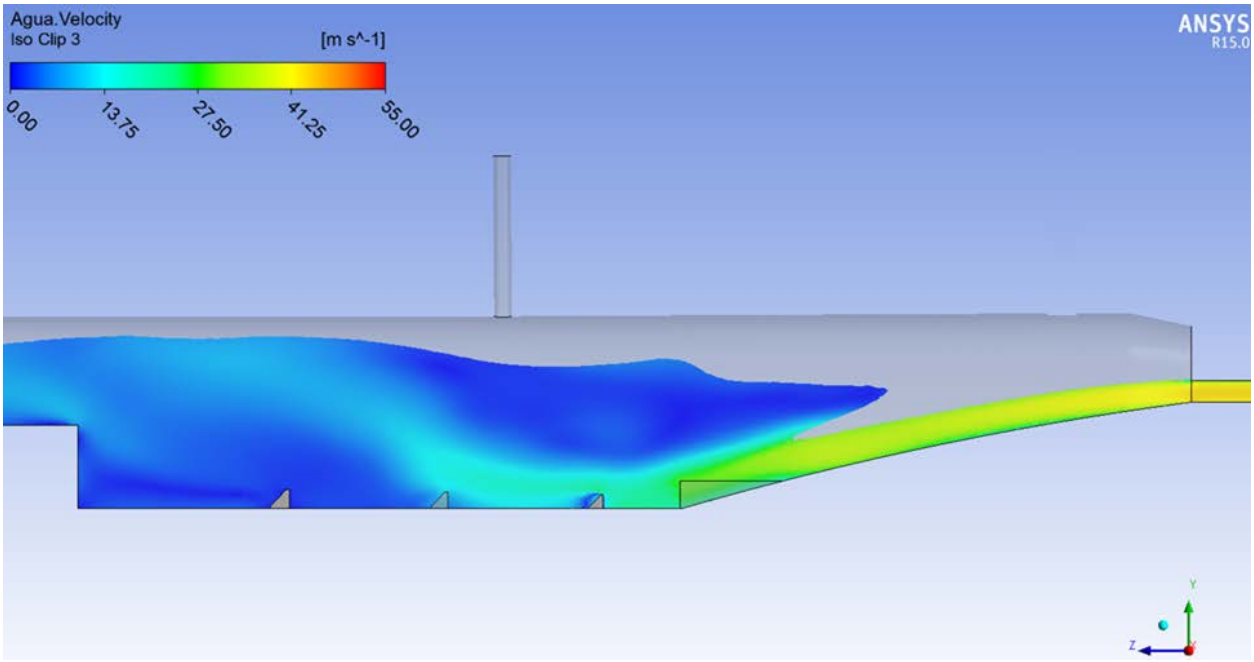

Figure 10.13-1. CFD Model of 30,000 cfs Flow in Emergency Outlet

Further analysis will need to be performed during detailed design, to confirm that the flow is stable and there is no contact on the tunnel crown by flow. This can be achieved by the refinement of the locations and sizes of energy dissipation blocks in the floor and wall, and by shaping of the steel conduits downstream of the gates before the jet enters the basin. The emergency outlet works is shown in Drawing 04-05G002.

10.14. Outlet Facilities

During the 1980s studies the primary function of the outlet facilities was deemed to be to discharge floods with recurrence frequencies of up to once in 50 years after they have been routed through the Watana reservoir. Those outlet facilities have been included in the present design. At an early stage in the derivation of the configuration, it was decided that the discharge valves could economically be served by two steel pipes embedded in the foundation of the chute spillway, and depending on the iteration of the layout, they have been variously located in the left or right abutment.

The final recommended location is on the north (right) side of the dam as shown on Drawings 04-01C002 and 04-03S001 and will consist of a gated intake structure, steel pipes, and an energy dissipation and control structure located beneath the spillway flip bucket. This structure will accommodate up to eight fixed-cone valves which will discharge into the river below, although after discussions with stakeholders the capacity may be reduced. The use of fixed-cone discharge valves will minimize downstream erosion and lower the dissolved nitrogen content in the discharges so as to avoid harmful effects on the downstream fish population. The facilities will also be used to provide additional outflow during any required reservoir evacuation down to El. 1850 ft.

10.14.1. Intake

The twin intake will have an invert elevation of El. 1800 ft., allowing operation down to normal minimum operating level. Each intake will contain three columns of steel trashracks on the face of the structure separated by concrete piers and spanning the openings to the water passage. The trashracks will be split into panels mounted one above the other in vertical steel guides installed at the upstream face. The trashrack panels can be raised and lowered for cleaning and maintenance by a mobile gantry crane located at deck level.

Two fixed-wheel gates will be located downstream of the trashracks between the pier and each of the sidewalls. These gates will be operated by hydraulic hoists mounted in the gate shaft. The fixed-wheel gates will not be used for flow control but will function as closure gates to isolate the downstream steel pipe and allow dewatering for maintenance of the pipe or ring gates located in the discharge structure.

Bulkhead guides will be provided upstream from the two fixed-wheel gates to permit dewatering of the structure and access to the gate guides for maintenance.

10.14.2. Intake Gate

The intake gate system for each intake tunnel will include an independently operated, hydraulically operated vertical wheel gate located downstream of the trashracks between pier and each of the sidewalls. The intake gates and hydraulic hoists will be identical for both intakes.

Each gate will be a fix-wheeled type vertical lift gate, approximately 23 ft. wide by 23 ft. high. Each gate will be spliced into two sections for the ease of transportation of gate sections to the site. The connection of the two sections will be sealed by bolting together two machined steel surfaces. Rubber seals will be provided on all four sides of gates and will seal against embedded stainless steel sealing surfaces around the perimeter of the gate opening.

Each gate will be provided with guide shoes which will engage side guide rails over the entire height of the intake for convenient lowering of the gate into the slot. A wheel track of uniform strength and construction will extend two gate heights above the sill elevation such that the gate wheels will always be engaged on the tracks over the entire opening range of the gate.

Each intake gate will be operated with hydraulic hoist mounted in the gate shaft. The gates will be capable of being lowered either from a pushbutton control station located in the remote control room or from a control station near the intake area. Raising will only be allowed from the stations located near the intake area. Both gates will be operated from a common hydraulic power unit. A backup HPU will also be provided.

10.14.3. Intake Bulkheads

Two sets of intake bulkheads will be provided for closing the two intakes upstream of the intake gates. The intake bulkheads will be used to permit inspection and maintenance of the intake gates and intake gate guides. The intake bulkheads will be designed to withstand the full differential head.

Each intake bulkhead will be approximately 23 ft. wide by 23 ft. high. Each bulkhead will be spliced into two sections for the ease of transportation of bulkhead sections to the site. Rubber seals will be provided on all four sides of the bulkhead on upstream side of the bulkhead. Bulkheads will be installed and removed under near balanced head conditions. Fill valves, operated by the lifting beam, will be provided in the bulkheads to fill the void space in the downstream tunnel.

10.14.4. Intake Trashracks

Three sets of steel trashracks will be provided at the entrance of each intake to prevent debris from being drawn into the discharge valves. Each of the three trashrack sets will include the following general design features.

Each trashrack set will be provided in four panels. All four panels will be stacked on top of each other and supported by each other. The trashrack frame load/support bars will be designed to span horizontally. The rack bar sub-panels will consist of vertical and horizontal bars forming a grill having clear opening of 6 inches by 6 inches. The rack bars will be designed to span vertically between the frame horizontal support plates. Trashrack structure will be designed for a maximum differential head of 40 ft. which corresponds to a fully clogged trashracks. For high-pressure, high-velocity intakes, the industry practice has been to design the trashrack structure to withstand a load equivalent to one-half the head on the racks, with a maximum of 40 ft. Trashrack structural components will be designed to prevent resonant vibration induced by the flow through the trashracks. The maximum net velocity through the racks will be approximately 5.0 ft. per second. Provisions will be made for monitoring the head loss across the trashracks.

10.14.5. Gantry Crane

The 75 ton gantry crane for the spillway facility will also be used for the low level outlet facility. As a result, a separate gantry crane for the low level outlet facility will not be required.

10.14.6. Pipes and Manifold

Discharges from each intake will be conveyed from the upstream gate structures by 23-ft. diameter steel pipes that will be embedded within the dam, near its downstream face. Each pipe will continue beneath the spillway chute before dividing into four pipes which will pass through the main spillway flip bucket structure to the fixed-cone valves mounted in line with the downstream face.

10.14.7. Discharge Structure

The concrete discharge structure will form a part of the flip bucket for the main spillway and will house the fixed-cone valves and individual upstream ring follower gates. Four valves will be set with a centerline elevation of El. 1569 ft. and four will be set at El. 1549 ft. and will discharge into the river below. Openings for the valves will be formed in the concrete and the valves will be recessed within these openings sufficiently to allow enclosure for ease of maintenance and heating of the movable valve sleeves. An access gallery upstream from the valves will run the length of the discharge structure, and will terminate in the access tunnel on the north side of the

structure. A vertical shaft to the powerhouse access tunnel will allow for installation and removal of the valves when required.

Housing for the butterfly valves will be located upstream from the fixed-cone valve chambers. The butterfly valves will serve to isolate the discharge valves. Provision will be made for relatively easy equipment maintenance and removal by means of a 25-ton service crane and a 25-ton monorail hoist.

10.14.8. Fixed-Cone Discharge Valves

Eight 79-inch diameter fixed-cone valves will be installed at the downstream end of the outlet manifold to control the discharge through the low-level outlet facility. The valves will be operated by hydraulic cylinder operators either from locally or remotely from control room.

The valve body will consist of a cylinder with a conical deflector head on the downstream end, internal radial ribs and an upstream mounting flange for attachment to the conduit liner. The valve gate will consist of a cylinder designed to slide over the valve body. The gate will slide upstream to open and downstream to close off the valve ports. Each valve will be operated with the two hydraulic cylinders, mounted diametrically opposite. Additionally, an embedded steel hood will be provided for each valve to reduce the spray and to reduce the risk of erosion from the water jet against the immediate environment. Each valve will be designed to withstand a total static head of approximately 530 ft.

The current valve design shows the piping and valves discharging straight out in the horizontal plane. This provides symmetric flow to the discharge valve. Depending on the constraints of a project, discharge valves can be angled above the horizontal plane to further “arc” the discharge path to either provide more energy dissipation in the air or change the “throw” distance out from the valve. So far there have not been any constraints to the discharge location identified that would require reconfiguring the outlet valves in such a way. Angling of the valves right at the end of the pipeline introduces issues such as asymmetric flow distribution though the valve, and off-axis loading on the valve and pipeline structures and their anchorages. There is no benefit to configuring the outlet with angled valves absent significant downstream constraints that would require such a design.

Plunger valves could also be used for controlling the discharge through the low-level outlet. The plunger valve is similar to needle, tube, or ring jet valves in that water flows around a central bulb within the valve body creating an annular flow path. The plunger valve has an axial cylinder that seals against the downstream edge of the flow path and retracts into the central bulb to increase the annular discharge area. This type of arrangement offers a much simpler design than the fixed cone valve. For the same size, the plunger valve is less expensive, but also has

smaller discharge capacity. In this case, a larger plunger to meet the same capacity would likely be comparable in cost to the fixed cone valves. The plunger valve would be relatively smaller in actual physical size, would require less surrounding structural support, and would likely provide comparable energy dissipation. The cylinder is also customizable to provide additional energy dissipation options.

Further investigation of the design features and cost comparison between the two types of valves will be carried out in the design phase to make the final selection of the discharge valve type.

10.14.9. Butterfly Valves

Butterfly valves will be installed upstream of each of the fixed-cone valve to permit inspection and maintenance of the fixed-cone valves; to relieve hydrostatic pressure on the fixed-cone valve when they are in closed position; and to close against flowing water in case of malfunction or failure of valves or the upstream gate. Each butterfly valve will be operated by hydraulic cylinders either from locally or remotely from a control room.

Each valve will have a nominal diameter of 90 inches and will be designed to withstand a total static head of approximately 530 ft. Each valve will be located within a heated enclosure with suitable provision for servicing the equipment. The valve will primarily consist of a cylindrical body with two flanges, valve blade, bypass system, and a hydraulic operator. Valves will be designed to be closed under flowing water condition and opened under balanced head condition. Prior to opening of the valve, pressure will be balanced by means of a bypass pipe.

The current valve sizing of a 90 inch butterfly guard valve and 79 inch fixed cone valve can work, but the velocities through those valves to achieve the required 4000 cfs flow rate are also very high and might usefully be lowered depending on the expected use of the valves. High velocity can lead to cavitation and vibration at various points along the butterfly valve disc or at the outlet surfaces of the fixed cone valve, as well increased turbulence and thus increased losses that can reduce discharge capacity. Early feedback from two valve manufactures is that either additional design considerations would need to be made, particularly for the butterfly valve disc design to minimize cavitation and vibration, or the valve sizing should be increased to 102 inch and 90 inch respectively. Also an increase to these sizes would allow the maximum required flow rate to be achievable throughout the entire head range, not just at full reservoir.

Further review of the design goals of the project and a comparison of costs and benefits should be performed in further detail in the project's design phase to optimize the valve sizing.

10.14.10. Monorail Hoist

One 25-ton monorail hoist will be provided above the fixed-cone discharge valves for the maintenance and handling of the valves. Primary function of the monorail hoists will be to mobilize valves and equipment to and from the service room during the maintenance.

10.14.11. Bridge Crane

One 25-ton overhead type, top running bridge crane will be provided for the maintenance and installation of butterfly valves in the discharge structure. Primary function of the crane will be to handle and mobilize valves and equipment to the service room during the maintenance.

10.14.12. Discharge Area

Immediately downstream from the discharge structure, the rock will be excavated at a slope of 2H:3V to a lower elevation of El. 1510 ft. The excavated face will be reinforced by rock bolts and protected by a concrete slab anchored to the face. The lower section of the rock slope extending to the river will be unlined.

10.15. Fish Passage Considerations

No provision has been made in the feasibility design of the project for the passage of anadromous fish. AEA is conducting separate studies on the incidence of such fish at the dam site and on the viability and economy of transporting them past the proposed dam under Study Plan 9.11. Options being investigated under the study plan include:

- Trap and haul;
- Fish ladder;
- Fish lift;
- Use of Tsusena Creek together with enhancement of flow; and,
- Other options developed from workshop sessions.

10.16. Power Intake

Each penstock (including the spare) will have its own separate power intake. The power intakes will be conventional concrete structures extending upstream from the dam upstream face and will be supported, if necessary for construction sequencing, on concrete extending to the dam foundation. The intakes will be fully accessible from the dam crest.

Each intake will contain pairs of openings at six levels in the upstream concrete wall of the structure, to facilitate withdrawal of water from the reservoir at specific levels over an expected drawdown range of 200 ft. For each vertical series of intake openings, flow through each opening will be capable of being obstructed (but not completely sealed) by a series of six sliding steel shutters operated in two common guides. Upstream trashracks will protect all openings. To maintain an ice-free trashrack system, a heated boom will operate in guides upstream of the racks. Behind the intakes at the entry to the penstocks, a control gate will be provided with routine maintenance being possible by the installation of a bulkhead gate upstream of the control gate.

Each intake will be 65 ft. wide with the upper level of the concrete structure set at El. 2065 ft. The level of the lowest intake is governed by the vortex criterion for flow into the penstock from the minimum reservoir level elevation of El. 1850 ft. The arrangement of the power intakes is shown on Drawings 05-06S002 and 05-06S003.

10.16.1. Intake Gates and Operators

The intake gate system for the power intake facility will act as a dependable emergency closure device in the event of a penstock rupture or a turbine runaway condition at the plant. The intake gates will also allow complete dewatering of the penstock for inspection and maintenance.

There will be an independent intake gate system for each of the four power intakes. Each intake gate system will include an independently operated, hydraulically operated vertical fix-wheeled gate, downstream of the bulkhead slots. Each gate will be approximately 21 ft. wide by 20 ft. high, and could be upstream sealing or downstream sealing. The decision on which type of gate to use will be made during detailed design, but will probably be downstream sealing – although substantial air would be required for this type of arrangement.

Each intake gate will be a welded fabricated construction with rubber seals. Rubber seals will be provided on all four sides of gates and will seal against embedded stainless steel sealing surfaces around the perimeter of the gate opening. Each gate will be provided with guide shoes which will engage side guide rails over the entire height of the intake for convenient lowering of the gate into the slot. A wheel track of uniform strength and construction will extend two gate heights above the sill elevation such that the gate wheels will always be engaged on the tracks over the entire opening range of the gate.

Each intake gate will be operated with a hydraulic hoist. The gates will be capable of being lowered either from a pushbutton control station located in the remote control room or from a control station near the intake area. Each of the two intake gates for each intake unit will be

operated using a common hydraulic power unit assigned to each intake unit. Furthermore, a backup hydraulic power unit will also be provided for each of the three power intake units.

During detailed design, the bypass arrangements will be addressed so that the penstock can be refilled and the gate opened. Options include a valve in one of the gates, built in pipework in the concrete structure for filling, cracking of the gate, or pumping in water.

10.16.2. Intake Bulkheads

Within each power intake, arrangements will be included for placing two sets of intake bulkheads to close the intake ports upstream of the intake gates. The intake bulkheads will be used to permit inspection and maintenance of the intake gates and intake gate guides. The intake bulkheads will be designed to withstand the full differential head.

One set of intake bulkheads will be placed in the spare intake, and a second set will be stored for use in any of the operating power intakes. Each intake bulkhead will be approximately 21 ft. wide by 27 ft. high, probably spliced into two sections for the ease of transportation to the site. Each intake bulkhead section will be of downstream sealing type and the transfer of the hydrostatic load from the two end posts of the leaf to the supporting structure will be through bearing pads mounted on the end posts. Intake bulkheads will be installed and removed with a semi-automatic lifting beam connected to a gantry crane. Intake bulkheads will be installed and removed under near balanced head conditions. Fill valves, operated by the lifting beam, will be provided in the bulkheads to fill the void space in the downstream tunnel.

10.16.3. Intake Shutters

The operators will be able to select the intake openings to be used for draw off to the penstocks, but movement of the shutters will be accommodated by using the intake gantry crane so remote operation will not be possible. To draw from the reservoir surface over an expected drawdown range of 200 ft., two adjacent openings at each of five levels will be provided in the upstream concrete wall of the structure for each of the intakes. Openings will be able to be closed off by steel shutters operated in two common guides. The downstream guide will accommodate the upper three shutters, and the upstream guide will accommodate the lower two shutters. Two guides are included to facilitate the accommodation of all the (individual) lifting cables (two for each shutter) in the protected environment of the guides. As the reservoir level varies, the shutters will be relocated as necessary using the power intake gantry crane.

Each shutter panel will be approximately 24 ft. wide by 25.5 ft. high and will be spliced into two sections for the ease of transportation to the site. Each shutter will be welded steel plate with upstream skin plate and downstream framing. No seals are envisaged, as some leakage around

the shutters is acceptable. Under normal conditions, shutter panels will always be under balanced head, and will be operated under balanced head. However, the shutter structure will be designed to withstand 15 ft. of differential head in case of blockage of intake openings. Flap gates or blow out sections will be provided in each shutter panel to prevent failure of the shutters in the event that the differential head exceeds 15 ft. due to unforeseen circumstances.

When an intake opening is selected, the appropriate shutter will be moved up to be shielded by the concrete wall between openings, so that they will not be subject to the hydraulic instability associated with partial opening. Shutters will be installed and removed under balanced head condition, with a semi-automated lifting beam connected to the power intake gantry crane.

10.16.4. Intake Trashracks

Each power intake will have a set of trashracks at the entrance to prevent debris from entering the penstocks. Each trashrack set will be provided in six panels. Each panel will be approximately 24 ft. wide by 29.5 ft. high, and delivered in two sections for the ease of transportation and handling.

The trashracks will be removable, and guide tracks will be provided for installation and removal of panels. The trashrack frame load/support bars will be designed to span horizontally. The rack bar sub-panels will consist of vertical and horizontal bars forming clear openings of six inches by six inches. The rack bars will be designed to span vertically between the frame horizontal support plates.

The trashrack structure will be designed for a maximum differential head of 40 ft. corresponding to a fully clogged condition, based on industry practice which has been (for high-pressure, high-velocity intakes) to design the trashrack structure to withstand a load equivalent to one-half the head on the racks, with a maximum of 40 ft. Structural components will be designed to mitigate resonant vibration induced by the flow through the trashracks. The maximum net velocity through the racks will be approximately five feet per second, and provisions will be made for monitoring the head loss across the trashracks. Trashracks will be installed and removed using a semi-automatic lifting beam connected to the power intake gantry crane.

Trash rakes have not been included, but accommodation can be made during final detailed design. The decision to include them in the project will depend on the reservoir clearing policy chosen.

10.16.5. Intake Gantry Crane

A 75 ton capacity electrical traveling gantry crane will be provided on power intake deck at El. 2065 ft. for handling and servicing the intake gates.

10.17. Penstocks

To convey water from each power intake to the powerhouse, one steel penstock will be provided for each generating unit. The penstock geometry encompasses a short horizontal reach through the dam structure, a 63° bend, a penstock down the (vertically curved) face of the dam, another 63° bend and a horizontal reach connecting to the spiral case. Drawing 05-06S001 shows the penstock alignment. The penstock will be supported by steel mountings in a "trench" in the downstream face of the RCC, and will be encased in conventional concrete.

The penstock diameter of 19 ft. was selected after applying velocity criteria for turbine flow of 6000 cfs at NMOL of El. 2050 ft. and industry recognized formulas to estimate economic diameters. Diameters estimated by four different methods are summarized in Table 10.17-1.

Table 10.17-1. Economic Penstock Diameter

Method	Diameter (ft.)
Sakaria (1979)	17.2
Warnick (1984)	19.6
Fahlbusch (1989)	19.9
Gulliver (1991)	18.0

The design static head on each penstock is 625 ft., at turbine centerline distributor El. 1425.5 ft. An allowance of up to 20 percent has been made for pressure rise in the penstock caused by hydraulic transients.

Further analysis will be performed during detailed design to verify the economic diameter of the penstocks.

The powerhouse design allows for the potential future addition of a fourth turbine-generating unit. The work would require converting the outlet bay of the sluice into the fourth turbine-generator bay. To enable future construction of the additional turbine bay while maintaining the normal operating level within the reservoir, the fourth power intake (including gates, bulkheads, and trashrack guides) for the future turbine and the penstock section through the dam will be constructed as part of this work, and the exposed downstream end of the penstock will be capped.

10.18. Powerhouse

10.18.1. General Arrangement

The powerhouse has been arranged based on similar surface powerhouse designs by MWH. It is of traditional design with standard bays and the following floors:

- Main floor and transformer deck at El. 1476 ft.
- Generator floor at El. 1457 ft.
- Turbine floor at El. 1439 ft.
- Scroll case floor at El. 1415 ft.
- Pump floor at El. 1382 ft.

The elevation selected for the main floor is based on the revised tailwater curve derived from cross sections of the river immediately below the site that were surveyed in 2014.

Access to the main floor will be via an access tunnel on the right bank sized for the generator step up (GSU) transformers, which are the largest single item to be delivered or removed from the powerhouse. From the access tunnel on the right abutment, entry to the powerhouse will be by a roller door in the north end of the powerhouse superstructure.

The main floor will be serviced by the main powerhouse crane which facilitates the installation and subsequent maintenance of all equipment, and the unloading of the GSU transformers onto the embedded rails for movement to the tailrace deck.

The substructure of the powerhouse below El. 1476 ft. will be conventional concrete. Above El. 1476 ft., the superstructure will be constructed using a steel frame, prefabricated cladding and roofing materials. The lower part of the downstream powerhouse wall, which will form the blast wall behind the transformers, will be of reinforced concrete. The steel superstructure has been chosen to allow the fastest possible construction of a weatherproof enclosure so that year-round work on the powerhouse can be initiated as soon as possible in the construction schedule. During detailed design, the extent to which the steel columns and crane rail supports can be founded and installed lower in the superstructure – together with precast concrete wall panels – will be investigated. As demonstrated in projects in northern Canada, by founding the crane and superstructure columns lower in the substructure, weatherproof cladding (even if temporary) can be installed earlier with the result that year-round powerhouse construction can begin earlier. This approach is illustrated in Figure 13.3-5.

The superstructure of the powerhouse will encompass three bays and an assembly area of approximately 1.5 bays, and the substructure will extend to the south to form the substructure for an extra bay – which will be available for future expansion if AEA needs warrant it. The design of the superstructure will be suitable for demolition of the south wall of the powerhouse and the extension of the superstructure over the fourth bay. During the construction of the project, the sluice through the dam will discharge through the spare bay, but will be finished to El. 1476 ft. between the spare bay and the dam so that emergency evacuation of the area is possible on the south side of the river on roads S4P and S6P.

Within the powerhouse, there will be two enclosed staircases through all floors at the northwest corner and at the southeast corner. In addition there will be a high capacity elevator at the northwest corner. A rotor pedestal will be built in on the main floor.

Equipment on the generator floor at El. 1457 ft. will include generator and excitation switchgear; station service transformer; motor control centers for the units; unit transformers and switchboard; neutral grounding cubicle; and station service switchgear.

The turbine floor at El. 1439 ft. will contain the governor control system; unit cooling water pumps, tanks and heat exchangers; air compression systems; and the station battery room.

The scroll case floor at El. 1415 ft. will house the inlet valve controls and the draft tube suppression system.

The pump floor at El. 1382 ft. will contain the main sump and dewatering pumps; drainage pumps; and the station oil-water separator.

The powerhouse will be constructed on the cleaned rock surface below the river, and rock excavation will be performed for the three unit bays and the spare bay. The final configuration of the powerhouse below the assembly bay will depend on the rock surface profile which will be derived during future site investigations. The powerhouse lower levels will be constructed to a configuration that minimizes the rock excavation.

The powerhouse will contain a control room, located either below the assembly bay or as a mezzanine room above the entrance door.

10.18.2. Turbine Inlet Valve

Each turbine inlet will have a butterfly shut-off valve, of about 14-ft. diameter (the diameter remains to be optimized) between the spiral case and penstock. The final diameter will be determined by the supplier of the turbine and in accordance with the final diameter of the spiral case inlet.

The valve will be capable of:

- Normal opening and closing times of less than 45 seconds.
- Isolating an individual turbine from the penstock so its spiral case can be emptied (in conjunction with closing the draft tube gate and dewatering the draft tube) for maintenance work without draining the penstock.
- Normal operational shut-off to eliminate leakage through the turbine wicket gates when the unit is shut down.
- Secondary independent means of emergency shut-off of flow in the event the turbine wicket gates are unable to close. If this function is adopted as a criterion, a metal-seated butterfly valve will be used.

The requirement for a shut-off valve will be reviewed during detailed design. A valve is considered good practice where the penstock or power tunnel is long or serves more than one turbine. In the case of the Susitna Watana Project, each penstock can be isolated at the power intake and each penstock is relatively short which will make emptying and refilling them a fairly straightforward operation. Many utilities elect to eliminate the valve as a matter of economy. The exclusion of the valve would reduce the overall width of the powerhouse, and that would have benefits in terms of reduced construction cost and construction duration.

10.19. Turbines

The powerhouse will contain three turbine-generating units, with provision for adding a fourth as noted above.

The rating of the units was determined in a two-step process. It is recognized that the units at Watana will be the largest capacity units on the Railbelt system and have the potential for transient disturbances to the entire Railbelt if a Watana unit trips while generating.

As discussed in Section 7 configurations with 6 x 100 MW, 4 x 150 MW and 3 x 200 MW units were considered and the capital costs estimated for comparison. From the perspective of machinery cost and construction cost, larger units were shown to be more economic.

During the analysis of the project energy, 200 MW units rated at minimum head were used to determine the initial annual output – leading to a rating at maximum head that would present a problem to system stability in the event of a unit trip. The maximum unit output under maximum head could be electrically limited to minimize that risk, but the units would then have a very narrow operating range at maximum head, reducing their operational flexibility.

However, the PROMOD studies described in other sections indicated that the optimum use of the project does not require maximum capacity at the minimum reservoir elevation.

As a result of the various modeling, the proposed turbine unit rating is 153 MW at a head of approximately 480 ft. (equivalent to an intermediate reservoir level of El. 1950 ft.). Turbine rated capacity at maximum normal operating level (equivalent to a head of 577 ft.) would be 206 MW, and at minimum operating level (equivalent to a head of 383 ft.) would be 106 MW. Note these values are different than those used in the system studies comparing the use of 200 MW and 150 MW units and recorded in Section 11.

The selected units will operate at a synchronous speed of 180 rpm, although this will be revisited during detailed design. Each turbine will be a vertical-shaft, single-runner, reaction type Francis turbine with movable wicket gates, fixed stay vanes, steel-plate spiral cases, and elbow type draft tubes.

The movable wicket gates are used to regulate flow through the turbines for regulation of power output and speed (system frequency), and for control of speed during starting, synchronizing, and shutting down the turbine. Preliminary turbine specifications are listed in Table 10.19-1.

Table 10.19-1. Preliminary Turbine Specifications

Item	Quantity
Rated output (each)	153 MW
Synchronous speed	180 rpm*
Runner throat diameter	13.3 ft.
Spiral case intake diameter	14.3 ft.
Total width of spiral case	47.9 ft.
Depth of draft tube (from spiral case center line to lowest point)	41.7 ft.

*A synchronous speed of 225 rpm is also feasible.

The dimensions given in the above table are estimated values based on parametric data obtained from other projects within MWH's experience. The final dimensions of the procured turbine will differ slightly from those provided above.

10.19.1. Turbine Components

The embedded turbine components consist of the draft tube liner, discharge ring, stay ring, spiral case and pit liner. These components are a structural part of the foundation for the turbine and generator. Access to the water passages will be provided by watertight doors in the spiral case and the draft tube liner.

Turbine rotating parts consist of the runner and the turbine shaft. The runner is bolted directly to the lower end of the flanged shaft. The turbine rotating parts, together with the generator rotating parts), are supported by the thrust bearing immediately below the generator. Radial movement loads on the turbine rotating parts are constrained by a turbine guide bearing mounted on and close to the turbine head cover. A turbine shaft seal is provided between the turbine guide bearing and the turbine head cover.

The distributor assembly includes the moveable wicket gates which are operated by levers and links attached to a wicket gate operating ring. The gate operating ring is moved by two or more servomotors, which are typically mounted on the pit liner wall, but may also be mounted on the turbine head cover. Also mounted on the head cover are the piping for the air, water, pressure equalizing, bearing oil and governor oil systems; and the pit maintenance platform and walkways. The turbine pit may also be provided with a monorail hoist to facilitate removal of the turbine wicket gates.

10.19.2. Governing System

Each turbine will be provided with an electro-hydraulic governing system, which will be of the solid-state, digital microprocessor type using proportional-integral-derivative speed control. The governing system will include speed and acceleration sensing, speed regulation, stabilizing, and diagnostic functions. The digital processor provides a control signal to an electro-hydraulic servo valve that controls positioning of oil-distributing valves directing pressure oil to the individual wicket gate servomotors, to move and position the wicket gates.

The governing system will have provisions for local and remote start/stop for automatic load control. Each governing system includes an electrical speed sensor, a digital microprocessor control, an actuator, restoring connection, an oil pump set, sump tank, pressure tank, oil piping to the wicket gate servomotors, and all controls, instruments and accessories necessary for a complete governing system. Additionally, the governor will have a digital interface to the overall unit and plant controls.

10.20. Generators

10.20.1. General

Various generator sizes were examined resulting in a generator rating of just over 200 MW at maximum normal operating level. Analysis of turbine performance resulted in a suggested rotational speed of 180 rpm. Therefore a generator rating of 225 MVA at 0.90 power factor and 180 rpm was chosen.

It is expected that under normal conditions, under-excited operation of the units will not be required; however, under abnormal system conditions, it may be necessary to energize part of the 230 kV system from the plant. Therefore, each generator will have a line charging capability of 140 MVA reactive which is adequate for energizing approximately 600 miles of 230 kV transmission line. This means that any one of the units will be capable of energizing the longest line connected (either present or planned) to the 230 kV switchyard.

10.20.2. Configuration and Ratings

The generators will be of the vertical-shaft, hydraulic-turbine driven synchronous type complete with bearings, fire protection system, and a closed system of ventilation with surface air-to-water coolers. Each generator will be of the semi-umbrella type construction with a lower thrust/guide bearing and upper guide bearing. The generator will be compatible with the turbine, particularly in terms of capacity, vibration, normal speeds and over speeds up to and including runaway speed, loadings, and stresses. All parts of the generator, including bearings, will be designed to withstand all electrical, mechanical and structural stresses resulting from operation under rated conditions, including stresses caused by temporary conditions of overspeed and short circuits.

The generator ratings will be as follows:

- Continuous rated capacity at rated voltage and power factor: 225 MVA
- Rated power factor: 0.90
- Rated frequency: 60 Hz
- Rated speed: 180 RPM
- Number of phases: 3
- Maximum stator winding temperature rise over 40°C ambient: 75°C

The generator system will be configured to operate in the condensing mode should transmission line voltage support be required. Each unit will have approximately 140 MVA reactive condensing capacity.

10.20.3. Generator Structure

10.20.3.1. Stator Frame

The stator frame will be supported on soleplates embedded in the concrete foundation. Bolts and dowels will be provided for fastening the stator frame to the soleplates and for preserving the alignment between the frame and the soleplates. An adequate number of dowels will be

provided to prevent any undue movement of the stator frame on the soleplates when the generator is subjected to stresses resulting from short circuit conditions.

The lower bracket supporting the thrust and guide bearing assemblies will support the weight of the entire rotating element of the generator together with the turbine runner and shaft and will have adequate rigidity and strength for safe operation under conditions of maximum unbalanced hydraulic thrust of the turbine runner or unbalanced conditions caused by short circuits, including short circuits of one-half of the field windings.

The generator brakes will be mounted on the lower bracket. The foundations for the brackets or supports will be designed so as not to reduce the clear opening for removal of turbine parts through the stator bore.

10.20.3.2. Bearings

The thrust bearing will have ample capacity to support the combined weight of the rotating parts of the generator and turbine, including the maximum unbalanced hydraulic thrust of the turbine. The thrust bearing will have a removable one-piece runner and be arranged to permit easy inspection, adjustment, dismantling and assembly of the thrust bearing shoes without disturbing the rotor, stator or bearing bracket other than jacking the rotor to remove the load from the bearing. The runner will be removable after lifting the rotor and the shaft from the pit.

The guide bearing will meet all normal and unbalanced operating requirements of the generator, including the unbalanced loads caused by a short circuit of one-half of the field windings. The guide bearing will be combined with the thrust bearing in the same enclosure. The guide bearing will be of the segmental, screw-adjustable, oil immersed, babbitted type. The bearing will be designed and constructed so that it can be easily dismantled, assembled and adjusted without disturbing the thrust bearing, the rotor or collector ring.

10.20.3.3. Lubrication

The generator will be provided with a complete, self-contained, lubricating system, which will include provisions to eliminate the throwing of oil and the escape of oil vapor from the bearings and lubricating system. Adequate provisions will be provided, if necessary, to prevent excessive churning or aeration of the oil.

10.20.3.4. Generator Housing

A generator stator housing will be provided to enclose the stator core, frame and cooling radiators. The enclosure will be sealed and provided with cooling air baffles and duct work to provide an enclosed cooling air circulation system for cooling the rotor, and stator components.

Access will be provided for maintenance and inspection of the generator winding and cooling components. The top of the enclosure will be provided with removable plates for purposes of rotor removal, access to the stator and field windings, and removal of the coolers. Lighting will be provided within the enclosure.

10.20.3.5. Stator Core

The stator core will be designed in such a way as to permit replacement of the core laminations without major disassembly of the stator frame. The stator design will permit partial or complete field replacement of the stator windings and/or core laminations without requiring major cutting, welding, heating or rework of the stator core, core retaining assembly or frame.

10.20.3.6. Stator Winding

The stator winding will be wye-connected, suitable for grounded operation. The winding will consist of Roebel bars with copper conductors completely (360°) transposed in the slot. The bars will be insulated for 20 kV with full Class F insulation.

Sufficient parallel circuits will be provided to keep the bar current less than 2,000 amps.

10.20.3.7. Circuit Rings

Circuit rings complete with all necessary connections, taps, adapters, braces, supports, and materials for making the necessary line and neutral connections between the windings and the terminals of the phase and neutral buses will be provided. The individual bars in each of the parallel paths which are connected to the circuit rings, will be connected in locations to minimize circulating currents between the parallel paths caused by misalignment of the rotor with respect to the stator.

10.20.3.8. Stator Air Coolers

The generators will be furnished with surface air coolers spaced symmetrically around the periphery of the stator frame for a closed, recirculating, cooling system. Water headers will be furnished with the coolers. The cooling system will be designed to fit within the generator housing while providing adequate space for inspection, maintenance, disassembly/reassembly, and air circulation.

The surface air coolers will have sufficient cooling capacity to maintain the temperature of the air leaving the coolers at 40°C, or less, with the generator delivering continuously rated output, and with 20°C cooling water temperature and 25 percent of the tubes blocked.

The circulation of air will be by means of the generator rotor fans. The air will circulate through the stator core, frame and coolers and back into the rotor.

10.20.3.9. Fire Protection

A high-pressure type water fire extinguishing system will be furnished for the generator and will conform to National Fire Protection Agency 851, *"Recommended Practice for Fire Protection for Hydroelectric Generating Plants"*. The system will consist of remote control stations, discharge nozzles, manual releases, automatic releases, thermostats, guards, and all appurtenances required for a complete operating system.

The system will be so designed that it can be discharged by action of the generator differential relays, by fixed temperature type and rate-of-rise-heat detectors and smoke detectors located inside the generator housing, by manual operation of remote emergency pushbuttons, or by direct manual operation of directional valves and cylinder releases.

10.20.3.10. Rotor

The rotor spider including a central hub will be a cast or weld fabricated steel structure, subdivided into a minimum number of sections to facilitate handling, transporting, and assembling. The spider will have adequate tangential and vertical rigidity to prevent undue deformation, center the rim and the poles, and to allow passage of the cooling air to the rim. The rotor rim will be shrunk fit and keyed to the rotor spider.

The pole pieces will be built up of high-grade, cold-finished, thin steel laminations fastened to the rotor rim secured in place by tapered keys. The poles will be replaceable without lifting the rotor.

10.20.3.11. Brakes

The generator will be provided with air-operated brakes of sufficient capacity to bring the rotating parts of the generator and turbine, under normal operating conditions, to a stop from 33 percent rated speed within sixty seconds after the brakes are applied, without injurious heating of the braking surface on the rotor, without field excitation on the generator, and with the leakage torque through the turbine wicket gate seals not exceeding an amount which will produce two percent of the full rated turbine torque. The brakes will also be designed to serve as hydraulic jacks to lift the generator rotor and the turbine runner for assembly, dismantling or adjustment of the thrust bearing. Provision will be made for blocking the rotor in the fully raised position.

10.20.3.12. Generator Shaft

The shaft will be made from forged, vacuum degassed, open hearth carbon or alloy steel properly heat treated. The shaft will be of ample size and strength to ensure safe operation at any speed up to the maximum runaway speed without harmful vibration or distortion.

The diameter of the generator main shaft will be coordinated with the turbine shaft diameter and will have a coupling flange for connection to the turbine shaft flange.

10.20.3.13. Generator Neutral Grounding

A generator neutral grounding cubicle will be provided for grounding the neutral point of the generator windings. A distribution transformer and secondary resistor will be furnished to provide a high resistance connection to ground for the generator neutral. Secondary side of the distribution transformer will be loaded by a resistor. This combination will be connected to a protection relay for stator earth fault protection.

The distribution transformer will be a conventional-type, single-phase, dry-type, and epoxy encapsulated with the following ratings:

- Capacity 75 kilovolt amperes
- Rated Primary Voltage 18,000 V
- Rated Secondary Voltage 240 V
- Basic Impulse Insulation Level 125 kV
- Time Rating 10 min

The resistor will be of the edge-wound, stainless steel, non-breakable type. All resistor components will be completely insulated ground. The resistor will have the following ratings:

- Resistance TBD
- Rated Voltage 240 V
- Rated 1-minute current TBD

The generator neutral cubicle will be a metal enclosed cubicle. The enclosure will provide protection against dust, insects and dripping water. All equipment installed within the cubicles will be fully accessible for inspection and maintenance.

10.21. Exciter

A digital type excitation system will be used. The digital excitation system will be designed to work directly into the generator main field complete with controls, limiters, and protection to safeguard the generator. The digital excitation system will also incorporate a Power System Stabilizer function operating in conjunction with the Automatic Voltage Regulator/Exciter function to dampen local mode, inter-area and inter-unit power system oscillations.

The exciter will consist of multiple thyristor power converters, each with its own digital firing control. Operator control will be provided through a local operator interface terminal, and the plant supervisory control and data acquisition (SCADA) system. Power to the exciter will be supplied via a power potential transformer powered from the generator bus. The exciter control channel will consist of microprocessor-based modules for digital sensing, regulation, silicon controlled rectifier firing control and sequence control algorithms. The cabinet lineup will include a logic cabinet and the required number of cabinets for the power converters and auxiliary devices.

10.22. Generator Step-up Transformers

10.22.1. General

For optimum performance, the GSU transformer will be a dual rated transformer, and will have normal rating of 225 MVA, a base rating of 185 MVA and a rating of 230 MVA with increased cooling. The base rating will be with natural circulation of oil and air (ONAN) with an increased rating using forced oil and air (OFAF) circulation.

Transformer design will be per the latest IEEE Standard C57 Series. The GSU transformer will be designed to withstand the sudden over excitation that can be produced when the transformer is separated from the line by the line breaker or other upstream device.

10.22.2. Ratings and Characteristics

The transformer will have the following ratings:

- Capacity 185/230 MVA at 60°C Rise
- Winding Temperature Rise by Resistance 65°C
- Hottest Spot Winding Temperature Rise 80°C
- Top Oil Temperature Rise by Thermometer 65°C
- Type of Cooling ONAN/OFAF

- Impedance at 75°C, ONAN Rating TBD
- Number of Phases 3
- Frequency 60 Hz
- High Voltage Winding, Rated Voltage 230.00 kV
- High Voltage Winding Connection Grounded Wye
- High Voltage Winding BIL at Phase Terminal 900 kV
- High Voltage Winding BIL at Neutral Terminal 550 kV
- Low Voltage Winding, Rated Voltage 18 kV
- Low Voltage Winding Connection Delta
- Low Voltage Winding BIL 150 kV
- High Voltage Side Taps (2) +2.5% above 230.00 kV, (2) -2.5% below 230.00 kV

10.22.3. Tank

The transformer tank and cover will be of welded construction, and such that the cover may be removed and rewelded without damage to the core and coil assembly. The transformer will be designed, where possible, so that components can be maintained without personnel entering the enclosed space of the tank. Access portals for essential maintenance and inspection will be provided as required. The transformer will have pulling eyes that are unobstructed by accessories to allow the transformer to be pulled in both directions.

10.22.4. Base

The transformer tank base will be designed to permit skidding on rollers in both directions and anchoring to a concrete foundation by welding/bolting to embedded steel angles or channels.

10.22.5. Core Assembly

The transformer will be designed and constructed either as a core-form or a shell-form type assembly. Exciting current for the core assembly will not exceed 0.5 percent of the rated current at rated voltage. The temperature rise limits will not be exceeded under the condition of maximum MVA with power factor of 0.80 and 105 percent voltage on the loaded winding.

10.22.6. Winding

Winding conductor will be copper. All windings will be a circular design. Individual conductors of the high and low-voltage windings will be rectangular with rounded edges. The high voltage winding will be furnished with full capacity taps.

10.22.7. Bushings

Bushings will conform to American National Standards Institute/Institute of Electrical and Electronics Engineers Standards and will be capable of carrying daily transformer overloads. Provisions will be made for connecting the isolated phase bus to the transformer low voltage bushings. A metal housing with flanges for terminating the isolated phase bus enclosure will be provided. Flexible braided copper bus connections will be provided for bolting the phase bus bars to the transformer bushings.

Each high voltage bushing will be furnished with one multi-ratio bushing current transformer with current ratios and accuracy class as required. Each current transformer will have a four-section winding with each winding section distributed along the full length of the secondary core to provide the tap ratios and accuracy classification required.

10.22.8. Surge Arresters

The transformer will be protected against surges on the high voltage windings by means of surge arresters. Surge arresters will be gapless metal-oxide station class suitable for operation on a solidly grounded neutral system for protection of the windings at the specified nominal and maximum line-to-line voltages and the insulation BIL rating.

10.22.9. Accessories

Temperature indicating and control equipment will be located not more than six ft. above the base of the transformer. Indicators (dials), thermometers, and relays will be constructed and located in such a manner that the temperature sensing portions can be removed from the transformer with the transformer energized.

The transformer will be equipped with the following devices:

- Magnetic Liquid Level Gauge
- Rapid Pressure Rise Relay
- Mechanical Relief Device

- Liquid Temperature (top oil) Indicator
- Electronic Temperature Monitor

10.22.10. Oil Preservation System

The transformer will include an oil preservation system of the atmospheric positive-pressure (sealed conservator) type with bladder, designed to prevent the oil from coming in direct contact with the air. The bladder membrane will prevent saturation of the oil with air. The oil connection to the main tank will be provided with a Buchholz-type (gas accumulation/excessive flow) relay.

10.22.11. Cooling System

Heat-exchangers will be so designed that there will be no recesses or surfaces on which water can accumulate and so arranged that surfaces will be readily accessible for cleaning and repainting without removing the heat-exchangers from the tank. Construction will be galvanized steel flat-plate type arranged in groups or banks for attachment to the main tank.

The heat-exchanger mounting flanges on the main transformer tank, both top and bottom, will be equipped with a butterfly valve to shut-off the oil flow from the main tank to the heat-exchangers. Drain valves and vent plugs will be furnished in the cooling system to permit draining oil from the heat-exchanger. Flexible connections will be furnished with pipe systems to minimize piping strains on coolers and to facilitate maintenance.

Fan and pump motors will be furnished in a National Electrical Manufacturers Association frame size and equipped with sealed bearings. Fan and pump groups will have in-line starters. Each motor will be protected by internal overload elements in each ungrounded conductor. Each motor will be furnished with an electrical disconnecting means to allow removal from the circuit without affecting other motor(s) in the same cooling group. Cooling equipment controls will be mounted in the control cabinet.

10.23. Unit Protection and Control System

10.23.1. General

The Protection and Control System (PCS) will be based on modern microprocessor based components networked together to provide a highly reliable system for monitoring and controlling the turbine-generator and associated plant equipment. Using software based technology for implementing the operating and monitoring functions allows for ease in

customizing the processes to fit specialized operating conditions, while also allowing for ease in making future changes.

While the PCS components and software will be designed to provide options for individual local control or centralized (SCADA stations) remote control of each of the turbine-generator systems, optimum utilization of generation will be through centralized remote dispatch operation. The plant SCADA system will be designed to interface with the remotely located generation dispatch center.

10.23.2. System Configuration

The PCS will be a programmable logic controller (PLC) based automation system with human machine interface (HMI) terminals for local monitoring and control. The PLC based system will be integrated with a plant SCADA system located in the Control Room. The PCS PLC based components will exchange information using a local area network (LAN). The LAN will transfer data over a fiber optic cable system using managed Ethernet switches for managing data traffic. The plant SCADA will be provided with a gateway connection into the LAN to monitor and initiate PCS automation functions. Access to the plant SCADA system from the remote dispatch center will be via a VPN connection to the plant LAN.

To provide the high level of availability required by the various critical applications a Hot Standby system will be required for each of the PLC based automation systems. The “Primary” PLC will execute the application program and control the system Inputs and Outputs (I/O). The “Standby” PLC will stay in the background, ready to take over if necessary. The “Standby” PLC will be connected to the “Primary” PLC via a high-speed fiber optic link. This link will update user application data cyclically on the “Standby” PLC. The Hot Standby system software will provide a smooth changeover from primary to standby at the I/O system. The changeover process will be transparent, and will continue to be managed without any permanent ill-effects from the occurrence of inoperative hardware.

A personal computer (PC) based SCADA system will be furnished to provide a centralized system (plant Control Room SCADA HMI stations) for monitoring and controlling the turbine-generator units and associated plant systems. SCADA servers will access the LAN through a secure gateway connection. PC HMI stations will be provided in the Control Room for accessing information from the servers and sending control initiating commands to the PCS PLCs. The SCADA software will generate HMI screens for use in monitoring the turbine-generator and plant systems and for initiating command signals for the PCS PLCs. When the plant SCADA system is in the “remote” mode of operation, generation control will be via the central dispatch center.

A GPS satellite controlled clock with an IRIG-B unmodulated time code output will be provided. The IRIG-B time code will be used for providing accurate time stamping for all alarm and fault recording.

All of the unit control systems will be designed for a "black-start" type situation. Critical systems required for unit starting will be supported by the station battery for a minimum of 8-hours upon loss of AC station service. Large AC station equipment and plant lighting will be supported by the standby diesel generator (32-hour local fuel supply). In the event that the transmission line system is down causing a loss of AC station service, it will be possible to start one of the units and operate locally in an islanded condition to provide local station service until the transmission line connection can be restored.

10.23.3. Unit Control Panel

A Unit Control Panel (UCP) will be provided for each of the turbine-generator units. The UCPs will be located in the plant Control Room. The UCP will be provided with features for either manual or automatic control of the turbine-generator system. Each UCP will be provided with a HMI for control and monitoring of the turbine-generator system. The UCP will also be provided with features for remote control from the Control Room HMI Operator Stations. Each UCP will be provided with a Mode Selection switch (Manual-Auto-Remote) for selecting unit mode of operation. UCP operating modes will be as follows:

10.23.3.1. Manual Mode Control

In Manual mode of operation the turbine-generator unit will be started, synchronized, connected to the system, and loaded using controls at the UCP. This control mode does not have automatic sequences; the operator will follow the standard manual operating procedures to start and connect the turbine-generator to the line. This mode of operation is typically used for maintenance and testing purposes.

10.23.3.2. Auto Mode Control

In Auto mode of operation the turbine-generator unit will be started, synchronized, connected to the system, and loaded using the UCP automation systems. Single action start or stop commands will be made from the UCP Start-Stop switch or from the UCP HMI terminal. The UCP PLC system will be programmed and interconnected with the plant LAN system to implement the required process for automatically starting, synchronizing, connecting to the line, and loading the unit.

10.23.3.3. Remote Mode Control

This is the preferred method of operation and transfers turbine-generator system control from the UCP location to the SCADA HMI Operator Stations located in the Control Room. Control commands will be issued to the UCP from the PC based SCADA/Operator Station servers.

10.23.4. Control Room Operations

The Control Room Operating Stations will permit centralized control of all units. The Control Room Operator Stations will be designed to initiate control functions on the units with their UCP in the "Remote" mode of operation. However, the Operator Stations will be able to monitor the systems under all UCP operating modes. The Operator Station HMIs will be provided with screens for displaying the required control and monitoring information. Standard SCADA software will be used to develop the required system screen displays. Interface with the HMI screens will be via standard PC keyboards and mouse. The Operating Stations will be configured to provide three automatic operating modes: Automatic Step-By-Step, Automatic Continuous, and Automatic Remote Dispatch. It is proposed that the normal mode of operation be Automatic Remote Dispatch.

10.23.4.1. Automatic Step-By-Step Sequence

In this mode the unit starting and stopping sequences are executed step by step. All prerequisites and conditions will be displayed on the HMI screen and when all step prerequisites are met, the operator can then proceed to the next step. This mode is primarily used for trouble shooting and maintenance operations.

10.23.4.2. Automatic Continuous Sequence

In this mode the unit start and stop sequences are initiated by the operator, but no additional operator intervention will be required. Once the process is initiated the unit will automatically sequence through all required steps. The operator will be able to monitor all conditions and actions on the Operator Station HMI screens. This will be the normal operating mode from the plant Control Room.

10.23.4.3. Automatic Remote Dispatch

In this mode, a remote computer located at the generation dispatch center will be able to connect to the PCS and perform the same monitoring and control functions available at the plant SCADA Operator Station HMIs (based on security privileges). The remote connection will be encrypted using virtual private network (VPN) technology. When in this mode of operation the dispatch

operator will have full control of the unit generation, including starting, stopping and loading. This is the intended normal operating mode.

10.23.5. Unit Protection

Unit protection panels will be provided for protection of the turbine-generator and GSU transformer systems. Multifunction microprocessor based generator and transformer protection relays will be provided. Each system will be fully redundant from the instrument transformers up through the protective relay. The relay trip signals will output to hand-reset type lockout relays (86-relay) for locking the systems out of operation. The relays will be provided with sequence of events recording retained in nonvolatile memory.

10.23.5.1. General Protection Features

The generator protection relay will contain as a minimum the following protective features:

- Loss-of-field detection
- 100 percent stator ground fault detection
- DC field ground protection
- Out-of-step protection
- Over excitation detection based on volts/hertz measurement
- Negative-sequence overcurrent elements
- Anti-motoring, over-power
- Two-zone mho phase distance, for backup protection
- Phase over voltage
- Phase under voltage
- Supervision of voltage transformers
- Over-under frequency elements
- Phase current differential elements

10.23.5.2. GSU Transformer Protection Features

The transformer protection relay will contain as a minimum the following protective features:

- Percentage Differential Protection
- Harmonic Restraint Elements

- Unrestrained Differential Protection for Severe Internal Faults
- Overcurrent Fault Protection
- Unit Breaker Failure Protection

10.23.5.3. Lockout Relays

The unit protection system will be provided with manually reset unit lockout relays to facilitate proper shutdown and lockout of the unit upon sensing a fault condition. The lock out relays (86) will be electrically tripped, manually reset, high-speed multi-contact type with an operating time of approximately 1/2 cycle. Built-in coil monitoring will be provided.

10.23.6. Station Monitoring

A Station Monitoring Panel will be provided for monitoring the station electrical and mechanical service equipment. The panel will use a hot backup PLC system connected to the LAN for gathering and processing the principle station service equipment. A HMI will be provided on the panel front for accessing status of the station equipment.

The following station service equipment will be monitored:

- Station 480V switchgear
- Station battery system
- Reservoir elevation
- Tail water elevation
- Fire alarm system
- Intrusion
- Station air system
- Station sump

10.23.7. Instrumentation Cabinet

A turbine-generator instrumentation cabinet will be provided at each unit for collection of the instrumentation signals associated with the turbine and generator assembly. The cabinet will use a PLC system for gathering the instrumentation signals and processing them for transfer to the LAN connected equipment. The temperature, pressure, position, and level signals monitoring the various systems will be collected at the PLC I/O. The signals will be sent to the UCP via the LAN for processing, alarming and monitoring.

10.23.8. Distributed Input / Output

Distributed I/O panels containing I/O and communication modules for collection of local I/O instrumentation will be provided at major equipment locations. Collected I/O information will be transferred to the appropriate control and monitoring panels via the LAN. Distributed I/O panels will be provided at each of the GSU transformers and the 480V switchgear.

10.23.9. HMI Terminals

10.23.9.1. General

In general, access to the system control and monitoring functions will be via HMI terminals located at the UCPs, Station Monitoring Panel, and the SCADA Operating Stations. The UCPs and Station Monitoring Panel HMIs will use color touch screens for accessing control and monitoring functions, while the Control Room SCADA Operating Stations will use LED widescreen monitors with keyboard and mouse interface.

10.23.9.2. UCP and Station Monitoring Panel HMIs

The UCP and Station Monitoring Panel HMIs will be provided with a touchscreen interface for accessing system control and monitoring functions. Software configured graphic screens will be provided for displaying the monitoring and control information. The graphic symbols used for equipment that change operating state such as the generator, circuit breakers, valves, brakes, pumps, etc. will be color coordinated. The graphic symbols will show red when in their operating state (circuit breaker closed, pump running, valve open, etc.), and green when in non-operating state (circuit breaker open, pump stopped, valve closed, etc.).

Each screen will be provided with a navigation bar with tabs for navigating to the various screens. Access to system control functions will be password protected to protect against unauthorized operations. The Overview Screen will have a location for entering the access password. The navigation bar will block access to secure screens until the proper password has been entered. All screens not password protected may be viewed by anyone, but all control functions will be blocked until the proper password has been entered and confirmed by the system. Access to the following screens and functions will be password protected:

- Unit Control Screen
- Valve Control Screens
- Alarm Acknowledge and Reset Functions

- Trending Screens
- Alarm and Trip Set Point Screens

An alarm banner will display on all of the screens at the initiation of an alarm condition. The alarm banner will remain until the alarm condition has been acknowledged via the Alarm Summary Screen.

10.23.9.3. Control Room SCADA Operating Station HMI

Each of the Control Room SCADA Operating Stations will be provided with two LED widescreen monitors with keyboard and mouse interface for accessing system control and monitoring functions. Software configured graphic screens will be provided for displaying the monitoring and control information. The graphic symbols used for equipment that change operating state such as the generator, circuit breakers, valves, brakes, pumps, etc. will be color coordinated. The graphic symbols will show red when in their operating state (circuit breaker closed, pump running, valve open, etc.), and green when in non-operating state (circuit breaker open, pump stopped, valve closed, etc.).

Each screen will be provided with a navigation bar with tabs for navigating to the various screens. Access to system control functions will be password protected to protect against unauthorized operations. The default, or Overview Screen, will have a location for entering the access password. The navigation bar will block access to secure screens until the proper password has been entered. All screens not password protected may be viewed by anyone, but all control functions will be blocked until the proper password has been entered and confirmed by the system. Access to the following screens and functions will be password protected:

- Unit Control Screens
- Alarm Acknowledge and Reset Functions
- Trending Screens

An alarm banner will display on all of the screens at the initiation of an alarm condition. The alarm banner will remain until the alarm condition has been acknowledged via the Alarm Summary Screen.

As a minimum, each of the SCADA HMIs will be provided with the following screens for control and monitoring of the turbine-generator systems:

- Overview Screen
- Unit Control Screens (one screen for each unit)

- Unit Start/Stop Sequence Screens (one screen for each unit)
- Governor Screen
- Exciter Screen
- Bearing Temperature Screens (one screen for each unit)
- Generator Temperature Screen (one screen for each unit)
- Alarm Summary Screen
- Alarm History Screen
- Trending Screens

10.24. Miscellaneous Mechanical Equipment

The powerhouse will be provided with the following miscellaneous mechanical systems and equipment.

10.24.1. Powerhouse Bridge Crane

One 300-ton capacity overhead traveling-bridge type crane will be installed in the powerhouse. The crane will be primarily used for installation of turbines, and other powerhouse equipment; and subsequent dismantling and reassembly of equipment during maintenance overhauls.

The powerhouse crane will be electrically operated double girder, overhead travelling bridge type, equipped with a main hoist and trolley and auxiliary hoist. The auxiliary hoist will be trolley-mounted or under-hung from the bridge girder. Bridge, hoist, and trolley drives will be provided to facilitate equipment transport in vertical, lateral, and longitudinal directions. The capacity of the main hoist will be sufficient for the heaviest equipment lift, which will be generator rotor plus the lifting device. The crane will be provided with operator's can to permit operation of the crane.

10.24.2. Draft Tube Bulkheads

Two sets of draft tube bulkheads will be provided to permit dewatering of the turbine water passages for inspection and maintenance of the turbines. Bulkhead guides will be installed at each draft tube openings. The bulkheads will be designed to withstand the full differential head.

Each draft tube bulkhead will be sectionalized into two sections for the ease of transportation of bulkhead to the site. Each section will be approximately 26.5 ft. wide by 13 ft. high. Each bulkhead section will be of downstream sealing type and the transfer of the hydrostatic load from the two end posts of the leaf to the supporting structure will be through bearing pads mounted on

the end posts. Bulkhead sections will be installed and removed with a semi-automatic lifting beam connected to a draft tube gantry crane. Bulkhead sections will be installed and removed under near balanced head conditions. Fill valves, operated by the lifting beam, will be provided in the bulkhead to fill the void space in the draft tube.

10.24.3. Draft Tube Gantry Crane

A 25 ton capacity electrical travelling gantry crane will be provided on powerhouse deck at El. 1475 ft. for installation, removal, and handling of draft tube bulkheads.

10.24.4. Station Drainage System

The powerhouse will be designed with a series of floor and trench drains to capture and route any water seepage or leakage. The drains will be routed to a central sump with an integral oil-water separator. The sump will be provided with two pumps to provide 100 percent redundancy for the design inflows. The pumps will pump the drainage water (after oil and other contaminants are separated out) to tailwater.

10.24.5. Unit Dewatering System

Each unit will be dewatered to tailwater through the main turbine water passages. To completely dewater each unit (after the draft tube gates and intake gate or inlet butterfly valve are closed), water will be piped from the low point of each draft tube to a dewatering pump which will pump the remaining water to the tailrace. After dewatering is complete, any leakage into the turbine water passages will be routed to the station sump and handled by the station sump pumps.

10.24.6. Station Raw Water System

The powerhouse will be provided with a raw water system. The system will either include a tap off each unit penstock, with a pressure reducer to reduce the penstock water pressure to 100 psi or less, or the water will be pumped from the tailrace to the required system pressure. Both systems would include redundant strainers at the system inlet to eliminate particulates and debris. Economic life-cycle cost analyses will determine which design concept is the lowest cost. Piping inside the powerhouse will distribute the water to suitable locations for general station use.

The raw water system will also be the source of water supply to the generator coolers, unit bearing coolers, and turbine shaft seal water. All these will be open-loop systems discharging to the tailrace. A secondary fine filter will be added to the shaft seal water supply to meet the cleanliness requirements of that water supply.

10.24.7. Compressed Air System

The powerhouse will be provided with a compressed air system for general station use and for the generator brakes. The system will consist of redundant compressors, an air dryer, an air receiver tank, distribution piping, and quick disconnect couplings in locations where pneumatic tools may be used.

10.24.8. HVAC Systems

The powerhouse will be provided with heating equipment to maintain suitable interior temperatures for worker comfort. Distributed electrical heaters will be the primary heating sources and using generator waste heat will be considered during detailed design. Forced air ventilation will be provided to all locations in the powerhouse, with the specific ventilation requirements determined for applicable ASHRAE codes. In addition air conditioning (cooling plus humidity control) will also be provided in the main control room, offices, and other spaces where workers will be routinely located.

10.24.9. Standby Generator

A diesel-powered standby generator will be located in an alcove in the powerhouse access tunnel. The generator will be used for black starts and for operation of the spillway gates and other equipment during a power failure.

10.25. Accessory Electrical Equipment

The powerhouse will be provided with the following accessory electrical systems and equipment.

10.25.1. Powerhouse Alternating Current System

The powerhouse will be provided with a distributed alternating current system to provide electrical power for the electrical equipment and miscellaneous system use. The system will be fed though redundant 13.8 kV/480V dry-type station service transformers that can be fed either from a generating unit or backfed from the Railbelt system through one of the generator step-up transformers. The system will distribute 480V AC power to the station motor control centers and other individual electrical demand sources. The system will also include step-down transformers to 120 VAC and a 120V distribution system for lighting and general station uses.

10.25.2. Powerhouse DC System

The powerhouse will be provided with a 125VDC system to power essential equipment when AC power is lost. The system will consist of a battery bank, redundant chargers, and a DC distribution system.

10.25.3. Powerhouse Lighting

The powerhouse will be provided with a lighting system to light all areas where workers may be located. Lighting types and lighting levels will be selected based on location, occupation levels, and specific lighting requirements.

10.25.4. Powerhouse Grounding System

The powerhouse will be provided with a comprehensive grounding system consisting of a ground grid inside the powerhouse and a grounding field located and sized to provide an acceptably low ground potential to the grounding grid. All equipment and ferrous metal elements will be connected to the ground grid. Grounding terminals will be provided at locations where workers may use electrical equipment that should be grounded.

10.26. Switchyard Structures and Equipment

10.26.1. Switchyard Arrangement

The switchyard will be a breaker-and-a-half arrangement with three bays and space for a future fourth bay. This configuration provides two normally energized main buses interconnected with three circuit breakers in each bay. Between each pair of bay breakers a circuit is provided (total of two circuits per bay). Each of the three bays provides two circuits, one circuit connects to one of the GSU transformers and the other provides a line connection to the transmission grid. The breaker-and-a-half configuration was chosen because of its high reliability and flexibility. Advantages include:

- Isolation of either main bus for maintenance without disrupting service;
- Isolation of any circuit breaker for maintenance without disrupting service;
- Double feed to each circuit;
- Bus fault does not interrupt service to any circuit; and,
- All switching done with circuit breakers.

Connection of each bay to the GSU transformers will be via a 230 kV overhead transmission line. A total of three transmission lines, with space for a fourth line, will be routed from the switchyard to the GSU transformers located on the powerhouse draft tube deck, and anchored to the downstream face of the dam or steel tower anchorages as appropriate. Three overhead 230 kV transmission lines will exit the switchyard with two connecting to the Gold Creek intertie and one to the Denali East intertie (arrangement selected for the cost estimate).

10.26.2. Circuit Breakers

The circuit breakers will be sulfur hexafluoride (SF_6) type breakers with dead-tank construction. Because of the low ambient temperatures experienced at the switchyard, the breakers will be provided with tank heaters to maintain the required SF_6 insulation levels. Bushing type current transformers will also be furnished to interface with the switchyard protection and control system.

The circuit breaker will have the following ratings and characteristics:

- Rated Nominal Voltage 230 kV
- Rated Maximum Voltage 245 kV
- Rated Frequency 60 Hz
- Rated Continuous Current 1200 A rms
- Rated BIL 900 kV
- Rated Short-Circuit Current TBD
- Max. Symmetrical Interrupting Capacity TBD
- Interrupting Time 3 cycles

Each circuit breaker will be provided with a three-pole, gang operated disconnect switch on the incoming and outgoing terminals of the circuit breaker.

10.26.3. Instrument Transformers

Voltage transformers will be provided for monitoring the voltage at the two main buses and at each line circuit termination. Capacitive coupled type voltage transformers will be used.

10.26.4. Bus, Overhead Lines and Structures

Aluminum tube bus will be used for overhead distribution with flexible type connector at equipment connections. Galvanized steel support structures with station post type insulators will be used for supporting the bus.

Galvanized steel tower supports will be used for supporting the 230 kV lines entering and exiting the switchyard. Each of the 230 kV lines will be provided with gang operated isolating switches and surge protection. Grounding switches will also be provided for each of the 230 kV lines

10.26.5. Grounding

The switchyard will be provided with a ground grid designed to limit step and touch potential to safe values. The ground grid will be designed using the latest IEEE 80 and IEEE 81 Standards. All steel structures and fencing will be bonded to the ground grid. It may be necessary to use chemically enhanced ground rods to reduce the grid-to-earth resistance to an acceptable value.

10.26.6. Control House

A control house will be provided to house the switchyard protection and control equipment, along with their required support systems. It is proposed that a prefabricated modular control house be provide. The control house will house the following:

- Switchyard Protection and Control Panels
- Switchyard Battery and Battery Charger
- Station Service Distribution Equipment

10.26.6.1. Protection and Control Panels

The protection and control panels will be PLC based with microprocessor type multifunction protection relays and HMI type interface. Provisions will be made for either local manual control of the circuit breakers, remote control from the powerhouse, or remote control from the dispatch center. Standard line protection relaying will be provided for the 230 kV transmission lines. A dedicated fiber optic communication link will be provided between the switchyard and powerhouse to integrate the GSU transformer protection with the required switchyard circuit breaker tripping.

A local SCADA system, similar to that used at the powerhouse will be provided at the switchyard. Desk-top operator terminals will be provided for monitoring the switchyard equipment status and for control of the circuit breakers. A server will be provided for storing alarm and operation information.

10.26.6.2. Station Service

Two station service transformers will be installed to provide 480V AC station service for the control house. The transformers will be connected to the switchyard's two main buses. Automatic switching at the 480V service will be provided to maintain station service in the event one of the switchyard main buses needs to be de-energized. Small distribution transformers will also be provided for lighting and other small 120V loads.

A lead acid, wet cell type battery with charger will be provided for operation of the switchyard circuit breakers and provide critical power for the control and protection systems.

A small standby generator will be provided to furnish backup AC station service in the event of an extended line outage. The standby generator will be sized to support the battery system and critical heating loads to protect the control house equipment during cold weather.

10.27. Reservoir

10.27.1. Reservoir Clearing

It has been assumed that complete reservoir clearing will not be undertaken. Complete clearing will only be performed for the first 3.5 miles upstream of the dam. Further upstream, the remaining reservoir perimeter will be cleared 200 ft. below the normal maximum water surface elevation.

10.28. Relict Channel Treatment

During this stage of the feasibility investigation, no work has been performed with respect to the relict channel that exists on the north bank of the Watana reservoir approximately 2,600 ft. upstream from the dam. Future geotechnical studies will revisit the feature and further site investigation will be carried out. At this stage, the results of the investigations carried out during the 1980s are repeated for clarity.

The relict channel runs from the Susitna River gorge to Tsusena Creek, a distance of about 1.5 miles. The surface elevation of the lowest saddle is approximately El. 2210 ft. Glacial deposits of depths up to 454 ft. have been identified. The maximum average hydraulic gradient along any flow path in the buried channel from the edge of the reservoir NMOL (El. 2050 ft.) to Tsusena Creek is approximately two percent. Tsusena Creek at the relict channel outlet area is at least 120 ft. above the natural river level. There are several surface lakes within the channel area, and some artesian water is present in places. Zones of permafrost have also been identified throughout the channel area.

To confirm the integrity of the rim of the Watana reservoir and to control losses due to potential seepage, a number of conditions were evaluated in the 1980s. Studies covered settlement of the reservoir rim, subsurface flows, permafrost, and liquefaction during earthquakes.

10.28.1. Surface Flows

Based on information gained from past exploration programs, the relict channel soils are either dense or cohesive and as such are not deemed to be subject to settlement resulting from seismic

shaking. Therefore, the low ground surface in the relict channel area will provide more than adequate freeboard as it is 135 ft. above the dam crest.

10.28.2. Subsurface Flows

The potential for progressive piping and erosion in the area of discharge into the Tsusena Creek will be controlled by the placement of properly graded granular materials to form a filter blanket over any zones of emergence. Field investigations will be carried out to further define critical areas, and mitigation measures will be developed. Subsequent to construction of the dam, the relict channel will be continuously monitored at the outlet area after reservoir filling to verify that a state of equilibrium is established with respect to permafrost and seepage gradients in the buried channel area.

10.28.3. Permafrost

Thawing of permafrost will occur in portions of the relict channel area. This thawing is expected to have minimum impact on subsurface flows and ground settlement. Although no specific remedial work is foreseen; flows, groundwater elevation, and ground surface elevation in the buried channel area will be carefully and continuously monitored by means of appropriate instrumentation systems and any necessary maintenance work carried out to maintain freeboard and control seepage discharge.

10.28.4. Liquefaction

Underground information compiled in the 1980s indicates that the buried channel area is filled with outwash, glacial till and lacustrine deposits. Initial evaluations, outlined in the original license application indicated concern with regard to the upper outwash deposits because they did not appear dense enough to resist seismic shaking without experiencing considerable loss in stability.

The most likely prospects for liquefaction are saturated foundations consisting of fine grained, poorly graded, cohesionless deposits (sands and silts), that are not laterally confined and are loose or moderately dense. Based on available data, an assessment of the liquefaction potential of the relict channel area indicates the deposits are either well graded, dense to very dense, or cohesive, and therefore, have low potential for liquefaction. Consequently, no remedial measures are currently considered necessary as a precaution against the effects of liquefaction.

Further geotechnical studies will be carried out to fully define the extent and characteristics of the materials in the relict channel. Should these studies indicate that mitigation is required, provisions will be made for treatment to cover the conditions identified.

10.28.5. Remedial Work Influence on Construction Schedules

Relict channel remedial treatment construction work, if necessary, will have no impact on the Watana Dam construction schedule.

10.28.6. Relict Channel Treatment

During future design investigations, additional boreholes and inspection trenches will be employed to further delineate the relict channel foundation. The area will also be thoroughly monitored by observation during reservoir filling to assess actual hydrological conditions in the relict channel. In response to the unlikely event that construction remedial measures are considered necessary following those observations and data assessment, a positive remedial treatment such as a downstream toe drain will be employed.